STUDIES ON WAVES
IN ELASTIC/VISCOPLASTIC MEDIA

by

PAUL E. ZANNIS

Diploma (Mech. Eng.) National Technical University of Athens, 1963

Diploma (Civil Eng.) National Technical University of Athens, 1967

M. Ph. Yale University, 1969

A Dissertation Presented to the Faculty of the

Graduate School of Yale University

in Candidacy for the Degree of

Doctor of Philosophy

1971

A B S T R A C T

This dissertation considers two applications of the theory of elastic/viscoplastic behavior of solids on wave propagation problems.

The first problem deals with waves emerging from an impact load suddenly applied uniformly on the surface of a cylindrical cavity. Due to the restriction of plane strain axial symmetry at the instant of impact, a pulse travels outwards in the form of cylindrical waves. Perzyna's constitutive equation for an isotropic work hardening material, together with the inelastic work as loading/unloading criterion, is applied for the presentation of the viscoplastic behavior under the present "multidimensional" state of stress. The system of partial differential equations is solved numerically along characteristic lines in the r-t plane. On the basis of these computations: 1) the influence of the several physical parameters (i.e., viscosity coefficient, work hardening parameter, magnitude of the applied pressure) will be discussed and 2) the existence of an elastic region within the inelastically deforming medium will be shown.

The second problem is an attempt to incorporate strain rate effects into an unloading problem. This wave propagation in a rod is used as the physical model for this effort. Malvern's constitutive equation is generalized to include the unloading processes for a material with a bilinear quasi-static stress-strain curve characterized by kinematic hardening. The method of solution is numerical along the characteristic lines in the x-t plane. It will be shown: 1) the inelastic deformations during unloading affect considerably the residual strain distribution and 2) by the end of the transient phenomenon a lower "quasi plateau" is developed along the bar.

A C K N O W L E D G M E N T S

It is a pleasure to record my gratitude to my teacher, advisor, and friend, Professor Aris Phillips, whose continuous interest and help guided the investigations reported in this dissertation.

My sincere appreciation must also be given to the other members of my doctoral committee, Professors B. T. Chu, P. M. Schultheiss, D. Rader, and W. Justusson.

In addition, I should acknowledge a debt owed to my teachers at the National Technical University in Athens, Greece as well as to Professors A. Phillips, B. T. Chu, and D. Rader at Yale University whose lectures helped me with the background necessary for this thesis.

I am deeply indebted as well to friends and colleagues at Yale University who kindly gave me their help at several occasions. Herewith I thank Professor M. Zabinski, now at Fairfield University, and Doctor D. Micholson, now at Goodyear and Rubber Company, for helpful suggestions, James Geary and Karen Kinsey for critical readings of my manuscript, Pranab Das for his beautiful figures, Joe Vitale for his genial services as a guide to the facilities at the Yale Computer Center, and June Yarosh for her superb typing.

Finally I would like to take this opportunity to express my belief that I would never have undertaken this study if I didn't have the privilege of having parents who set the example of pursuing higher education. To them, who were my source of inspiration and motivation, I dedicate this thesis.

TABLE OF CONTENTS

LIST OF ILLUSTRATIONS

SYMBOLS

σ	stress
ε	strain
σ_o	yield stress in simple tension
ε_o	yield strain in tension
r	radius
t	time
x	distance along the bar
K_o	initial value of the radius of the yield surface
K	radius of the yield surface
s	deviatoric stress
e	deviatoric strain
E	Young's modulus
ν	Poisson's ratio
K	Bulk modulus
μ	shear modulus
u	displacement
v	velocity
c	wave speed
C_o	elastic wave speed
ρ	density
II_s	second invariant of the deviatoric stress tensor
II_p	second invariant of the inelastic strain rate
W	work done during the deformations
m	viscosity coefficient
$e\ell$	as superscript: the elastic part

vp	as superscript: the viscoplastic part
in	as superscript: the inelastic part
r	as subscript: the radial part
θ	as subscript: the tangential part
z	as subscript: the axial part
N, S, E, W	points on the characteristic net
Δt	time increment
Δr	radial distance increment

I N T R O D U C T I O N

Increasing activity in the study of wave propagation during the last two decades contributed significantly towards a better understanding of the dynamic behavior of solids, both theoretically and experimentally.

A considerable amount of this research has been devoted to wave propagation of strain-rate sensitive materials. The majority of these efforts has been concentrated on solving one-dimensional wave problems and special emphasis was given to the problem of a semi-infinite bar subjected to an axial impact load. The first formal theory describing this problem is credited to Malvern (1951). Malvern's rate-of-strain dependent theory successfully applied by B. Wood and A. Phillips (1969) gave complete agreement between experiment and theory predicting the existence of a strain plateau and the incremental plastic wave velocity.

An extension of Malvern's theory to the spherical wave propagation problem was proposed by Zabinski (1969) in his doctoral dissertation.

On the other hand, a general theory describing the

elastic/viscoplastic behavior under a multidimensional state of stress was proposed by Perzyna in 1966. In the same publication, Perzyna offered a detailed application of his theory for the case of spherical waves together with a general, though not carefully presented, discussion of the case of cylindrical waves.

This case of an infinite elastic/viscoplastic medium with a cylindrical cavity will be considered in the first part of this dissertation. A radial impact load is suddenly applied uniformly on the surface of the cavity. Due to the restriction of cylindrical symmetry and the boundary condition of plane strain deformation, at the instant of impact, a pulse travels outwards in the form of a cylindrical wave. Thus a transient process is set up. Cylindrical divergence rapidly reduces the radial amplitude of the pulse. As the pulse emanates from the cavity, it travels at the elastic wave speed into an undisturbed region. The region immediately behind the wave front is no longer stress free. As a consequence of continuity and the fact that the pulse travels into an undisturbed region, the jump conditions across the wave front are elastic in nature (i.e., no inelastic work). Due to the type of loading program assumed, the only possible displacement is along the radial direction. Furthermore, cylindrical symmetry requires variations of stresses and strains to be radial.

The applied pressure is largest in magnitude at the cavity's surface; due to the cylindrical divergence it di-

minishes with radial position and vanishes in the limit. Thus, if the pulse is large enough, yielding will first occur at the cavity. A plastic region will subsequently spread outwards and due to viscous effects and cylindrical divergence it will terminate at a finite radial position followed by an elastic region. The location of the elastic-plastic boundary within the cylinder is unknown a priori. It changes also with increasing time since increasing inelastic work will shift points from the viscoplastic to the elastic region.

The first phase of this part consists of formulating a constitutive equation. The Hohenemser-Prager and Perzyna's theories will be used as the starting point for this effort. The von Mises yield condition together with isotropic hardening will be applied. For simplicity, the quasi-static stress-strain relation will be assumed as bilinear. The ratio between the slopes of these two lines will introduce a concrete way by which the effects of strain hardening could be studied. The quasi-static stress-strain curve will produce a relationship between the inelastic work and the radius of the yield surface. In order to simplify the mathematics, this relation will be approximated with a piece-wise linear curve. In addition to the constitutive equation, it is necessary to establish loading/unloading criteria. This will be done by means of the inelastic work in a way similar to the one suggested by Cristescu (1967).

The fundamental equations relating the unknown quantities will be derived from the following considerations:

1. Equation of motion along the radial direction.
2. Radial strain as a function of the radial displacement.
3. Tangential strain as a function of radial displacement.
4. Elastic compressibility.
5. Two independent applications of the constitutive equation for the strain rates along the radial and tangential directions.

The six equations in conjunction with the initial conditions are sufficient to solve for the three stress components (radial, tangential, and axial), the two strain components (radial and tangential) and the radial velocity. This set of first order non-linear partial differential equations will be integrated numerically by the method of characteristics in the radius-time space. The solutions for the unknowns will be obtained by means of a finite difference scheme. The trapezoidal rule for a reasonably small time increment Δt will be used.

The material data assumed in the calculations will be those for aluminum. Due to the large number of calculations involved in the numerical method, the procedure will be programmed in FORTRAN IV for the IBM 7094-7040 or IBM 360/67 digital computer. The program provides time histories in the radius-time space for the three components of the stress, the radial and tangential strains, and the radial velocities. Con-

clusions, also, will be derived about the position of the elastic-plastic boundary, the magnitude of the second invariant of the deviatoric stress tensor, and the change in the radius of the yield surface during the transient process.

The final phase consists of examining the influence of such parameters as impact load, Poisson's ratio, viscosity coefficients, strain hardening ratio, and radius of the cylindrical cavity on the transient process. Comparison between the computer outputs will allow us to determine the combined effect of these variables and will advance our understanding of the nature of the cylindrical waves in elastic/viscoplastic materials.

Although cylindrical geometry presents more mathematical difficulty than rectangular geometry, as in the rod problem, or spherical geometry, in the case of spherical waves, certain distinct advantages are gained by examining cylindrical waves. First it should be observed that the mathematical model for cylindrical waves has only one direction of symmetry, namely the axial direction. Therefore, in contrast to the two other types of waves (i.e., rod and sphere), the cylindrical problem retains all three stress components and represents one of the simplest applications for a "multidimensional" theory of viscoplastic behavior. Secondly, experiments producing plane-strain cylindrical waves in elastic/viscoplastic materials are readily feasible. (For more details, see Chapter I, section 5). The theoretical treatment of the problem will contribute to a better evaluation of the experimental

results and eventually will increase our understanding of the viscoplastic behavior under multidimensional states of stress.

In the second part of this dissertation, an attempt will be made to incorporate rate effects into an unloading wave problem. The simplest case of one dimensional wave propagation, i.e., that in a semi-infinite bar, will be used as the model for this investigation.

The constitutive equation proposed by Malvern to describe the dynamic behavior during inelastic loading will be generalized to cover the inelastic behavior during the unloading process.

The quasi-static stress-strain curve of a kinematically hardening material will be approximated by linear segments for the purpose of computing the inelastic strain rates during the loading as well as the unloading part of the dynamic stress-strain curves.

The basic equations relating the three unknowns (i.e., stress, strain, and velocity) will be derived from the following condierations:

1. Equation of motion along the axis of the bar
2. Strain as a function of the displacement
3. Application of the constitutive equation for the strain rates.

This set of first order linear partial differential equations will be integrated numerically by the method of characteristics in the x-t (i.e., distance-time) space. The applied

pressure at the free end of the bar will be the boundary condition. This gives rise first to the loading waves and at a later time, as the pressure decreases, to the unloading waves within the bar. Again, a finite difference scheme is used in connection with a simplified version of the trapezoidal rule. This scheme provides the solution for the unknowns at the points of the characteristic net. On choosing the dimensions of the net to be sufficiently small, we find the solutions to be of the desired accuracy.

The computations are done with an IBM 7094-7040 digital computer. The program provides the dynamic stress-strain curves for several points inside the bar and allows us to derive conclusions about the influence of the several parameters involved.

As in Malvern and Wood and Phillips, special attention will be given to the residual strain distribution along the bar.

The existence of a strain plateau at the end of the transient phenomenon and its comparison to the plateau in the case of continued loading will provide a better understanding of the physical processes taking place during the inelastic unloading. It will be seen first that the inelastic unloading will produce the "quasi-plateau" by shifting the end point of the dynamic stress-strain curves close to the intersection point of the lower yield point line and the strain axis. On the other hand, it will be observed that points far away from the free end of the semi-infinite bar, due to the

viscous dispersion, will experience only elastic unloading and will not contribute to the plateau at the end of the transient phenomenon.

So far, in the second part of this dissertation, we discussed a problem involving only one stress component. If we wish to generalise the inelastic unloading problem to multidimensional states of stress, we need a method of determining the analogue of the lower quasi-static reference yield point. However, a theory that will provide criteria for this determination has not been reported in the literature.

C H A P T E R I

HISTORICAL DEVELOPMENTS OF THE THEORY OF WAVES IN ELASTIC/VISCOPLASTIC MEDIA

1. Introduction

It is a well known fact that whenever the time effects are included in the equations describing a mechanical problem the solution shows that the stresses and strains propagate into the medium in a wave form.

The original work on the wave problem was concentrated on the linear elastic materials, and the strain-rate effects were neglected. Work of this type has been done by famous elasticians like D'Alembert, Euler, Bernoulli, Young, Cauchy, Poisson, Saint Venant, and Boussinesq. For more details regarding the elastic waves see references [1] - [14] as well as several standard books dealing with the historical developments of the theory of elasticity(1).

(1) See for example

1. - Timoshenko, S.P. History of Strength of Materials, McGraw-Hill, New York, 1953.

In the late nineteenth century work done by J. Hopkinson [20] gave rise to the question of strain-rate dependence. Studying the propagation of longitudinal waves in iron wire he found the dynamic yield stress to be approximately twice as high as the static yield stress, and this observation opened the question of the influence of the strain-rate in the wave propgation problem. Further experiments by B. Hopkinson [21], Ludwik [22] and others have shown that this influence is important for some materials, while others have shown that for other materials and for certain types of experiments this influence is negligible.

On the other hand wave propagation within a solid having a stress strain relation other than the Hooke's law has been considered only relatively recently. The earliest work on a one dimensional inelastic problem was done by DONNELL [23]

---

2. - Todhunter and Pearson, A History of the Theory of Elasticity and of the Strength of Materials, Dover Publications, New York, 1960.
3. - Robert Bruce Lindsay, "Historical Introduction" to Lord Rayleigh's Theory of Sound, Dover, New York, 1945.
4. - Struik, O. J., A Concise History of Mathematics, Dover Publications, New York, 1948.
5. - Love, A. E. H., The Mathematical Theory of Elasticity, Dover Publications, New York, 1944.

(1930) who considered wave propagation in a rod. This problem is important because it provides a vehicle for generating three-dimensional theories and provides a standard and revealing application for new advanced theories such as viscoplasticity which are now being applied in wave problems.

Even though in his publication DONNELL deals mostly with elastic materials finally he considers the case of a bilinear stress strain curve. From Newton's second law the following equation of motion can be obtained:

$$\frac{\partial \sigma}{\partial x} = \rho \frac{\partial^2 u}{\partial t^2} \tag{1.1}$$

where σ is the engineering stress, ρ the density, and u the displacement. Substituting σ with its expression as a function of ε from the bilinear stress-strain curve the equation (1.1) yields eq. (1.2) below

$$\frac{\partial^2 u}{\partial x^2} = \frac{1}{c_i^2} \frac{\partial^2 u}{\partial t^2} \tag{1.2}$$

$$i = 1, 2$$

where the two wave speeds c_1 and c_2 correspond to the two parts of the bilinear curve.

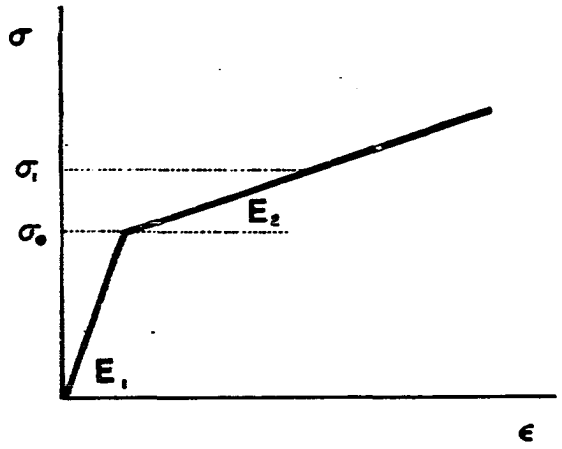

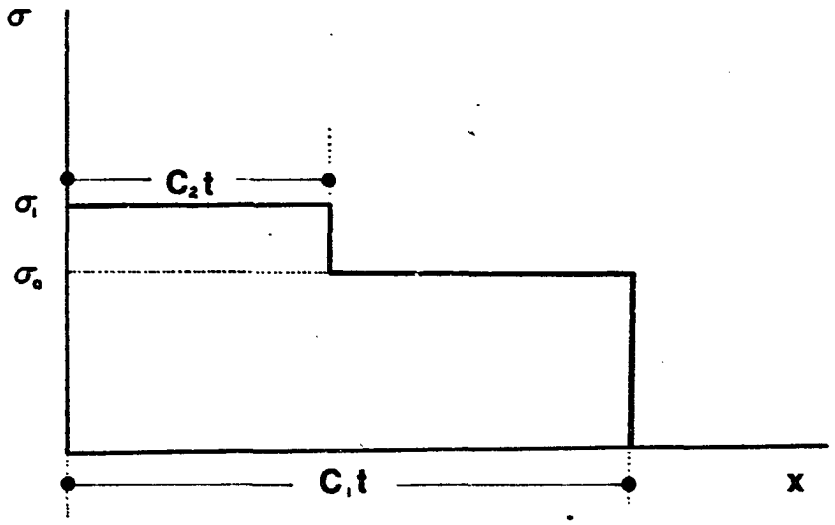

stress wave profile for bilinear stress-strain curve (after Donnell)

FIG. 1.1

$$c_1^2 = \frac{E_1}{\rho} \qquad \text{and} \qquad c_2^2 = \frac{E_2}{\rho}$$

(E_1 and E_2 are the two slopes of the bilinear stress strain curve of figure 1.1).

DONNELL's theory therefore establishes the existence of two distinct wave speeds and hence two separate wave fronts arising from the same load applied at the end of the bar. The distance between these wave fronts increases with time as the respective waves propagate within the inelastic medium. DONNELL's research also laid the ground work for formal solutions of other wave problems, including those in two and three dimensions and for more realistic stress-strain relationships.

As it will be shown in this chapter where we review the historical developments of the wave propagation problem, all these problems finally reduce to a system of partial differential equations which are hyperbolic in form. Solutions of the system show that in inelastic bodies, in general, many types of wave propagate and have different velocities. Each of these solutions may have in general both a dilatational and shear wave having many kinds of discontinuities. On this account some authors[1] call them "c o m p l e x w a v e s".

---

(1) For further details regarding the inelastic waves in

At this point, it should be emphasized that there are three major factors which determine the nature of waves propagating in a solid and their interactions:

1) The geometry of the body in which they propagate,

2) The magnitude and the distribution of the forces from which they originate, and

3) The response of the material to the applied forces as given by its constitutive equation.

It should be noticed however that the system of equations which describe the propagation of complex waves in a two or three dimensional elastic-plastic body, degenerates into several independent equations of wave propagation if the system is particularized for the elastic case or if certain components of the shear strain do not exist. Therefore "s i m p l e w a v e s" (in the sense that the phenomenon of propagation is described by a single equation of hyperbolic type producing the propagation of a single type of discontinuity) are characteristic for the elastic body or for inelastic bodies in which certain shear strains are absent.

---

solids, see Cristescu, N "European Contributions to Dynamic Loading and Plastic Waves" in Plasticity, Proceedings of the second Symposium of Naval Structural Mechamics, edited by E. H. Lee and P. S. Symonds, Pergamon Press, New York 1960, p. 386-387.

This property of inelastic bodies means that only those spatial problems (where many components of the displacement occur) which depend on only one single spatial coordinate can be conveniently examined by the method of characteristics. This is the so-called "non-linearity" effect.

For an isotropic inelastic medium easily can be seen that only three types of simple waves are possible:

1) Plane waves propagating in a rod.
(they are usually treated by means of the elementary rod theory where the assumptions of plane stress and plane strain coincide).

2) Spherically symmetric waves coming from a cylindrical cavity, and

3) Cylindrical waves under plane strain conditions coming from a cylindrical cavity.

It is of interest to notice at this point that all these simple waves can be studied, according to PERZYNA [24], by means of one single matrix equation:

$$U_t + A\ U_r + B = 0 \qquad (1.3)$$

where U is a column vector whose n elements are the n unknown functions (stresses, strains, and particle velocities) of the wave problem, A is an nxn matrix and B is an n column vector.

A and B are generally functions of one spatial coordinate, say r, and the time. U_t and U_r denote the column vectors whose elements are the time and spatial derivatives respectively of the elements of the vector U. As it will be discussed later, PERZYNA produced formal solutions of all three possible simple wave problems mentioned before.

As the previous discussion suggests, a complete historical review of the problem of the propagation of cylindrically symmetric waves in an elastic/viscoplastic medium should include all three one-dimensional wave cases. First the developments of the wave propagation in a rod are discussed. Secondly the spherical wave problem is reviewed. Thirdly the cylindrical waves are considered. This last section is divided in two parts. Firstly research done for the elastic cylindrical waves, which laid the groundwork for the present problem, is briefly reviewed, and secondly several publications dealing with inelastic cases are discussed. Finally in a fourth section experimental results are presented and techniques suitable for obtaining dynamic stress-strain curves are discussed.

2. One dimensional wave propagation in a rod

As has been mentioned in the introduction to this chapter the first work published about non-elastic waves is that by Donnell. Starting with eq. (1.1) he considered not only a bilinear stress-strain curve but also a curve gradually decreasing in slope like the one in figure 1.2 and came to the following conclusions:

1) The plastic wave train is characterized by a continuous change in its slope due to the continuous change in the slope of the stress-strain curve and

2) The back of the plastic wave train is determined by the unloading condition with a final particle velocity determined by the unloading relationship of the material.

These original observations led to a complete rate independent theory developed simultaneously by Th. von KARMAN, BOHNEMBLUST, and HYERS [26], NDRC Report No. A-103 1942, in this country and by TAYLOR [27] in England. Applications and extensions of this theory have been made by several investigators, see Ref. [28] to [30] and a substantially similar theory was developed independently in Russia [31] to [33]. The major feature of the rate independent theory is the constitutive equation expressed in the following form:

$$\frac{\partial \sigma}{\partial x} = \frac{\partial \sigma}{\partial \varepsilon} \frac{\partial \varepsilon}{\partial x} = \frac{\partial \sigma}{\partial \varepsilon} \frac{\partial^2 u}{\partial x^2}.$$

which, with the equation of momentum conservation

$$\frac{\partial^2 u}{\partial t^2} = \frac{1}{\rho} \frac{\partial \sigma}{\partial x}$$

implies a wave speed given by eq. (1.4)

$$c = \sqrt{\frac{1}{\rho} \frac{d\sigma}{d\varepsilon}} \qquad (1.4)$$

The basic features of the Karman-Taylor theory can be shown in a velocity type problem, i.e. in a problem where the boundary conditions have the following form:

1. - $$v(0,t) = \begin{cases} 0 & \text{for} \quad t < 0 \\ -V_1 & \text{for} \quad t \geq 0 \end{cases}$$

2. - All the other quantities like stresses, strains etc. are required to vanish everywhere along the bar just before the impact.

The solution to this problem, shown in figure 1.2, decomposes into four regions:

1) For $x > c_o t$ (i.e. before the travelling wave front) $t = 0$, $\sigma = 0$, $v = 0$, since the rod is assumed initially at

rest.

2) At $x = C_o t$ (i.e. exactly on the wave front) there is a discontinuity in σ and ε. The wave front is travelling at the elastic wave speed

$$C_o = \sqrt{\frac{E}{\rho}}$$

3) For $x \leq C_1 t$ a steady state has been developed where $v = -V_1$ (the given boundary condition) and $\varepsilon = \varepsilon_1$. The strain ε_1 is the one that corresponds to the given impact velocity V_1 through the equation

$$V_1 = = \int_0^{\varepsilon_1} \sqrt{\frac{1}{\rho} \cdot \frac{\partial \sigma(\varepsilon)}{\partial \varepsilon}}\, d\varepsilon$$

and C_1 is given from eq. (1.4)

$$C_1 = \sqrt{\frac{1}{\rho} \frac{\partial \sigma}{\partial \varepsilon}}$$

$\frac{\partial \sigma}{\partial \varepsilon}$ is the slope at the point $\sigma(\varepsilon_1)$

4) In the region $C_1 t < x < C_o t$ the stresses, strains, and particle velocities are increasing from the values at the

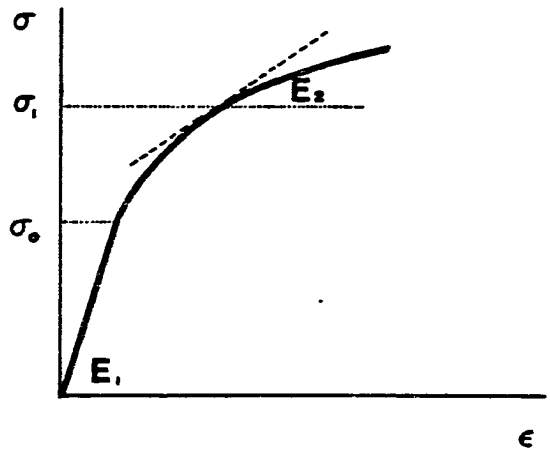

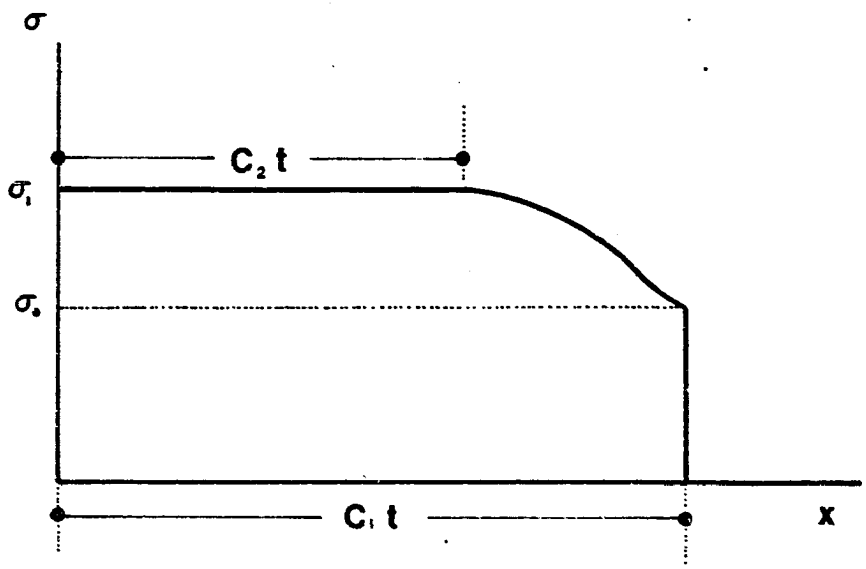

stress wave profile (after Donnell)

FIG. 1.2

wave front to the values they finally have in section 3. So far the presentation was similar to the one given by von Karman where Lagrangian coordinates have been used. Taylor on the other hand worked with Eulerian coordinates and came to the same conclusions.

Early experimental investigations dealt primarily with the propagation of longitudinal waves in wires and rods. The complete mathematical analysis associated with such waves is extremely difficult. As the previous theoretical analysis indicates, assumptions were made which were often hard to justify. Uniformity of the axial stress distribution across the thickness of the bar and neglecting the effect of the lateral inertia are the most questionable basic assumptions. Despite these limitations it will be seen that the theory did give fair agreement with experimental results.

Through a series of experiments DUWEZ and CLARK [34] and [35] in 1947 generally confirmed parts of the theoretical predictions of the rate independent theory. Specifically, though they observed a good agreement between theory and experiments in the existence and the shape of the strain plateau at the loaded end of the bar, and the correlation between strain at the impact end and impact velocity, they did not find that the distribution of strain along the specimen in the region ahead of the strain plateau was that theoretically predicted.

Further experimental work by WHITE and GRIFFIS [36] and

[37] with specimens of annealed copper showed that the mechanism of compressive impact produces five different modes of compressive behavior depending upon the impact velocity.

1) E l a s t i c I m p a c t, with low impact velocities up to 100 ips and stress proportional to impact velocity.

2) N o r m a l P l a s t i c I m p a c t, coming from the concave downward portion of the stress-strain curve. The resulting travelling wave can be considered as the superposition of a large number of small but finite increments. Due to the slope of the stress-strain curve the higher stressed wavelets move at lower velocities. Therefore the wave train lengthens with time. This occurs for velocities between that of 100 to 5000 ips.

3) N o r m a l S h o c k W a v e B e h a v i o r. This is produced from the concave upward region of the stress-strain diagram. For copper normal shock wave impact occurs in the velocity range of 5000 to 7000 ips.

4) F l o w i n g D e f o r m a t i o n. The material behavior becomes intermediate between a plastic solid and a fluid. The possible velocities are up to 125000 ips where the latter figure represents the elastic wave speed.

5) S u p e r s o n i c I m p a c t. Here the impact velocity exceeds the speed of an elastic wave and the disturbance can no longer escape from the neighborhood of the point of impact.

WHITE [38] (1949) later produced a theory based on these experimental observations, while DE JUHASZ [39] at the same time offered a graphical treatment of the impact of bars stressed above the elastic range.

Finally discussion of the question of strain-rate dependence and comparisons between experiments and the theory were given in a paper by von KARMAN and DUWEZ [40] in 1950. Conclusions given include the following:

1) Constant velocity tests showed that a strain plateau did exist, that its magnitude is a function of the velocity alone and that its magnitude agreed with that predicted by the theory.

2) Tests carried out at various impact velocities revealed fairly good agreement with theory with regard to the variation of impact stress with impact velocity.

3) The distribution of permanent strain along wires during the Duwez and Clark experiments showed a considerable deviation between theory and experiments. This deviation was attributed to inaccuracy in the values of the duration of impact and also to transient effects due to the sudden stopping of the impact.

4) Comparison of measured and calculated reflected strain distribution at the fixed end showed relatively good agreement. However, as the authors remarked, the difference between the two curves certainly indicates some influence of strain rate.

5) Unquestionable strain rate effects were observed for iron specimens subjected to both tension and compression. In this case tests showed that the plastic strain did not occur near the moving end until the magnitude of the stress reached a value of the order of three times the quasi static yield stress.

Further experimental work questioning the validity of the rate-independent theory has been presented by BELL [41] in 1951, STERNGLASS and STUART [42] in 1953, and ALTER and CURTIS [43] in 1956. From eq. (1.4) it follows that the plastic wave propagates at a velocity associated with the corresponding tangent modulus to the quasi-static stress-strain curve. To test this prediction of the Taylor theory, they subjected cold-rolled medium carbon steel specimens pre-stressed into the plastic range to incremental impact loads. In contrast to the theory they found the wave speed of the disturbance equal to the elastic wave speed.

While Sternglass and Stuart attributed this major discrepancy to the strain rate effects, Bell explained the propagation of incremental waves at the elastic wave speed by discontinuous yielding. However because of additional experimental work to be discussed in a later section of this chapter, there seems to be little disagreement to the fact that strain rate plays a role in the strain rate curves measured for the range

$$10^{-6}\ \text{sec}^{-1} \leq \dot{\varepsilon} \leq 10^{-1}\ \text{sec}^{-1}$$

where constant stress machines, hydrolic machines and screw machines are used.

A theory to account for the strain rate effects was presented by MALVERN in 1951. Malvern [44], [45] assumed that in longitudinal impact on a cylindrical or prismatic bar a relation of the form

$$\sigma = \phi\ (\varepsilon'', \dot{\varepsilon}'') \qquad (1.5)$$

exists between the values of the nominal tensile stress σ, plastic strain ε'' (= permanent change in length per unit initial length) and plastic strain rate $\dot{\varepsilon}''$ • o is in general a strictly increasing function in which case it is possible to invert eq. (1.5) and have $\dot{\varepsilon}''$ as a function of σ and ε''. This relation may be expressed as

$$E_o \dot{\varepsilon}'' = g(\sigma,\varepsilon) \tag{1.6}$$

where E_o is the Young modulus and ε the total strain.

The elastic part of the deformation was assumed to be independent of the strain rate.

$$E_o \dot{\varepsilon}' = \dot{\sigma} \tag{1.7}$$

(ε' is the elastic part of the deformation)

Therefore the relation between stress and strain has the form

$$E_o \dot{\varepsilon} = \dot{\sigma} + g(\sigma,\varepsilon) \tag{1.8}$$

The static stress-strain relation $\sigma = f(\varepsilon)$ is interpreted as a succession of equilibrium states so that viscoplastic deformation occurs when the condition given by eq. (1.9) is satisfied.

$$\sigma > f(\varepsilon) \tag{1.9}$$

The propagation problem in a rod is then governed by the system of equations given below

$$\frac{\partial \sigma}{\partial x} = \rho \frac{\partial u}{\partial t}$$

$$\frac{\partial \varepsilon}{\partial t} = \frac{\partial u}{\partial x} \tag{1.10}$$

$$E_o \frac{\partial \varepsilon}{\partial t} - \frac{\partial \sigma}{\partial t} = g(\sigma, \varepsilon)$$

According to Malvern this system of equations has in the t - x plane the following three families of straight lines as characteristics

$$1 - \quad dx = 0$$

$$2 - \quad dx - C_o dt = 0$$

$$3 - \quad dx + C_o dt = 0$$

where C_o is the elastic wave speed

$$C_o = \sqrt{\frac{E_o}{\rho}} \tag{1.11}$$

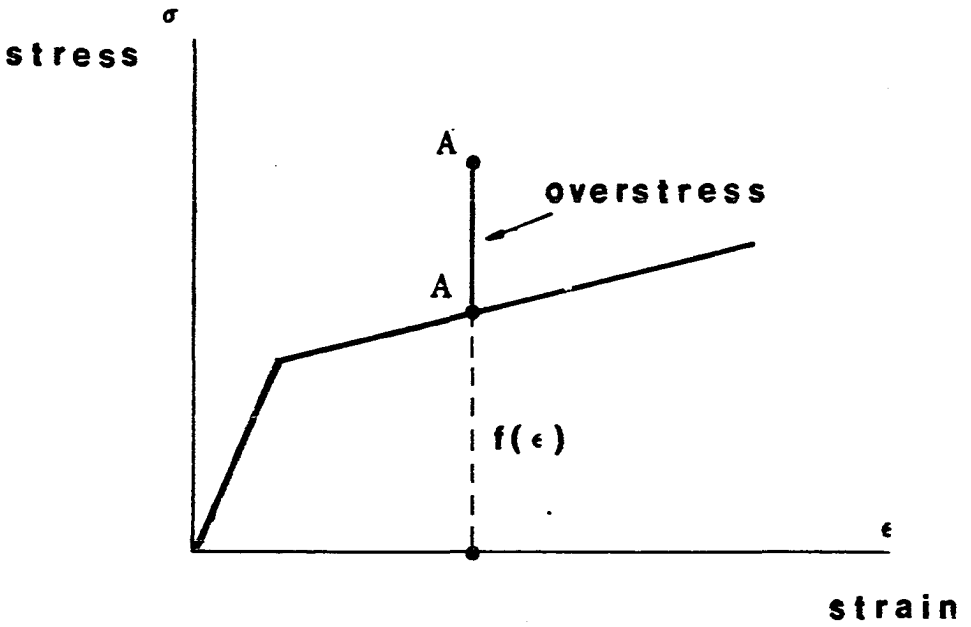

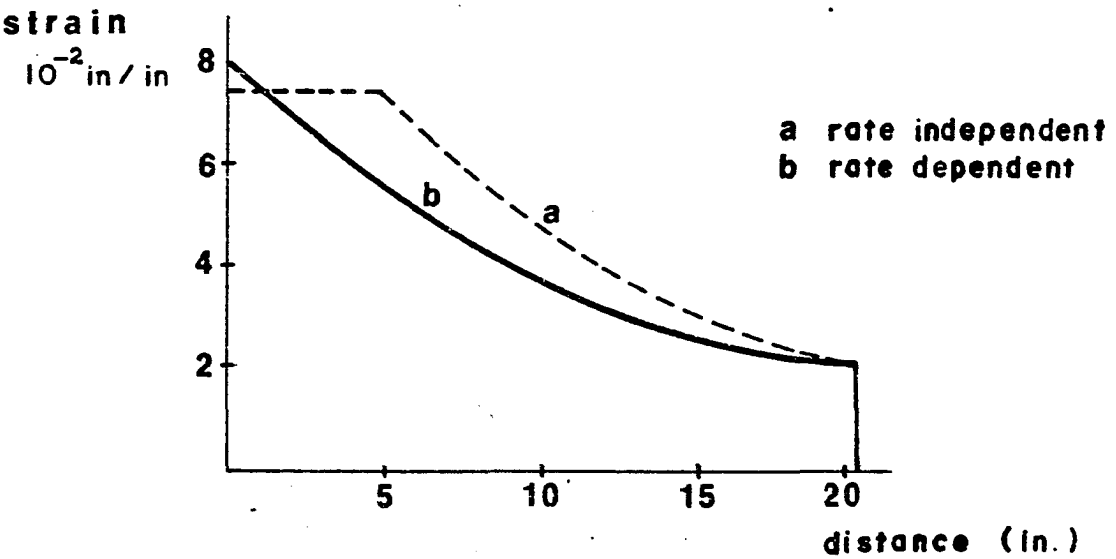

strain distribution (after Malvern)

FIG. 1.3

The remainder of Malvern's two papers are concerned with applications of the previous differential equations to several problems with different boundary conditions.

From eq. (1.11) easily can be seen that the rate dependent theory successfully explains the discrepancies observed in Karman's theory with regard to incremental impact leads travelling at the elastic wave speed. On the other hand both theories generally agree, as figure 1.3 shows, on the strain distribution along the bar with the only exception that the strain rate dependent theory does not predict according to Malvern the experimentally well established existence of a strain plateau.

In a later paper MALVERN [46] indicated that a stain plateau may be obtained with his theory. As from figure 1.4 can be seen a stain plateau is clearly visible in a bar when a constant load was applied.

PERZYNA (1966) also studied the wave propagation in a rod as a special case of eq. (1.3) and presented a formal solution to the problem without any further discussion of the parameters involved.

On the other hand, WOOD and PHILLIPS [47] (1967) working on the same problem with the strain-rate dependent theory and a Malvern type relationship between the inelastic strain rate and the overstress showed that there is a characteristic time τ_{char} which governs the time required for the strain plateau to appear.

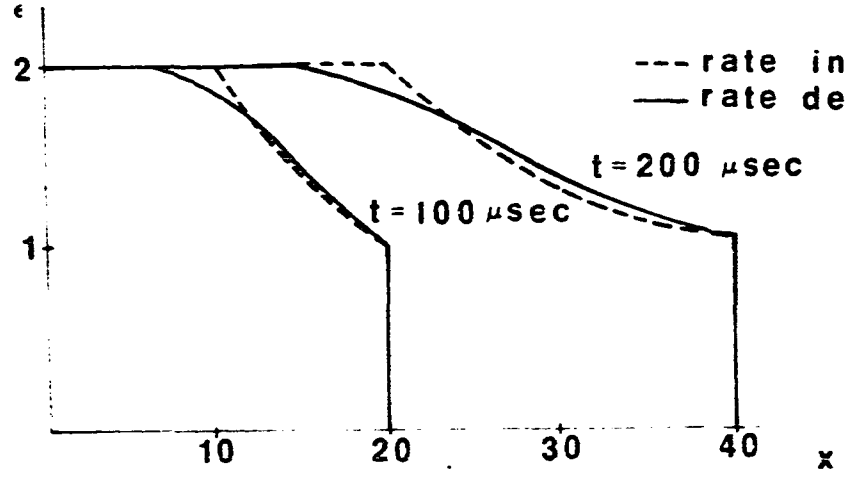

strain distribution after Malvern

FIG. 1.4

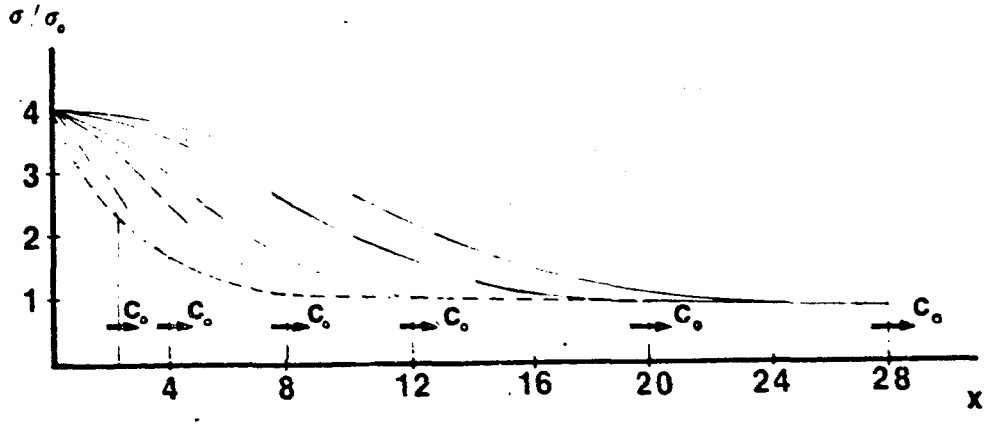

Development of the elastic/plastic wave front after Wood and Phillips

FIG. 1.5

This can be seen from eq. (1.6) written in the following way:

$$E_o \frac{\partial \varepsilon^{vp}}{\partial t} = g(\sigma,\varepsilon) = k\ [\sigma - f(\varepsilon)]$$

This equation can be written in the non-dimensional form

$$\frac{\partial \varepsilon^{vp}}{\partial \left(\frac{kt\sigma_o}{E_o}\right)} = \frac{\sigma - f(\varepsilon)}{\sigma_o} \qquad (1.12)$$

where σ_o denotes some appropriate reference stress. Eq. (1.12) introduces the characteristic time τ_{char}

$$\tau_{char} = \frac{E_o}{k\sigma_o}$$

A zero characteristic time corresponds to a value of $k \to \infty$ and this corresponds to the rate independent theory, since from eq. (1.6) $\sigma - f(\varepsilon) \to 0$. Increasing characteristic time τ_{char} requires more time for the plateau to appear. This conclusion is very important because it eliminates the strain plateau as a distinguishing feature of the rate-independent or the rate-dependent behavior and presents a connection between the two theories.

Figure 15 shows the stress distribution along a semi-infinite bar composed from a material having a bilinear quasi-static stress-strain curve at several instants of time. The results are given for an impact stress 4 times the yield stress σ_o. The figure clearly shows the elastic wave travelling ahead at constant velocity c_o and indicates the existence of a strain plateau at the end of the bar.

In a recent paper E. A. RIPPERGER and H. WATSON [48] in 1968 studied the influence of the constitutive equation on the wave propagation problem assuming several forms of the function $g(\sigma,\dot{\varepsilon})$ in eq. (1.6). The experimentations were done with a computer. For $g(\sigma,\dot{\varepsilon})$ the following forms have been investigated

$$g(\sigma,\dot{\varepsilon}) = \frac{1}{\tau}\left(\frac{\sigma - \bar{\sigma}}{\bar{\sigma}}\right)^m$$

$$g(\sigma,\dot{\varepsilon}) = k\,(\sigma - \bar{\sigma})$$

$$g(\sigma,\dot{\varepsilon}) = k\,(\sigma - \sigma_o)$$

σ_o is the yield stress and $\sigma - \bar{\sigma}$ is the dynamic overstress used by Malvern. The figure 1.6 shows the wave front profile at 40 μsec for these constitutive equations.

The analytical solution of the wave propagation in a rod problem using the rate dependent theory is given by D. NICHOLSON [49] (1971) in his doctoral dissertation.

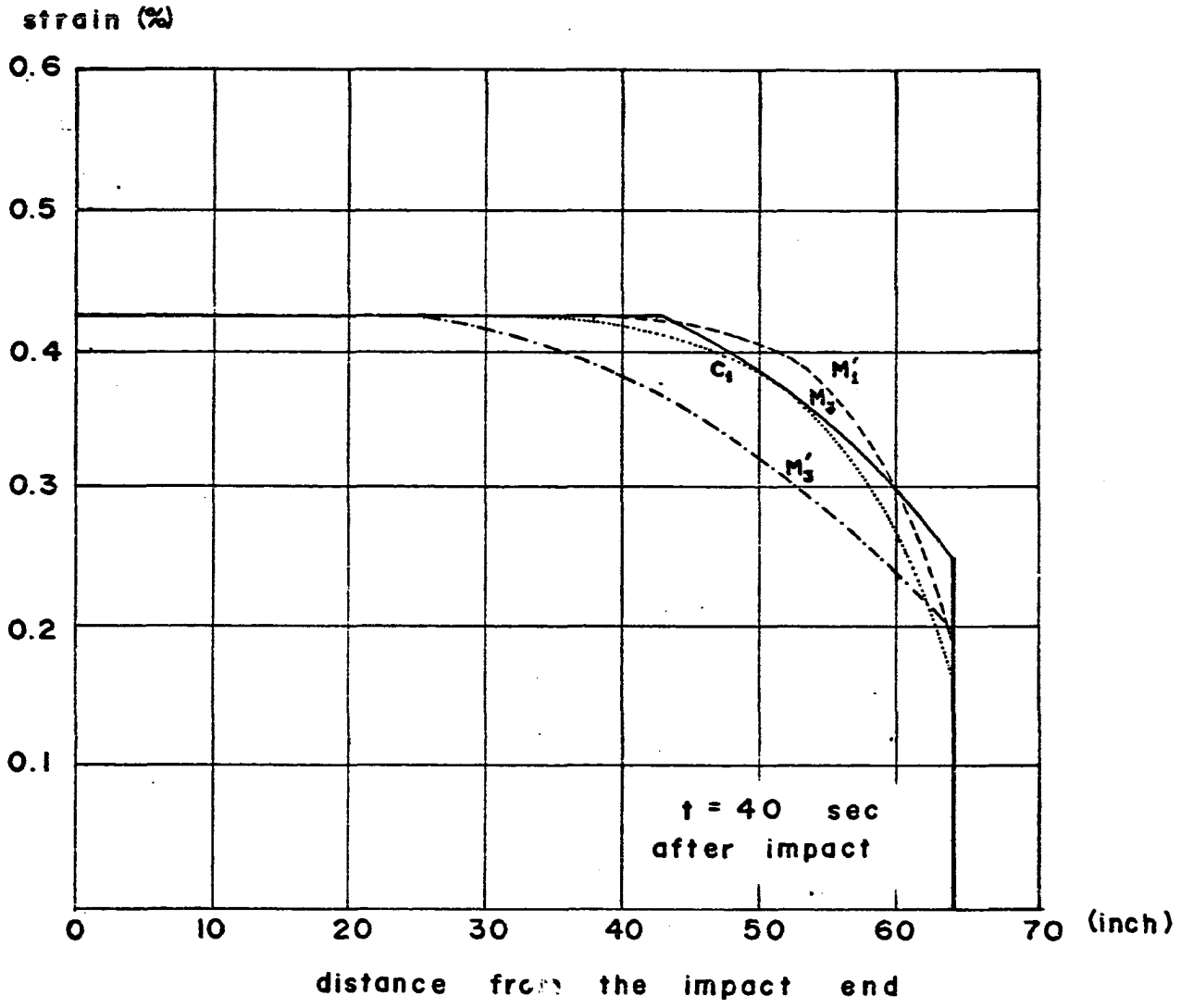

M_3 —— $\sigma = \sigma(\epsilon)$ from a dynamic stress-strain curve

C_1 ..... $g(\sigma,\varepsilon) = 1/\tau\left(\frac{\sigma-\bar{\sigma}}{\bar{s}}\right)^m$, $\tau = 8\cdot10^{-6}$ sec, $m = 1.92$

M_3' —·—·— $g(\sigma,\varepsilon) = K\cdot(\sigma-\bar{\sigma})$, $K = 1.125\cdot10^6\ sec^{-1}$

M_1' ----- $g(\sigma,\varepsilon) = K\cdot(\sigma-\bar{\sigma})$, $K = 2.25\cdot10^6\ sec^{-1}$

FIG. 1.6

Specifically, he obtained again the strain plateau as a limiting case of the exact solution for a material with a general rate-dependent constitutive equation.

3. Spherical Wave Propagation

Papers studying the propagation of viscoplastic spherical waves have been presented only relatively recently. To the knowledge of this writer, WIERZBICKI [50] (1963) was the first who applied PERZYNA's theory for multidimensional viscoplastic deformation to describe spherical wave propagation. Wierzbicki's work, however, was concentrated on a spherical container of a rigid-perfectly plastic strain-rate sensitive material undergoing impulsive loading.

In 1964 PERZYNA and BEJDA [51] considered the case of an elastic/viscoplastic work hardening strain-rate sensitive material with a constitutive equation of the type:

$$\dot{e}_{ij} = \frac{1}{2\mu}\,\dot{s}_{ij} + \gamma\,\langle\phi(F)\rangle\,\frac{\partial F}{\partial \sigma_{ij}}$$
$$\varepsilon_{ii} = \frac{1}{3k}\,\dot{\sigma}_{ii} \qquad (1.13)$$

(more details about the constitutive equations of viscoplasticity are given in Chapter II).

where the symbol $\langle\phi(F)\rangle$ is defined as follows:

$$\langle\phi(F)\rangle = \begin{cases} 0 & \text{when} \quad \phi(F) \leq 0 \\ \phi(F) & \text{when} \quad \phi(F) > 0 \end{cases} \qquad (1.14)$$

The quasi-static yield surface is defined through the function F describing the work - hardening effects

$$F(\sigma_{ij}, \varepsilon_{ij}^{p\ell}) = \frac{f(\sigma_{ij}, \varepsilon_{ij}^{p\ell})}{K} - 1 \qquad (1.15)$$

where the function $f(\sigma_{ij}, \varepsilon_{ij}^{p\ell})$ depends on the state of stress σ_{ij} and the state of the inelastic strain $\varepsilon_{ij}^{p\ell}$. On the other hand, for the work hardening parameter κ the following relation was given:

$$K = K(W_{p\ell}) = K\left(\int_0^{\varepsilon_{ij}^{p\ell}} \sigma_{ij} d\varepsilon_{ij}^{p\ell}\right) \qquad (1.16)$$

As the origin of the spherical waves they considered a radial uniform time dependent pressure p(t) applied on the surface of a spherical cavity. Due to the symmetry of the problem they remarked that only one component of displacements tensor exists. The application of eq. (1.13) led to a one-dimensional problem in which $\sigma_r - \sigma_\phi$, the so-called effective stress, is employed. Finally a formal numerical solution of the problem was presented by means of a difference equation along the characteristics.

In 1966 PERZYNA in a review article gave again the same solution by considering the spherical wave problem as a second

special case of eq. (1.3).

The influence of the strain hardening parameter, expressed in terms of E_1/E_o in figure 1.7a and the influence of the viscosity coefficient γ in eq. (1.13) have been studied by ZABINSKI [52] in his doctoral dissertation (1969). His solution was based on the previously mentioned observation that $\sigma_r - \sigma_\phi$ effectively can be used as the equivalent stress reducing the problem to a one-dimensional one. For the inelastic strain a Malvern's type overstress has been used. Figure 1.7a shows the effective stress and the overstress. For a stress history like the one shown in figure 1.7b, figures 1.7c and 1.7d show the two main features of the spherical waves in elastic/viscoplastic media, namely the unexpected considerable influence of both strain hardening ratio and viscosity coefficient on the results. These conclusions are also of interest for comparison purposes between the spherical and cylindrical waves.

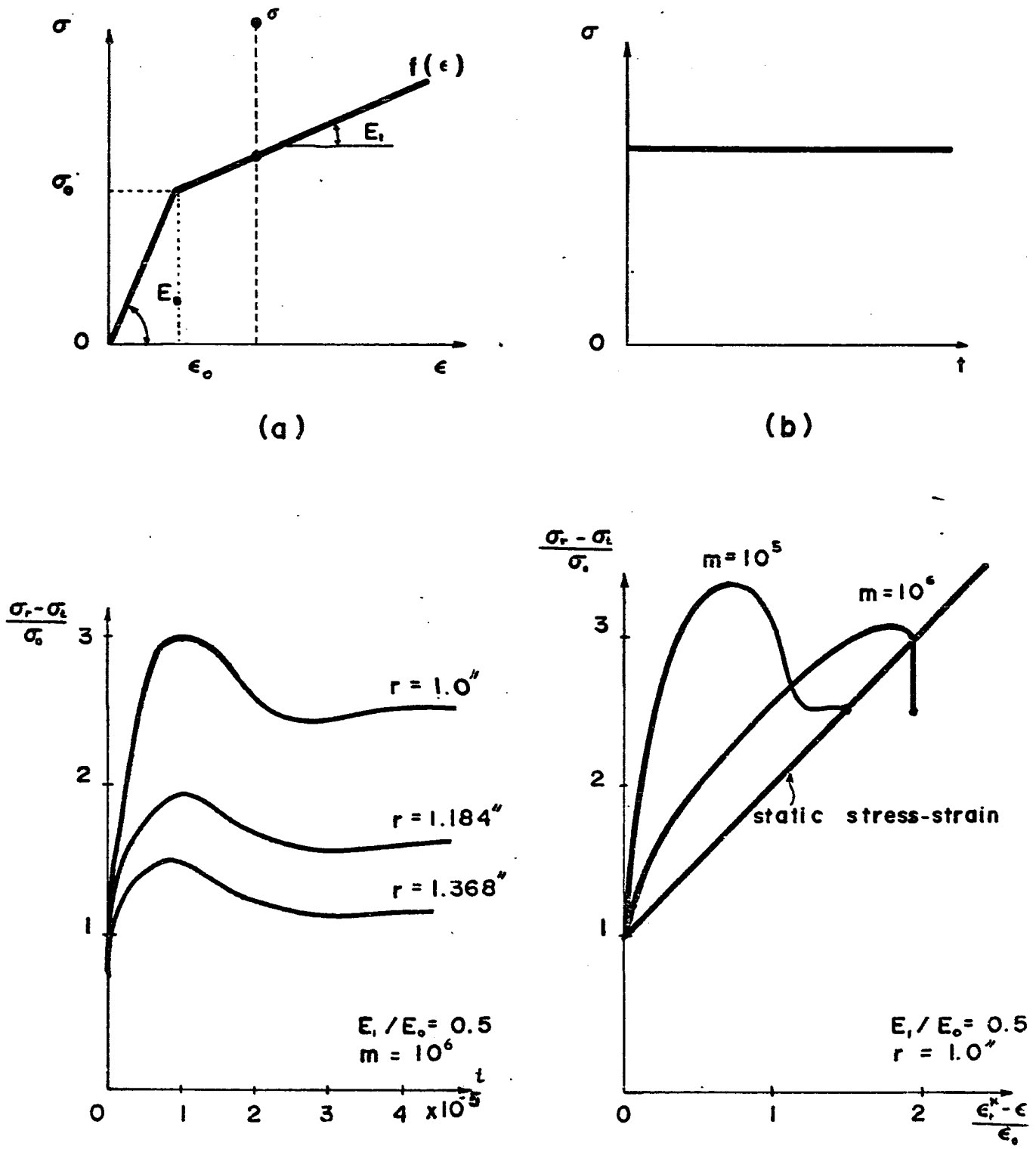

spherical waves (after Zabinski)

FIG. 1.7

4. Cylindrical waves

1. Elastic waves.

The studies of vibrations of cylindrical cavities go back to JAERISH [53], [54], CHREE [55], BASSET [56], and SEZAWA [57]. KROMM [58] however was the first who published a paper on the more restricted problem of a circular cavity subject to uniform blast loading. He used Hooke's law and studied plane-stress cylindrical waves by expressing σ_r and σ_ϕ in terms of the radial displacement only and wrote the equation of equilibrium along the r direction as an equation for the displacement $u = u(r,t)$ in the following way

$$\frac{\partial^2 u}{\partial r^2} + \frac{1}{r}\frac{\partial u}{\partial r} - \frac{u}{r^2} = \frac{1}{c^2}\frac{\partial^2 u}{\partial t^2}$$

where $c = \left(\frac{E}{(1-r^2)\rho}\right)^{1/2}$ is the elastic plate wave speed. He considered then the solution of the initial value problem

$$u = 0 \text{ and } \frac{\partial u}{\partial t} = 0 \quad \text{for } t = 0 \text{ and } r > a$$

by means of eq. (1.18) where the unknown function is the Laplace transform of $u(r,t)$

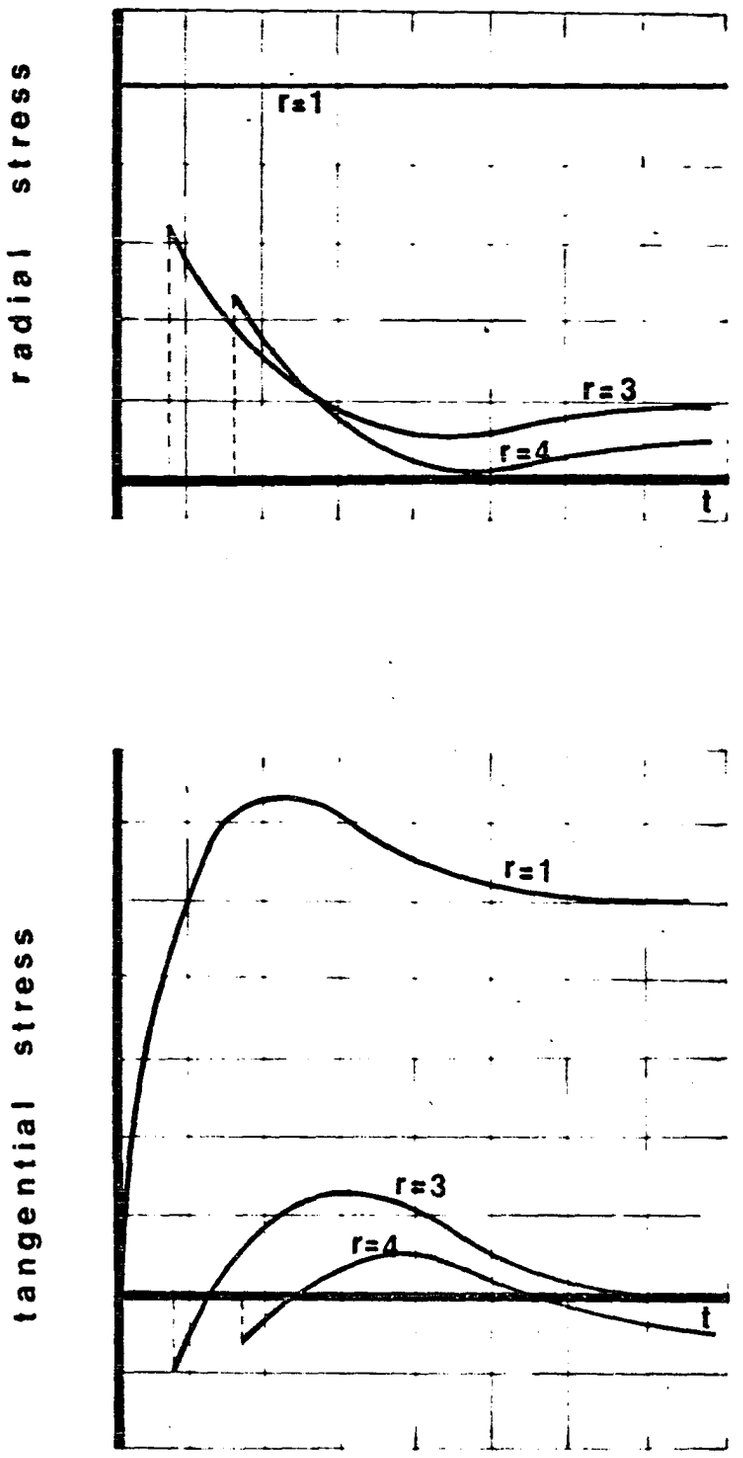

elastic cylindrical waves, after KROMM

FIG. 1.8

$$\frac{\partial^2 U}{\partial r^2} + \frac{1}{r}\frac{\partial U}{\partial r} - \left(\frac{h^2}{c^2} + \frac{1}{r^2}\right)U = 0 \qquad (1.18)$$

The solution of eq. (1.18) can be written immediately in terms of Bessel and Hankel functions:

$$U(r,p) = A(p)\, K_1\left(\frac{pr}{c}\right) + B(p)\, I_2\left(\frac{pr}{c}\right) \qquad (1.19)$$

The most important feature of this solution was his way of deriving the inverse Laplace transform of eq. (1.19) by means of a Volterra integral. Figures 1.8a through 1.8d, due to Kromm, reproduce the most important results of his solution.

H. L. SELBERG [59] in 1952 considered the same problem again by means of a Laplace transform and derived formal solutions in terms of Hankel functions. The asymptotic expression for that solution proved that for $t \to \infty$ (i.e. static equilibrium) the stresses decrease in proportion to r^{-2} with increasing radius r, while the stresses along the wave front decrease proportionally to $r^{-1/2}$.

In 1956 J. N. GOODIER and W. E. JAHSMAN [60] presented results for the two plane-stress problems of an elastic plate with a hole from which a symmetrical disturbance (shear stress or rotary velocity) is suddenly applied and maintained at the hole. Their way of solving the problem was similar to the one by Kromm. W. E. JAHSMAN [61] in a second publication considered the case of plane waves under several boundary conditions applying the method of characteristics to the

equations of motion.

An other application of Kromm's plate-stress solution was presented by J. MILKOWITZ [62] in 1960. Namely, he considered the case of stretched elastic plate in which a circular hole is suddenly punched and derived a solution by means of a Laplace transform. An application of the Fourier-transform technique to solve the exterior elasto-dynamic problem concerning the region outside a circular cavity has been given by A. C. ERINGEN [63] for the first time in 1961. There he described the boundary conditions, normal and tangential tractions acting at the surface of the cylindrical cavity as arbitrary functions of the polar angle θ , and the time t; and presented a formal solution by means of infinite Fourier series for the unknown functions.

The method of characteristics, widely used in the solution of inelastic wave propagation problems, has been used by H. J. PLASS and B. C. ELLIS [64], and PEI CHI CHOU and H. A. KOENIG [65] in two very similar papers dealing with cylindrical plane-stress elastic waves. Numerical results presented in both papers and shown in figure 1.9 are in excellent agreement with the results obtained by the analytical method (see Kromm, Selberg etc.).

The problem of the inverse Laplace transform was the subject of a recent paper by M. J. FORRESTAL [66]. There a new simpler way to derive the inverse transform of the solution given by Kromm is presented.

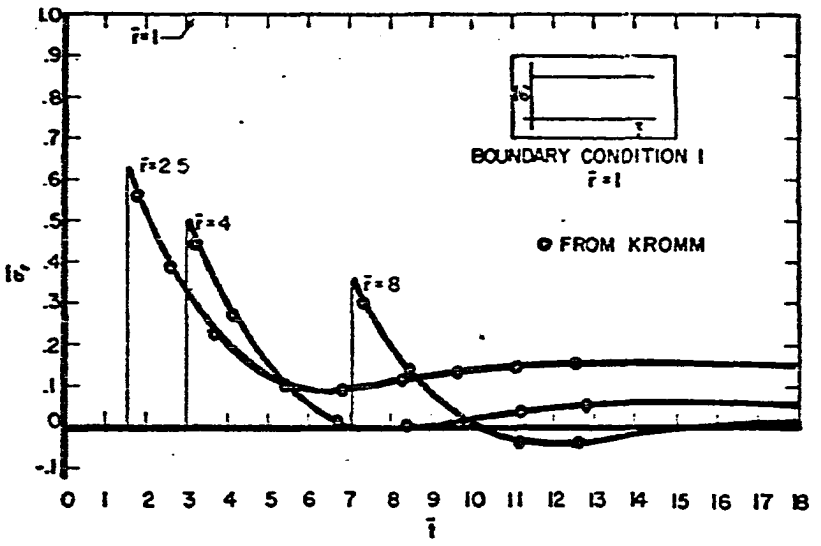

radial stress

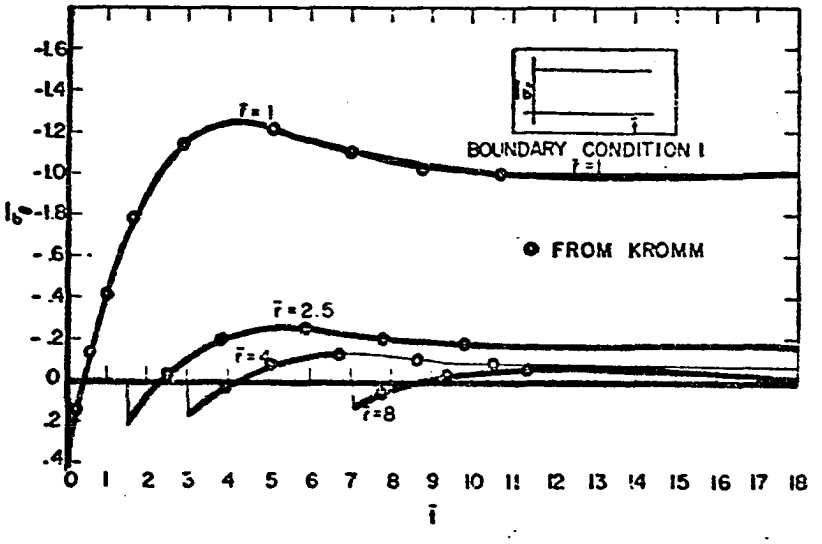

tangential stress

elastic cylindrical waves

FIG. 1.9

An elementary solution using a harmonic analysis for the cases of plane strain and plane stress elastic cylindrical waves has been presented by D. RADER [67] in 1969. The paper is divided in two parts. First the problem of the change of the pulse shape has been fully discussed in terms of a generalized phase velocity and the effects of the lateral inertia are considered by means of a modified plane stress equation which accounts for the energy of lateral motion. In the second part experimental results are presented and compared with the computed results from the first part showing a remarkably good agreement, particularly for the head of the pulse.

ii. Inelastic waves

The problem of cylindrical waves in inelastic materials has been considered only relatively recently in the literature.

In 1966, PERZYNA [24], in a review article, presented the case of cylindrical waves in an elastic/viscoplastic material as a particular case of the general one dimensional wave equation (1.3). Starting with the basic relations along the wave front he derived the general equations governing the wave propagation. However the inelastic part of the strains, given by the matrix B in eq. (1.3), was not the correct one and therefore the numerical approximation to the problem did not produce any valuable information.

The case of elastic-plastic waves has been considered

by several authors. In 1967 P. K. MEHTA [68], [69] presented solutions for the case of linearly strain hardening materials by means of an analysis of the physical laws rather than the differential equations derived from them. J. N. JOHNSON [70] on the other hand studied the decay of the elastic precursor for cylindrical, spherical and plane flow and presented results showing the influence of the magnitude of the cavity to the form of the elastic decay for a particular material (Sioux Quartzite). A general discussion of the same problem in matrix notation is given by T. C. T. TING [71]. The relations between the stresses on both sides of an elastic-plastic boundary and the restrictions on the speed of the elastic-plastic boundary are the main objectives of this publication.

H. D. McNIVEN and Y. MENGI [72] studied the propagation of cylindrical waves in a linear viscoelastic material using the method of characteristics. The basic results of this investigation are presented in figures 1.10a and 1.10b. The influence of the viscosity easily can be seen from these figures. Namely, the more viscous the material is the less steep is the decay behind the wave front and for stations apart from the cylindrical surface of the hole the smaller is the amplitude of the discontinuity at the front of the wave.

The propagation of waves in inhomogeneous elastic media with cylindrical symmetry has been considered by G. EASON [73]. A numerical solution for an elastic/viscoplastic material with

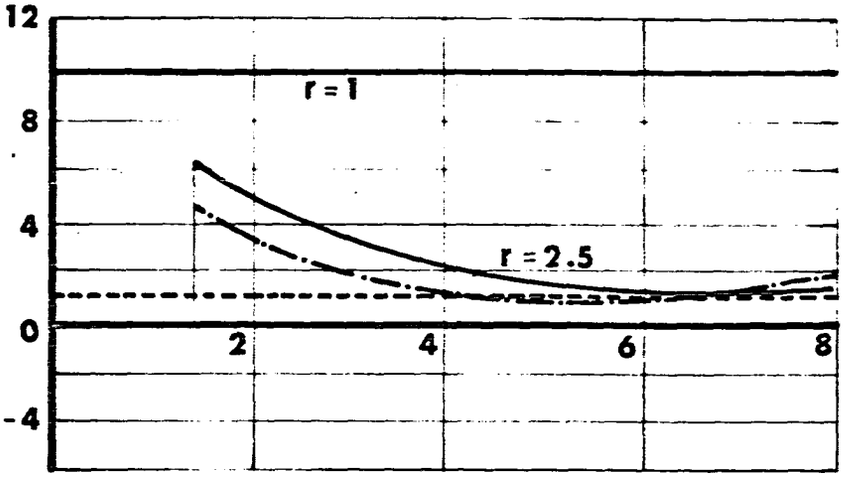

radial stress

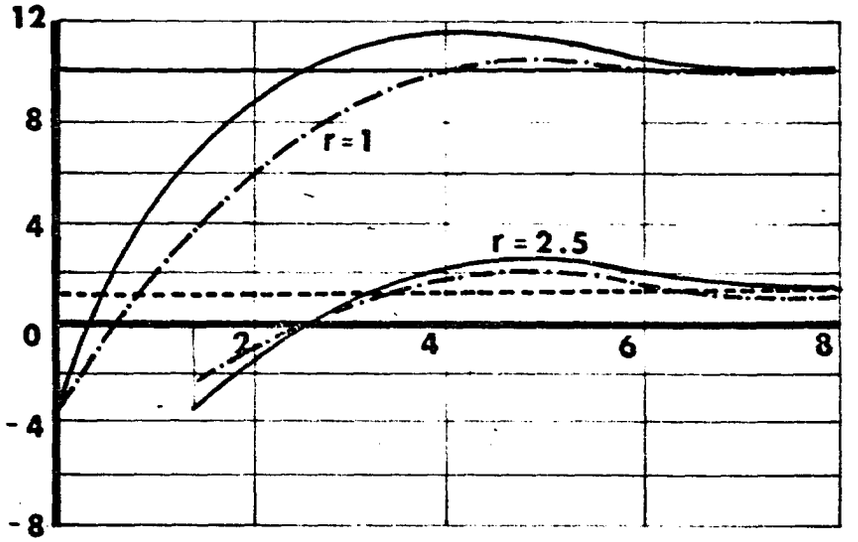

tangential stress

viscoelastic cylindrical waves, after H. McNIVEN

FIG. 1.10a, b

a Perzyna type constitutive equation and a hardening low of the type

$$K = K(\bar{\varepsilon}_p)$$

where

$$\bar{\varepsilon}_p = k\left(\int_o^t \sqrt{\frac{2}{3}\,\varepsilon^p_{ij}\,\varepsilon^p_{ij}}\,dt\right)$$

has been given by R. P. SWIFT [74]. A comparison between experimental data and the results from the numerical calculations for a particular material (1100-0 aluminum) and an evaluation of the constitutive equations in viscoplasticity through this comparison are the main purposes of this publication.

Finally, in a recent publication, S. MURAKAMI and J. BEJDA [75] considered the case of two-dimensional cylindrical waves in an elastic/viscoplastic material. The Perzyna's constitutive equation for the viscoplastic behavior has been used again, though the material was assumed non-work hardening. A numerical solution for the unknown quantities was presented in the form of a system of equations with finite differences. However the presentation of the results of actual calculations was postponed for a later paper.

5. A survey of the experimental Procedures, Problems and Results

The main objectives of this section are two in number. First a review of the procedures used to obtain dynamic stress strain curves will be given together with some typical experimental data. These results will be used later as the starting point for generalizations necessary to describe the mechanical behavior of materials under the multidimensional state of stress of the cylindrical wave propagation problem.

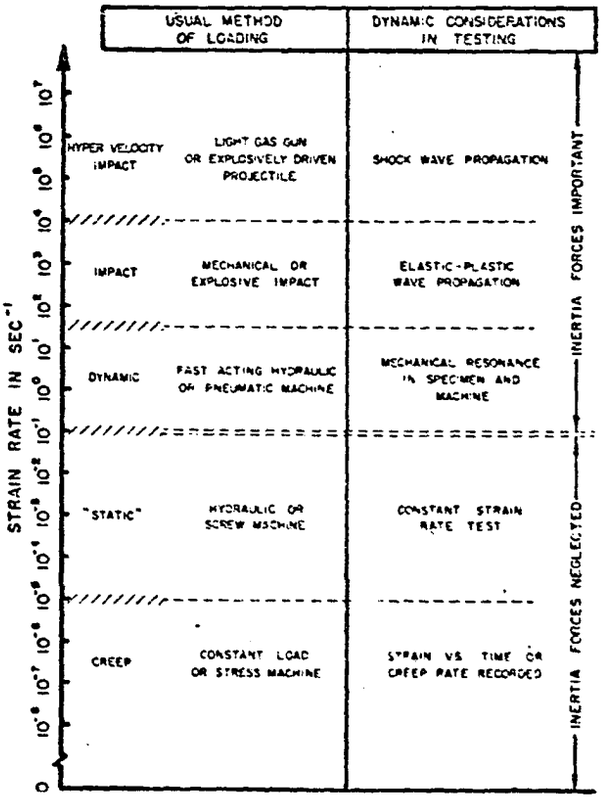

TABLE 1

Experimental methods used in investigation of the dynamic behavior of metals (after U. S. Lindholm, 1967)

Secondly papers dealing specifically with experiments with cylindrical waves will be presented and discussed.

Literature dealing with experiments of dynamic loading of metals beyond the elastic limit uses the term dynamic in the same sense as "time dependent". Obviously any tests, even the commonly called static, are actually dynamic. However the distinction between static and dynamic is made not on the basis of time dependence of the material behavior, but rather on the necessity of including inertia forces in any dynamic analysis.

The previous Table 1, due to U. S. LINDHOLM [76], shows the usual methods of obtaining data from dynamic loading and the corresponding strain-rates.

It is disputed however what procedures are valid, and it is disputed even more strongly what alternative claims regarding dynamic inelastic behavior have been verified from these experiments. Two surveys presenting the two differing positions, one due to BELL [77] and one due to LINDHOLM will be reviewed here.

Generally it seems that strain-rate plays a role in stress-strain curves measured in the strain-rate range

$$10^{-6}\ \text{sec}^{-1} < \dot{\varepsilon} < 10^{-1}\ \text{sec}^{-1}$$

In the range

$$10^{-1}\ \text{sec}^{-1} < \dot{\varepsilon} < 10\ \text{sec}^{-1}$$

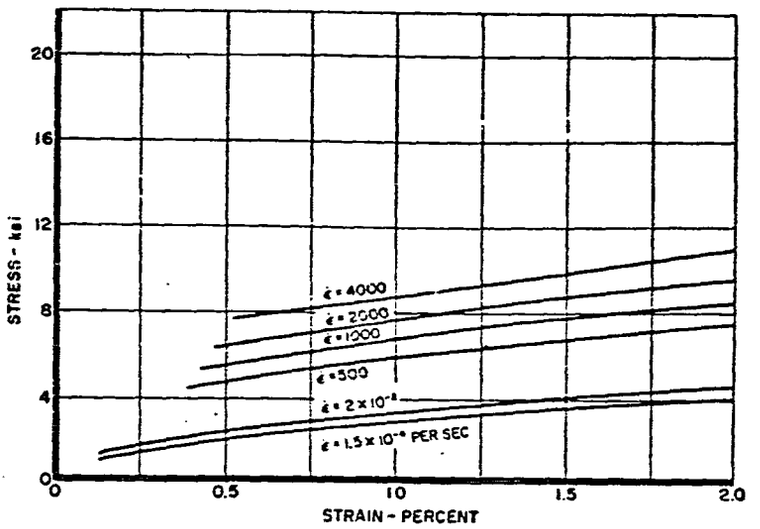

CONSTANT STRAIN-RATE CURVES FOR ANNEALED ALUMINUM

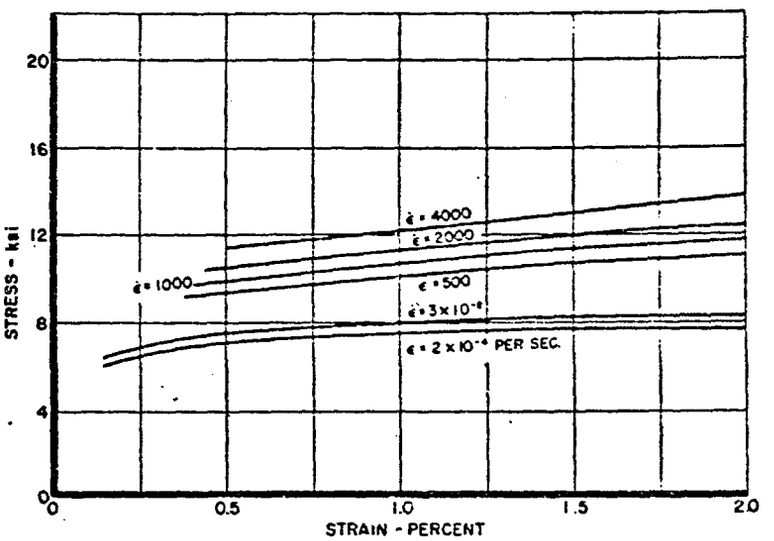

CONSTANT STRAIN-RATE CURVES FOR 10 PER CENT COLD-WORKED ALUMINUM

FIG. 1.10

increasing difficulties due to mechanical resonance appear. For higher strain rates impact tests are apparently needed. The basic question in impact testing is to find some direct method to study dynamic properties. BELL, on the one hand, claims to be able to measure by optical means particle velocities and strains in two identical specimens experiencing impact in free flight. LINDHOLM, on the other hand, employing the split Hopkinson bar technique, claims to measure constant strain-rate stress-strain curves on a thin wafer placed between two striker bars that remained elastic during impact. Other experimental procedures also have been used. For a survey of such procedures see HAUSER [78].

There remains the question of which approach is to be preferred. For the present dissertation however it is enough to observe the general form of the experimental constant strain-rate curves presented in the figure 1.10 for two common metals. Many others are available in articles named in the References

Experiments with cylindrical waves producing only radial displacements must, according to R. R. ENSMINGER and I. M. FYFE [79], be designed to accomplish the following three basic objectives:

1. To provide a rapid loading pulse on the inner surface of the cylindrical specimen, with the requirement that the pulse be uniform along the axis of the cylinder and symmetric about the axis.

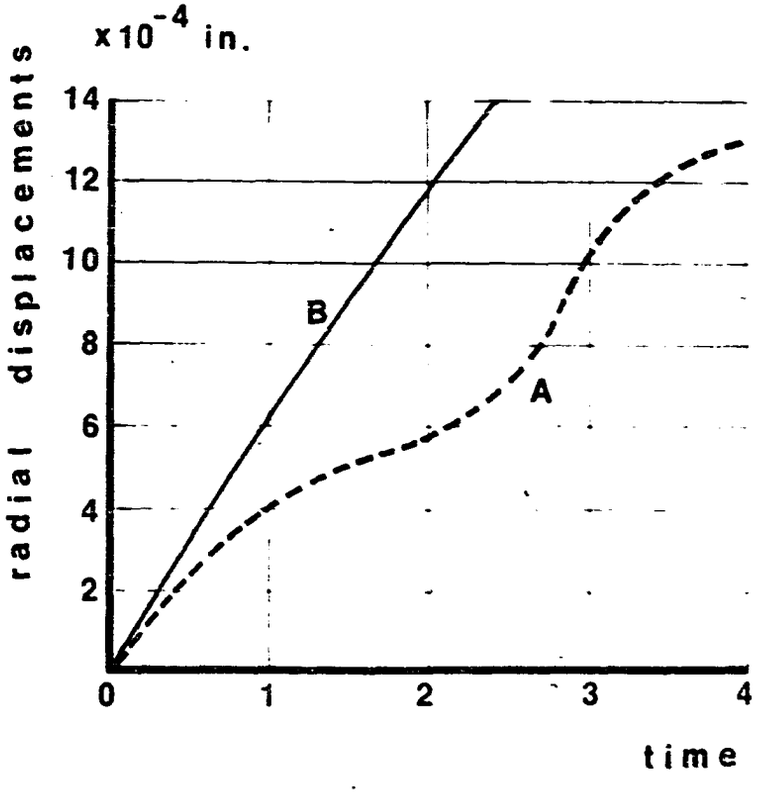

computed (A) and measured (B) radial dispacements (after I.M.FYFE)

FIG. I.II.

2. To measure the pressure-time history of the applied pulse on the inner surface of the specimen. This measurement is necessary as a time dependent boundary condition to determine uniquely a theoretical prediction of the response.

3. To measure the response of the specimen to the aforementioned loading. This is a direct measurement of the free surface displacement of the specimen.

Due to the finite thickness of the specimen the period of observation is limited to a short finite time controlled by the length-to-thickness ratio of the cylinder. The response is measured at the free surface with an optical surface motion defection system (see R. R. ENSMINGER and I. M. FYFE, I. M. FYFE [80], and R. P. SWIFT [81]) or by a condenser microphone of the type devised by DAVIES [82] (see D. RADER).

Usually experimental investigations of this type are associated with an analytical evaluation of the measured data. By measuring the pressure-time history of the loading pulse at the inner surface of the specimen, sufficient information is obtained to calculate the unique response of the material once a constitutive model is chosen. A comparison of the measured displacement-time history at the outer surface of the cylinder with the calculated response permits a judgment about the validity of the particular constitutive equation under consideration. Since the mathematics which model the physical situation in cylindrical waves are more nearly exact than other stress wave propagation experiments, a better

judgment as to the quality of the constitutive equation describing the behavior of the material is possible.

However, as Chapter IV of this dissertation will show, because

1. The combined effect of all parameters used in the constitutive equation can provide only minor changes in the solution of the problem, and
2. It is very questionable if the actually applied dynamic load on the surface of the cavity is the one used for the analytical calculations

it is very unlikely that any valuable information can be obtained through those experiments. In addition, the number of experiments necessary to define the constants of a general theoretically derived functional constitutive equation is beyond present capabilities.

The following figures show some experimental results and the corresponding values after analytical calculations with several different models. The results in figure 1.11 are given by I. M. FYFE [80] and the ones in figure 1.12 are given by R. P. SWIFT [75].

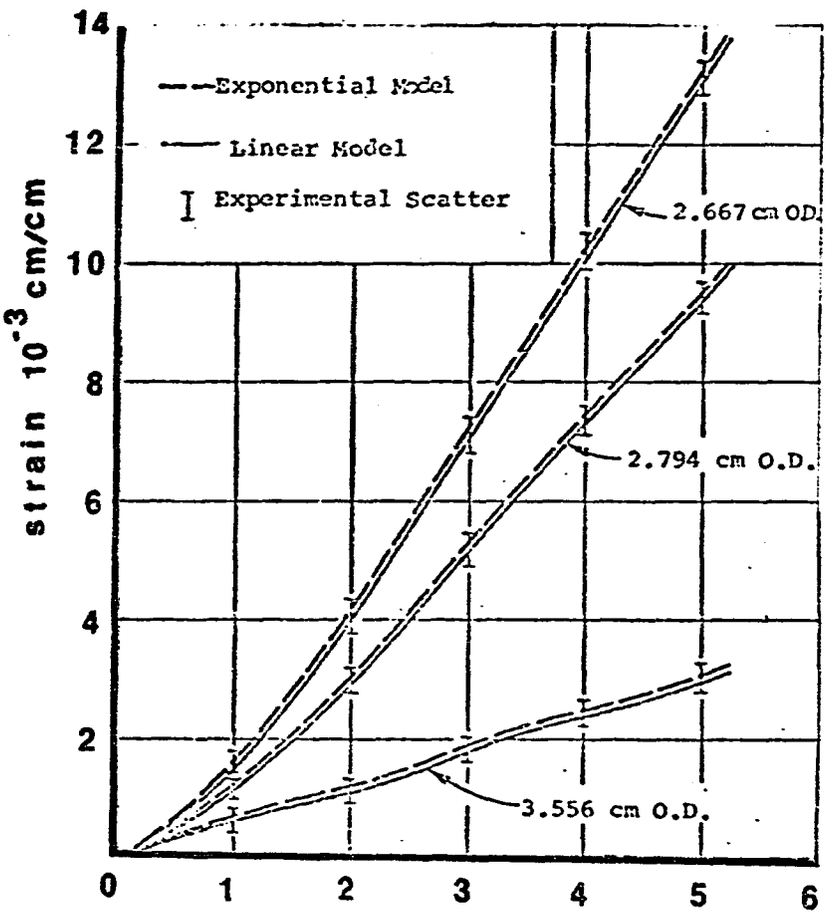

experimental – theoretical free surface responce, after R. SWIFT

FIG. 1.12

C H A P T E R II

CONSTITUTIVE EQUATIONS IN VISCOPLASTICITY

1. Introduction

The question whether the dynamic loading of a material produces effects different from its response to a static load has been an important problem for long time in the theory of plasticity. In a previous section (section 5, Chapter I) where the experimental results have been reviewed it was observed that many materials exhibit rate and time scale effects during yielding. The theory of viscoplasticity, to be presented in the present chapter, provides a beginning to the understanding and a tool to the analysis of such effects.

Many authors have proposed various constitutive equations in order to describe these mechanical properties. The constitutive equations in viscoplasticity to be discussed in this chapter represent a summary of these efforts.

All have started from the assumption, well supported by experimental evidence that, when the stress increases continuously, there exists no one-to-one correspondence between stress and strain. One of the earliest attempts to incor-

porate strain-rate effects into the wave propagation problem was developed by MALVERN [44] through the equation

$$E_o \dot{\varepsilon} = \dot{\sigma} + g(\sigma,\varepsilon) \tag{2.1}$$

where ε and $\dot{\varepsilon}$ denote the total strain and the total strain-rate respectively, σ denotes the stress and E_o tye Young's modulus.

Equation (2.1) implies that the total strain-rate is composed by two parts, the elastic $\dot{\varepsilon}^e$ given by eq. (2.2a)

$$\dot{\varepsilon}^e = \frac{\dot{\sigma}}{E_o} \tag{2.2a}$$

and the inelastic part $\dot{\varepsilon}^{in}$ given by eq. (2.2b).

$$\dot{\varepsilon}^{in} = \frac{g(\sigma,\varepsilon)}{E_o} \tag{2.2b}$$

If the function $g(\sigma,\varepsilon)$ takes the special form $g(\sigma - f(\varepsilon))$, where σ is the actual stress and $f(\varepsilon)$ is the stress at the same strain ε in a quasi-static test, then eq. (2.1) becomes

$$E_o\dot{\varepsilon} = \dot{\sigma} + g(\sigma - f(\varepsilon)) \tag{2.1a}$$

This formulation implies that the material is brought to a state of incipient plastic flow after a given amount of elastic strain, independent of the elastic strain rate, but that the

plastic flow requires time in which to become appreciable so that the additional strain beyond the quasi-static yield strain is at first mainly elastic. Therefore, even when the applied load is well above the yield limit, the elastic law applies beyond the ordinary yield strain along the wave front, since time is required for plastic flow to occur.

Equation (2.1a) also suggests that the inelastic strain rate is a function of $\sigma - f(\varepsilon)$, the so-called overstress, i.e. the excess of the instantaneous stress over the stress at the same strain in a quasi-static test. The flow law (2.1) applies only when the condition

$$\sigma > f(\varepsilon) \tag{2.3}$$

is satisfied; otherwise the elastic law applies. The use of this eq. as a loading-unloading criterion implies that the amount of strengthening obtained is independent of the strain-rate history. This is, as Malvern [44] pointed out, probably not strictly true.

The particular function g selected by Malvern to express the inelastic strain rate as a function of the overstress was the linear relation given by the following equation

$$g(\sigma - f(\varepsilon) = k\ [\sigma - f(\varepsilon)] \tag{2.4}$$

The equation (2.2) can be written therefore in the form of eq. (2.5)

$$E\dot{\varepsilon} = \dot{\sigma} + k \cdot [\sigma - f(\varepsilon)] \qquad (2.5)$$

Malvern's theory is a well formulated and effective theory of one-dimensional viscoplasticity. Applied in the wave propagation in a rod problem it eliminates the disagreements between the rate independent theory of von Karman and the experimental results that incremental impact loads travel at the elastic wave velocity. It provides also, as Wood and Phillips showed, enough theoretical background for the understanding of the existence of a strain plateau in the vicinity of the impact.

The flow condition (2.3) is however too simple to describe more complicated loading/unloading conditions for the elastic/viscoplastic materials. The applied loads also generally produce multiaxial states of stress. Finally the function g must have more complicated forms than the simple linear case studied before in order to reproduce with enough accuracy the actual mechanical behavior of the materials. These remarks provide the starting point for the generalizations of eq. (2.2) to be presented in the following sections of this chapter.

2. The theory of HONENEMSER-PRAGER

The attempts to represent elastic/viscoplastic behavior under a multidimensional state of stress go back to HENCKY [84] in 1924.(1) The general stress-strain-rate relations however that provide the starting point for the theory of viscoplasticity, given by eq. (2.6), are due to HOHENEMSER-PRAGER [85], ILYUSHIN [86], and OLDROYD [87].

$$\dot{e}_{ij} = \frac{\dot{s}_{ij}}{2\mu} + \eta\,(s_{ij} - k_{ij}) \qquad \text{if } s_{ij} > k_{ij} \qquad (2.6)$$

and

$$\dot{e}_{ij} = \frac{\dot{s}_{ij}}{2\mu} \qquad \text{if } s_{ij} \leq k_{ij} \qquad (2.6b)$$

where

$\dot{e}_{ij}$ is the deviatoric stress rate, $\dot{e}_{ij} = \dot{\varepsilon}_{ij} - \delta_{ij}\,\dot{\varepsilon}_{kk}$

$\dot{s}_{ij}$ is the deviatoric stress rate $\dot{s}_{ij} = \dot{\sigma}_{ij} - \delta_{ij}\,\dot{\sigma}_{kk}$

μ is the elastic shear modulus

η is the viscosity coefficient

k_{ij} the yield stress.

---

(1) For further details see "Handbuch der Physik", Band VI, "Elastizität und Plastizität" page 288.

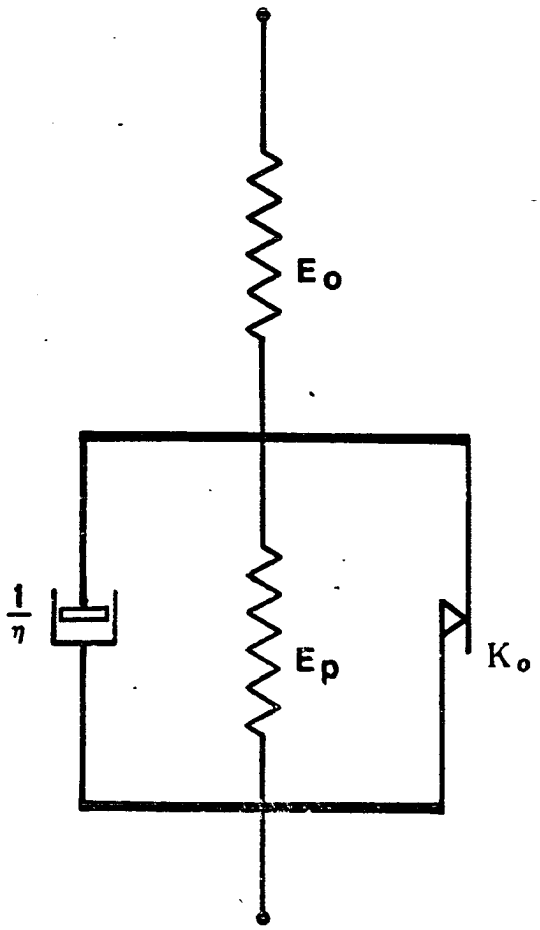

Model of an elastic/viscoplastic material

FIG. 2.1

Viscoplasticity therefore can be viewed, according to H-P, as generalizing the model of Figure 2.1. This model, due to BINGHAM [88], represents in a very simple manner the presence of viscous effects beyond initial yield. It contains a spring (Hooke's solid) for the elastic part, a dashpot (Newtonian fluid) for the viscous effects, and a solid friction element (St. Venant-Prandtl body) for the yield condition. Equation (2.6) has been rederived later by Oldroyd [87] through the assumption that we can write

$$\text{(a)} \qquad s_{ij} = k_{ij} + 2\eta\, \dot{e}^{in}_{ij}$$

In addition, Oldroyd has assumed that the proportionality

$$\text{(b)} \qquad s_{ij} = A\, k_{ij}$$

holds, A being a proportional factor. Moreover, the Mises yield condition

$$\text{(c)} \qquad \frac{1}{2}\, k_{ij}\, k_{ij} = k_o^2$$

has been assumed. Introducing II_s as the second invariant of the deviatoric stress tensor, equation (2.7) follows easily from equations (2.6), (b) and (c)

$$\dot{e}_{ij} = \frac{\dot{s}_{ij}}{2\mu} + \eta \left(1 - \frac{k_o}{\sqrt{II_s}}\right) s_{ij} \qquad \text{if} \quad II_s > k^2 \qquad (2.7)$$

and

$$\dot{e}_{ij} = \frac{\dot{s}_{ij}}{2\mu} \qquad \text{otherwise.}$$

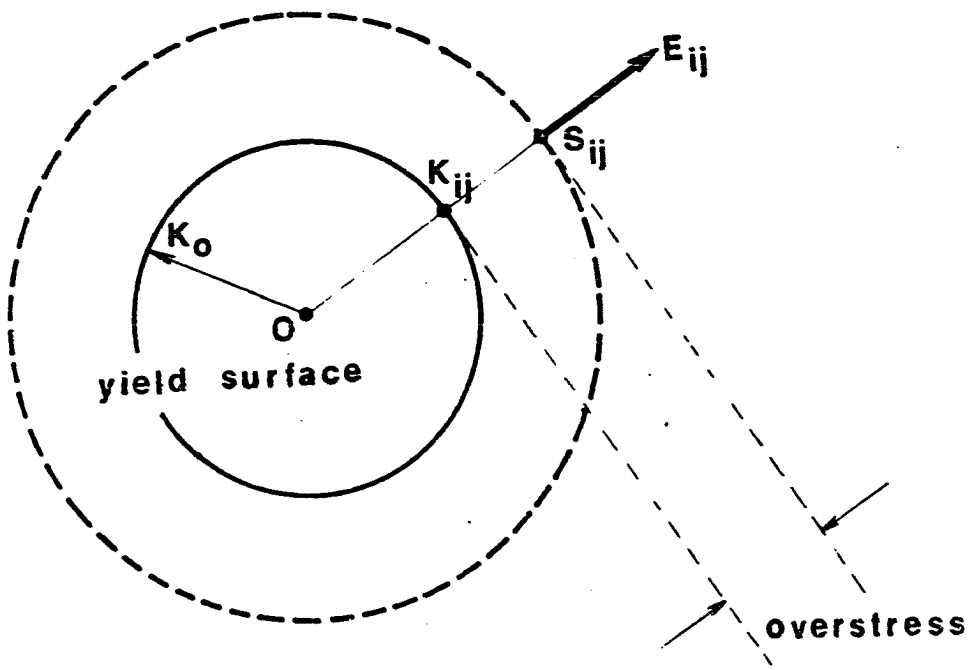

Geometrical presentation of the H – P theory

FIG. 2.2

The geometric interpretation of these ideas and results is given in Figure 2.2.

It is of interest at this point to summarize the assumptions that lead to the Hohenemser-Prager constitutive equations.

a. Kinematic Decomposition

The strain rate decomposes into an elastic and an inelastic component

$$\dot{e}_{ij} = \dot{e}^{e}_{ij} + \dot{e}^{in}_{ij} \tag{2.8}$$

where

$$\dot{e}^{e}_{ij} = \frac{\dot{s}_{ij}}{2\mu}$$

and

$$\dot{e}^{in}_{ij} = \eta \left(1 - \frac{k_o}{\sqrt{II_s}}\right) s_{ij} \quad \text{only if} \quad \sqrt{II_s} > k_o$$

b. Inelastic Incompressibility

$$\dot{\varepsilon}^{in}_{ij} = \dot{e}^{in}_{ij} \tag{2.9}$$

c. Yield Condition

The von Mises yield condition for an isotropic non work hardening material has been assumed

$$\frac{1}{2} k_{ij} k_{ij} = k_o^2 \qquad (2.10)$$

d. Loading-Unloading Criterion

Inelastic deformation will occur when the magnitude of the second invariant of the deviatoric stress tensor exceeds some critical value which is a material property

$$\frac{1}{2} \dot{e}^{in}_{ij} \dot{e}^{in}_{ij} \neq 0 \qquad \text{if} \qquad \frac{1}{2} s_{ij} s_{ij} > k_o^2$$

$$\frac{1}{2} \dot{e}^{in}_{ij} \dot{e}^{in}_{ij} = 0 \qquad \text{if} \qquad \frac{1}{2} s_{ij} s_{ij} \leq k_o^2$$

We observe finally that equations (a) and (b) lead to the co-axiality of the tensors s_{ij}, k_{ij}, and $\dot{e}^{in}_{ij}$. Further because of the von Mises yield condition $\dot{e}^{in}_{ij}$ becomes perpendicular to the yield surface at the point k_{ij}.

3. PERZYNA's generalization of the HOHENEMSER-PRAGER theory

The previously discussed Hohenemser-Prager theory is a very restricted one since it assumes the existence of a yield surface expressed in terms of the von Mises equation and ignores the influence of the inelastic deformation on the yield surface. PERZYNA's generalization, to be presented in this section, goes beyond these limitations and includes the work hardening effects, allows the yield surface to be more general than the von Mises and describes the viscoplastic behavior of solids in a better way since it includes more parameters to be chosen in order to fit with known experimental data.

For a better understanding of the generalizations introduced by the new theory, this section is divided into two parts. First the H-P theory will be reconsidered from a more general point of view, and second a summary of the PERZYNA's theory will be presented in a way that will lead to the constitutive equations to be used in the present dissertation.

The introduction of the symbol $< \Phi >$ defined through eq. (2.11)

$$< \Phi > = \begin{cases} \Phi & \text{if } \Phi > 0 \\ 0 & \text{otherwise} \end{cases}$$

and the two functions F and Φ given through eqs. (2.12) and (2.13)

$$F(s_{ij}) = (\tfrac{1}{2}\, s_{ij}\, s_{ij})^{1/2} \qquad (2.12)$$

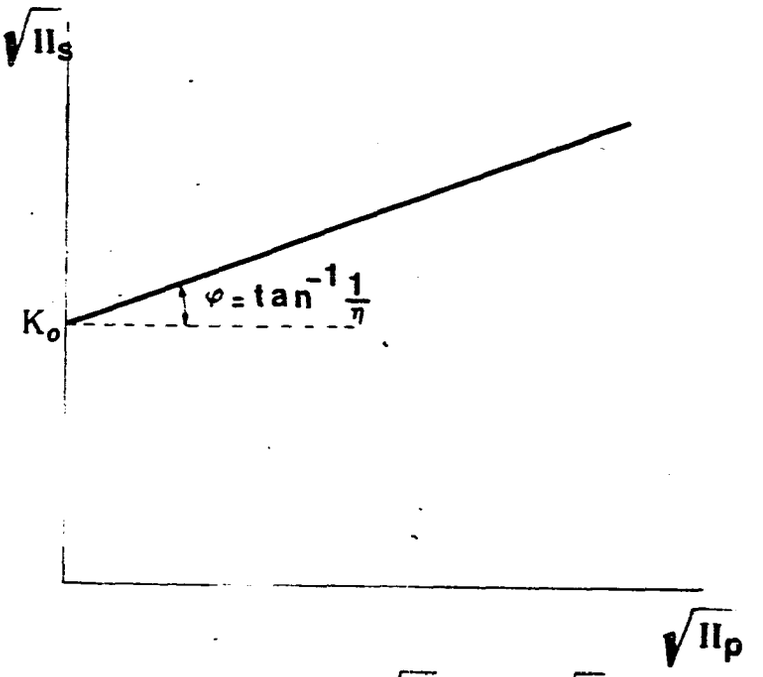

Relationship between $\sqrt{II_s}$ and $\sqrt{II_p}$ according to the H − P theory

FIG. 2.3

$$\Phi\ (s) = x \tag{2.13}$$

allow us to rewrite eq. (2.7) in the following form

$$\dot{e}_{ij} = \frac{\dot{s}_{ij}}{2} + \eta < \Phi\ (F\ (s_{ij}) - k_o)> \frac{\partial F}{\partial s_{ij}} \tag{2.14}$$

Using the second part on the right hand side of eq. (2.14) and the definition of the second invariant of the deviatoric viscoplastic strain-rate tensor

$$II_p = \frac{1}{2}\ \dot{e}_{ij}^{vp}\ \ \dot{e}_{ij}^{vp} \tag{2.15}$$

the following relation can be obtained

$$\sqrt{II}_p = \eta < \Phi\ (F\ (s_{ij}) - k_o)> \sqrt{\frac{1}{2}\ \frac{\partial F}{\partial s_{ij}}\frac{\partial F}{\partial s_{ij}}} \tag{2.16}$$

Equation (2.16) can be solved in terms of Φ^{-1}, the inverse function of Φ, for $F(s_{ij})$

$$F(s_{ij}) = k_o + \Phi^{-1}\left\{ - \frac{\sqrt{II}_p}{\sqrt{\frac{1}{2}\ \frac{\partial F}{\partial s_{ij}}\frac{\partial F}{\partial s_{ij}}}}\right\} \tag{2.17}$$

From the definition of $F(s_{ij})$ eq. (2.17) can be written in the following form

$$\sqrt{II}_s = k_o + \frac{1}{\eta}\ \sqrt{II}_p \tag{2.18}$$

The geometrical interpretation of this last equation is that during inelastic deformation the actual state of stress is located on a surface, the so-called "dynamic yield surface", given by eq. (2.17), enveloping the static yield surface. Eq. (2.18), derived from the assumption that the material obeys the von Mises yield condition, indicates that the distance between the exterior surface and the static yield surface, represented here as the difference between their radii, is a monotonically increasing function of the second invariant of the deviatoric strain-rate-tensor.

PERZYNA's theory on the other hand introduces the strain-rate through eq. (2.19)

$$\dot{e}_{ij} = \frac{\dot{s}_{ij}}{2\mu} + \eta < \Phi (F)> \frac{\partial F}{\partial \sigma_{ij}} \qquad (2.19)$$

First it should be noticed that the choice of

$$\Phi (F) = 1 - \frac{k_o}{F} \qquad (2.20)$$

with the relation $\frac{\partial II_s}{\partial \sigma_{pq}} = s_{pq}$ shows that the Hohenemser-Prager theory is a special case of PERZYNA's theory. Second the introduction of the two functions F and Φ will provide the starting point for a more general concept of elastic/viscoplastic behavior.

For instance F may have the general form

$$F = \frac{f(II_s,\ III_s)}{c} - 1 \qquad (2.21)$$

where III_s is the third invariant of the deviatoric stress tensor.

Also the function Φ may have any one of the following forms introduced by PERZYNA [89], [90].

$$\begin{aligned} \Phi\ (F) &= F^{\delta} \\ \Phi\ (F) &= F \\ \Phi\ (F) &= \exp F - 1 \end{aligned} \qquad (2.22)$$

Or any linear combination of them as in eq. (2.23)

$$\begin{aligned} \Phi\ (F) &= \sum_{\alpha=1}^{N} A_{\alpha}(\exp F^{\alpha} - 1) \\ \Phi\ (F) &= \sum_{\alpha=1}^{N} B_{\alpha}\ F^{\alpha} \end{aligned} \qquad (2.23)$$

A further generalization of eq. (2.14) has been introduced by Perzyna in order to describe the work hardening effects. This is done by rewriting the equation for the quasi-static yield surface in the following form.

$$F = F\ (s_{ij}\ ,\ e_{ij}^{vp})$$

As it is done in equation (2.21), F is assumed to be equal to the expression given by eq. (2.24)

$$F = \frac{f(s_{ij},\ e^{vp}_{ij})}{K} - 1 \qquad (2.24)$$

and the points of the quasi-static yield surface satisfy the equation

$$f(s_{ij},\ e^{vp}_{ij}) = K$$

For the work hardening parameter K the following expression holds:

$$K\ (W^{vp}) = K\left(\int_{o}^{\varepsilon^{vp}_{ij}} \sigma_{ij}\, d\varepsilon_{ij}\right) \qquad (2.25)$$

or more precisely

$$\dot{K} = k_{ij}\ (s_{pq},\ e^{vp}_{pq},\ K)\ \ \dot{e}^{vp}_{ij} \qquad (2.26)$$

It should be emphasized however at this point that the approach followed in this section is slightly different than the one presented by PERZYNA. This is done by assuming the quasi-static yield surface as a function of the deviatoric stress tensor instead of the stress tensor. This is an assumption closer to the experimental result that hydrostatic pressure does not affect the yielding point.

The quasi-static yield surface introduced through eq. (2.24) is not restricted to the von Mises yield condition. The function F may be of any form. The point k_{ij} satisfying the equation (2.24) belongs to the quasi-static yield surface and is the intersection point of the actual deviatoric

stress vector with the present quasi-static yield surface. In order to introduce a meaningful concept through that definition it is necessary that the quasi-static yield surface for any magnitude of the plastic strain always includes the origin of the coordinate system in the deviatoric stress space. Also this reference surface must remain regular and convex.

There is also another difference between the inelastic components of the deviatoric strain rate given by eq. (2.12) for the Hohenemser-Prager theory and the corresponding eq. (2.19) in Perzyna's generalization. At this point the usual assumption has been made that the deviatoric stress space and the deviatoric strain space are superposed to one coordinate system. For the H - P theory because the von Mises yield condition has been used, s_{ij}, k_{ij}, and $\dot{e}_{ij}^{vp}$ are perpendicular to the dynamic yield surface. On the other hand, eq. (2.14) indicates that the inelastic part of the strain rate has the direction of the perpendicular to the dynamic yield surface through the point of actual stress s_{ij}. This difference between the original Hohenemser-Prager theory and the generalization by Perzyna is shown in figure 2.4.

From equations (2.16) or (2.19) a relation can be obtained for the inelastic strain rate as a function of Φ and f.

$$\dot{e}_{ij}^{vp} = \eta < \Phi \left(f \left(s_{ij}, e_{ij}^{vp} \right) - K \right) > \frac{\partial f}{\partial s_{ij}} \qquad (2.27)$$

By the same process outlined through the equations

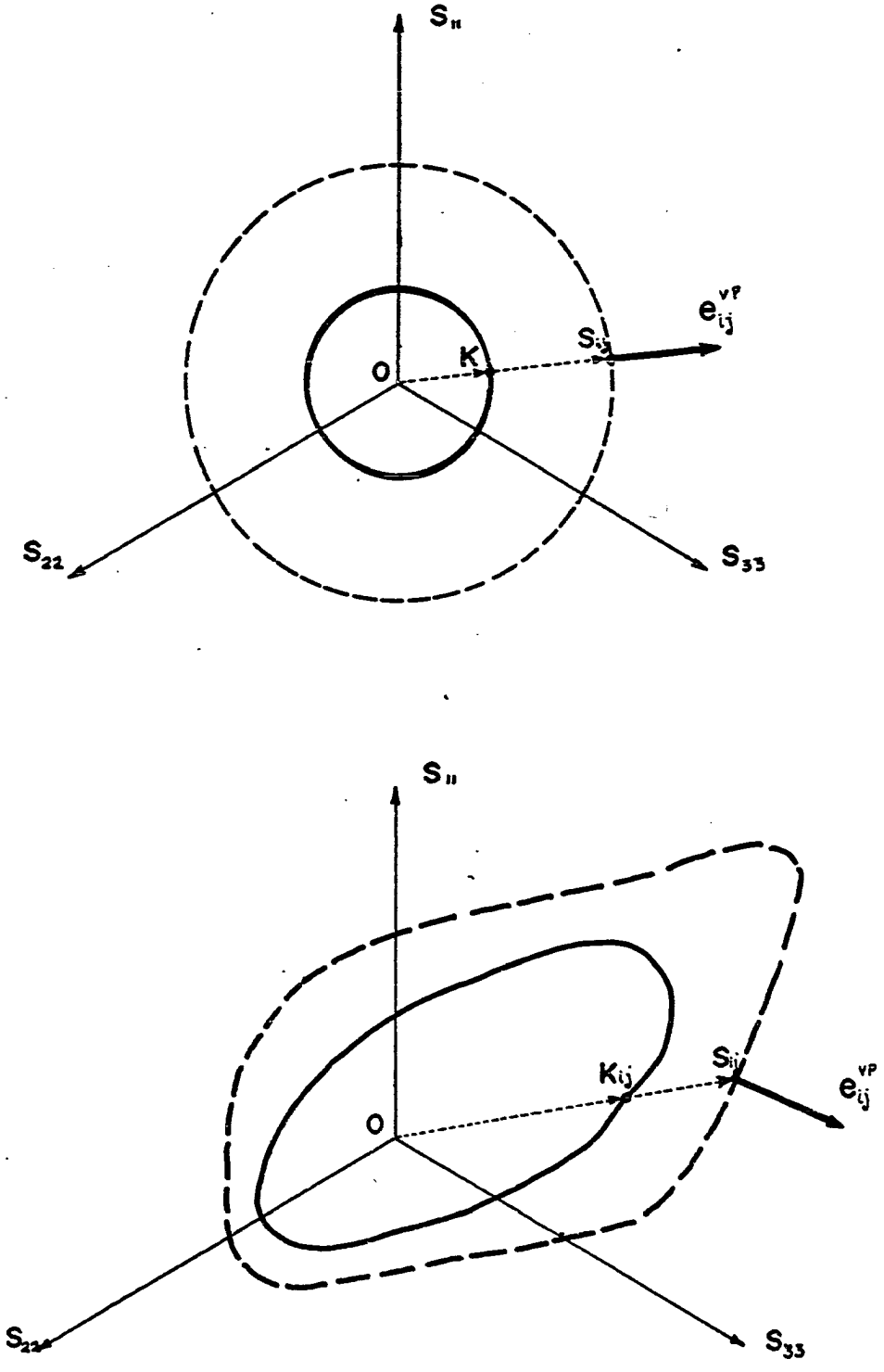

FIG. 2.4

(2.15) to (2.17) the dynamic yield surface can be obtained. As a first step, the eq. (2.24) can be written in the following way:

$$f(s_{ij},\ e_{ij}^{vp}) = K\,(W^{vp})\cdot\left\{1+\phi^{-1}\left(\frac{\sqrt{II_p}}{n\sqrt{\frac{1}{2}\frac{\partial F}{\partial s_{ij}}\frac{\partial F}{\partial s_{ij}}}}\right)\right\} \qquad (2.28)$$

This expression according to Perzyna implicitly represents the "dynamic yield condition" for elastic/viscoplastic, work hardening materials. It describes also the dependence of the yield criterion, for a given amount of inelastic work, on the inelastic strain rate. A further discussion about the physical meaning of the dynamic yield surface is to be presented in the following section.

One additional question should be briefly discussed in order to complete the review of the Perzyna's generalization to the constitutive equation presented by H - P. This is the question about the class of materials that cannot be described by this theory. Obviously the case of a yield surface not including the origin of the coordinate system in the deviatoric stress space has been excluded from the previous discussion. A more general theory taking account of this restriction has been recently proposed by H. C. WU [91] in his doctoral dissertation.

strain rate is determined from the constitutive equation presented before. On the other hand, if the inelastic strain-rate is prescribed, the excess stress is also determined. Thus the dynamic yield surface is defined as the surface which encloses the present quasi-static yield surface and is formed from all the stress points which produce the same magnitude of the viscoplastic strain-rate vector. This definition implies however that the original as well as the subsequent yield surfaces are of the von Mises type equation.

For a more general form of the quasi-static yield surface given by the function F in equation (2.24), two points 1 and 2 belong to the same dynamic yield surface if according to eq. (2.28) the following relation is satisfied:

$$f(s_{ij}^{1}, \varepsilon_{ij}^{1}) = f(s_{ij}^{2}, \varepsilon_{ij}^{2}) \quad (1) \tag{2.29}$$

and by considering the right hand side part of eq. (2.28)

$$K(W^{vp}) \left\{ 1 + \phi^{-1}\left(\frac{\sqrt{II_p}}{\sqrt{\frac{1}{2}\frac{\partial F}{\partial s_{ij}}\frac{\partial F}{\partial s_{ij}}}} \right) \right\}^{1} = K(W^{vp}) \left\{ 1 + \phi^{-1}\left(\frac{\sqrt{II_p}}{\sqrt{\frac{1}{2}\frac{\partial F}{\partial s_{ij}}\frac{\partial F}{\partial s_{ij}}}} \right) \right\}^{2} \tag{2.30}$$

---

(1) The superscripts 1 or 2 on s_{ij} and ε_{ij} indicate the numerical values of these functions at the points 1 or 2.

4. The dynamic yield surface

It has been shown through eq. (2.28) that for a given stress point s_{ij} a surface can be associated in the deviatoric stress space, the so-called dynamic yield surface. The definition of this surface as well as the common property of its points will be discussed in this section.

In the previously presented theory it has been noticed that the magnitude of the viscoplastic strain rate is given as a function of the "excess stress". The excess stress in the deviatoric stress space was introduced as the difference between s_{ij} and k_{ij}, where k_{ij} was the intersection point between the vector representing the current dynamic stress point and the current quasi-static yield surface. According to this definition the excess stress even for a constant stress point A is a decreasing function of time, since under the assumption of a work hardening material, the inelastic strain produces an expansion of the quasi-static yield surface, i.e. an increase of the magnitude of the vector k_{ij}.

The figure 2.5 shows the change of the quasi-static yield surface as a function of the inelastic strain and the corresponding change of the vector $s_{ij} - k_{ij}$. This idea agrees completely with the experience gained through the uniaxial tests as it is shown in figure 2.6. An increment in the inelastic strain from ε_1^{vp} to ε_2^{vp} decreases the overstress from $\Sigma_1 K_1$ to $\Sigma_2 K_2$ for a constant load σ_o.

For a certain amount of the excess stress the inelastic

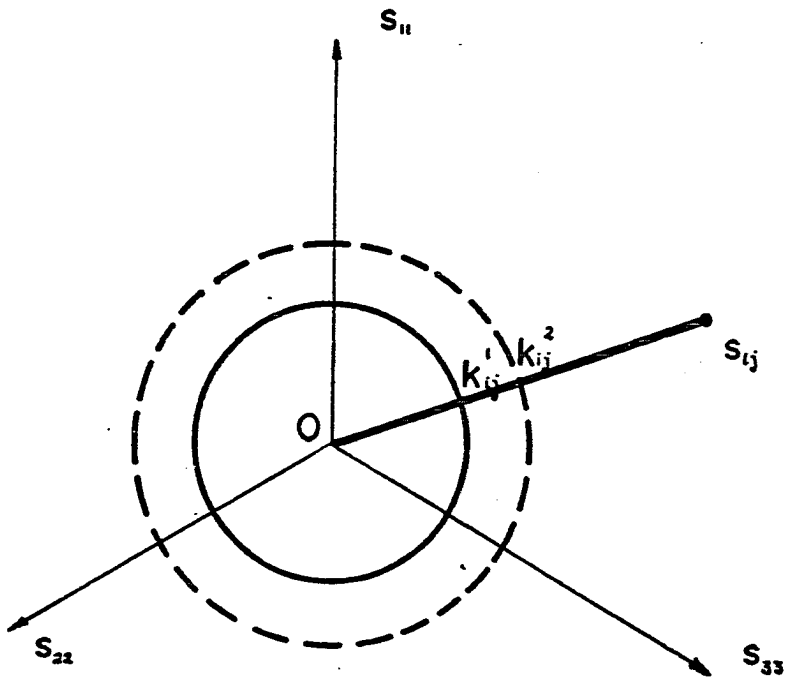

FIG. 2.5

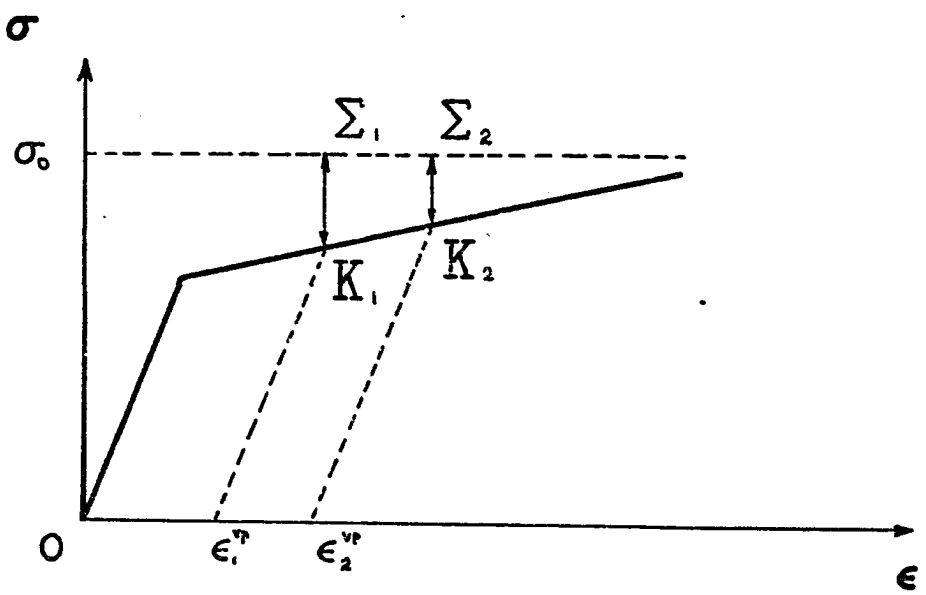

FIG. 2.6

where the work hardening parameter $K = K(W^{vp})$ has the same value in both sides in eq. (2.30) since the points 1 and 2 of the dynamic yield surface are associated with the same present quasi-static yield surface.

The dynamic yield surfaces corresponding to the two states of stress 1 and 2 coincide if the following eq. (2.31) is satisfied:

$$\left(\frac{\sqrt{II_p}}{\sqrt{\frac{1}{2}\frac{\partial F}{\partial s_{ij}}\frac{\partial F}{\partial s_{ij}}}}\right)^1 = \left(\frac{\sqrt{II_p}}{\sqrt{\frac{1}{2}\frac{\partial F}{\partial s_{ij}}\frac{\partial F}{\partial s_{ij}}}}\right)^2 \qquad (2.31)$$

For quasi-static yield surfaces of the von Mises type this relation implies that the dynamic yield surface is defined by the actual points of stress in deviatoric stress space that produce an inelastic strain rate vector of a constant magnitude. For a more general case however, when the gradient $\frac{\partial F}{\partial s_{ij}}$ is of varying magnitude, not simply $\sqrt{II_p}$ but the whole expression in eq. (2.31) must be a constant.

In the deviatoric stress space shown in figure 2.7, the original as well as the subsequent quasi-static yield surfaces are shown. Each one of these subsequent surfaces is associated with some value of the inelastic strain. In a later section a simple linear law describing the expansion of the von Mises yield surface is to be presented. For the time being it is enough to observe that the radius of the yield surface is an increasing function of the inelastic

strain. The actual stress point A is assumed outside the quasi-static yield surfaces. According to the previous discussion, a dynamic yield surface given by eq. (2.28) passes through the point A. Any expansion of the quasi-static yield surface produces a decrease of the magnitude of the visco-plastic strain rate and therefore a change in the dynamic yield surface, which now must be the one that passes again through A and corresponds to the expanded quasi-static yield surface. Finally after a certain amount of inelastic strain has been developed, the quasi-static yield surface will pass through the point A. The quasi-static yield surface through A is introduced then as the limit case of the family of dynamic yield surfaces through A when the inelastic strain rate is zero. This remark introduces an additional restriction on the mathematical definition of the dynamic yield surface because the continuous change in the shape of the dynamic yield surface as the magnitude of the inelastic strain rate decreases must have as limit the quasi-static yield surface through A given independently through the work hardening law.

Figure 2.7 shows the change of the quasi-static yield surface on the one hand and the corresponding dynamic yield surfaces on the other.

Finally it can be observed very easily that whenever the state of stress s_{ij} degenerates into a one dimensional stress distribution, the previous discussion reproduces the well known experimental results shown in figure 2.8. There it is shown that to a given value of the stress σ_o different

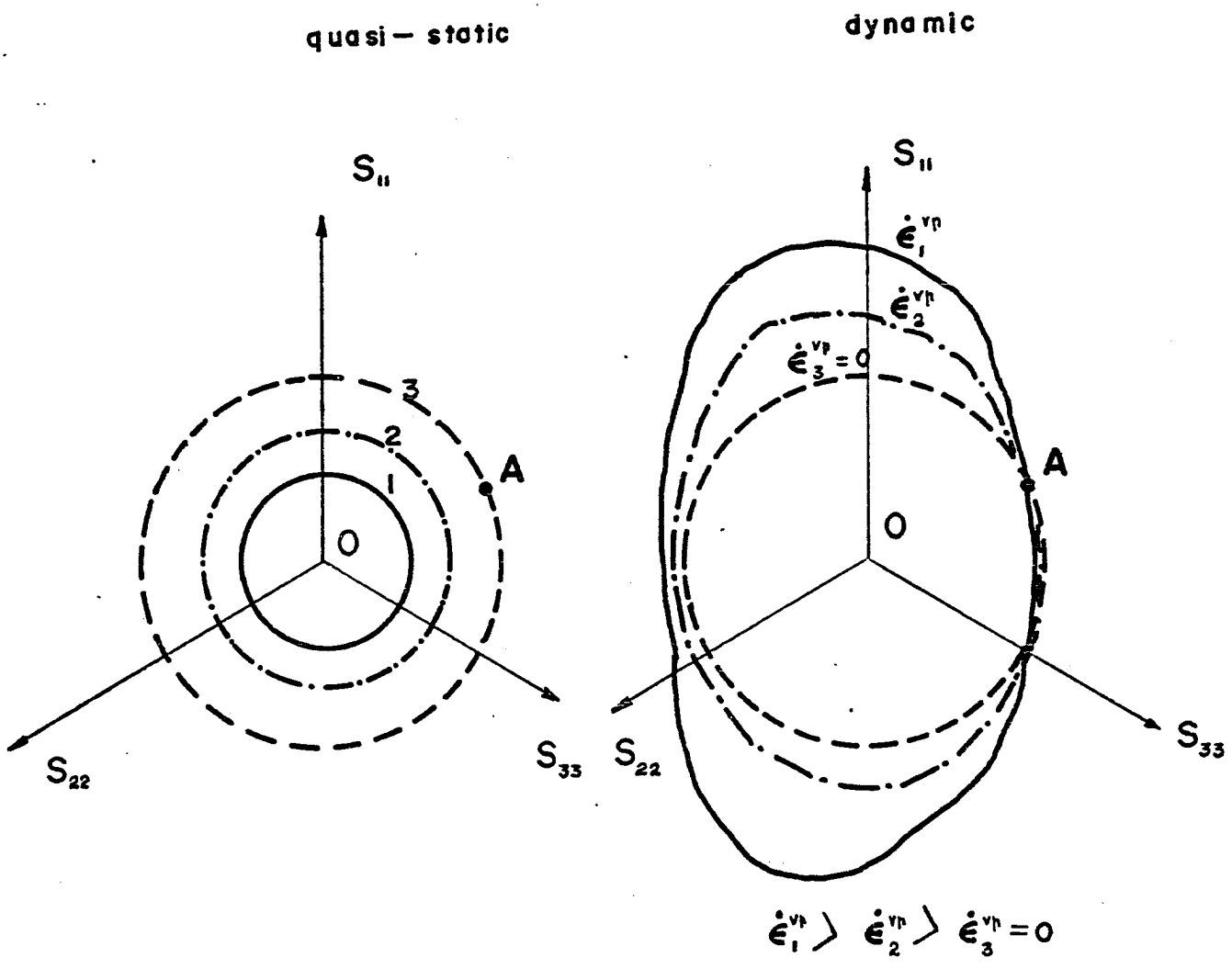

FIG. 2.7

values of $\dot{\varepsilon}$ may be associated pending on ε^{vp}. The inelastic strain rate $\dot{\varepsilon}$ is a decreasing function of ε^{vp}.

5. Loading-Unloading criterion

All the work mentioned so far was related to the two fundamental questions of the theory of visco/plasticity, namely the constitutive equation and the dynamic yield surface. As the applied load at the boundaries of the elastic/viscoplastic material may increase, remain constant or decrease criteria must be introduced describing loading and unloading processes and their corresponding modes of deformation.

In the theory of plasticity an increase of the stresses beyond the yield point, in the case of a one dimensional problem, will give rise to an increase of the plastic strain. A decrease of the stress on the other hand will leave the plastic strain intact. If the stress does not exceed the yield limit the material behaves elastically. Both increasing and decreasing stresses result in elastic deformation and the plastic strain remains zero. In this case the constitutive equation is represented by the Hooke's law.

In the theory of viscoplasticity, although an increase of the stress will produce an increase of the inelastic strain, a decrease of the stress will produce either an increase of the inelastic strain or no variation at all.

In figure 2.9 all possible motions of the stress-strain point A are in any direction D to the right of line AB[1] or

---

(1) AB is the parallel to the elastic part of the quasi-static stress-strain curve from the point A.

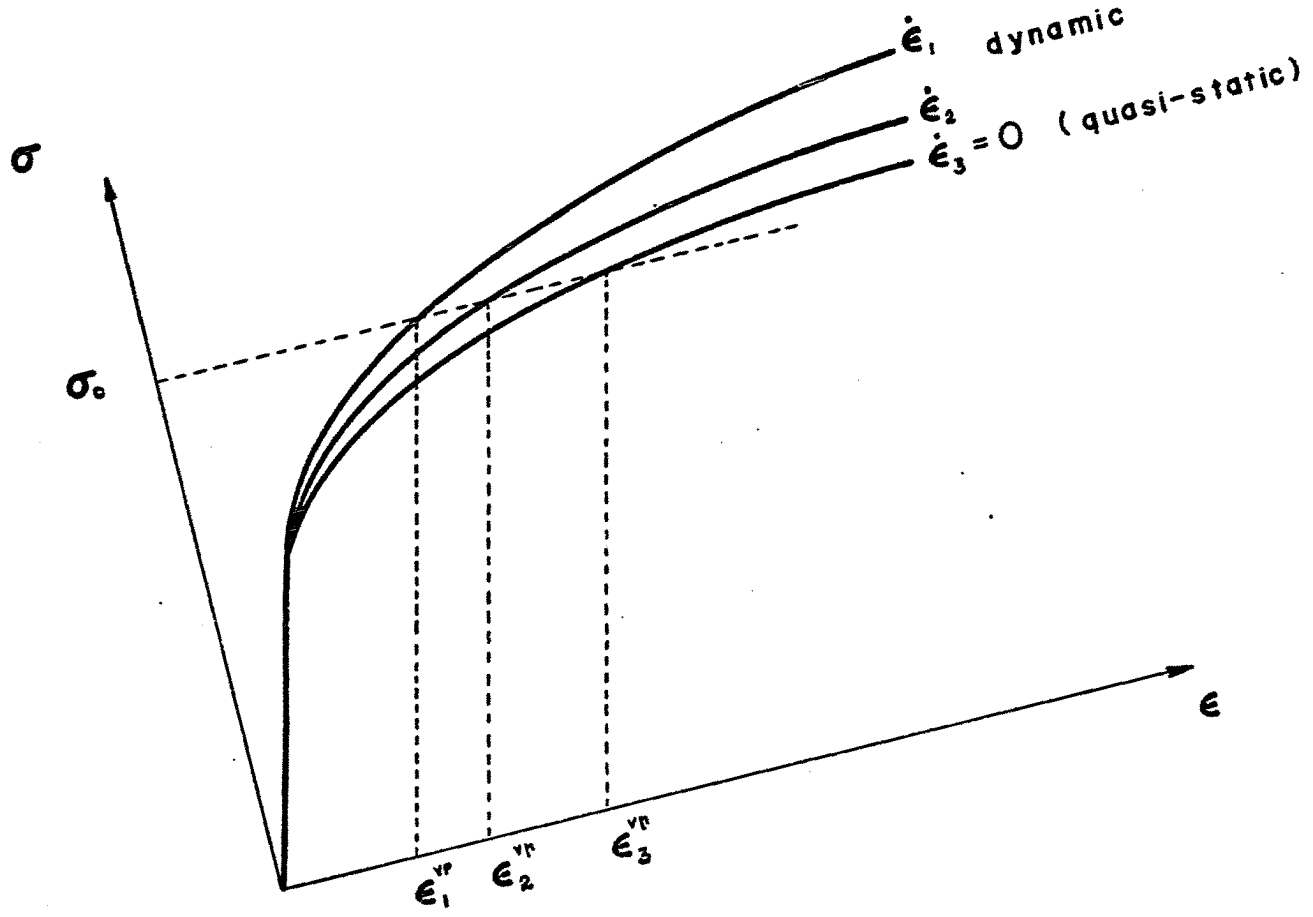

FIG. 2.8

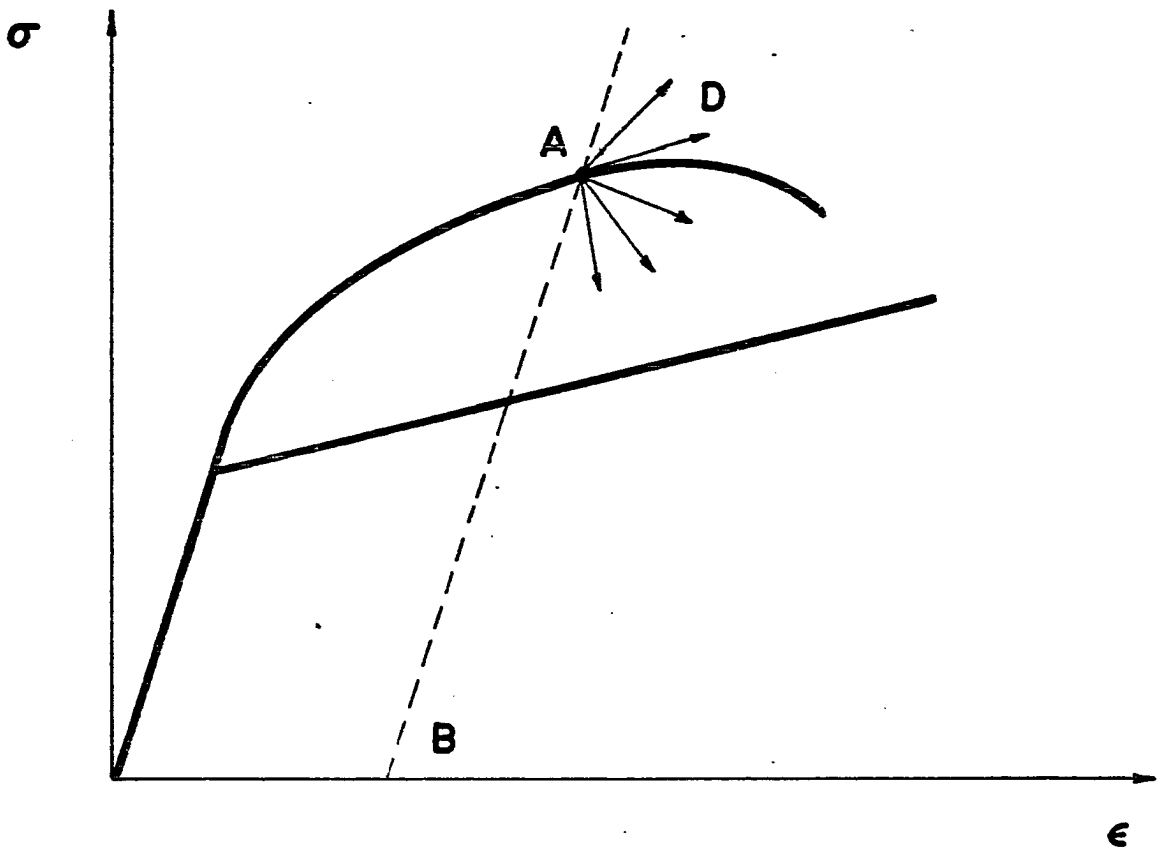

FIG. 2.9

downwards along AB.

The mathematical conditions which define the changeover between material loading and material unloading, in other words, the passage from the region in which the inelastic strain is an increasing function of time to a region in which it is constant at every point, are called the loading/unloading criteria.

As mentioned before and it is shown in figure 2.9, the material is assumed to work harden. A classical loading/unloading criterion in viscoplasticity is

$$\sigma > f(\varepsilon^{vp}) \quad \text{for loading i.e.} \quad \frac{\partial \varepsilon^{vp}}{\partial t} > 0$$

and

$$\sigma < f(\varepsilon^{vp}) \quad \text{for unloading i.e.} \quad \frac{\partial \varepsilon^{vp}}{\partial t} = 0$$

where $f(\varepsilon)$ is the stress that corresponds to a given state of strain long the quasi-static stress-strain curve.

This criterion however cannot describe the relaxation phenomena discussed in a paper by CRISTESCU and MIHAILESCU [92]. It does not provide also any information about the elastic and the inelastic part of the strain rate. A more realistic loading/unloading criterion has been introduced by CRISTESCU [93] and is shown by the dotted lines in figure 2.10.

If it is assumed that the present state of stress and strain are presented by the point A, then the following cases may be developed (the numbers correspond to the dotted lines in the figure 2.10).

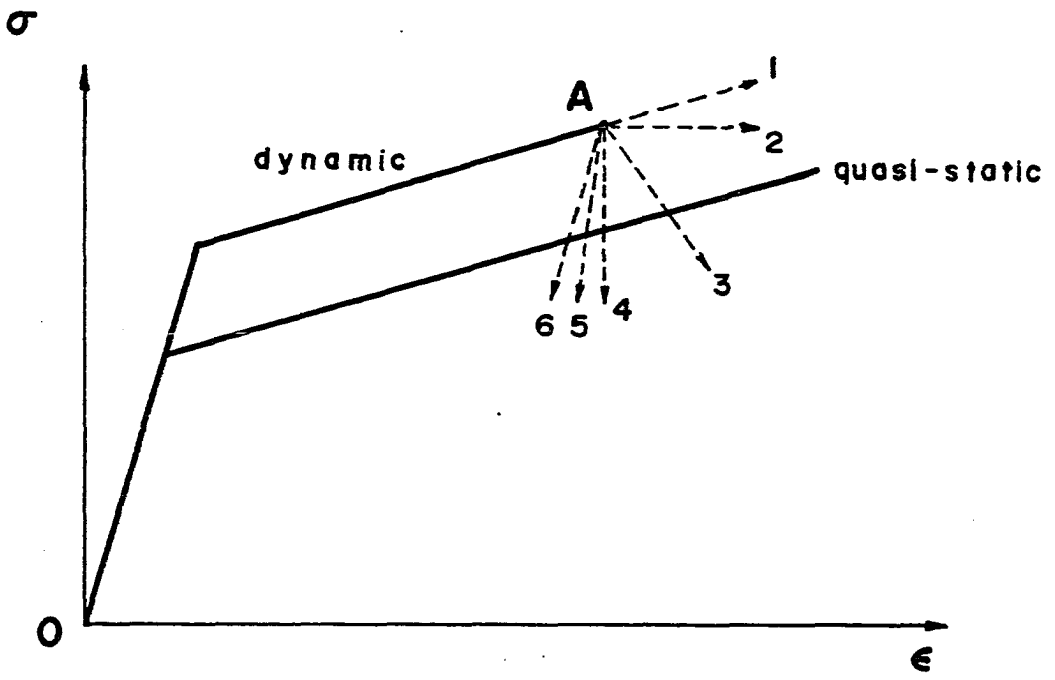

FIG. 2.10

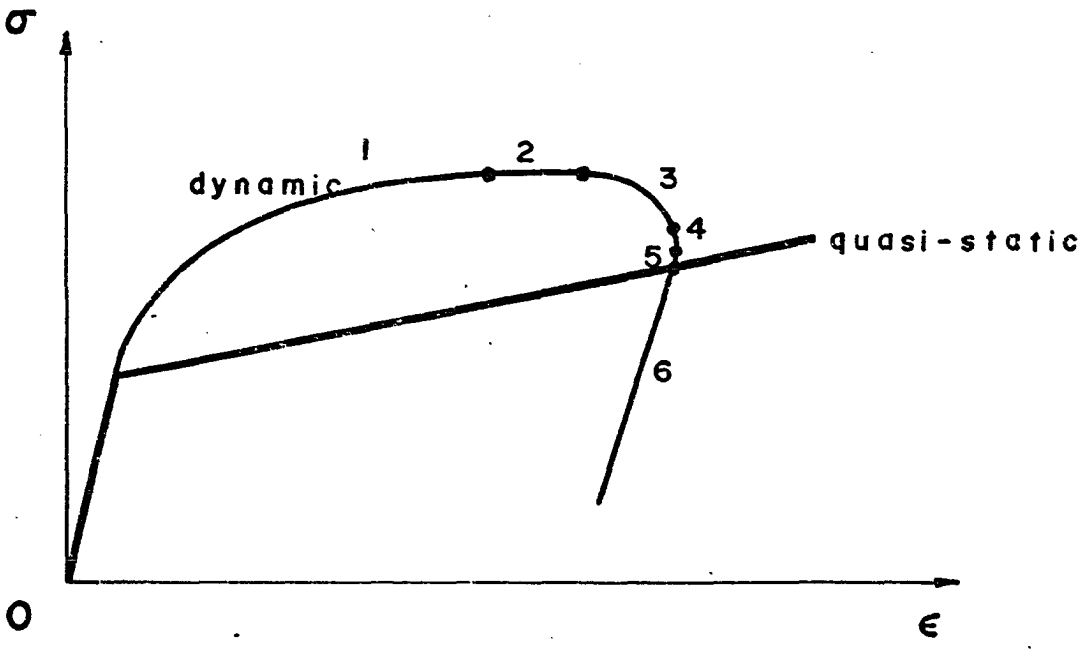

FIG. 2.11

1. T o t a l l o a d i n g. During this deformation

$$d\sigma > 0 \quad \text{and} \quad \dot{\varepsilon} > 0$$

therefore $\dot{\varepsilon}^{e}$ and $\dot{\varepsilon}^{vp} > 0$

2. C r e e p. During this process

$$d\sigma = 0 \quad \text{and} \quad \dot{\varepsilon} > 0$$

in this case $\dot{\varepsilon}^{e} \doteq 0$ and $\dot{\varepsilon}^{vp}$ 0

3. P a r t i a l l o a d i n g. During this process

$$d\sigma < 0 \quad \text{and} \quad \dot{\varepsilon} > 0$$

The previous relations imply that $\dot{\varepsilon}^{e} = 0$ and $\dot{\varepsilon}^{vp} > 0$

4. R e l a x a t i o n. The relaxation occurs when

$$\dot{\varepsilon} = \dot{\varepsilon}^{e} + \dot{\varepsilon}^{vp} = 0$$

then $d\sigma < 0$ and $\dot{\varepsilon}^{e} < 0$, $\dot{\varepsilon}^{vp} > 0$

5. P a r t i a l u n l o a d i n g. During this process $d\sigma < 0$, $\dot{\varepsilon} < 0$

It follows then that $\dot{\varepsilon}^{e} < 0$ and from the slope of the dotted line 5 $\dot{\varepsilon}^{vp} > 0$, but as the equation indicates the decrease of the stress is more rapid than it is during the relaxation process.

6. T o t a l u n l o a d i n g. The total unloading happens only for instantaneous unloading when $\frac{d\sigma}{dt} = -\infty$. This is like the elastic unloading starting at A.

A typical dynamic stress strain curve showing the various stages of loading/unloading conditions during a de-

crease of the applied stress is shown in figure 2.11.

This criterion can be generalized to the case of multi-axial states of stress for materials satisfying various kinds of constitutive equations. For the Hohenemser-Prager constitutive equation the rate of work has been introduced by Cristescu as a loading/unloading criterion. The definition of $\dot{W}$ is given through the equation (2.32)

$$\dot{W} = s_{ij}\ \dot{e}_{ij} = s_{ij}\dot{e}^{e}_{ij} + s_{ij}\ \dot{e}^{vp}_{ij} \qquad (2.32)$$

The dissipated inelastic rate of working is positive if the following inequality holds:

$$II_s > k^2$$

The loading/unloading stages 1 to 6 presented before for the uniaxial state of stress correspond to the following cases:

1. T o t a l l o a d i n g. During this process

$II_s > k^2$, $\dot{W} > 0$ and $\dot{II}_s > 0$

therefore $\dot{W}^{vp} > 0$ and $\dot{W}^{e} > 0$

2. N e u t r a l l o a d i n g. During this process

$II_s > k^2$, $\dot{W} > 0$ and $\dot{II}_s = 0$

also $\dot{W}^{vp} > 0$ and $\dot{W}^{e} = 0$

3. P a r t i a l l o a d i n g. In this case

$II_s > k^2$, $\dot{W} > 0$ and $\dot{II}_s < 0$

and therefore $\dot{W}^{vp} > 0$ and $\dot{W}^{e} < 0$

4. P u r e r e l a x a t i o n. A pure relaxation occurs if $II_s > k^2$ and $\dot{W} = 0$
i.e. if $-\dot{W}^{e} = \dot{W}^{vp}$ and $\dot{W}^{vp} > 0$

5. P a r t i a l u n l o a d i n g. During this process $II_s > k^2$ and $\dot{W} = 0$
Therefore $\dot{II}_s < 0$ (= unloading) and as in the partial loading $\dot{W}^{vp} > 0$ and $\dot{W}^{e} < 0$. In this case however the decrease of the stress is more rapid than the relaxation process while the viscoplastic component of the rate of working $\dot{W}^{vp}$ is greater than zero.

6. P u r e u n l o a d i n g.
This is an instantaneous process corresponding to $\dot{II}_s = -\infty$.

This loading/unloading criterion is good in the general scheme. It provides enough information about the development of the elastic and the viscoplastic part of the deformation and their relation to the changing stresses. It is also in complete agreement with the constitutive equation (2.27). For the present investigation where materials experiencing only work hardening effects are considered the rate of working presents a very powerful tool to express the loading/unloading criterion.

6. Constitutive equations for the present problem

The purpose of the present section is to study the dynamic behavior of an isotropic work hardening elastic/visco-plastic material to be used in the present investigation.

The material is considered as initially isotropic with a yield criterion obeying the von Mises equation. In the deviatoric stress space the initial yield surface is a cylinder with radius K. The stress points k_{ij} that belong to the initial yield surface satisfy the equation

$$F = 0, \qquad F = \frac{f(s_{ij})}{K} - 1$$

or written in another way:

$$f(k_{ij}) = K$$

Also all the subsequent yield surfaces are assumed to be the von Mises type. The radius K of any of these surfaces is assumed to be a function of the inelastic work W^{vp}.

$$K = K(W^{vp}) \qquad (2.33)$$

The function representing the relationship between the radius K and the inelastic work W^{vp} is assumed piecewise linear of the following type:

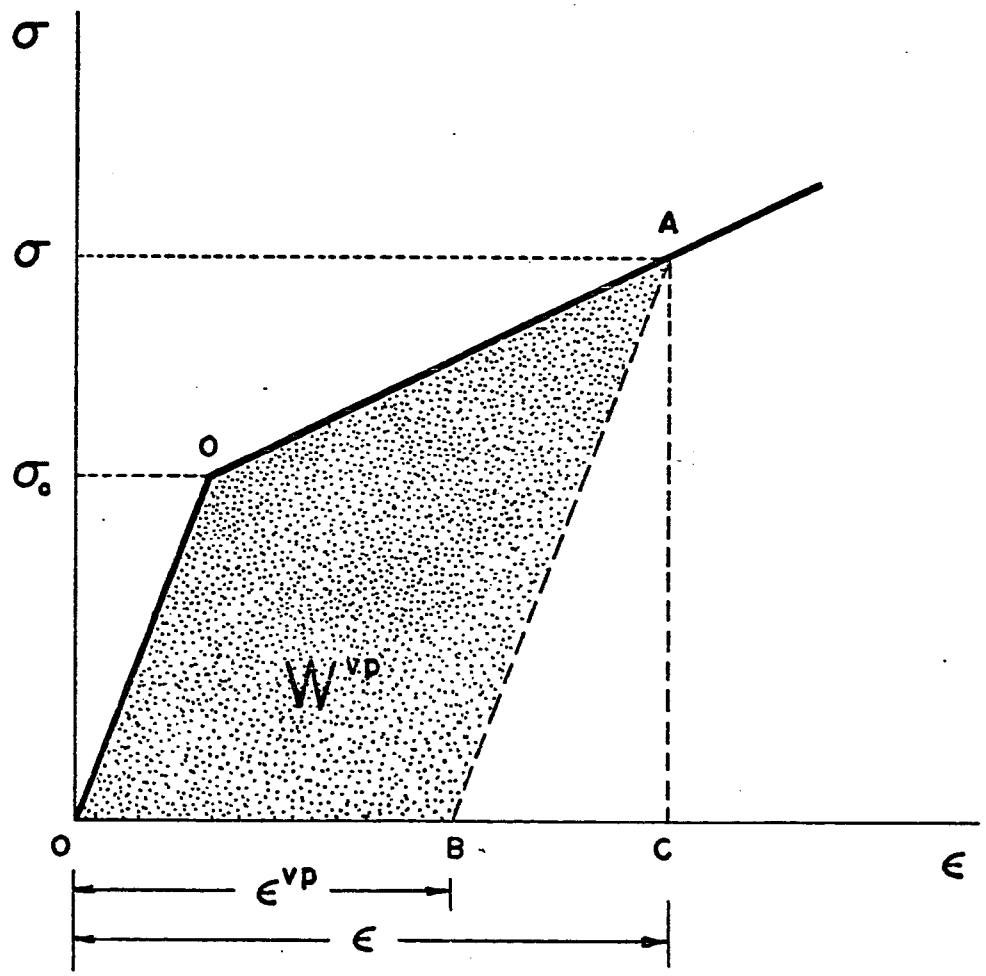

FIG. 2.12

$$K\,(W^{vp}) = K^{i-1} + A^{i}(W^{vp} - {}^{i-1}W^{vp}) \qquad (2.34)$$

for

$$(W^{vp})^{i-1} < W^{vp} \leq (W^{vp})^{i}$$

where A^{i}, K^{i-1}, and ${}^{i-1}W^{vp}$ are constants

The coefficients A^{i} can be found from the basic principle constantly used throughout this work that whenever the state of stress degenerates to a one-dimensional problem all the constitutive relations should reproduce well known results from the one-dimensional stress-strain curves.

Figures 2.12 shows a bilinear approximation of the actual quasi-static stress-strain curve. The stress σ that corresponds to a strain δ is given by eq. (2.35)

$$\sigma = \sigma_{o} + (\varepsilon - \varepsilon_{o})\, E_{1} \qquad (2.35)$$

The ratio between the slopes in the inelastic and the elastic region defines the level of strain hardening. The point σ_{o}, ε_{o} is the yield point.

The unloading from any point A of the viscoplastic region occurs along the straight line A B which is parallel to the elastic line with slope E_{o}. Therefore to any point A the viscoplastic work associated with the stress σ is given by the area OO'AB in figure 2.12. As it can be seen from this figure this work is equal to the total work done by the

stress point whenever it moves along the quasi-static curve from the zero stress point to the final stress σ minus the elastic work gained back after total unloading along the straight line A B.

$$W^{vp} = W^{total} - W^{elastic\ unloading} \tag{2.36}$$

$$W^{vp} = \int_0^{\varepsilon} \sigma d\varepsilon - \frac{(\sigma_o + (\varepsilon - \varepsilon_o)E_1)^2}{2E_o}$$

and finally

$$W^{vp} = \frac{1}{2}E_o\varepsilon_o^2 \left\{ 2\frac{\varepsilon}{\varepsilon_o} - 1 + \frac{E_1}{E_o}\left(\frac{\varepsilon}{\varepsilon_o} - 1\right)^2 - \left(1 + \left(\frac{\varepsilon}{\varepsilon_o} - 1\right)\frac{E_1}{E_o}\right)^2 \right\} \tag{2.37}$$

On the other hand, in the one dimensional case, any stress beyond the yield limit σ_o produces an expansion of the elastic region. The new yield point in simple tension is the stress point A itself. This remark establishes the relationship between the radius K of the current, i.e. after some viscoplastic deformation, yield surface and the viscoplastic work. Figures 2.13, 2.14, and 2.15 present the graph of this relationship for several values of the strain hardening ratio E_1/E_o.

The previous relationship between inelastic work and yield stress can be generalized to a six dimensional state of stress very easily. For a multidimensional state of stress the constitutive equation representing the response from the material to the applied stress is assumed to be like the one given by eq. (2.12)

$$\dot{e}_{ij} = \frac{\dot{s}_{ij}}{2\mu} + (1 - \frac{K}{\sqrt{II_s}})s_{ij} \qquad (2.38)$$

where μ is the shear modulus. Introducing a new material constant m through the relation

$$m = 2\eta\mu$$

the equation (2.38) may be written in the following way:

$$\dot{e}_{ij} = \frac{\dot{s}_{ij}}{2\mu} + \frac{m}{2\mu}(1 - \frac{K}{\sqrt{II_s}})s_{ij} \quad \text{for } II_s > k^2 \qquad (2.39)$$

and

$$\dot{e}_{ij} = \frac{\dot{s}_{ij}}{2\mu} \quad \text{for } II_s \leq k^2 \qquad (2.39a)$$

Obviously m has dimensions T I M E^{-1} and represents the inelastic, i.e. the viscous behavior of the material.

The total viscoplastic work for a multidimensional state of stress is equal to the following expression:

$$W^{vp} = \int_0^{\varepsilon_{ij}^{vp}} \sigma_{ij} d\varepsilon_{ij}^{vp}$$

A fundamental assumption about the work hardening behavior of the material must be made at this point. Namely, that the relationship established in a monoaxial stress test between the radius K of the yield surface and the inelastic work also holds in a multiaxial state of stress. In this case the figures 2.13, 2.14, and 2.15 can be used for the present problem. Between the yield stress σ in the previous figures and the radius K of the subsequent yield surfaces the following relation holds:

$$K = \sqrt{\frac{2}{3}}\,\sigma$$

This assumption is used throughout the chapter VI of this dissertation where other possibilities will be investigated.

As a loading-unloading criterion, the rate of working proposed by Cristescu and presented in the section 5 of this chapter will be used.

$E_1 / E_0 = 0.99$

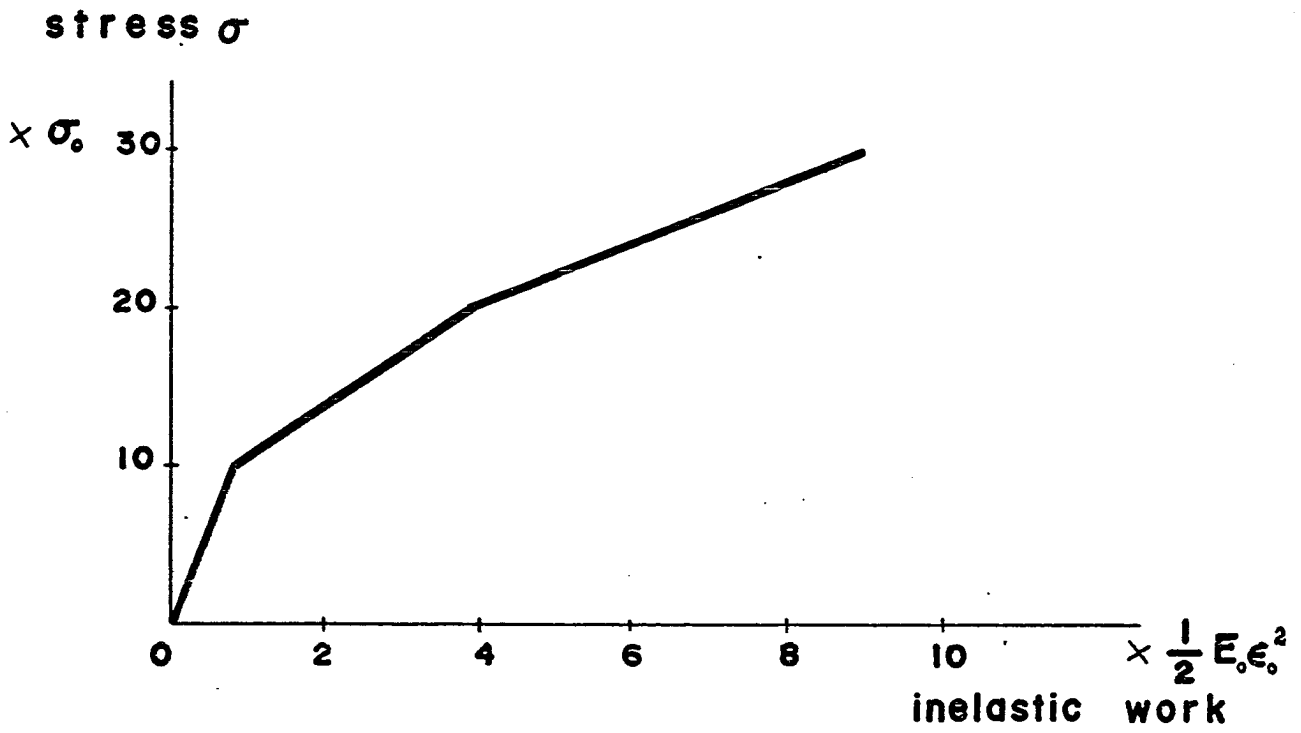

INELASTIC WORK	STRESS
$0 \leqslant W < 0.8$	$1 + \frac{9}{0.8} W$
$0.8 \leqslant W < 3.8$	$10 + 3.333(W - 0.8)$
$3.8 \leqslant W < 8.8$	$20 + 2.0(W - 3.8)$

FIG. 2.13

$E_1 / E_0 = 0.50$

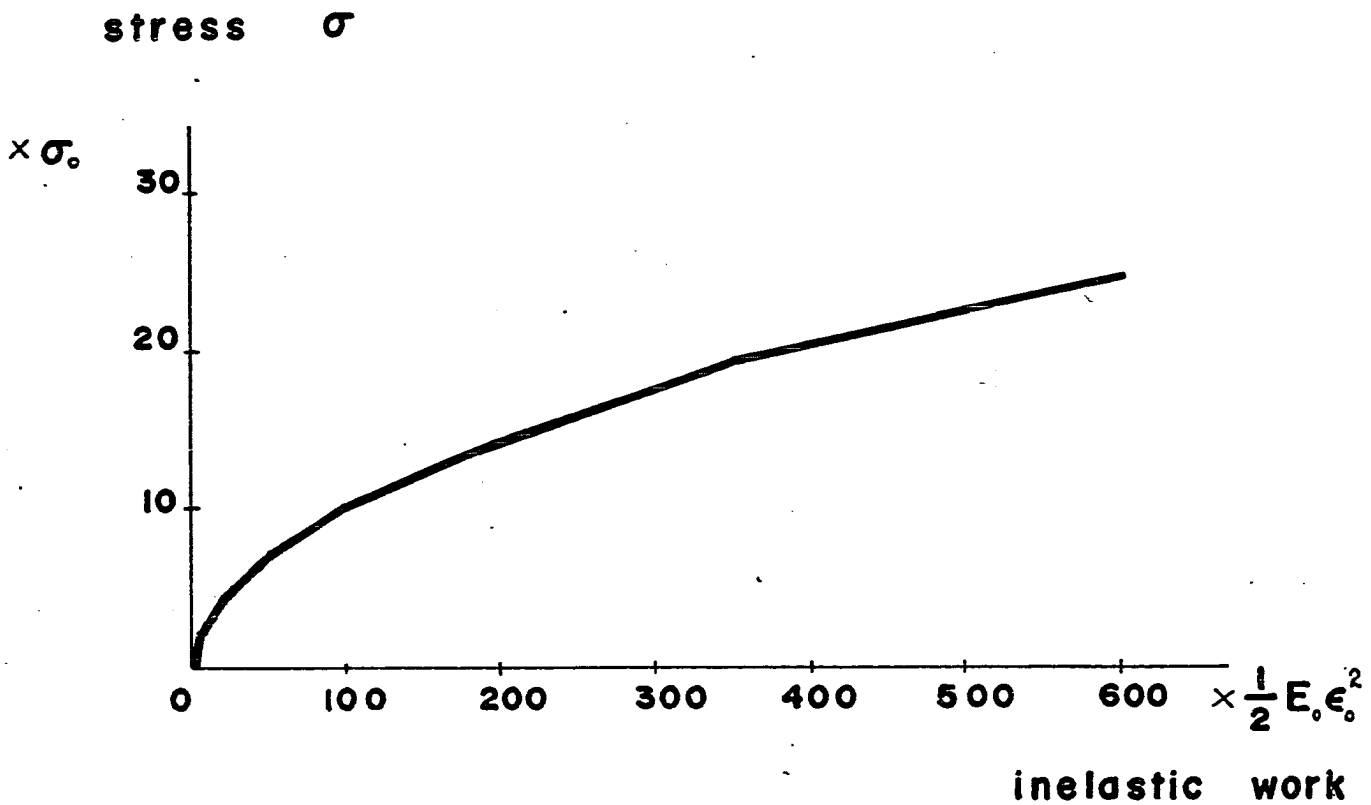

INELASTIC WORK	STRESS
$0 \leq W < 5$	$1 + 0.32\,W$
$5 \leq W < 20$	$2.60 + 2.02\,\frac{W-5}{15}$
$20 \leq W < 50$	$4.62 + 2.66\,\frac{W-20}{30}$
$50 \leq W < 100$	$7.28 + 2.80\,\frac{W-50}{50}$
$100 \leq W < 150$	$10.08 + 2.30\,\frac{W-100}{50}$
$150 \leq W < 200$	$12.38 + 1.90\,\frac{W-150}{50}$
$200 \leq W < 350$	$14.28 + 3.54\,\frac{W-200}{150}$
$350 \leq W < 600$	$18.82 + 5.80\,\frac{W-350}{250}$

FIG. 2.14

$E_1 / E_0 = 0.25$

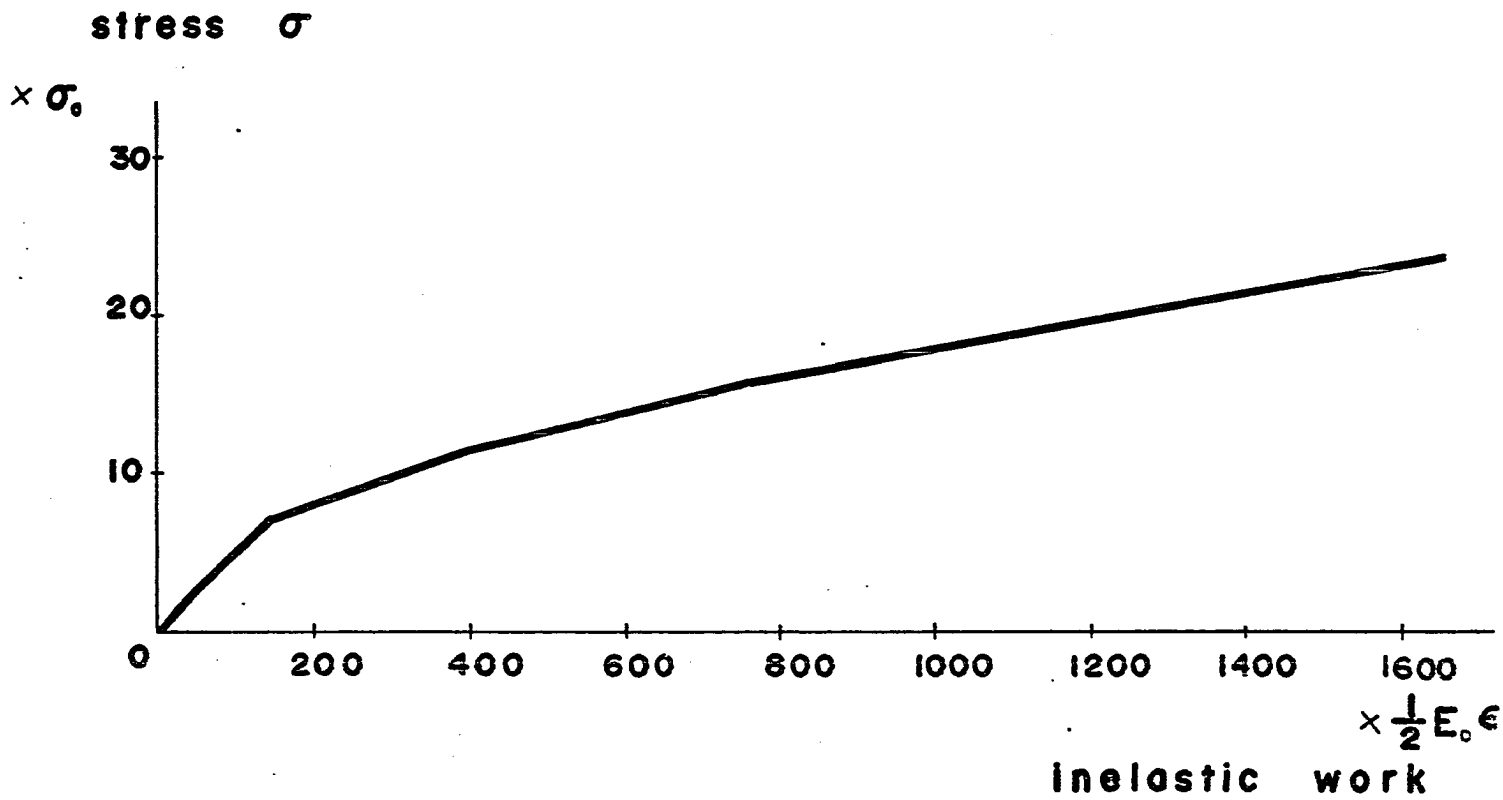

INELASTIC WORK	STRESS
$0 \leq W < 15$	$1 + 1.58 \frac{W}{15}$
$15 \leq W < 50$	$2.58 + 1.70 \frac{W-15}{35}$
$50 \leq W < 150$	$4.28 + 3.00 \frac{W-50}{100}$
$150 \leq W < 400$	$7.28 + 4.44 \frac{W-150}{250}$
$400 \leq W < 750$	$11.72 + 4.20 \frac{W-400}{350}$
$750 \leq W < 1650$	$15.92 + 7.55 \frac{W-750}{900}$

FIG. 2.15

C H A P T E R III

THE PROBLEM OF CYLINDRICAL WAVES IN ELASTIC-VISCOPLASTIC MATERIALS

1. Introduction

The problem to be investigated in the present dissertation consists of the wave propagation in an elastic/viscoplastic medium. This medium is considered as infinitely extended around a cylindrical hole where the external load is applied. As figure 3.1 indicates the axis of the cylinder is the Z - axis for the cylindrical coordinate system chosen to describe the wave propagation. The length along the Z-axis of the medium where the wave propagates is considered as very large compared with the radius r_o of the cylindrical hole. Also the stress distribution on the surface of the cylindrical cavity at any cross section perpendicular to the Z-axis is independent of the Z component of the coordinates. The medium is supposed homogeneous. Generally under the previous assumptions and without any further boundary conditions a volume element, defined as the volume between two perpendicular to the Z-axis planes in a distance dz from each other, two

cylindrical surfaces with radius r and r+dr, and two planes through the Z-axis, shown in figure 3.2, is subjected to two displacements. The one is on the radial direction and the other on the axial direction. Due to the symmetry both are functions of one variable only, the distance from the Z-axis r.

At this point an additional assumption has to be made. Namely, though the distance along the Z-axis is very large compared to the radius r_o, displacements on the direction parallel to the axis of symmetry Z are not allowed. The realization of that restriction is shown in figure 3.1 where the medium where the waves propagate is bounded between two planes which are considered as fixed and undeformed during the wave propagation. Obviously the presence of the two fixed planes introduces additional stresses and changes the independent of the z coordinate symmetry of the problem. However because the length along the Z-axis is very large, it is possible to neglect the influence of these additional non-independent of z stresses in a large region around the origin O of the coordinate system.

There is therefore a region into the elastic/viscoplastic medium where only cylindrical waves propagate. Superposition and other coupling effects coming from the fixed boundaries are outside the slope of the present investigation. The two planes in figure 3.1 serve only as kinematic restrictions without any dynamic effect on the wave propagation process. In other words, the problem is the wave propagation of plane

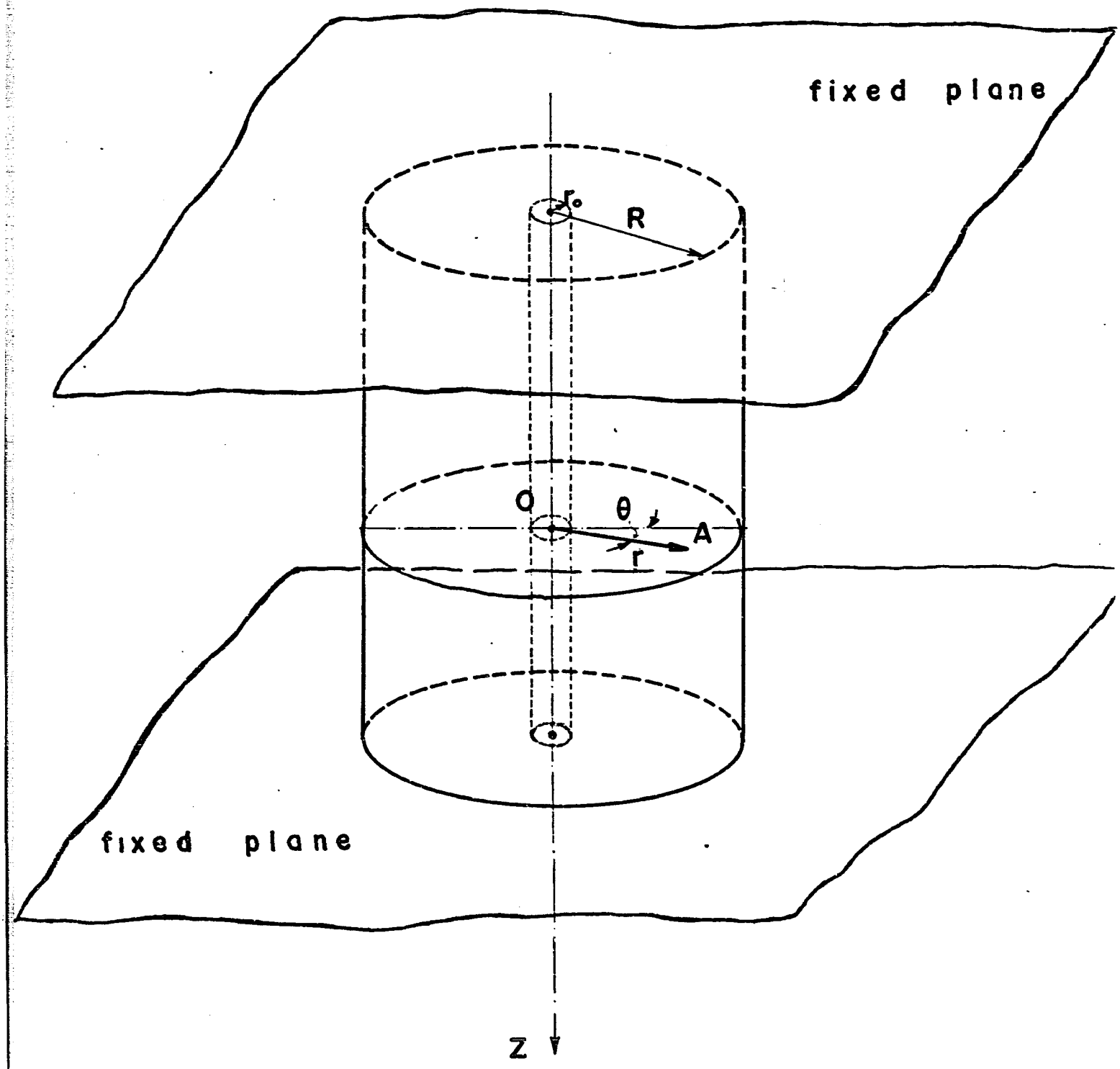

FIG. 3.1

strains in an infinite elastic/viscoplastic medium.

Under these conditions at each point inside the medium the following three principal stresses along the three directions r, θ , and z exist

$$\sigma_r = \sigma_r(r,t)$$

$$\sigma_\theta = \sigma_\theta(r,t)$$

$$\sigma_z = \sigma_z(r,t)$$

As it will be shown later by increasing the radius r_o of the cylindrical hole and keeping at the same time the magnitude of the applied pressure as a constant, the effects of the curvature of the surface of the hole, where the load is applied, decrease and the stress σ_θ becomes more and more negligible. The solution at the limit case as $r \to \infty$ should be like the one of a wave propagation in a rod. On the other hand for small r_o the present problem and the already investigated spherical one are very similar. The only existing difference is a quantitative one,since,in the case of a sphere, there is a double curvature in two perpendicular to each other directions and,in the case of a cylinder, only one.

Summarising the above discussion, it can be said that the present problem of plane strain cylindrical waves in elastic/viscoplastic media is a problem with one only displacement u_r along the radial direction, two strains ε_r and ε_t and three stresses σ_r, σ_ε, and σ_z. All the unknown functions are functions of only one space variable, the radius r, and the time t.

2. The geometry of the deformation

In a volume element like the one shown in Figure 3.2 the applied stresses along the radial direction are three σ_r, $\sigma_r + \frac{\partial \sigma_r}{\partial r} dr$, and the radial force coming from the combined effect of the two σ_θ acting on the plane surfaces of the volume element. Figure 3.3 and 3.4 show the radial forces. The equilibrium equation along the r-direction should be

$$(\sigma_r + \frac{\partial \sigma_r}{\partial r} dr)\ (r+dr)\ d\theta - \sigma_r\ r\ d\theta - 2\sigma_\theta\ dr\frac{d\theta}{2} = F \qquad (3.1)$$

where F is the inertial force coming from the acceleration of the mass inside the volume element along the r-direction. Neglecting the higher order terms in eq. (3.1) the following relation can be written:

$$dr\ d\theta\ (r\ \frac{\partial \sigma_r}{\partial r} + \sigma_r - \sigma_\theta) = F \qquad (3.2)$$

Also for F the following expression can be used:

$$F = r\ dr\ d\theta\ \rho\ \frac{\partial v}{\partial t} \qquad (3.3)$$

where ρ is the density (mass per volume) and $\frac{\partial v}{\partial t}$ the acceleration (v is the speed along the r axis).

From eqs. (3.2) and (3.3) the equation of motion, NEWTON's second law, can be written in the following form for the displacements along the radial direction

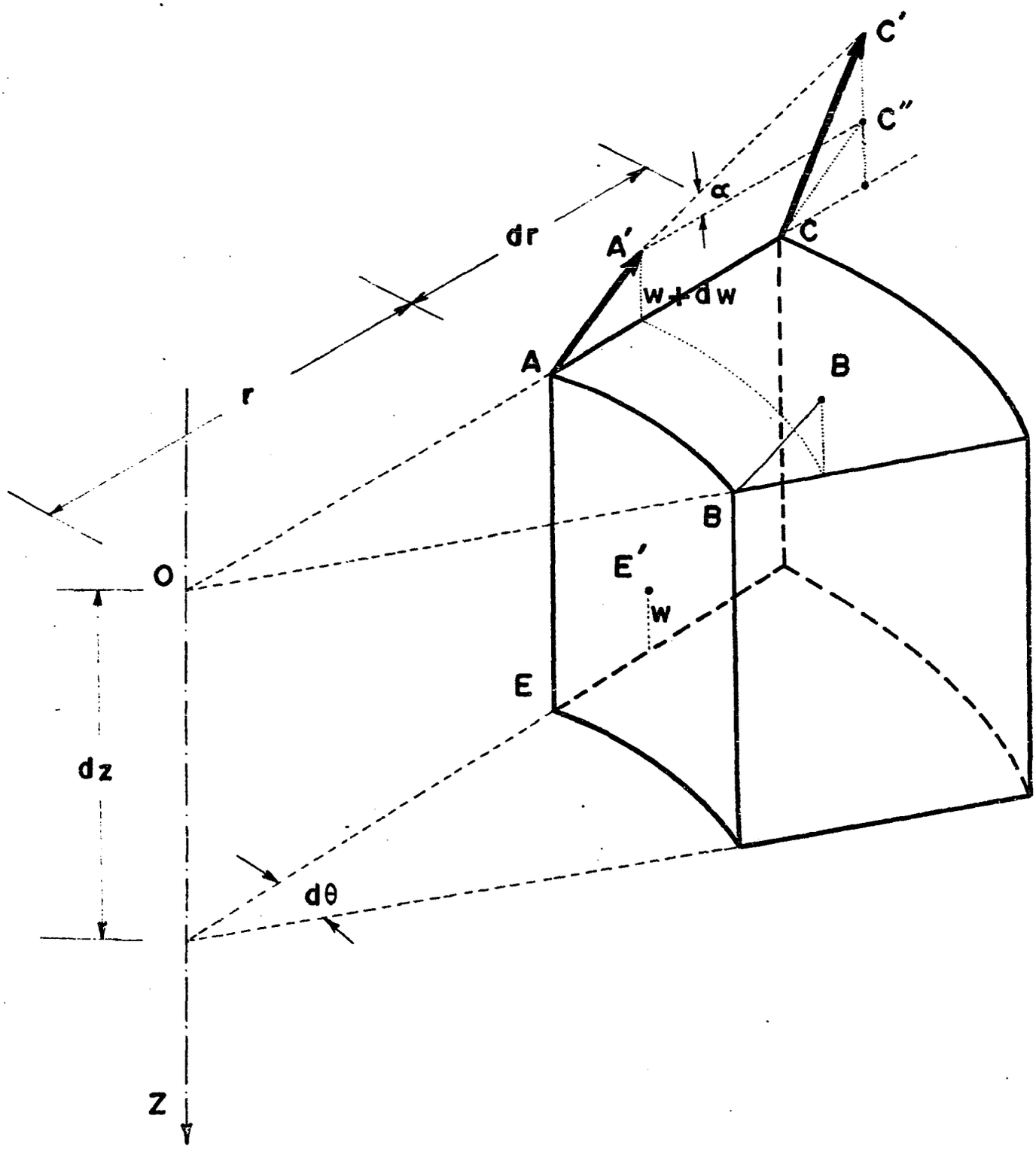

FIG. 3.2

$$\frac{\partial \sigma_r}{\partial r} + \frac{\sigma_r - \sigma_o}{r} = \rho \frac{\partial u}{\partial t} \qquad (3.4)$$

The displacements along one radial direction are a function of the distance from the axis of symmetry only.

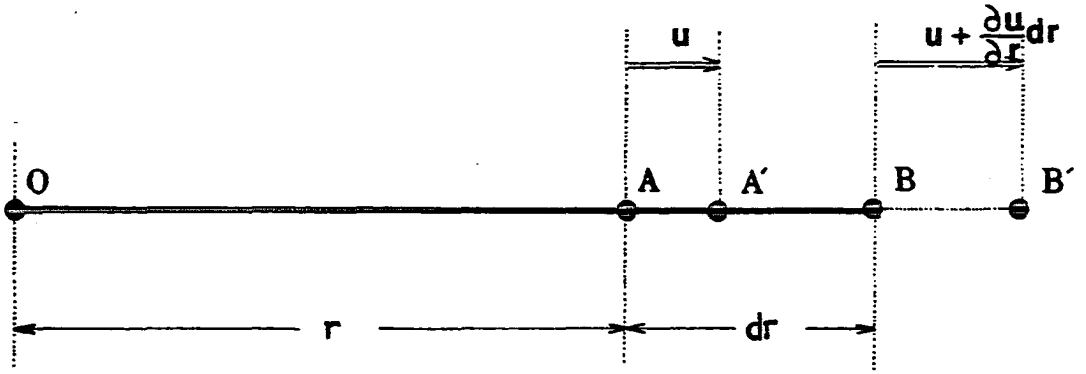

From the definition of the strain in the radial direction applied on the length element A B the following equation can be written:

$$\varepsilon_r = \frac{A'B' - A\,B}{A\,B}$$

(the point A' is the new place for the point A and B' is the new place for the point B)

$$\varepsilon_r = \frac{u + \frac{\partial u}{\partial r}\,dr - u}{dr} \qquad (3.5)$$

or

$$\varepsilon_r = \frac{\partial u}{\partial r} \tag{3.6}$$

where $u = u(r,t)$ is the equation for the displacements of any point A.

From figure 3.5 the equation for the strains on the direction θ can be found

$$\varepsilon_\theta = \frac{M'K' - M\,K}{M\,K}$$

(M and K are two points on a cylindrical surface of radius r around the Z-axis and M' and K' are the same points after the deformation when the corresponding radial displacement u(r,t) took place).

$$\varepsilon_\theta = \frac{(u+r)d\theta - rd\theta}{rd\theta}$$

therefore

$$\varepsilon_\theta = \frac{u}{r} \tag{3.7}$$

Equations (3.4), (3.6), and (3.7) describe the dynamic and kinematic conditions for a plane-strain wave propagation. The displacement u as well as σ_r and σ_θ are functions of r and t only.

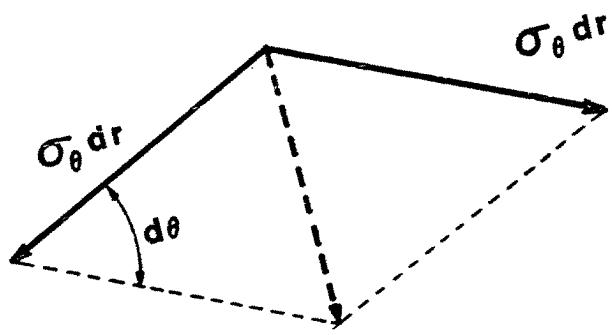

FIG. 3.3

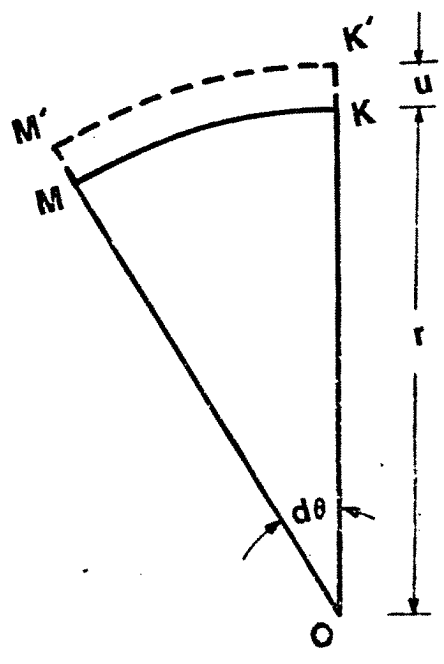

FIG. 3.5

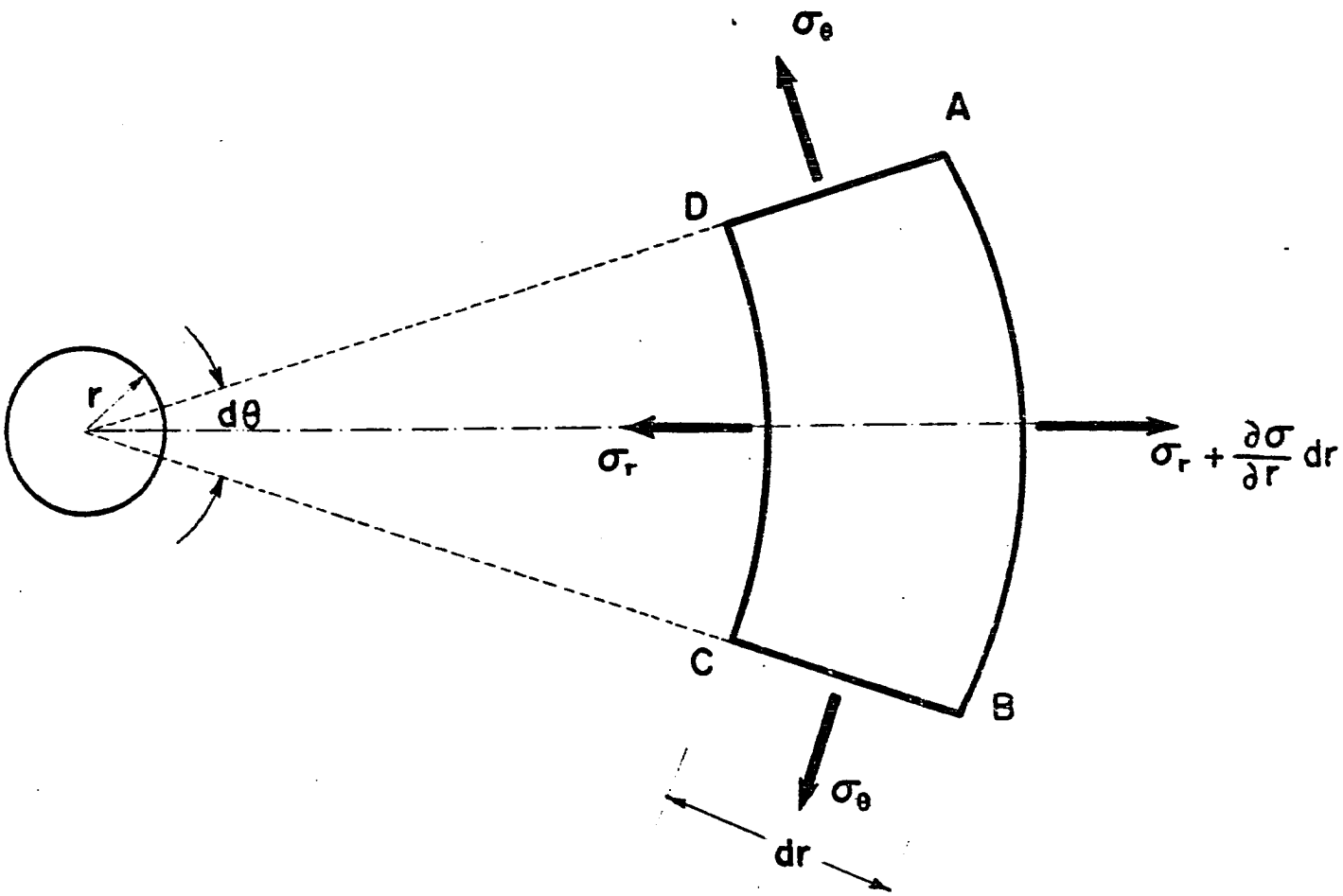

FIG. 3.4

3. Mechanical properties

The equations to be derived in this section are straightforward specializations of the general constitutive equations for the present cylindrically symmetric wave propagation problem.

As we stated before, see eq. (2.8), in viscoplasticity the total strain rate is decomposed into two elements, the elastic and the viscoplastic. Consequently the total volume change is to be divided in two parts.

1. In the elastic part, where the material is compressible, equation (3.8) expresses the elastic volume change $\varepsilon_r^{e\ell} + \varepsilon_\theta^{e\ell}$ as function of the applied stresses by means of the bulk modulus K.

$$\sigma_r + \sigma_\theta + \sigma_z = 3K(\varepsilon_r^{e\ell} + \varepsilon_\theta^{e\ell}) \tag{3.8}$$

2. In the inelastic part where we postulate that the material is incompressible

   Therefore

$$\varepsilon_r^{vp} + \varepsilon_\theta^{vp} = 0 \tag{3.9}$$

A combination of equations (3.8) and (3.9) yields the following relation between stresses and total strains

$$\sigma_r + \sigma_\theta + \sigma_z = 3K(\varepsilon_r + \varepsilon_\theta) \tag{3.10}$$

Note that eqs. (3.8) through (3.10) were found under the assumption of plane strain deformation, i.e. $\varepsilon_z = 0$. As a final step to complete the system of equations the constitutive equation (2.38) should be applied for the total strain-rate. The geometry of the problem suggests that σ_r, σ_θ, and σ_z are along the principal directions of the actual stress tensor σ. For the same reasons ε_r and ε_θ are also along the principal directions of strain tensor ε.

The elements of the deviatoric stress tensor are given by definition through eq. (3.11)

$$s_{ij} = \sigma_{ij} - \frac{1}{3}\sigma_{KK}\delta_{ij} \tag{3.11}$$

where

$$\sigma_{KK} = \sigma_r + \sigma_\theta + \sigma_z$$

Also

$$e_{ij} = \varepsilon_{ij} - \frac{1}{3}\varepsilon_{KK}\delta_{ij} \tag{3.11a}$$

where

$$\varepsilon_{KK} = \varepsilon_r + \varepsilon_\theta$$

Therefore s_{ij} and e_{ij} are also the principal values of the deviatoric stress and the deviatoric strain tensors respectively.

The equation (2.36) applied along the principal di-

rections of the s and e tensors yields to only two independent relations. The third possible equation does not provide any additional information due to the obvious identities

$$s_{kk} = 0 \qquad \dot{s}_{kk} = 0$$

$$e_{kk} = 0 \qquad \dot{e}_{kk} = 0$$

The two independent constitutive relations to be considered for the present cylindrically symmetric problem are the ones describing the total strain rate along the r and θ directions.

$$\dot{e}_r = \frac{\dot{s}_r}{2\mu} + \frac{m}{2\mu} < 1 - \frac{K}{\sqrt{II_s}} > s_r$$

$$\dot{e}_\theta = \frac{\dot{s}_\theta}{2\mu} + \frac{m}{2\mu} < 1 - \frac{K}{\sqrt{II_s}} > s_\theta \qquad (3.12)$$

Using equations (3.11) and (3.11a) the equation (3.12) can be written in the following way:

$$\frac{1}{3}(2\dot{\varepsilon}_r - \dot{\varepsilon}_\theta) = \frac{1}{6\mu}(2\dot{\sigma}_r - \dot{\sigma}_\theta - \dot{\sigma}_z) + \frac{m}{6\mu} < 1 - \frac{K}{\sqrt{II_s}} > (2\sigma_r - \sigma_\theta - \sigma_z)$$

$$\frac{1}{3}(2\dot{\varepsilon}_\theta - \dot{\varepsilon}_r) = \frac{1}{6\mu}(2\dot{\sigma}_\theta - \dot{\sigma}_r - \dot{\sigma}_z) + \frac{m}{6\mu} < 1 - \frac{K}{\sqrt{II_s}} > (2\sigma_\theta - \sigma_r - \sigma_z) \qquad (3.13)$$

where K is the work hardening parameter. Recalling the results given in chapter II, section 6, where the constitutive equation used in the present problem has been studied, the following piecewise linear relationship between the radius K of the yield surface and the total viscoplastic work W_{vp}

can be written:

$$K(W^{vp}) = K^{i-1} + A^{i}\,(W^{vp} - {}^{i-1}W^{vp})$$

where

$$W^{vp} = \int_{o}^{\varepsilon_{ij}^{vp}} \sigma_{ij}\, d\varepsilon_{ij}^{vp}$$

Along the principal axes the viscoplastic work is

$$W^{vp} = \int_{o}^{\varepsilon_{r}^{vp}} \sigma_{r}\, \varepsilon_{r}^{vp} + \int_{o}^{\varepsilon_{\theta}^{vp}} \sigma_{\theta} d\varepsilon_{\theta}^{vp} + \int_{o}^{\varepsilon_{z}^{vp}} \sigma_{z} d\varepsilon_{z}^{vp}$$

On the other hand the second invariant of the deviatoric stress tensor in terms of the principal stresses is given by the following equation

$$II_{s} = \frac{1}{9}\left\{ (2\sigma_{r}-\sigma_{\theta}-\sigma_{z})^{2} + (2\sigma_{\theta}-\sigma_{z}-\sigma_{t})^{2} + (2\sigma_{z}-\sigma_{r}-\sigma_{\theta})^{2} \right\}$$

According to the flow law used in this dissertation the second term in the right hand side in eqs. (3.13) representing the inelastic part of the strain rate exists only if $II_{s} \geq K$ For $II_{s} < K$ eqs. (3.13) can be written as follows:

$$\frac{1}{3}(2\dot{\varepsilon}_{r}-\dot{\varepsilon}_{\theta}) = \frac{1}{6\mu}(2\dot{\sigma}_{r}-\dot{\sigma}_{\theta}-\dot{\sigma}_{z})$$

$$\frac{1}{3}(2\dot{\varepsilon}_{\theta}-\dot{\varepsilon}_{r}) = \frac{1}{6\mu}(2\dot{\sigma}_{\theta}-\dot{\sigma}_{r}-\dot{\sigma}_{z}) \qquad (3.13a)$$

Equations (3.10) and (3.13) or (3.13a) describe the mechanical properties of the elastic/viscoplastic material during the cylindrical wave propagation.

4. Solution of the System of Differential Equations by the Method of Characteristics

The method to be developed here is based on the following two observations. First, the equations governing the propagation of waves in an elastic/viscoplastic medium are hyperbolic, and second, the lines of the time-space plane that locate wave fronts coincide with characteristic lines. The method of characteristics is the only practical in solving this type of problems with two independent variables. Using this method the system of differential equations reduces to two types of equations. The first type is the decay equation which is integrated directly on the space-time space to find the behavior of the first wave front. The domain beyond the first wave front is explored by means of the canonical form of the governing equations. These are valid along the characteristic lines and are integrated using finite differences. The method has many advantages. The conditions on the surface of the cylindrical cavity can be any mixture of conditions including those that can be realized experimentally and the time dependence can be arbitrary. There are perhaps two shortcomings of the method. The first arises if the response at stations far from the surface of the cavity is investigated. The second, if distances far behind the head of impulse are considered. This is true not only because the response would be needed far from the origin of the time-space plane where the numerical analysis originates but the mesh

size (see figure 3.10) would have to be small to obtain accurate results.

In the previous two sections the equations describing the propagation of cylindrical waves in an elastic/visco-plastic material were derived. After introducing the velocity v given by the eq. (3.14)

$$v = \frac{du}{dt} \tag{3.14}$$

equations (3.4), (3.6), (3.7), (3.10),and (3.13) may respectively be written in differential form as

$$\frac{\partial \sigma_r}{\partial r} + \frac{\sigma_r - \sigma_\theta}{r} = \rho \frac{\partial v}{\partial t}$$

$$\frac{\partial \varepsilon_r}{\partial t} = \frac{\partial v}{\partial r}$$

$$\frac{\partial \varepsilon_\theta}{\partial t} = \frac{v}{r}$$

$$\frac{\partial \sigma_r}{\partial t} + \frac{\partial \sigma_\theta}{\partial t} + \frac{\partial \sigma_z}{\partial t} = 3K \left(\frac{\partial \varepsilon_r}{\partial t} + \frac{\partial \varepsilon_\theta}{\partial t}\right)$$

$$2\frac{\partial \varepsilon_r}{\partial t} - \frac{\partial \varepsilon_\theta}{\partial t} = \frac{1}{2\mu}\left(2\frac{\partial \sigma_r}{\partial t} - \frac{\partial \sigma_\theta}{\partial t} - \frac{\partial \sigma_z}{\partial t}\right) + \frac{m}{2\mu}\left\langle 1 - \frac{K}{\sqrt{II_s}}\right\rangle (2\sigma_r - \sigma_\theta - \sigma_z)$$

$$2\frac{\partial \varepsilon_\theta}{\partial t} - \frac{\partial \varepsilon_r}{\partial t} = \frac{1}{2\mu}\left(2\frac{\partial \sigma_\theta}{\partial t} - \frac{\partial \sigma_r}{\partial t} - \frac{\partial \sigma_z}{\partial t}\right) + \frac{m}{2\mu}\left\langle 1 - \frac{K}{\sqrt{II_s}}\right\rangle (2\sigma_\theta - \sigma_r - \sigma_z)$$

This system of equations must be solved simultaneously for the six unknowns $\sigma_r(r,t)$, $\sigma_\theta(r,t)$, $\sigma_z(r,t)$, $\sigma_r(r,t)$, $\varepsilon_\theta(r,t)$, and $v(r,t)$. For this purpose they must be integrated numeri-

cally along the characteristic lines.

The previous system of differential equations can be written in the following form

$$\frac{\partial \sigma_r}{\partial t} - (\tfrac{4}{3}\mu+K)\frac{\partial v}{\partial r} + (\tfrac{2}{3}\mu-K)\frac{u}{r} + \frac{m}{3}\left\langle 1-\frac{K}{\sqrt{II_s}}\right\rangle(2\sigma_r-\sigma_\theta-\sigma_z)=0 \qquad (3.15)$$

$$\frac{\partial \sigma_\theta}{\partial t} + (\tfrac{2}{3}\mu-K)\frac{\partial v}{\partial r} - (\tfrac{4}{3}\mu+K)\frac{u}{r} + \frac{m}{3}\left\langle 1-\frac{K}{\sqrt{II_s}}\right\rangle(-\sigma_r+2\sigma_\theta-\sigma_z)=0 \qquad (3.16)$$

$$\frac{\partial \sigma_z}{\partial t} + (\tfrac{2}{3}\mu-K)\frac{\partial u}{\partial r} + (\tfrac{2}{3}\mu-K)\frac{u}{r} + \frac{m}{3}\left\langle 1-\frac{K}{\sqrt{II_s}}\right\rangle(-\sigma_r-\sigma_\theta+2\sigma_z)=0 \qquad (3.17)$$

$$\frac{\partial \varepsilon_r}{\partial t} - \frac{\partial v}{\partial r} = 0 \qquad (3.18)$$

$$\frac{\partial \varepsilon_\theta}{\partial t} - \frac{u}{r} = 0 \qquad (3.19)$$

$$\frac{\partial v}{\partial t} - \frac{1}{\rho}\frac{\partial \sigma_r}{\partial r} - \frac{\sigma_r-\sigma_\theta}{\rho\, r} = 0 \qquad (3.20)$$

All six equations can be written in the following way

$$\frac{\partial u_i}{\partial t} + \sum_{j=1}^{n} a_{ij}\frac{\partial u_j}{\partial r} + b_i = 0 \qquad i=1,2,\ldots 6 \qquad (3.21)$$

where u_j is any of the six unknown functions.

The solution of the initial value problem of the system of equations (3.21) has been studied by numerous authors. First existence and uniqueness were discussed in full (see K. O. FRIDRICHS [94], C. COURANT and LAX [95], HARTMAM and

H. WINTER [96]). Secondly to obtain solutions for given initial and boundary conditions in the practice, the method of finite differences is used.

According to COURANT and HILBERT [97] the characteristic directions are given by the equation:

$$\frac{dr}{dt} = \lambda$$

where λ are the solutions of the matrix equation

$$|\alpha_{ij} - \lambda\delta_{ij}| = 0 \tag{3.22}$$

For the system of equations (3.15) to (3.20) equation (3.22) gives the following six roots

$$\lambda_1 = 0, \quad \lambda_2 = 0, \quad \lambda_3 = 0, \quad \lambda_4 = 0$$
$$\lambda_5 = \sqrt{\frac{4\mu+3k}{3\rho}} \qquad \lambda_6 = -\sqrt{\frac{4\mu+3k}{3\rho}} \tag{3.23}$$

There is therefore a fourfold characteristic given by the equation

$$\frac{dr}{dt} = 0$$

and two additional distinct characteristics

$$\frac{dr}{dt} = +\sqrt{\frac{4\mu+3k}{3\rho}}$$

and

$$\frac{dr}{dt} = -\sqrt{\frac{4\mu+3k}{3\rho}}$$

The characteristic relation between the variables along the characteristic line $\frac{dr}{dt} = \lambda_k$ in the r-t plane is

$$\sum_{j=1}^{6} v_{kj}\left(\frac{\partial u_j}{\partial t} + \lambda_k \frac{\partial u_j}{\partial r}\right) + \sum_{i=1}^{6} v_{ki} b_i = 0 \qquad (3.24)$$

k equations, $\quad k = 1,2,\ldots,6$

where the coefficients v_{kj}, v_{ki} are the solution of the system of equations:

$$\sum_{i=1}^{6} v_{ki}\ \alpha_{ij} = \lambda_k v_{kj} \qquad (3.25)$$

k and j take values 1, 2, 3, 4, 5, and 6

Obviously the expression into parenthesis in eq. (3.24) involves differentiation in a single direction $\frac{dr}{dt} = \lambda_k$ because after the chain rule of differentiation the following relation can be written

$$\frac{\partial u_j}{\partial t} + \lambda_k \frac{\partial u_j}{\partial r} = \frac{\partial u_j}{\partial t} + \frac{dr}{dt}\ \frac{\partial u_j}{\partial r} = \frac{du_j}{dt}$$

Finally along the characteristics of the system of differential equations the following relations can be written:

1. Along $\frac{dr}{dt} = 0$

$$d\varepsilon_\theta = \frac{v}{r} = 0 \tag{3.26}$$

$$d\sigma_r + d\sigma_\theta + d\sigma_z = 3k\,(d\varepsilon_r + d\varepsilon_\theta) \tag{3.27}$$

$$\frac{1}{2\mu}(2d\sigma_r - d\sigma_\theta - d\sigma_z) = (2d\varepsilon_r - d\varepsilon_\theta) - \frac{m}{2\mu}\left\langle 1 - \frac{K}{\sqrt{II_s}}\right\rangle (2\sigma_r - \sigma_\theta - \sigma_z)dt \tag{3.28}$$

$$\frac{1}{2\mu}(-d\sigma_r + 2d\sigma_\theta - d\sigma_z) = (-d\varepsilon_r + 2d\varepsilon_\theta) - \frac{m}{2\mu}\left\langle 1 - \frac{K}{\sqrt{II_s}}\right\rangle (-\sigma_r + 2\sigma_\theta - \sigma_z)dt \tag{3.29}$$

2. Along $\frac{dr}{dt} = +\sqrt{\frac{4\mu+3k}{3\rho}}$

$$d\sigma_r - \rho\sqrt{\frac{4\mu+3k}{3\rho}}\,dv + \left\{ A + \sqrt{\frac{4\mu+3k}{3\rho}}\;\frac{\sigma_r - \sigma_\theta}{r} \right\} dt = 0 \tag{3.30}$$

3. Along $\frac{dr}{dt} = -\sqrt{\frac{4\mu+3k}{3\rho}}$

$$d\sigma_r + \rho\sqrt{\frac{4\mu+3k}{3\rho}}\,dv + \left\{ A - \sqrt{\frac{4\rho+3k}{3\rho}}\;\frac{\sigma_r - \sigma_\theta}{r} \right\} dt = 0 \tag{3.31}$$

where

$$A = \left(\frac{2}{3}\mu - k\right)\frac{u}{v} + \frac{m}{3}\left\langle -\frac{K}{\sqrt{II_s}}\right\rangle (2\sigma_r - \sigma_\theta - \sigma_z)$$

and

$$II_s = \frac{1}{9}\left\{ (2\sigma_r - \sigma_\theta - \sigma_z)^2 + (-\sigma_r + 2\sigma_\theta - \sigma_z)^2 + (-\sigma_r - \sigma_\theta + 2\sigma_z)^2 \right\}$$

Some additional remarks must be made about the physical meaning of the characteristic slopes. Using the values of λ given by the equations (3.23) the straight lines

$$r = r_o + \lambda_i t \qquad i = 1,2,\ldots 6$$

can be found. These lines represent the fronts of the travelling inelastic waves. The values λ_5 and λ_6 are equal to the dilation wave speed (for waves moving along the positive or negative r direction). This result should be expected since the deformation takes place on a plane and is a function of r only. No rotation therefore occurs during the deformation and the wave speed must be the irrotational wave speed. On the other hand the fourfold characteristic line $\lambda = 0$ does not represent travelling waves. The relations (3.26) to (3.29) represent relations between the unknowns on a steady wave or rather a local static deformation. Quoting R. J. CLIFTON [98] it can be said that "....the extra factor λ indicates a characteristic surface with zero velocity. It has no physical significance since it is known that the equations of elastodynamics do not yield a zero wave velocity, it is a consequence by introducing an additional dependent variable by choosing stresses and velocities as the dependent variables...".

It should be emphasized finally that the equations along the characteristic direction $\lambda = 0$ could be obtained from eqs. (3.7), (3.10), and (3.13) without the theory of hyperbolic differential equations since they involve differentiation with respect to one independent variable only.

5. Equations along the wave front

From the physical point of view a wave front traveling into an undisturbed medium may be considered as a moving surface of discontinuity. With this notion a model is defined here where waves are depicted as surfaces of discontinuity. Once this model is defined the theory of surfaces of discontinuity based on HADAMARD [99] and applied by ZIV [100], [101], [102] is introduced to present the discontinuity relations which hold across the wave surface.

The model to be considered is a surface $S(r,t)=0$ in the medium. Two basic conditions are imposed on this surface:

(a) It is required that this surface presents the locus of possible discontinuities in the first partial derivatives of the dependent variables appearing in the dynamic field equations (3.4), (3.6), (3.7), (3.10), and (3.13). The dependent variables themselves are assumed to be continuous everywhere, but differentiable only in regions which are in the rear and the front of the discontinuity surface. In that sense the wave is considered as a weak wave.

(b) It is required of the surface of discontinuity to present a wave surface in the sense that,while moving in the medium, it affects different material particles as it moves.

The figure 3.6 shows the traveling wave front in the r - t plane and the relationship between the dependent variables f (where f stands for any of the dependent variables σ_r, σ_θ, σ_z, ε_r, ε_θ, and v) and their first partial derivatives.

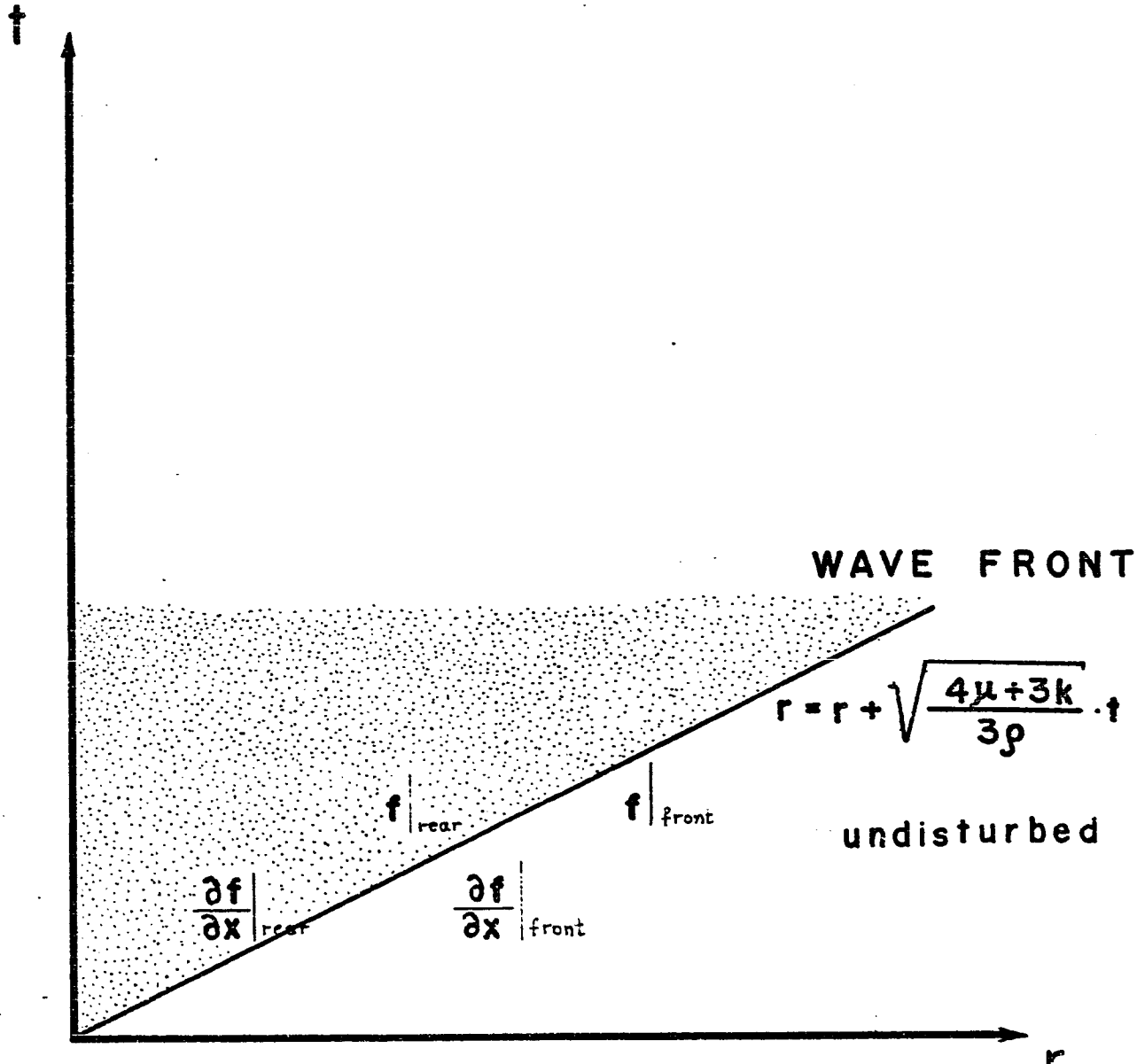

f stands for any of the variables

$$f|_{rear} = f|_{front} \qquad [f] = 0$$

$$\frac{\partial f}{\partial x}\Big|_{rear} \neq \frac{\partial f}{\partial x}\Big|_{front} \qquad \left[\frac{\partial f}{\partial x}\right] \neq 0$$

FIG. 3.6

The fact that a discontinuity in derivatives of the functions f persists at each instant t over a singular surface results in certain relations called conditions of compatibility. According to THOMAS [103] two kinds of discontinuities are to be presented in a wave problem. The kinematic discontinuity which connects the displacements only, i.e. strains and velocities, across the wave front and the dynamic discontinuity which is a relation between the velocity of each particle on the radial direction and the stresses developed on the wave front.

A brief discussion of the physical meaning of the discontinuity relations is given now similar to a presentation by HOPKINS [104] of the spherically symmetric problem. Under the present restrictions of cylindrically symmetric conditions any possible jumps in the physical quantities must necessarily take place across cylindrical surfaces concentric with the hole. Let S denote a cylindrical surface, say $r = r_1(t)$ and suppose that an isolated jump in at least one physical quantity, say $f(r,t)$, occurs everywhere across S. This discontinuity is to be regarded as the limit of a continuous distribution that changes by a definite amount across a thin cylindrical cell enclosing S as this cell everywhere shrinks up to S. The magnitude of the jump in f across S is defined as

$$[f] = f^+ - f^- \tag{3.32}$$

where

$$f^{\pm} = \lim_{r \to r_1 \pm 0} f(r,t) \tag{3.33}$$

The position of S will, in general, vary with t, and this variation may be presented by the curve

$$g(r,t) = r - r_1(t) = 0 \tag{3.34}$$

drawn in a plane in which r and t are taken as rectangular cartesian co-ordinates (see figure 3.7).

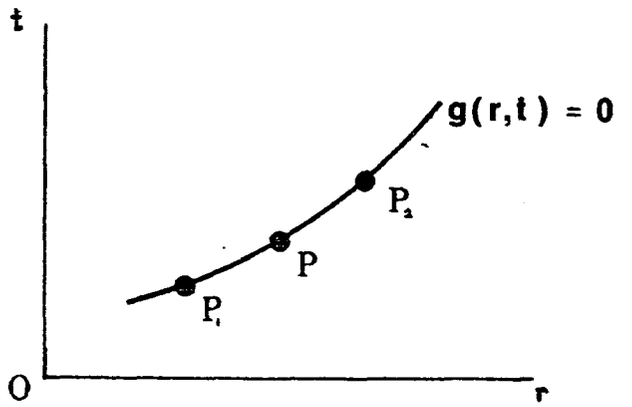

FIG. 3.7

For simplicity the arguments developed here will be largely formal, the exact statement of analytical conditions sufficient for the validity of the results being omitted.

Suppose that a physical quantity is continuous across S throughout some interval. Let p_1, p, p_2 be points, taken

in order on a small segment of g. Then

$$f_{p_1} = f_p = f_{p_2}$$

therefore

$$[f]_{p_1,p_2} = f_{p_1} - f_{p_2} = 0 \tag{3.35}$$

and hence

$$\frac{1}{\delta s} \left([f]_{p_2,p} - [f]_{p_1,p}\right) = 0 \tag{3.36}$$

where δ_s is the distance $p_1\ p_2$. Therefore, proceeding to the limit as $\delta_s \to 0$

$$\left.\frac{\partial f}{\partial s}\right|_{p^+} - \left.\frac{\partial f}{\partial s}\right|_{p^-} = \left[\frac{\partial f}{\partial s}\right] = 0 \tag{3.37}$$

(see also figure 3.6 and figure 3.7)

or from eq. (3.34)

$$\lambda\left[\frac{\partial f}{\partial r}\right] + \left[\frac{\partial f}{\partial t}\right] = 0 \tag{3.38}$$

where the above relation introduces also the wave speed λ.

Along the wave front λ, i.e. the speed of propagation of S, is given through the equation:

$$\lambda = \frac{dr_1}{dt}$$

Assuming as before (see (b) at the beginning of this section) that $\lambda \neq 0$ equation (3.38) gives

$$[\frac{\partial f}{\partial r}] = - \frac{1}{\lambda} [\frac{\partial f}{\partial t}] \neq 0 \qquad (3.39)$$

The fundamental restrictions on the jump permissible in various physical quantities will now be given.

First elastic/viscoplastic waves into an undisturbed (stress free) medium without fracture (i.e. separation of contiguous particles) requires particle displacements equal to zero immediately behind the wave front.

$$[u] = 0 \qquad (3.40)$$

Since according to eq. (3.7) $\varepsilon_\theta = u/r$ and since in the undisturbed region $u = 0$ it follows from eq. (3.40) and eq. (3.7) that on the wave front

$$\varepsilon_\theta = 0 \qquad (3.41)$$

Secondly the laws of conservation of mass and momentum show that

$$[\rho\ (v-\lambda)] = 0 \qquad (3.42)$$

and

$$[\sigma_r - \rho\, v(v-\lambda)] = 0 \qquad (3.43)$$

where v is the particle velocity. The remaining laws of conservation of energy and non decrease of entropy are not directly of interest here.

Consider now for the present problem f=u. From equation (3.39), because u=0 in front of the wave front, the following relation can be obtained:

$$\frac{\partial u}{\partial r} = -\frac{1}{\lambda}\frac{\partial u}{\partial t}$$

Or, because $\frac{\partial u}{\partial r}$ from eq. (3.7) is equal to ε_r and by definition $\frac{\partial u}{\partial t} = v$

$$\varepsilon_r = -\frac{1}{\lambda}v \qquad (3.44)$$

Therefore

$$\lambda\varepsilon_r + v = 0 \qquad (3.44a)$$

Also because $v << \lambda$ eq. (3.43) yields to the relation

$$\sigma_r + \rho v\lambda = 0 \qquad (3.45)$$

(Notice that the equation (3.45) comes from direct integration of eq. (3.31) as the time interval $dt \to 0$).

Assuming that $dt \to 0$ from equations (3.28) and (3.29) a relation between σ_r, σ_θ, and σ_z can be obtained

$$\sigma_\theta = \sigma_r \left(1 - \frac{2\mu}{\rho\lambda^2}\right) \tag{3.46}$$

$$\sigma_z = \sigma_r \left(1 - \frac{2\mu}{\rho\lambda^2}\right) \tag{3.47}$$

The relations (3.44), (3.45), and (3.47) indicate that σ_θ, σ_z, ε_r, ε_θ, and v along the wave front are given in terms of the radial component of the stress tensor σ_r.

It is of interest to notice that the deformation along the wave front is purely elastic. From eqs. (3.44) and (3.45)

$$\varepsilon_r = \frac{\sigma_r}{\rho\lambda^2}$$

The total strain can be decomposed in two parts

$$\varepsilon_r = \varepsilon_r^e + \varepsilon_r^{vp}$$

The elastic part can be calculated from HOOKE's law

$$\varepsilon_r^e = \frac{1}{E}\left(\sigma_r - \nu\sigma_\theta - \nu\sigma_z\right)$$

Using eqs. (3.46) and (3.47) for σ_θ and σ_z it can be shown that for the elastic component of ε_r the following relation holds

$$\varepsilon_r^e = \frac{\sigma_r}{\rho\lambda^2}$$

By combining equations (3.44), (3.45), (3.46), and (3.47) with equation (3.30) the following equation for σ_r can be obtained

$$2d\sigma_r + \left\{ A + \frac{\lambda}{r} (\sigma_r - \sigma_\theta) \right\} \frac{dr}{\lambda} = 0 \qquad (3.48)$$

where

$$A = (\frac{2}{3}\mu - k)\frac{u}{r} + \frac{m}{3} \left\langle 1 - \frac{K_0}{\sqrt{II_s}} \right\rangle (2\sigma_r - \sigma_\theta - \sigma_z)$$

Obviously A through II_s is a function of σ_r. From the definition of II_s in terms of the principal stresses of the deviatoric stress space

$$II_s = s_{rr}^2 + s_{\theta\theta}^2 + s_{zz}^2$$

where

$$s_{ij} = \sigma_{ij} - \frac{1}{3} \sigma_{kk} \delta_{ij}$$

using eqs. (3.46) and (3.47) the following relations for the principal stresses on the deviatoric stress space can be written

$$s_{rr} = \frac{4\mu}{3\rho\lambda^2} \sigma_r$$

$$s_{\theta\theta} = -\frac{2\mu}{3\rho\lambda^2} \sigma_r$$

$$s_{zz} = -\frac{2\mu}{3\rho\lambda^2}\,\sigma_r$$

and finally for II_s the relation given by eq. (3.49) can be obtained.

$$\sqrt{II_s} = \frac{\sqrt{24}\mu}{4\mu+3k}\,\sigma_r \qquad (3.49)$$

Using eq. (3.49) the eq. (3.48) can be written as follows

$$2d\sigma_r + \left\{\left(\frac{2}{3}\mu-k\right)\frac{u}{r} + \frac{m}{3}\left\langle 1 - \frac{4\mu+3k}{\sqrt{24}\,\mu}\frac{K_o}{\sigma_r}\right\rangle (2\sigma_r-\sigma_\theta-\sigma_z) + \right.$$

$$\left.\frac{\lambda}{r}(\sigma_r-\sigma_\theta)\right\}\frac{dr}{\lambda} = 0 \qquad (3.50)$$

this equation holds for $II_s \geq K_o^2$, i.e. $\frac{\sqrt{24}\,\mu}{4\mu+3k}\,\sigma_r \geq K_o$ or written in any other way

$$\sigma_r \geq \frac{4\mu+3k}{\sqrt{24}\,\mu}K_o$$

and

$$2d\sigma_r + \left\{\left(\frac{2}{3}\mu-k\right)\frac{u}{r} + \frac{\lambda}{r}(\sigma_r-\sigma_\theta)\right\}\frac{dr}{\lambda} = 0 \qquad (3.50a)$$

for

$$\sigma_r < \frac{4\mu+3k}{\sqrt{24}\mu}K_o$$

Equations (3.50) and (3.50a) can be written respectively

$$d\sigma_r + \frac{\sigma_r dr}{2r} + \frac{2}{3}\frac{\mu m}{\rho \lambda^3}\sigma_r dr - \frac{m K_o}{\sqrt{6}\,\lambda} dr = 0 \qquad (3.50b)$$

and

$$d\sigma_r + \sigma_r \frac{dr}{2r} = 0 \qquad (3.50c)$$

From the previous analysis it is obvious that yielding occurs whenever the second invariant of the deviatoric stress tensor is equal to K_o. In case of monoaxial tension the components of the deviatoric stress tensor are given by the following relations

$$s_{11} = \frac{2}{3}\sigma_{11}, \quad s_{22} = -\frac{1}{3}\sigma_{11}, \quad s_{33} = -\frac{1}{3}\sigma_{11}$$

and therefore

$$II_s = \frac{6}{9}\sigma_{11}^2$$

Assuming now that the monoaxial stress is equal to the yield stress in pure tension the following relation between K_o and σ_y can be obtained

$$II_s = K_o = \sqrt{\frac{2}{3}}\,\sigma_y$$

Introducing the new constants

$$A = \frac{1}{2}$$

$$B = -\frac{m K_o}{\sqrt{6}\,\lambda}$$

$$C = \frac{2}{3}\,\frac{\mu m}{\rho \lambda^3}$$

the differential equation (3.50b) or (3.50c) can be written as follows

$$r d\sigma_r + A\sigma_r dr + (Br + Cr\sigma_r)dr = 0 \qquad (3.50d)$$

or

$$r d\sigma_r + A\sigma_r dr = 0 \qquad (3.50e)$$

Equation (3.50e) represents the elastic part of the problem and the term $A\sigma_r dr$ is due to the geometric dispersion of the cylindrical waves. On the other hand the additional term in eq. (3.50d) , i.e. the term $Br + Cr\sigma_r$, represents the visco/plastic dispersion (notice that from the flow rule this additional term is always a positive decreasing function of r).

The solution of the eq. (3.50d) can be obtained by direct integration after a transformation to an exact differential by means of an integrating factor. The integrating factor h(r) is given by the following equation [1]

---

(1) See for example Morris Tenenbaum and Harry Pollard: "Ordinary Differential Equations", page 84.

$$\frac{dh(r)}{h(r)} = \frac{\frac{\partial}{\partial \sigma_r}(A\sigma_r+Br+Cr\sigma_r) - \frac{\partial}{\partial r}(r)}{r}\, dr$$

$$\frac{dh(r)}{h(r)} = \frac{A+Cr-1}{r}\, dr$$

therefore

$$h(r) = r^{A-1}e^{Cr}$$

Equation (3.50d) can be written in the following form using the previously found integrating factor h(r).

$$r^A e^{Cr} d\sigma_r + r^{A-1}e^{Cr}(A\sigma_r+Br+Cr\sigma_r)dr = 0 \qquad (3.50f)$$

The general solution of eq. (3.50f) is given by eq. (3.51)

$$\int_r^{\sigma_r} r^A e^{Cr} d\sigma_r + \int_{r_o}^{r} r^{A-1}e^{Cr}(Ap+Br+Crp)dr=0 \qquad (3.51)$$

or, after using the boundary condition that $\sigma_r=p$ at $r = r_o$

$$\sigma_r = p - \frac{Ap\int_{r_o}^{r} r^{A-1}e^{Cr}dr + (B+Cp)\int_{r_o}^{r} r^A e^{Cr}dr}{r^A e^{Cr}} \qquad (3.51a)$$

This solution holds from $r = r_o$ where $\sigma_r=p$ up to the radius r_y where $\sigma_r = \frac{4\mu+3k}{\sqrt{24\mu}} K_o$. After r_y, eq. (3.50e) describes the wave propagation of σ_r along the wave front and the fol-

lowing eq. (3.51b) gives σ_r as a function of the distance r from the center of the cylindrical cavity under the boundary condition that $\sigma_r = \frac{4\mu+3k}{\sqrt{24\mu}} K_o$ at $r = r_y$.

$$\sigma_r = \frac{4\mu+3k}{\sqrt{24\ \mu}} K_o \left(\frac{r_y}{r}\right)^{1/2}$$

From the previous discussion it is obvious that the solution given by eq. (3.51b) holds when the viscoplastic part of the strain is equal to zero. Also it has been shown that in any case the strains along the wave front are only elastic, i.e. $\varepsilon_r = \varepsilon_r^e$. It is therefore possible to consider the wave propagation for the wave front after the radius r as purely elastic. In chapter I it has been mentioned that for plane strain and under the same boundary conditions as in the present problem SELBERG presented a solution using transform techniques. Even though the method there is quite different from the present one, it is useful as a check. Eq. (3.51a) here is exactly the same as eq. (25) in SELBERG's paper.

A more detailed discussion of the features of the stress distribution along the wave front will be given in a later chapter. There (see figures 4.1 to 4.6) the influence of all the parameters involved will be fully investigated.

After the evaluation of σ_r along the wave front, σ_t, σ_z, ε_r, ε_t, and v can be found from eqs. (3.46), (3.47), (3.41), and (3.45). It is therefore possible to complete the solution

of the hyperbolic-type system of partial differential equations under any given boundary-initial conditions. This is done by a step by step numerical procedure in the r-t plane. A discussion of this method is given in the following section.

6. Numerical analysis

In the r - t plane the region between $r = r_o$ and $r = r_o + \lambda t$ is divided into a grid system by the three physical characteristics as shown in figure 3.10. The unknowns will be calculated at each one of these grid points, thus the continuous domain is replaced by discrete points.

In the region $r > r_o+\lambda t$ the stresses, strains, and the velocity are equal to zero. Along the straight line $r=r_o+\lambda t$ the stresses, strain, and the velocity are also zero if the initial input at $r = r_o$ is continuous (rather than a step input). If however a discontinuous input (step input) is applied at $r = r_o$ and $t = 0$ then the values of $\sigma_r(r,t)$, $\sigma_\theta(r,t)$, $\sigma_z(r,t)$, $\varepsilon_y(r,t)$, and $v(r,t)$ are different from zero along the wave front (ε_θ is always equal to zero anyway) and may be determined from eqs. (3.50) or (3.50a), (3.46), (3.47), (3.44) and (3.45).

Inside the wave front the finite difference approach is to be applied by means of a simplified version of the trapezoidal rule. In order to illustrate the necessity as well as the extent of this simplification the following differential form should be considered as a typical example of any one of the equations (3.26) to (3.31):

$$dz = f(z)dt \qquad (3.52)$$

where z represents any of the unknown variables. The function

f may as well depend on time or on any other of the unknowns z.

In a step by step numerical integration z and t are known at the previous point, say z_o, t_o, and by means of eq. (3.52) are to be found at a later point t.

A first order or linear approximation of z is given by eq. (3.53a)

$$z^1 = z_o + f(z_o)(t-t_o) \tag{3.53a}$$

representing a first approximation to the correct solution given by eq. (3.53b) below

$$z = z_o + \int_{t_o}^{t} f(x)dt \tag{3.53b}$$

Obviously z given by eq. (3.53b) can be found only if z were a known function of time. The question to be considered at this point is what can be a good approximation to the correct value of z at time t. Using eq. (3.53a) as the start point the following "predictor-corrector" method has been applied by means of eqs. (3.54)

$$z^2 = z_o + \frac{1}{2}\left\{ f(z_o)+f(z^1) \right\} (t-t_o)$$

$$z^3 = z_o + \frac{1}{2}\left\{ f(z_o)+f(z^2) \right\} (t-t_o)$$

. . . . . .

$$z = z_o + \frac{1}{2} \left\{ f(z_o) + f(z) \right\} (t-t_o) \qquad (3.54)$$

As the last of the eqs. (3.54) indicates, the iteration process stops at the point when successive approximations do not produce any significant change on z.

From the Taylor series expansion for z as a function of t at the point z_o, the following eq. (a) can be written

$$\text{(a)} \quad z = z_o + f(z)\Big|_{z_o} (t-t_o) + \frac{\partial f}{\partial z}\frac{\partial z}{\partial t}\Big|_{z_o} \frac{(t-t_o)^2}{2} + O\left((t-t_o)^3\right)$$

On the other hand, from the last of the eqs. (3.54) z is given through the equation (b), where a Taylor series expansion for f(z) has been used again.

$$\text{(b)} \quad z = z_o + \frac{1}{2} \left\{ f(z_o) + f(z_o) + \frac{\partial f}{\partial z}\Big|_{z_o} \frac{1}{2} \left\{ f(z_o) + f(z) \right\} (t-t_o) + \right.$$

$$\left. \frac{\partial^2 f}{\partial z^2}\Big|_{z_o} \frac{\frac{1}{4} \left\{ f(z_o) + f(z) \right\}^2 (t-t_o)^2}{2} + \cdots \right\} (t-t_o)$$

Finally, substituting for the second time f(z) with its Taylor series expansion, the following relation can be written

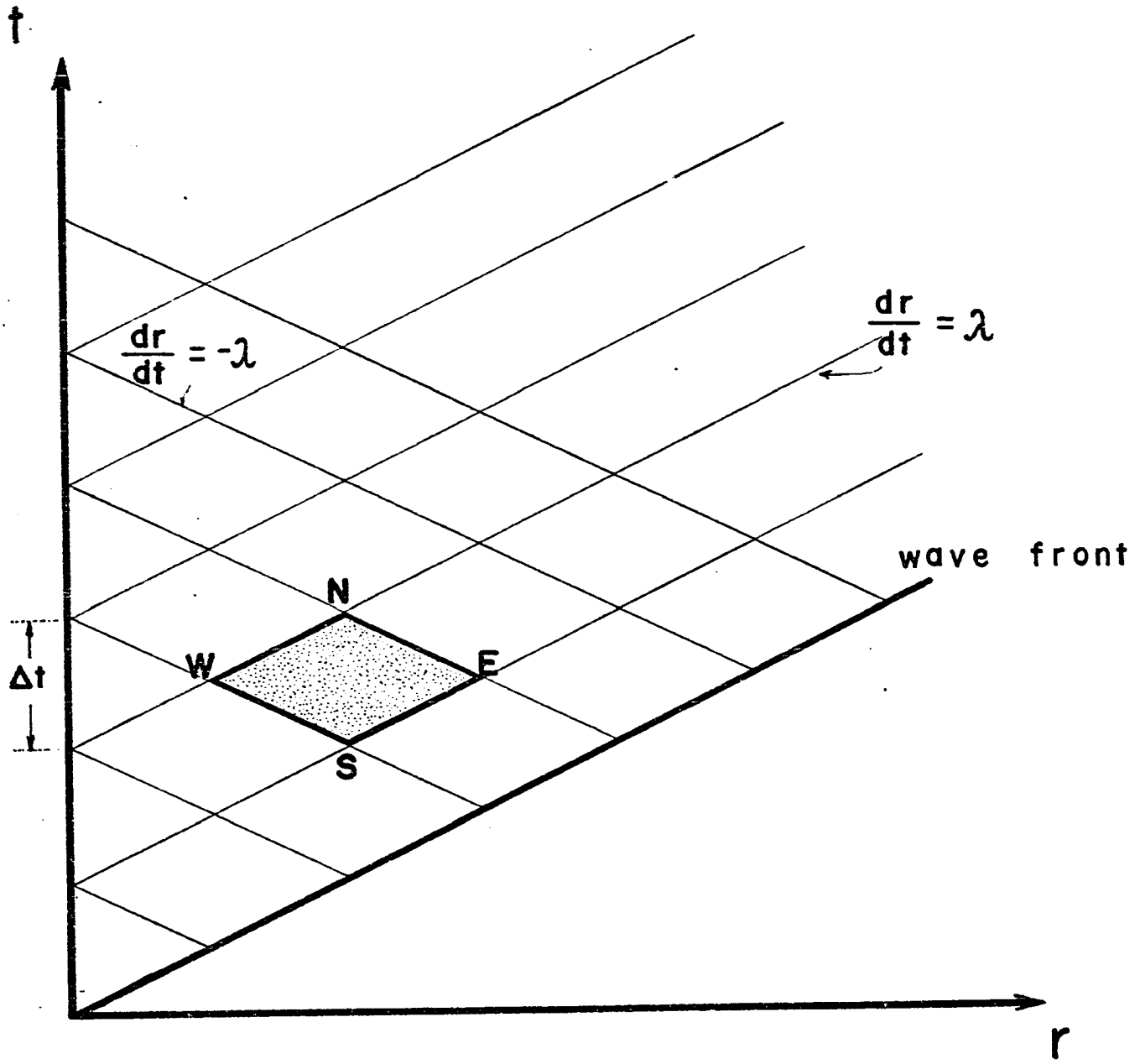

FIG. 3.8

$$(c) \quad z = z_o + f(z_o)(t-t_o) + \frac{1}{2}\left.\frac{\partial f}{\partial z}\right|_{z_o} f(z_o)(t-t_o)^2 + \cdots O\left((t-t_o)^3\right)$$

Comparison of eq. (c), where z is found through the iteration process, with (a), where the exact solution of the differential equation (3.52) is given in terms of a Taylor series, shows that the iterations increased the accuracy of the calculations by one order of magnitude compared with the solution given by eq. (3.53a) before the iterations. (The order of magnitude is expressed in terms of the power coefficient for the small quantity $t-t_o$). The application of the simplified version of the trapezoidal rule with the notation of figure 3.8 yields the following finite difference form of the original system of differential equations

$$\varepsilon_\theta^N - \varepsilon_\theta^S = \frac{\Delta t}{r^S} 2v^S \tag{3.55}$$

$$(\sigma_r^N - \sigma_r^S) + (\sigma_\theta^N - \sigma_\theta^S) + (\sigma_z^N - \sigma_z^S) = 3K \left\{ (\varepsilon_r^N - \varepsilon_r^S) + (\varepsilon_\theta^N - \varepsilon_\theta^S) \right\} \tag{3.56}$$

$$\frac{1}{2\mu} \left\{ 2(\sigma_r^N - \sigma_r^S) - (\sigma_\theta^N - \sigma_\theta^S) - (\sigma_z^N - \sigma_z^S) \right\} = \left\{ 2(\varepsilon_r^N - \varepsilon_r^S) - (\varepsilon_\theta^N - \varepsilon_\theta^S) \right\} \tag{3.57}$$

$$- \frac{m}{2\mu} \left\langle 1 - \frac{\kappa^S}{\left(\sqrt{II_S}\right)^S} \right\rangle (2\sigma_r^S - \sigma_\theta^S - \sigma_z^S) 2\Delta t$$

$$\frac{1}{2\mu}\left\{-(\sigma_r^N-\sigma_r^S)+2(\sigma_\theta^N-\sigma_\theta^S)-(\sigma_z^N-\sigma_z^S)\right\} = \left\{-(\varepsilon_r^N-\varepsilon_r^S)+2(\varepsilon_\theta^N-\varepsilon_\theta^S)\right\}$$

$$-\frac{m}{2\mu}\left\langle 1-\frac{\kappa^S}{\left(\sqrt{II_S}\right)^S}\right\rangle(-\sigma_r^S+2\sigma_\theta^S-\sigma_z^S)2\Delta t \qquad (3.58)$$

$$(\sigma_r^N-\sigma_r^W)-\rho\lambda(v^N-v^W)+\left\{A^W+\lambda\frac{\sigma_r^W-\sigma_e^W}{r^W}\right\}\Delta t = 0 \qquad (3.59)$$

$$(\sigma_r^N-\sigma_r^E)+\rho\lambda(v^N+v^E)+\left\{A^E-\lambda\frac{\sigma_r^E-\sigma_\theta^E}{r^E}\right\}\Delta t = 0 \qquad (3.60)$$

Where

$$A^W=\left(\frac{2}{3}-K\right)\frac{v^W}{r^W}+\frac{m}{3}\left\langle 1-\frac{\kappa^W}{\left(\sqrt{II_S}\right)^W}\right\rangle(2\sigma_r^W-\sigma_\theta^W-\sigma_z^W)$$

$$A^E=\left(\frac{2}{3}-K\right)\frac{v^E}{r^E}+\frac{m}{3}\left\langle 1-\frac{\kappa^E}{\left(\sqrt{II_S}\right)^E}\right\rangle(2\sigma_r^E-\sigma^E-\sigma_z^E) \qquad (3.61)$$

As it stated before, the application of the simplified trapezoidal rule introduces errors which can be eliminated to some extent by successive approximations through the iteration

scheme outlined at the beginning of this section. The system of equations (3.55) to (3.60) determines the values of the unknown functions $\sigma_r(r,t)$, $\sigma_\theta(r,t)$, $\sigma_z(r,t)$, $\varepsilon_r(r,t)$, $\varepsilon_\theta(r,t)$, and $v(r,t)$ at the point N (i.e. the unknowns are σ_r^N, σ_θ^N, σ_z^N, ε_r^N, ε_θ^N, and v^N) in terms of the final values that have been assigned to the same variables after the iteration process has been completed at the S, E, and W points. Equations (3.55) to (3.60) are respectively rewritten to include the iteration process in the following way:

$$ {}^{i}\varepsilon_\theta^N - {}^{\lambda}\varepsilon_\theta^S = \frac{\Delta t}{r^S}\left({}^{\lambda}v^S + {}^{i-1}v^N\right) \tag{3.62} $$

$$ \begin{aligned} &\left({}^{i}\sigma_r^N - {}^{\lambda}\sigma_r^S\right) + \left({}^{i}\sigma_\theta^N - {}^{\lambda}\sigma_\theta^S\right) + \left({}^{i}\sigma_z^N - {}^{\lambda}\sigma_z^S\right) = \\ &3K\left\{\left({}^{i}\varepsilon_r^N - {}^{\lambda}\varepsilon_r^S\right) + \left({}^{i}\varepsilon_\theta^N - {}^{\lambda}\varepsilon_\theta^S\right)\right\} \end{aligned} \tag{3.63} $$

$$ \begin{aligned} &\frac{1}{2\mu}\left\{2\left({}^{i}\sigma_r^N - {}^{\lambda}\sigma_r^S\right) - \left({}^{i}\sigma_\theta^N - {}^{\lambda}\sigma_\theta^S\right) - \left({}^{i}\sigma_z^N - {}^{\lambda}\sigma_z^S\right)\right\} \\ &= \left\{2\left({}^{i}\varepsilon_r^N - {}^{\lambda}\varepsilon_r^S\right) - \left({}^{i}\varepsilon_\theta^N - {}^{\lambda}\varepsilon_\theta^S\right)\right\} - \frac{m}{2\mu}\left\{\left\langle 1 - \frac{\kappa^S}{\lambda\left(\sqrt{II_S}\right)^S}\right\rangle\right. \\ &\left.\left(2{}^{\lambda}\sigma_r^S - {}^{\lambda}\sigma_\theta^S - {}^{\lambda}\sigma_z^S\right) + \left\langle 1 - \frac{{}^{i-1}\kappa^N}{{}^{i-1}\left(\sqrt{II_S}\right)^N}\right\rangle\left(2\,{}^{i-1}\sigma_r^N - {}^{i-1}\sigma_\theta^N - {}^{i-1}\sigma_z^N\right)\right\} \end{aligned} \tag{3.64} $$

$$\frac{1}{2\mu}\left\{-\left({}^{i}\sigma_r^N - {}^{\lambda}\sigma_r^S\right) + 2\left({}^{i}\sigma_\theta^N - {}^{\lambda}\sigma_\theta^S\right) - \left({}^{i}\sigma_z^N - {}^{\lambda}\sigma_z^S\right)\right\} = \left\{-\left({}^{i}\varepsilon_r^N - {}^{\lambda}\varepsilon_r^S\right)\right.$$

$$\left.+2\left({}^{i}\varepsilon_\theta^N - {}^{\lambda}\varepsilon_\theta^S\right)\right\} - \frac{m}{2\mu}\left\{\left\langle 1 - \frac{{}^{\lambda}\kappa^S}{{}^{\lambda}\left(\sqrt{II_S}\right)^S}\right\rangle\left(-{}^{\lambda}\sigma_r^S + 2{}^{\lambda}\sigma_\theta^S - {}^{\lambda}\sigma_z^S\right)\right.$$

$$\left.+\left\langle\frac{{}^{i-1}\kappa^N}{{}^{i-1}\left(\sqrt{II_S}\right)^N}\right\rangle\left(-{}^{i-1}\sigma_r^N + 2\,{}^{i-1}\sigma_\theta^N - {}^{i-1}\sigma_z^N\right)\right\} \qquad (3.65)$$

$$\left({}^{i}\sigma_r^N - {}^{\lambda}\sigma_r^W\right) - \rho\lambda\left({}^{i}v^N - {}^{\lambda}v^W\right) + \left\{{}^{\lambda}A^W + {}^{i-1}A^N + \lambda\,\frac{{}^{\lambda}\sigma_r^W - {}^{\lambda}\sigma_\theta^W}{r^W}\right.$$

$$\left.+\lambda\,\frac{{}^{i-1}\sigma_r^N - {}^{i-1}\sigma_\theta^N}{r^N}\right\}\frac{\Delta t}{2} = 0 \qquad (3.66)$$

$$\left({}^{i}\sigma_r^N - {}^{\lambda}\sigma_r^E\right) + \rho\lambda\left({}^{i}v^N - {}^{\lambda}v^E\right) + \left\{{}^{\lambda}A^E + {}^{i-1}A^N - \lambda\,\frac{{}^{\lambda}\sigma_r^E - {}^{\lambda}\sigma_\theta^E}{r^E}\right.$$

$$\left.-\lambda\,\frac{{}^{i-1}\sigma_r^N - {}^{i-1}\sigma_\theta^N}{r^N}\right\}\frac{\Delta t}{2} = 0 \qquad (3.67)$$

where i is the current number of iteration and λ is the final number of iterations.

The symbols ${}^{i}\sigma_r^N$, ${}^{i}\sigma_\theta^N$, ${}^{i}\sigma_z^N$, ${}^{i}\varepsilon_r^N$, ${}^{i}\varepsilon_\theta^N$, and ${}^{i}v^N$ indicate the intermediate values for σ_r^N, etc. after the i iteration and ${}^{\lambda}\sigma_r^S$, ${}^{\lambda}\sigma_\theta^S$, ${}^{\lambda}\sigma_z^S$, ${}^{\sigma}\varepsilon_r^S$, ${}^{\lambda}\varepsilon_\theta^S$, and ${}^{\lambda}v^S$ (the same for the E and W points) the final values for the unknowns when all the calculations have been completed in these points (i.e. after the λ iterations).

For i = 1 the first values for the unknown quantities at the point N have to be calculated from the eqs. (3.55) to (3.60) where the values used for the same unknowns at the points S, E, and W are the final ones.

7. Convergence and stability of the solution

In the stepwise numerical solution, one encounters the question of construction of finite difference systems, methods of solving them, their stability and their accuracy.

In the previous section a plausible procedure has been constructed for obtaining the solution of the finite difference system. Let y_j be this numerical solution and let $y_j^{k,\ell}$ be its value at the point k,ℓ in the r - t plane. In the present section the important question of whether these values actually represent a good approximation to the solution of the original differential equations at the grid points is to be considered.

For a better understanding of the notion of a "good" approximation according to B. CARNAHAN, H. A. LUTHER and J. O. WILKES [111] the following aspects of the numerical analysis should be considered.

1. The departure of the finite-difference approximation $y_j^{k,\ell}$ from the solution of the partial differential equation p_j due to the particular numerical solution procedure selected is to be considered. This is known as local d i s c r e t i z a t i o n e r r o r v (sometimes it is also called truncation). This error is produced by the nature of the approximations present in the numerical method and is independent of the computing equipment characteristics.

By definition

$$v_j = y_j^{k,\ell} - p_j \quad (k\Delta r, \ \ell\Delta t) \tag{3.68}$$

The finite difference method is said to converge if $v_j \to 0$ as the grid spacings Δr and Δt tend to zero.

2. The computational procedure is assumed to be capable of the exact representations of the solution of the finite difference equation. This is not quite true in the practice, since only a finite number of digits can be retained by the computer. This phenomenon introduces the so-called r o u n d - o f f - e r r o r . It should be emphasized however that this kind of error results from computing-machine design.

It has been said previously that the numerical approximation to the system of the partial differential equations must be convergent. The term convergent is understood to mean that the exact solution of the finite-difference problem (in the absence of round-off-errors) tends to the solution of the partial differential equation as the grid spacings in time and distance tend to zero. There are two concepts closely associated with a particular finite-difference procedure, namely, those of consistency and stability.

Referring to a certain computational procedure, the term stability denotes a property of the particular finite-difference equations used as the time increment is made vanishingly small. It means that there is an upper limit to the extent to which any error can be amplified in the compu-

tations. The term consistency, on the other hand, means that the procedure used in the numerical analysis, in fact, approximates the problem under study and it is not the solution of some other system of partial differential equations.

The error definition, given by eq. (3.68), arises therefore through the following two basic questions, according to RICHTMYER [112].

1. What is the behavior of $|y_j^{k,\ell} - p_j(k\Delta r, \ell\Delta t)|$ as $\ell \to \infty$ for fixed $k\Delta r$ and Δt?

2. What is the behavior of $|y_j^{k,\ell} - p_j(k\Delta r, \ell\Delta t)|$ as the mesh size is refined, i.e. as $\Delta t \to 0$ for a fixed value of $k\Delta r$ and t (t is equal to $\ell\Delta t$ originally).

For both questions the number of cycles of the calculation becomes infinite in the limit and there is a possibility of unlimited amplifications of the errors. The first question deals with the stability of the method for larger time intervals and the second with the accuracy of the solution as the net of points along the characteristics is refined and the number of calculations in order to get $y_j^{k,\ell}$ at a given point $r = k\Delta r$ increases.

The second question is to be considered first in a way similar to the one introduced by R. MENGI and H. D. Mc NIVEN [115] which is in fact a simplification of a more general case discussed by R. COURANT, E. ISAACSON and M. REES [116].

According to the previous derivations in the sections 5 and 6, the equations along the characteristics can be

written in the following general form

$$a_{ij} \frac{du_j}{dt} = b_{ij} u_j \tag{3.69}$$

This is the i equation of the system, summation on j is understood and the symbol u_j stands for any of the unknown functions. Equation (3.69) holds along the characteristic direction defined by the following equation

$$\frac{dr}{dt} = c_i$$

where for the present problem c_i takes the following values

for i = 1 $\qquad c_1 = \sqrt{\frac{4\mu+3k}{3\rho}}$

for i = 2 $\qquad c_2 = -\sqrt{\frac{4\mu+3k}{3\rho}}$

for i = 3, 4, 5, and 6 $\qquad c = 0$

Let as before y_j be the solution of the finite difference equations that correspond to the system of equations given by eq. (3.69), then by definition it must be

$$a_{ij} \frac{y_j(A) - y_j(A_i)}{s_i \Delta t} = b_{ij} y_j(A) \tag{3.70}$$

where A is any point in the r - t plane. For s_i, as figure 3.8 shows, the following relations hold

for i = 1,2 $\quad s_i = 1$

for i = 3,4,5, and 6 $\quad s_i = 2$

Also it should be noticed that the definition of the derivative used in eq. (3.70) in connection with the directions of the characteristics given by c_i in figure 3.10 requires that the point A_i has as coordinates:

$(k-1)\Delta r,\ (\ell-1)\Delta t$ $\quad$ for i = 1

$(k+1)\Delta r,\ (\ell-1)\Delta t$ $\quad$ for i = 2

$k\Delta r,\ (\ell-1)\Delta t$ $\quad$ for i = 3, 4, 5, and 6

From equation (3.70) the following relation can be obtained:

$$a_{ij}y_j(A) = s_i\Delta t\ b_{ij}y_j(A) + a_{ij}y_j(A_i) \qquad (3.71)$$

(there is no summation on the i symbol)

Let p_j be the exact solution of the equation (3.69) i.e. according to the definition of the derivative

$$a_{ij}\frac{p_j(A)-p_j(A_i)}{s_i\Delta t} + O_i(\Delta t) = b_{ij}p_j(A) \qquad (3.72)$$

where $O_i(\Delta t)$ represents a quantity, generally depending on the equation i of the system (3.69) as well as on the particular point A under consideration which goes to zero as Δt goes to zero.

From equation (3.72) it follows that

$$a_{ij}p_j(A) = s_i\Delta t\, b_{ij}p_j(A) + a_{ij}p_j(A_i) + O_i(\Delta t^2) \qquad (3.73)$$

(there is no summation on i)

Taking the difference of equations (3.71) and (3.73) the following equation can be written

$$a_{ij}v_j(A) = s_i\Delta t b_{ij}v_j(A) + a_{ij}v_j(A_i) + O_i(\Delta t^2) \qquad (3.74)$$

or, written in any other way

$$a_{ij}v_j^{k,\ell} = s_i\Delta t b_{ij}v_j^{k,\ell} + a_{ij}v_j^{k,\ell-2} + O_i(\Delta t^2) \qquad (3.74a)$$

for i = 3, 4, 5, and 6

or

$$a_{ij}v_j^{k,\ell} = s_i\Delta t b_{ij}v_j^{k,\ell} + a_{ij}v_j^{k+1,\,\ell-1} + O_i(\Delta t^2) \qquad (3.74aa)$$

for i = 2

and

$$a_{ij}v_j^{k,\ell} = s_i\Delta t b_{ij}v_j^{k,\ell} + a_{ij}v_j^{k-1,\,\ell-1} + O_i(\Delta t^2) \qquad (3.74aaa)$$

for i = 1

From the previous equations taking the absolute value in both sides, the following relation can be obtained:

$$|a_{ij}v_j^{k,\ell}| \leq s_i\Delta t|b_{ij}v_j^{k,\ell}| + |\alpha_{ij}v_j^{-,-}| + |O_i(\Delta t^2)| \qquad (3.75)$$

where the term $a_{ij}v_j^{-,-}$ stays for $a_{ij}v_j^{k,\ell-2}$ or $a_{ij}v_j^{k-1,\ \ell-1}$ or $a_{ij}v_j^{k+1,\ \ell-1}$ pending on i.

At this point it is necessary to introduce a measure of the error. This is done in a rather arbitrary way through the following equation

$$E^{k,\ell} = \max_i |a_{ij}v_j^{k,\ell}|$$

where the error is defined as the maximum value of $a_{ij}v_j^{k,\ell}$ over all the equations i of the given system of differential equations.

From the previous equations, the following expression for the error can be written

$$E^{k,\ell} \leq t\beta_1 E^{k,\ell} + E^{-,-} + \beta_2\Delta t^2 \qquad (3.76)$$

where $E^{-,-} = E^{k,\ell-2}$, $E^{k-1,\ \ell-1}$, $E^{k+1,\ \ell-1}$

$$\beta_1 = \frac{s_i |b_{ij} v_j^{k,\ell}|}{|a_{ij} v_j^{k,\ell}|}$$

and

$$\beta_2 = \frac{|O_i(\Delta t^2)|}{\Delta t^2}$$

Obviously from the above definitions both β_1 and β_2 are positives. Finally eq. can be written in the following form

$$E^{k,\ell}(1-\beta_1\Delta t) \leq \beta_2\Delta t^2 + E^{-,-} \qquad (3.77)$$

Starting from the given boundary and initial conditions and applying eq.(3.77) $1-\ell$ times along the characteristics eq. (3.78) can be obtained

$$E^{k,\ell} < \frac{\beta_2\Delta t^2}{1-\beta_1\Delta t} \sum_{n=0}^{\ell=1} \frac{1}{(1-\beta_1\Delta t)^n} \qquad (3.78)$$

or

$$E^{k,\ell} < -\frac{\beta_2\Delta t}{\beta_1} \left\{ 1 - \left(\frac{1}{1-\beta_1 t} \right)^{\ell} \right\} \qquad (3.78a)$$

Equation (3.79) introduces the new quantity $H^{k,\ell}$:

$$H^{k,\ell} = -\frac{\beta_2\Delta t}{\beta_1} \left\{ 1 - \left(\frac{1}{1-\beta_1\Delta t} \right)^{\ell} \right\} \qquad (3.79)$$

For fixed values of r,t and taking the limit of eq. (3.79) as ℓ goes to the infinity (this is equivalent to saying that $\Delta t \to 0$) the following relation can be found

$$\lim_{\ell\to\infty} H^{k,\ell} = -\lim_{\ell\to\infty} \frac{\beta_2 t}{\beta_1 \ell} \left\{ 1 - \left(\frac{1}{1-\beta_1 \frac{t}{\ell}} \right)^{\ell} \right\}$$

$$= -\lim_{\ell\to\infty} \frac{\beta_2 t}{\beta_1 \ell} \cdot \lim_{\ell\to\infty} \left\{ 1 - \left(\frac{1}{1-\beta_1 \frac{t}{\ell}} \right)^{\ell} \right\}$$

$$= 0$$

because $\lim_{\ell\to\infty} \frac{\beta_2 t}{\beta_1 \ell}$ is zero and $\lim_{\ell\to\infty} (1 - \frac{\beta_1 t}{\ell})^{\ell} = e^{-\beta_1 t}$

The previous derivation leads to the conclusion that, for a fixed point (r,t) on the r - t plane, the error becomes zero as the mesh size goes to zero. Hence, the convergence of the numerical procedure used in this dissertation is established.

Finally, it is necessary to obtain the maximum value of the time increment Δt that will preserve the stability of the calculations done with the computer. This is particularly important since, even if for $\Delta t \to 0$ the convergence of the finite difference scheme to the exact solution has been established, "it can happen", according to Richtmyer [1], "that for the finite

[1] For more details, see Richtmyer [112] page 270.

Δt used in practice the errors are nevertheless unacceptably amplified".

From equations (3.62) to (3.67) we observe that the coefficients of the unknowns are nonlinear. Then, according to Fox [108] (page 183), the best way to solve our problem of stability is to experiment with several different time increments. Using this practical criterion we realized at an early stage that the accuracy of the approximation and not the stability of the computations was the principal criterion that governed the choice of the maximum Δt. In fact, we observed that the solution remained stable for time increments Δt well above any reasonable upper limit imposed on these increments by requirements of accuracy.

C H A P T E R IV

DISCUSSION OF RESULTS

1. Introduction

The type of loading considered was that of a constant radial stress suddenly applied on the surface of a cylindrical cavity. Initially the material was assumed to be at rest and stress free. At time t = 0, a symmetrically distributed pressure p was applied. Thereafter it was assumed that the radial stress on the surface of the cavity remained constant. The stress-time diagram shown in the following figure was the boundary condition throughout the entire transient phenomenon.

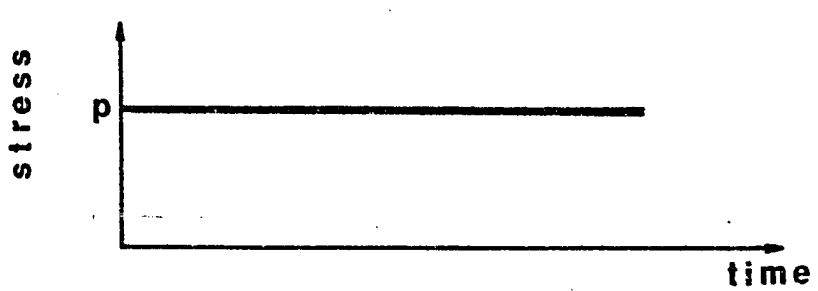

Stress-time curve at the surface of the cylindrical cavity.

As a consequence of this boundary condition, cylindrical waves travelled inside the elastic/viscoplastic solid. The purpose of this chapter is to describe these waves and to study the influence of the several parameters involved in their propagation.

The major features to be discussed in this study are two in number. First the wave front, i.e., the solution along the first characteristic line. From the experimental viewpoint this part of the solution is very important since it prescribes the optimum dimensions for the specimens and predicts the order of magnitude of the measurements that should be made. The second feature concerns the stress and strain histories at selected points within the inelastic solid. Figures will be shown that describe stresses, strains and velocities as functions of time. This will be done for a wide range of values for the several parameters involved, i.e. applied pressure p, viscosity coefficient m, strain hardening ratio E_1/E_o, etc. On the basis of these curves, an attempt will be made to understand better the influence of the previously mentioned parameters on the transient phenomenon.

An interesting aspect of this investigation is the comparison of the second invariant of the deviatoric stress tensor to the radius of the yield surface in the deviatoric stress space. The magnitude of p will be such that inelastic flow at the surface of the cylindrical cavity may or may not occur (i.e. according to the loading/unloading criterion at $r = r_o$ we may have $II_s \gtrless K_o^2$). However, for any given p, there is

always a cylindrical surface of radius r_p within the solid, such that for $r > r_p$, because of the decay of stresses due to geometrical dispersion, only elastic deformations take place. On the other hand, we will observe that at a later time a second elastic region is formed inside the inelastically deforming region. This second elastic region expands towards the cylindrical cavity on one side, and towards the original elastic region on the other.

Unless otherwise stated, the material data used for the computations throughout this study are those of aluminum

Density	$2.585 \ 10^{04}$ lbs sec^2/in^4
Poisson's ratio	0.3 - 0.34
Young's modulus	10^7 psi
Yield stress in pure tension	2200 psi
Viscosity coefficient	10^5 - 10^7 sec^{-1}

The radius of the cylindrical cavity is assumed equal to 1 inch.

Finally, we will select the time increment Δt (i.e. the distance between any two characteristic lines in figure 3.8). Obviously, this choice will effect the accuracy of the calculations, since all the errors introduced from the approximations associated with the trapezoidal rule are proportional to the mesh size.

POINT 1

Grid size Δt

10^{-7} sec	2.10^{-7} sec	4.10^{-7} sec
0.10837917	0.10891262	0.10997655
0.09780006	0.09833820	0.09947675
0.08988228	0.09027536	0.09145442
0.08330999	0.08367844	0.08512780

POINT 2

Grid size Δt

10^{-7} sec	2.10^{-7} sec	4.10^{-7} sec
0.12963571	0.12963281	0.12962808
0.10799135	0.10828167	0.11011777
0.09711456	0.09723279	0.09793461

Table 2

Results of calculations are shown in Table 2. They show the influence of grid size upon the accuracy of numerical results. The computed stresses at two locations within the infinite medium are given for several instants of time. For this comparison two representative points of the r-t plane were selected. Similar comparisons were made at several other points of the r-t plane. Based upon these studies, a time increment of $\Delta t = 2.10^{-7}$ sec was selected. It is felt that this value provides the best compromise between the desire for accuracy and our unwillingness to compute an unrealistic number of points.

2. The Wave Front

Figures 4.1 to 4.4 describe the behavior of σ_r as a function of radius r along the first characteristic line. It is evident from the solution of equation (3.50d) (or eq. (3.50e)) that σ_r is a function only of r, m, and p. Equations (3.45), (3.46) and (3.47) show that a linear relationship exists between σ_r, σ_θ, σ_z, ε_r and v (ε_θ is always equal to zero) at any point r along the first characteristic. Because of this linear relationship, the above figures can be used to represent the strength of the discontinuities in σ_θ, σ_z, ε_r, and v across the wave front merely by a change of scale. Then the magnitude of each dependent variable is given on a function of its corresponding original value at the surface of the cylindrical cavity at time t = 0.

First, it should be noticed that the leading wave is purely elastic. Consequently, the work hardening parameter does not affect the solution. It is therefore possible to use figures 4.1 to 4.4 in connection with any of the three elastic/viscoplastic materials presented in figures 3.13 to 3.15.

Secondly, we should recall that from equation (3.49) a linear relationship between the magnitude of the deviatoric stress tensor and σ_r has been established. There is therefore a critical value of σ_r, called $\sigma_{r,crit}$, such that the second invariant of the deviatoric stress tensor will become equal to K_o^2 whenever along the wave front the radial com-

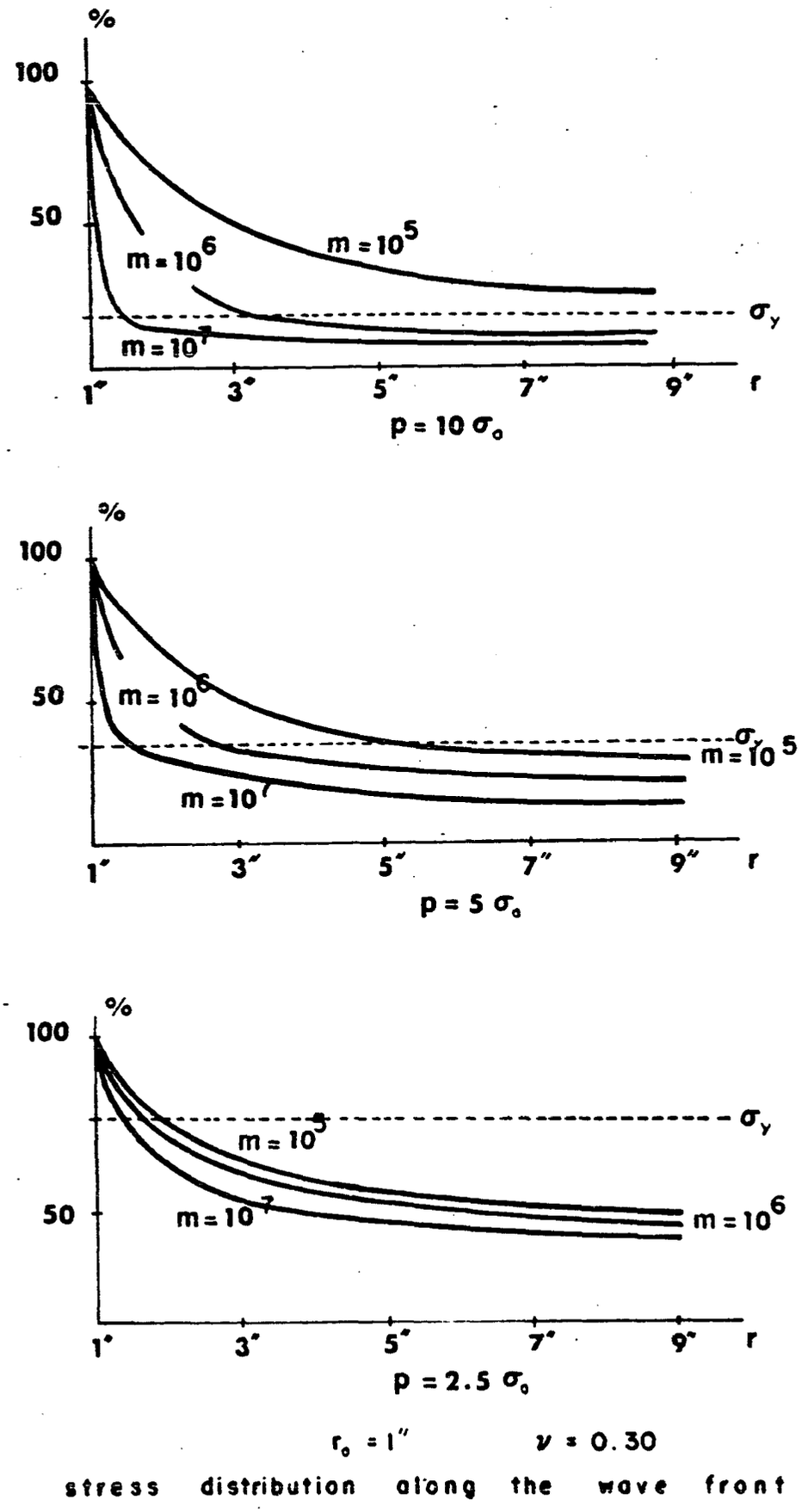

$r_o = 1''$ $\nu = 0.30$

stress distribution along the wave front

FIG. 4.1

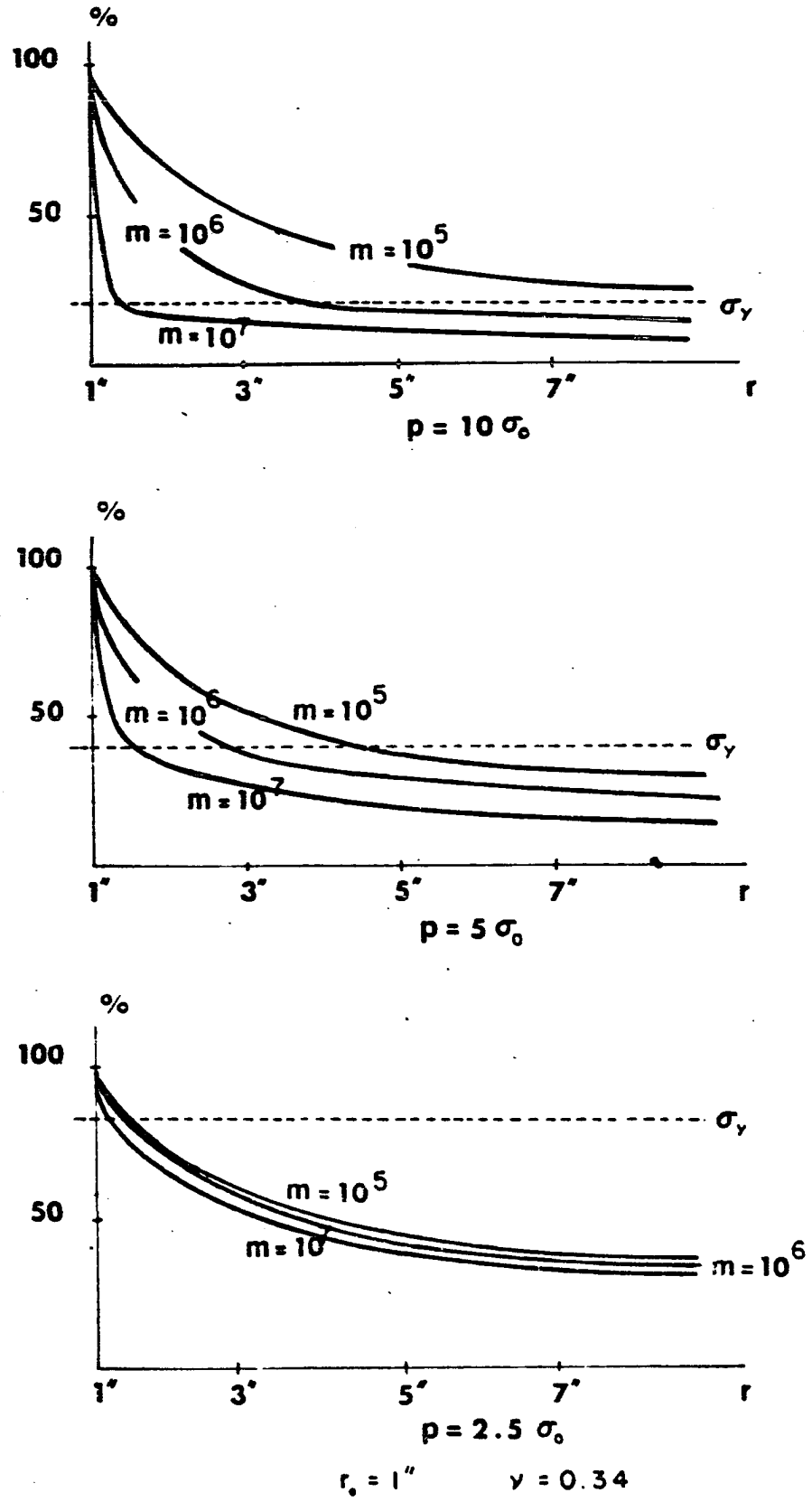

stress distribution
along the
wave front

FIG. 4.2

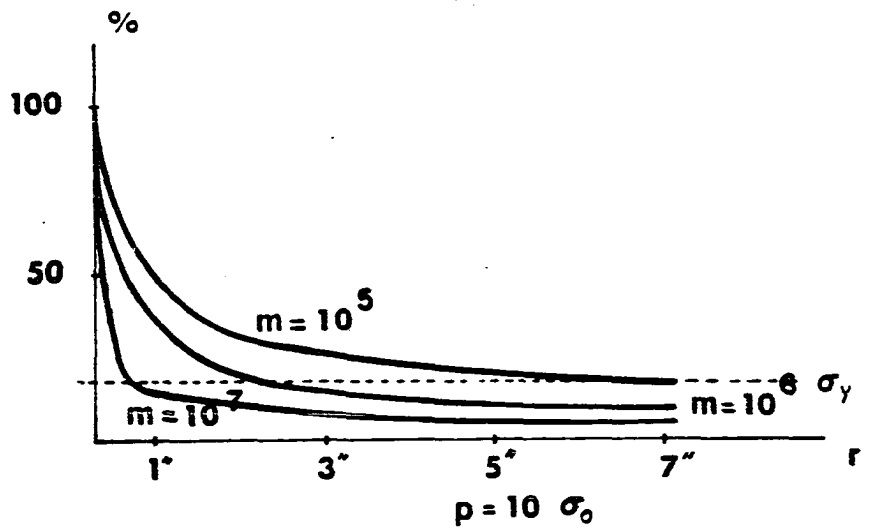

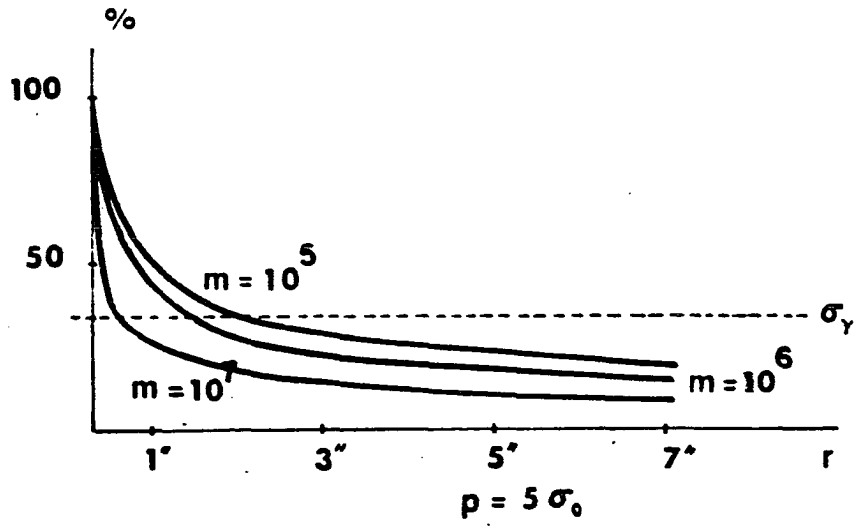

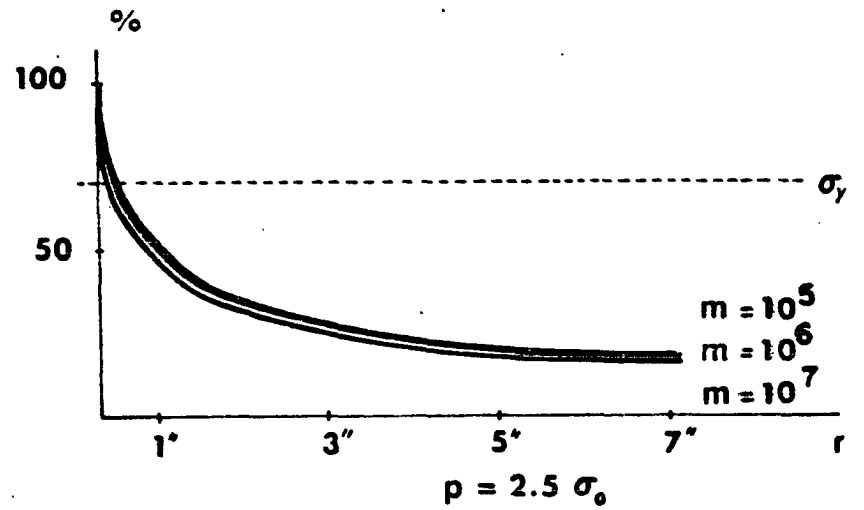

$r_0 = 0.25''$ $\nu = 0.30$

stress distribution along the wave front

FIG. 4.3

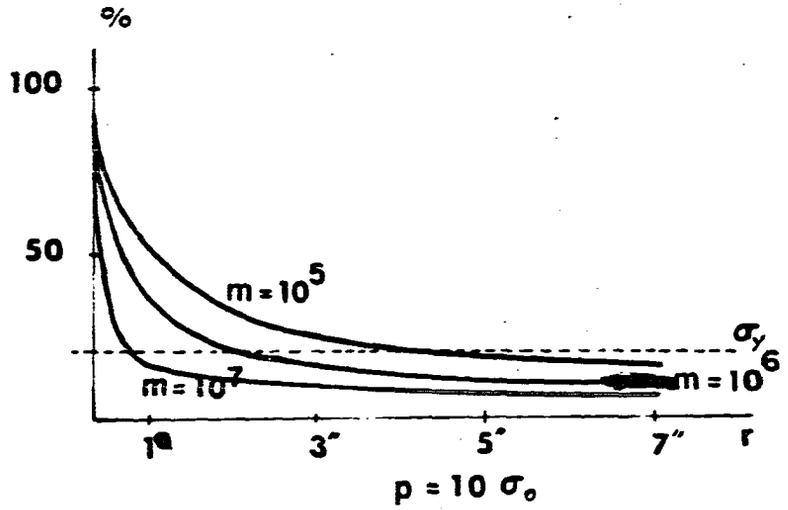

$p = 10\ \sigma_o$

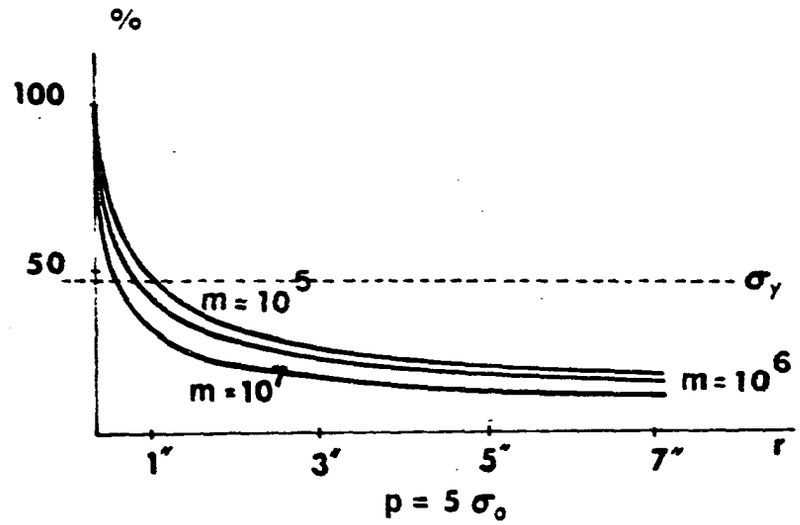

$p = 5\ \sigma_o$

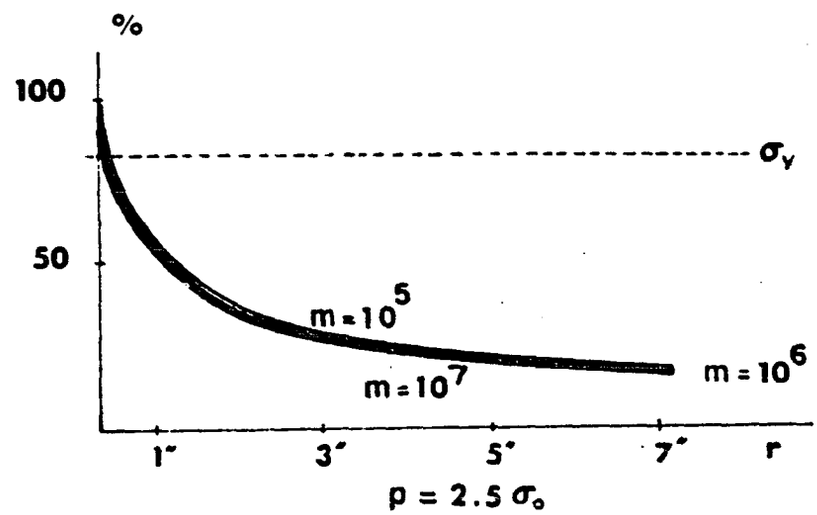

$p = 2.5\ \sigma_o$

$r_o = 0.25"$ $\quad \nu = 0.34$

stress distribution along the wave front

FIG. 4.4

ponent of stress is equal to $\sigma_{r,crit}$. Figures 4.1 to 4.4 show that σ_r is a decreasing function of r. There is therefore always a distance r_y (that depends on p and ν) with the following properties.

1. at $r = r_y$ $II_s = \frac{2}{o}$
2. for $r > r_y$ the solution becomes independent of m.

Thirdly, the influence of the viscosity coefficient on the decay of the dependent variables can be deduced from any of the previously mentioned figures. It is shown there, that the magnitude of the discontinuity is a decreasing function of r and vanishes as r tends to infinity. The rate of decrease is a decreasing function of m. This influence is most pronounced in a small region near the surface of the cylindrical cavity and is very severe in this region. Unless the impact load is "greatly" in excess of the $\sigma_{r,crit}$, viscous effects will not be significant outside the "immediate vicinity" at the cavity. (see figures 4.1 to 4.4 for estimates of "greatly" and "immediate vicinity").

Fourthly, the influence of the radius r_o of the cavity on the solution can be obtained by comparing either figures 4.1 and 4.3 or figures 4.2 and 4.4. For any p, m, and r, a decrease in r_o produces a corresponding decrease in the size of the region where stress decay along the wave front is very severe. Upon lowering p to values close to $\sigma_{r,crit}$, the effects of the viscosity coefficient can be eliminated by using a sufficiently small radius r_o.

Finally, we will associate with every point (i.e., distance r) within the elastic/viscoplastic material, the notion of the "instantaneous strength". This is the minimum pressure p that should be applied on the surface of the cavity in order to have σ_r on the wave front equal to $\sigma_{r,crit}$ (i.e., yield takes place at the point r whenever the wave front reaches this point). Obviously the "instantaneous strength" depends on ν and r_o. Figures 4.5 and 4.6 present the "instantaneous strength" as a function of m. There it is shown that the "1.s." is an increasing function of m as we should expect,since m increases the ratio of decay for σ_r along the wave front. We also observe that it is an increasing function of r and ν.

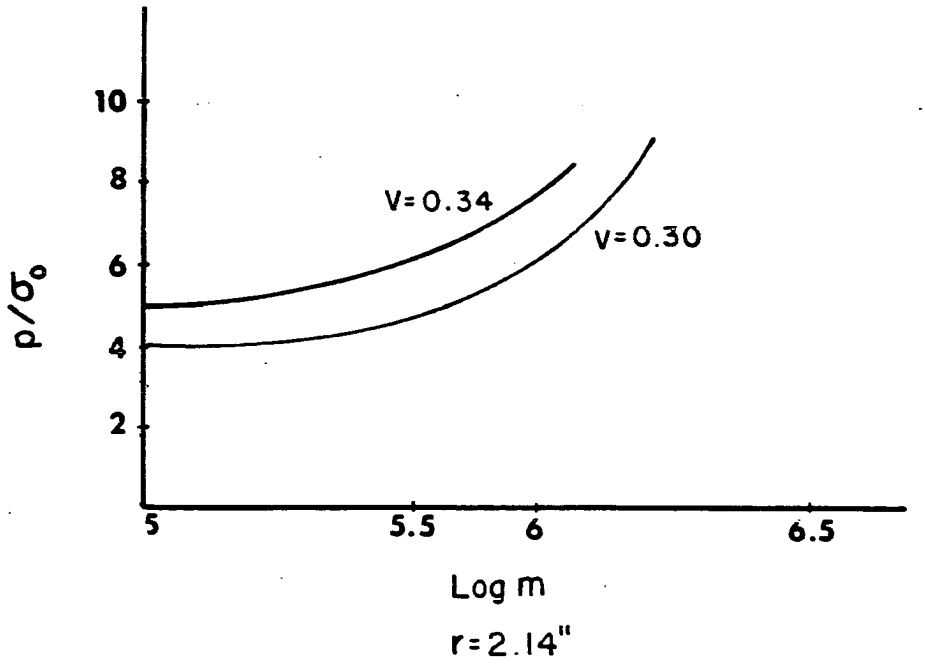

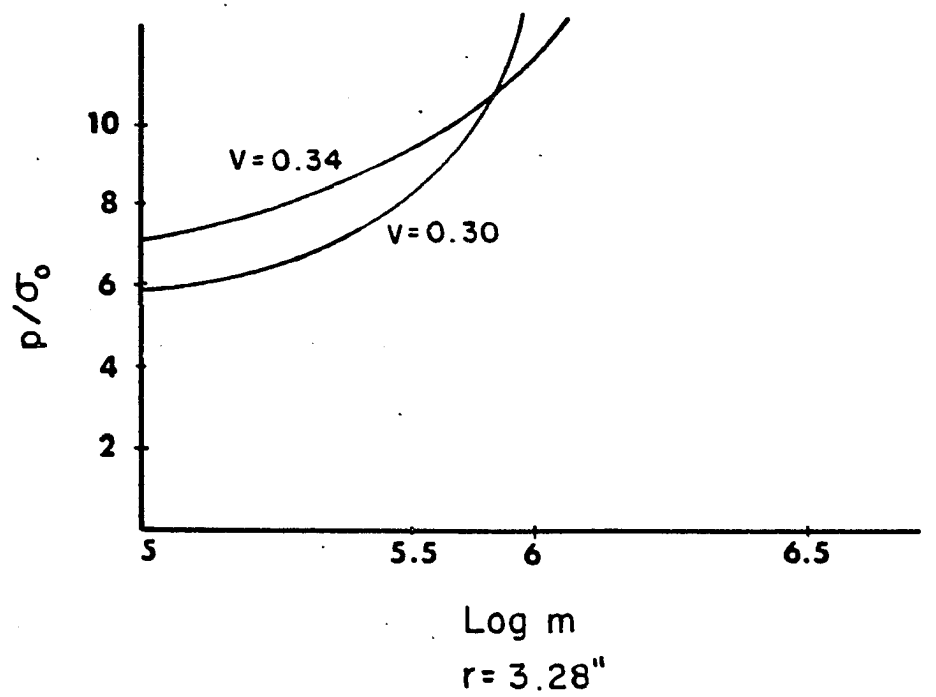

Instantaneous strength

FIG. 4.5

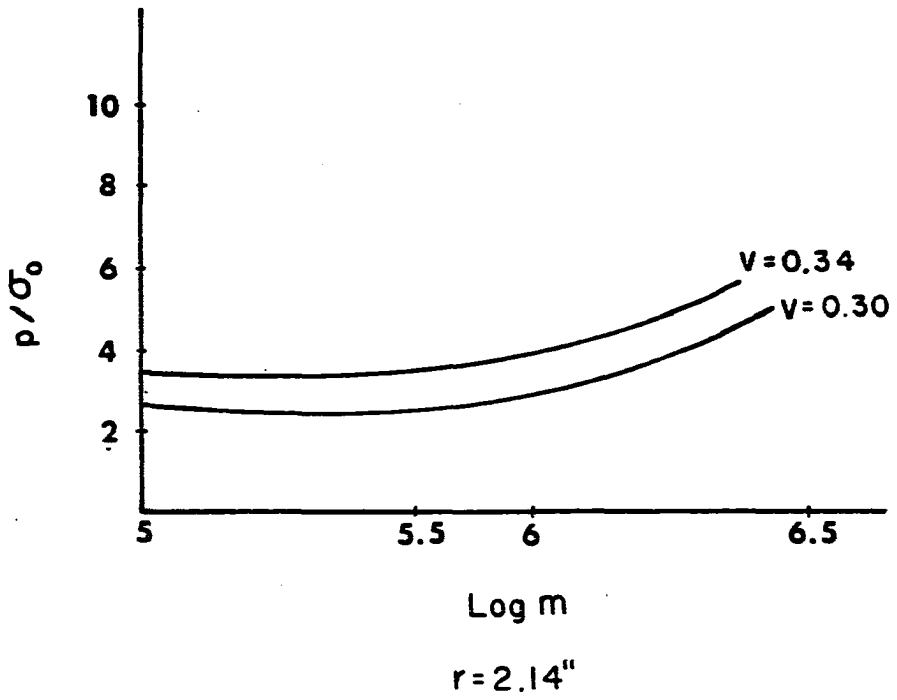

r=2.14"

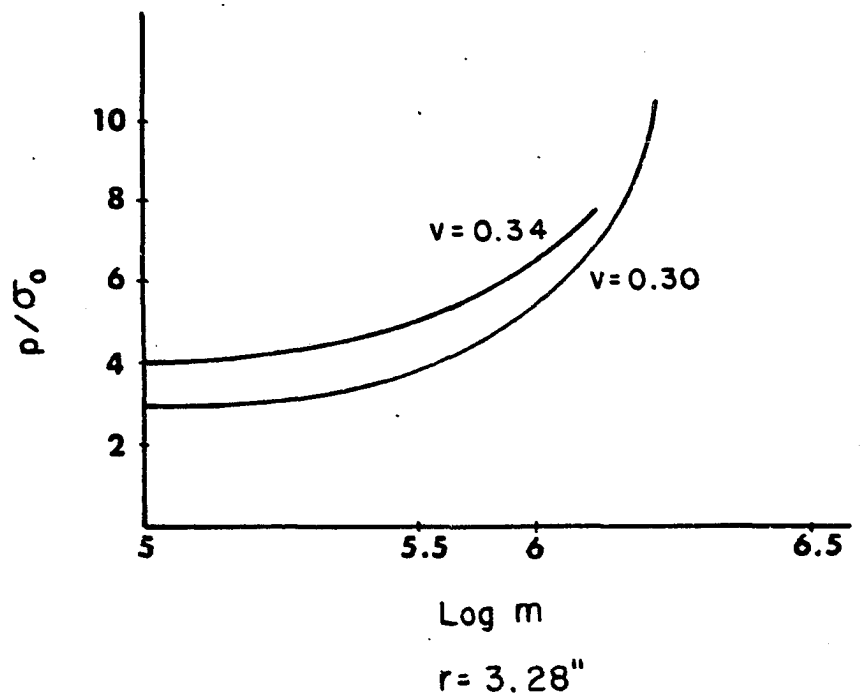

r= 3.28"

Instantaneous strength

FIG. 4.6

3. Stress and strain histories

The time histories of the dependent variables (σ_r, σ_1, σ_2, ε_r, and ε_t) are presented in the following figures 4.7 through 4.12 for a value of the viscosity coefficient m equal to 10^6, the working hardening parameter $E_1/E_2 = 0.25$, and applied pressure $p = 10\sigma_o$. This is done for three points ($r = 1.27"$, $r = 1.54"$, and $r = 3.43"$) inside the medium. It is shown there that the dependent variables decrease from their initial values (i.e., the values at the moment when the traveling wave reaches the corresponding point) and reach a local minimum after about 5μ sec. Thereafter they start increasing and finally reach their final value after about 30μ sec. A comparison between the values associated with the points $r = 1.27"$ and $r = 3.43"$ shows the influence of the dispersion on the cylindrical viscoplastic waves.

Now we will examine the influence of m and E_1/E_o on the dependent variables. This will be shown for the radial stresses in figures 4.12, 4.13 and 4.14.

The influence of the viscosity coefficient for a given pressure and work hardening parameter is shown in figure 4.12. There it is shown that, as m decreases, the corresponding values of σ_r decrease as the result of a larger

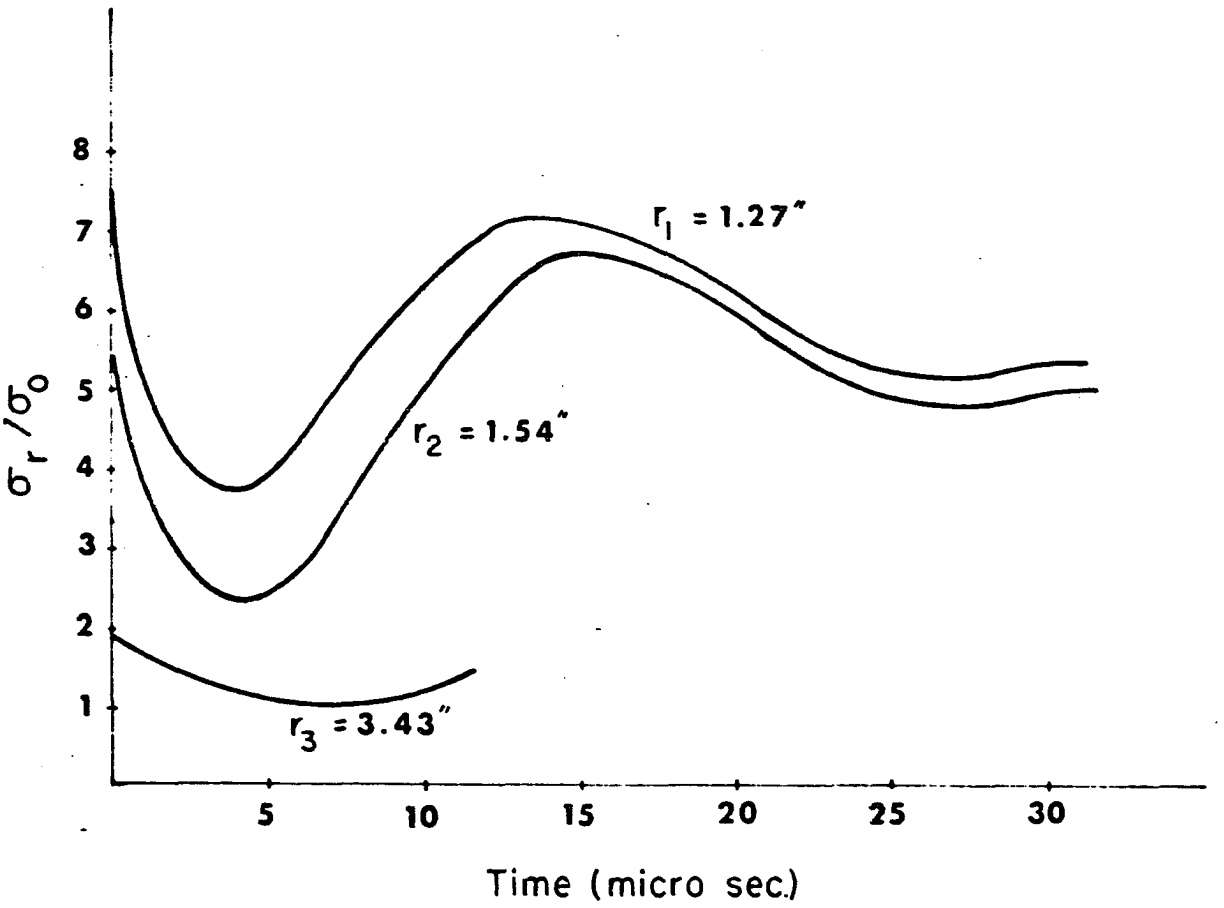

Radial stress histories for several points

($p=10\sigma_0$, $E_1/E_0=0.25$, $m=10^6$)

FIG. 4.7

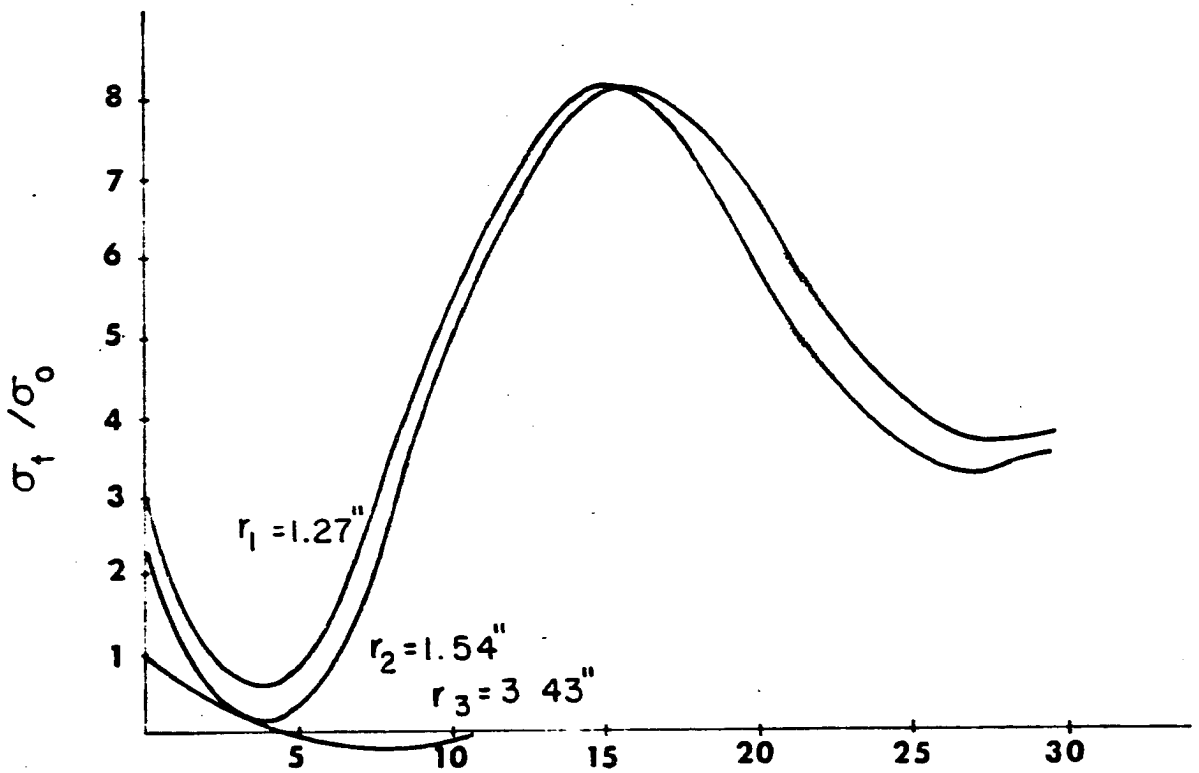

Tangential stress histories for several points

($p = 10\sigma_0$, $E_1/E_0 = 0.25$, $m = 10^6$)

FIG. 4.8

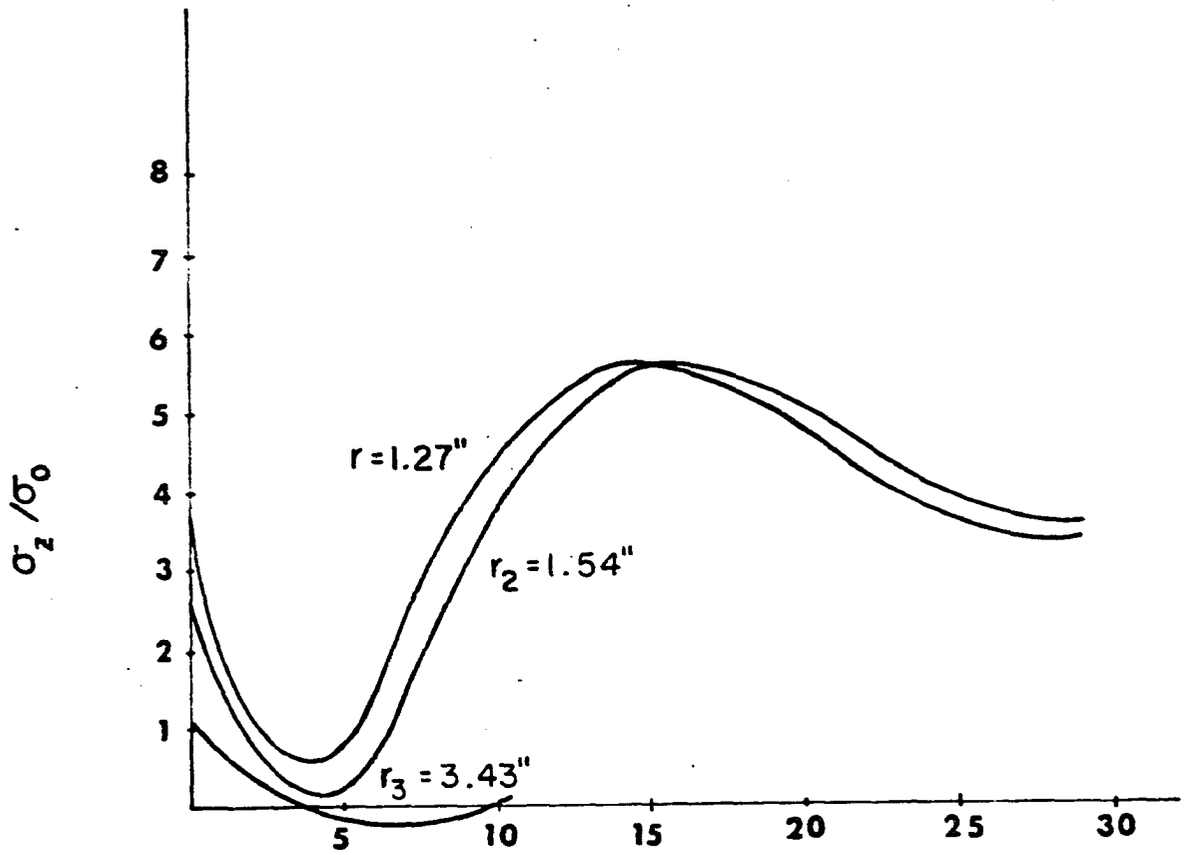

Axial stress histories for several points

($p=10\sigma_0, E_1/E_0=0.29, m=10^6$)

FIG. 4.9

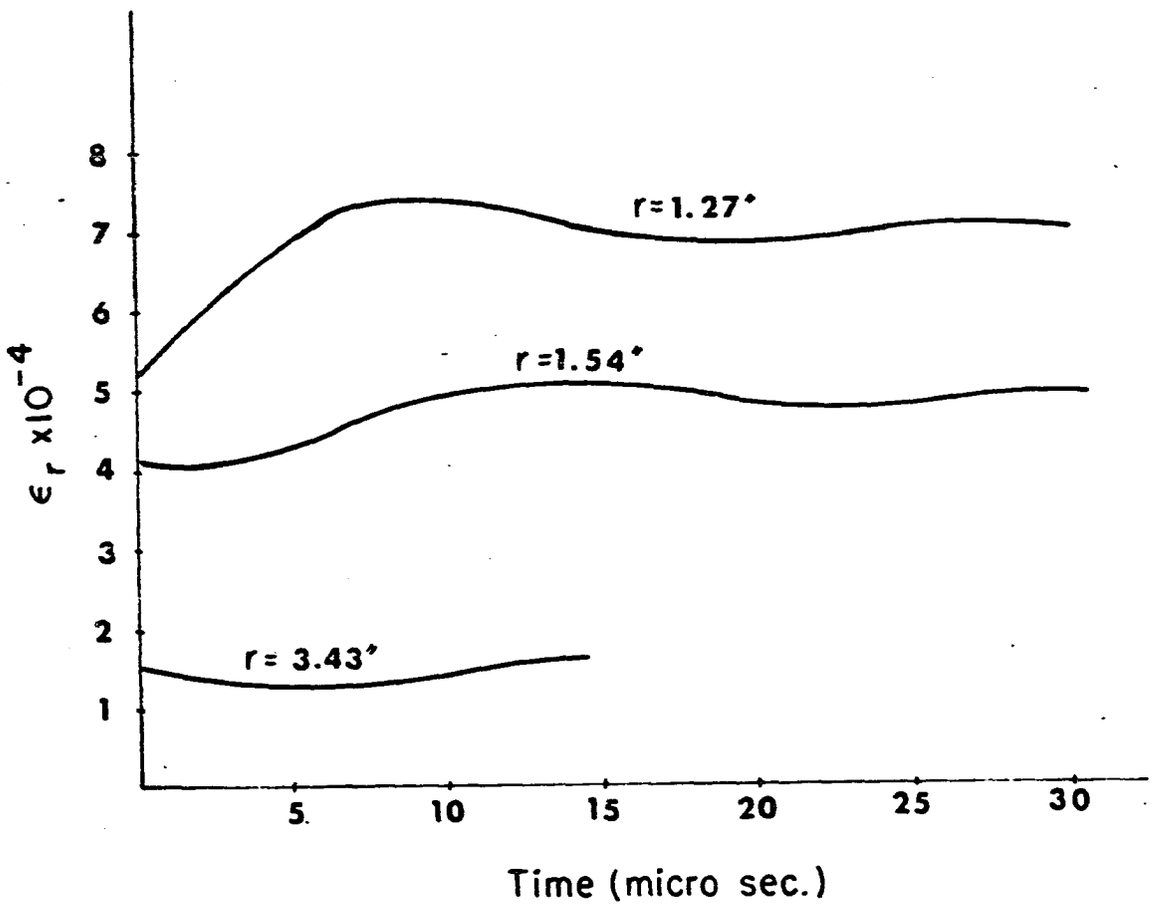

Radial strain histories at several points

($p=10\sigma_0$, $E_1/E_0=0.25$, $m=10^6$)

FIG. 4.10

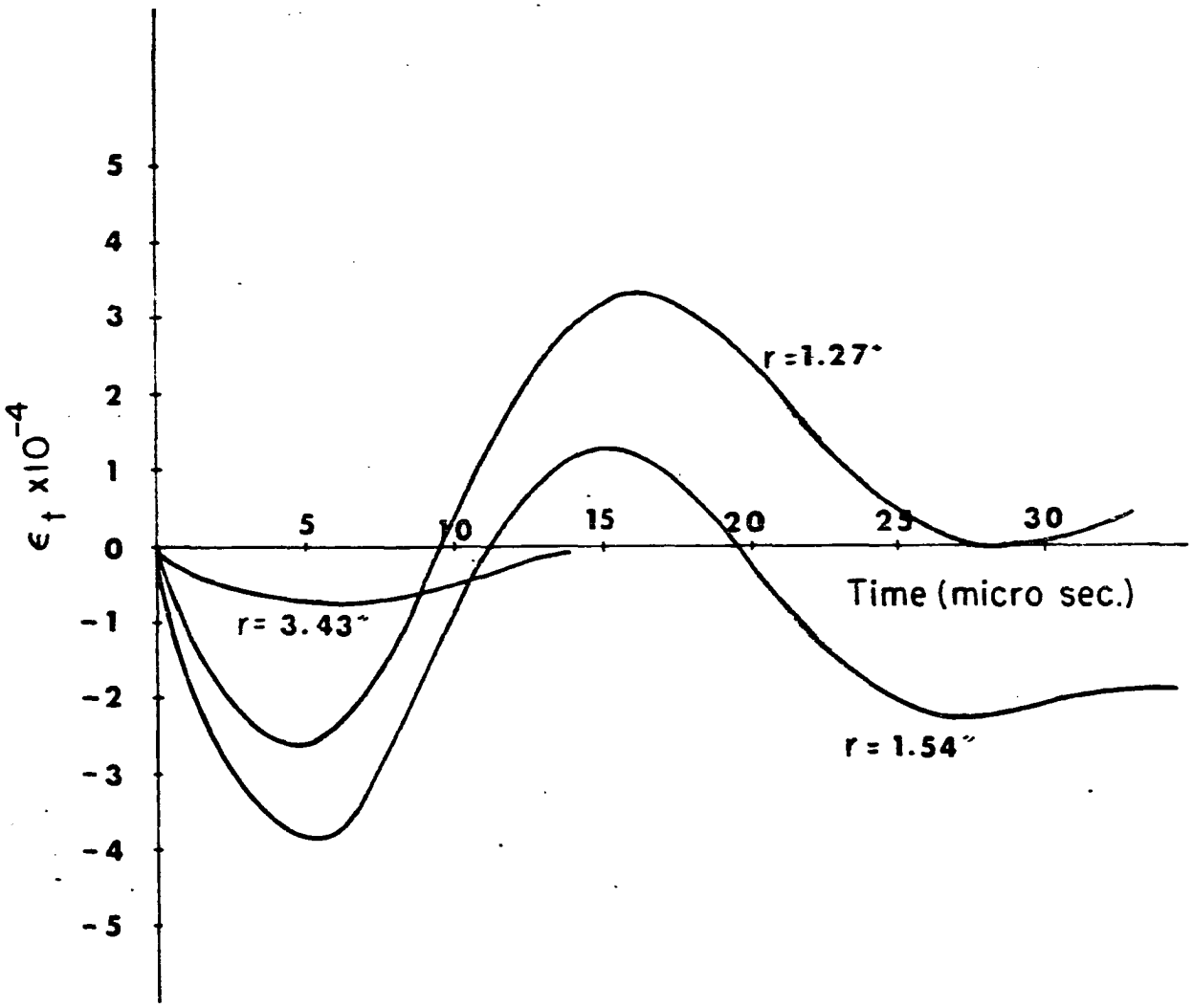

Tangential strain histories at several points

($p = 10\sigma_0$, $E_1/E_0 = 0.25$, $m = 10^6$)

FIG. 4.11

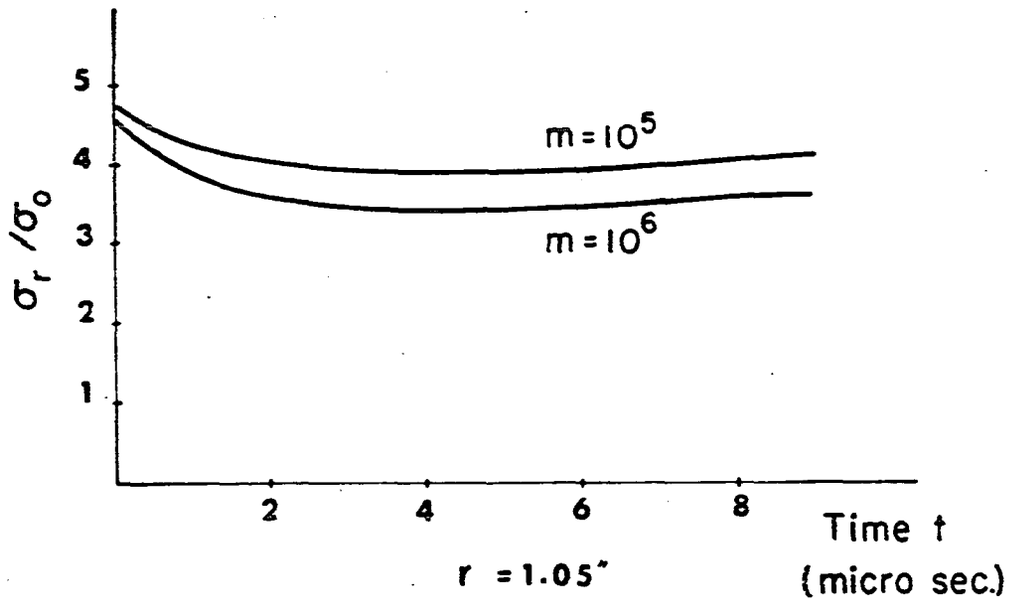

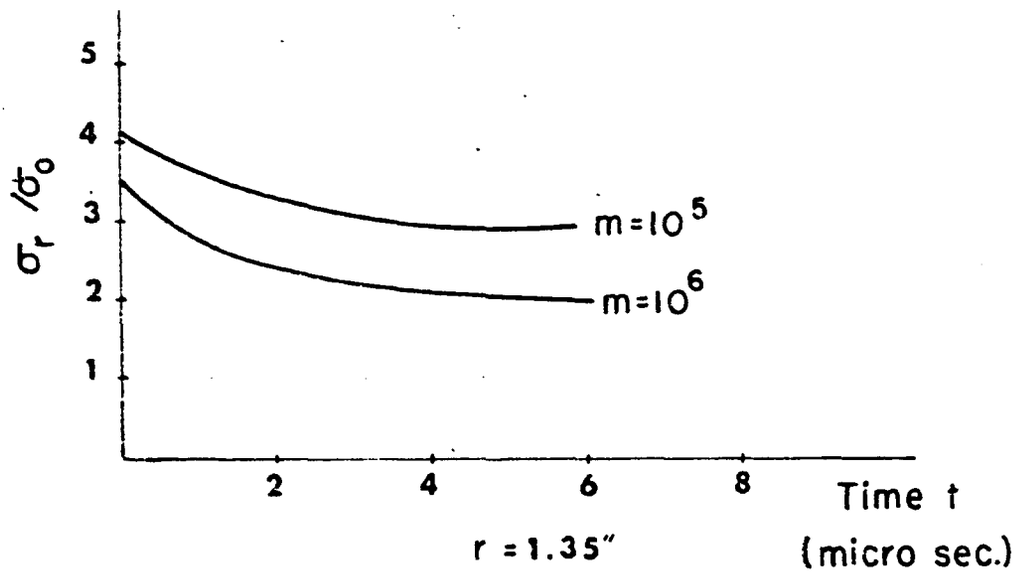

$(E_1/E_0=0.50,\ p=5\sigma_o)$

The influence of viscosity coefficient on the radial stress distribution

FIG. 4.12

viscous dispersion. This viscous dispersion is also evident at stress histories for the point r = 1.35" in the initial value of σ_r. Notice also that a comparison of the previously mentioned figure with the results reported by McNiven (and presented in figure 1.10a) for a viscoelastic material shows a qualitative agreement between the two solutions.

The influence of the work hardening parameter for a constant value of the viscosity coefficient is presented in figures 4.13 and 4.14. The curves there show the radial stress histories at two points (r = 1.05" and r = 1.34") inside the medium. As we see for both values of p as E_1/E_o decreases, the corresponding values of σ_r also decrease. This effect is more intense for the larger value of p since, in this case, the solution remains inelastic and therefore depends on E_1/E_o for a larger period of time.

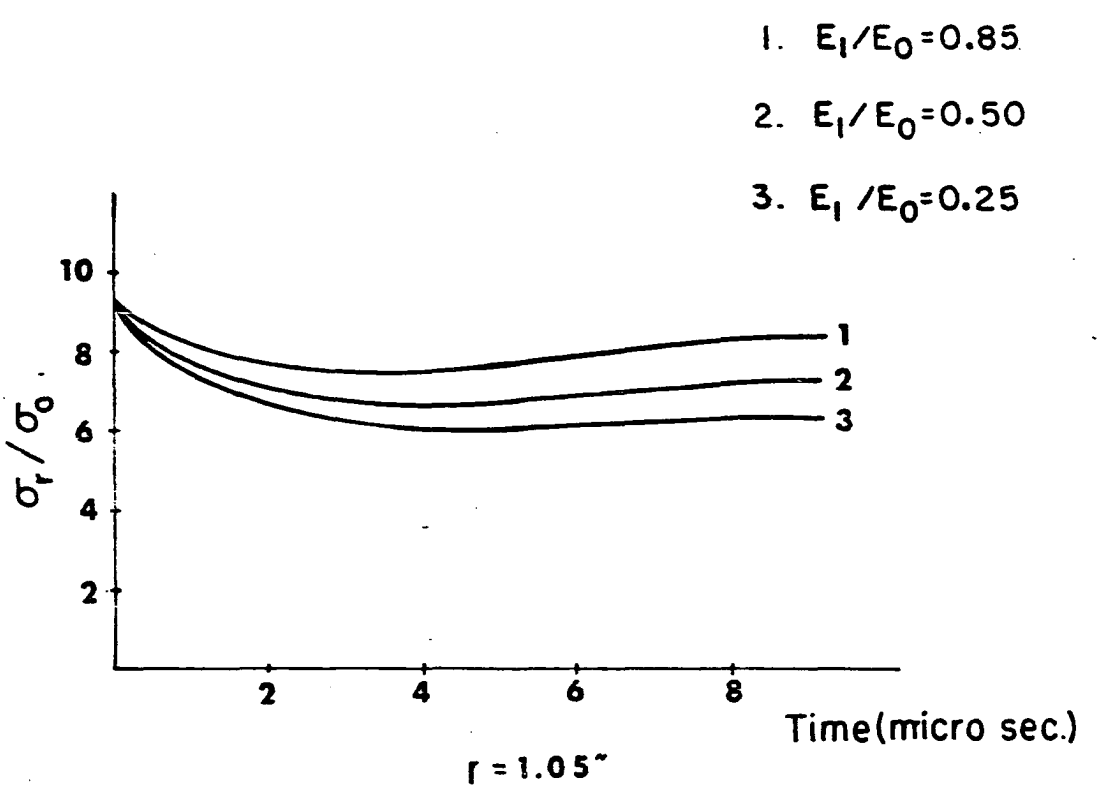

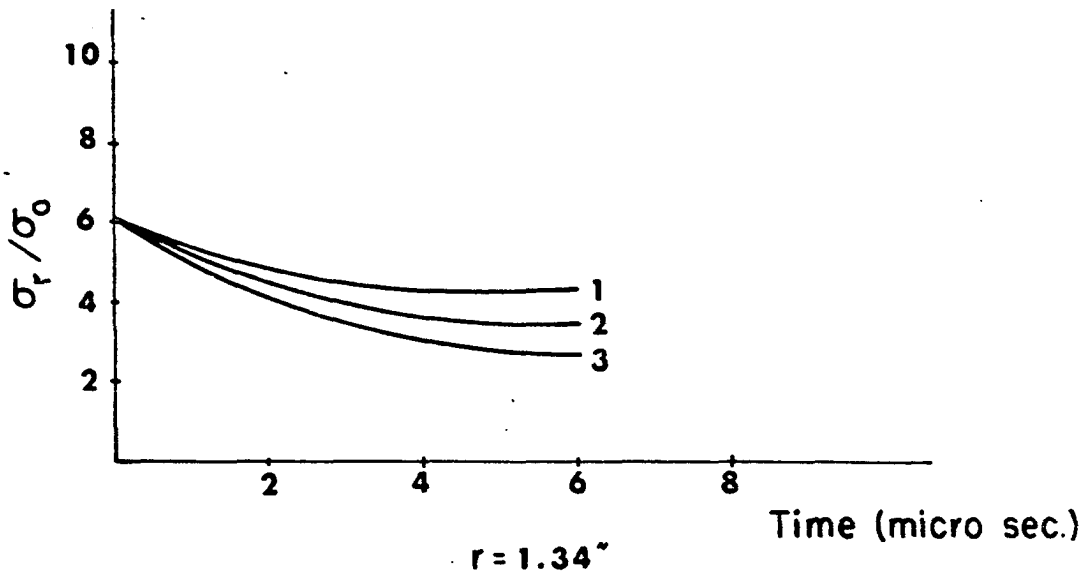

The influence of E_i/E_0 on the radial stress histories

($m = 10^6$, $p = 10\sigma_0$)

FIG. 4.13

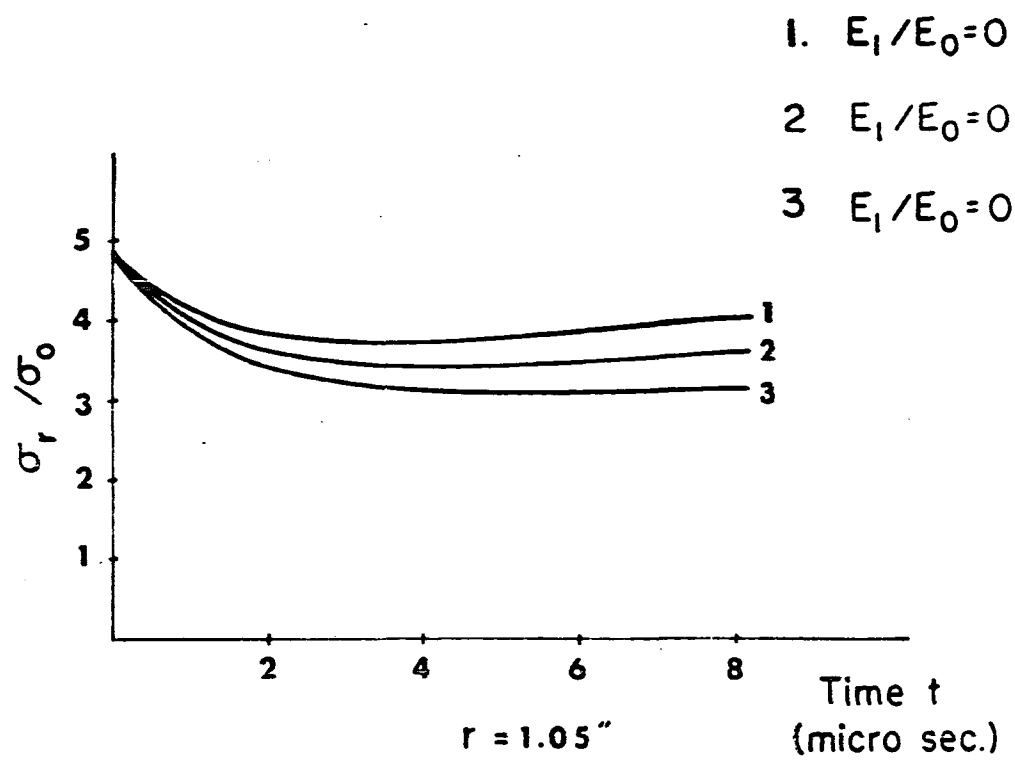

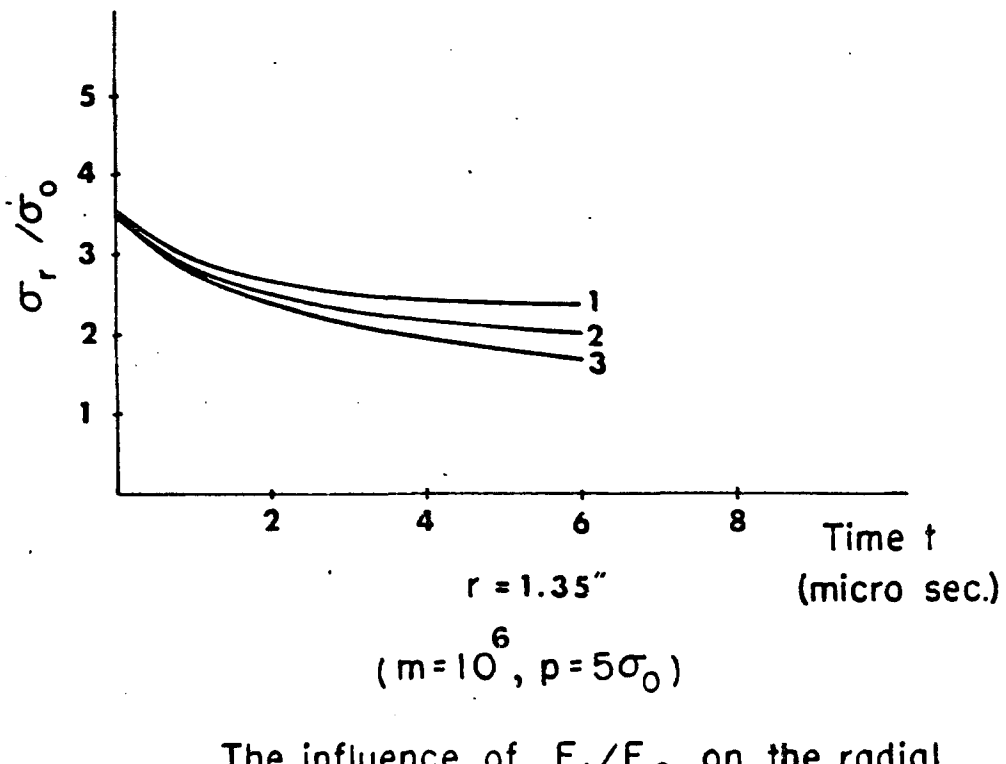

($m=10^6$, $p=5\sigma_0$)

The influence of E_1/E_0 on the radial stress histories

FIG. 4.14

4. The elastic-viscoplastic boundary

The II_S, t relationship (i.e., the magnitude of the second invariant of the deviatoric stress tensor vs time) is plotted in fig. 4.15. This figure shows that at any point within the medium the magnitude of II_S decreases with time from initial value. As we expected, the magnitude of this initial value of $\sqrt{II_S}$ is a decreasing function of r. According to the discussion in section 2 of this chapter, for radius r smaller than r_y, $\sqrt{II_S}$ is larger than the radius of the yield surface κ. Therefore viscoplastic flow takes place, according to the loading/unloading criterion. Consequently inelastic work develops and the radius of the yield surface increases from its initial value K_o.

In the same figure we observe that the rate of increase for κ is a decreasing function of time. There are two reasons for this behavior. First $\sqrt{II_S}$ itself is a decreasing function of time and secondly the rate of increase for is a decreasing function of W^{in} (as it is shown in figures 2.13 to 2.15).

After a certain time interval $\sqrt{II_S}$ decreases to a local minimum value. The time taken to reach this minimum value depends on r.

After this minimum has been reached, two new modes of inelastic behavior are possible. The first is that presented by the curve corresponding to the point r_1. Namely, the magnitude of $\sqrt{II_S}$ (and consequently of κ) starts to increase again and continues to increase at an almost constant rate throughout the remaining of the transient phenomenon. As we see in

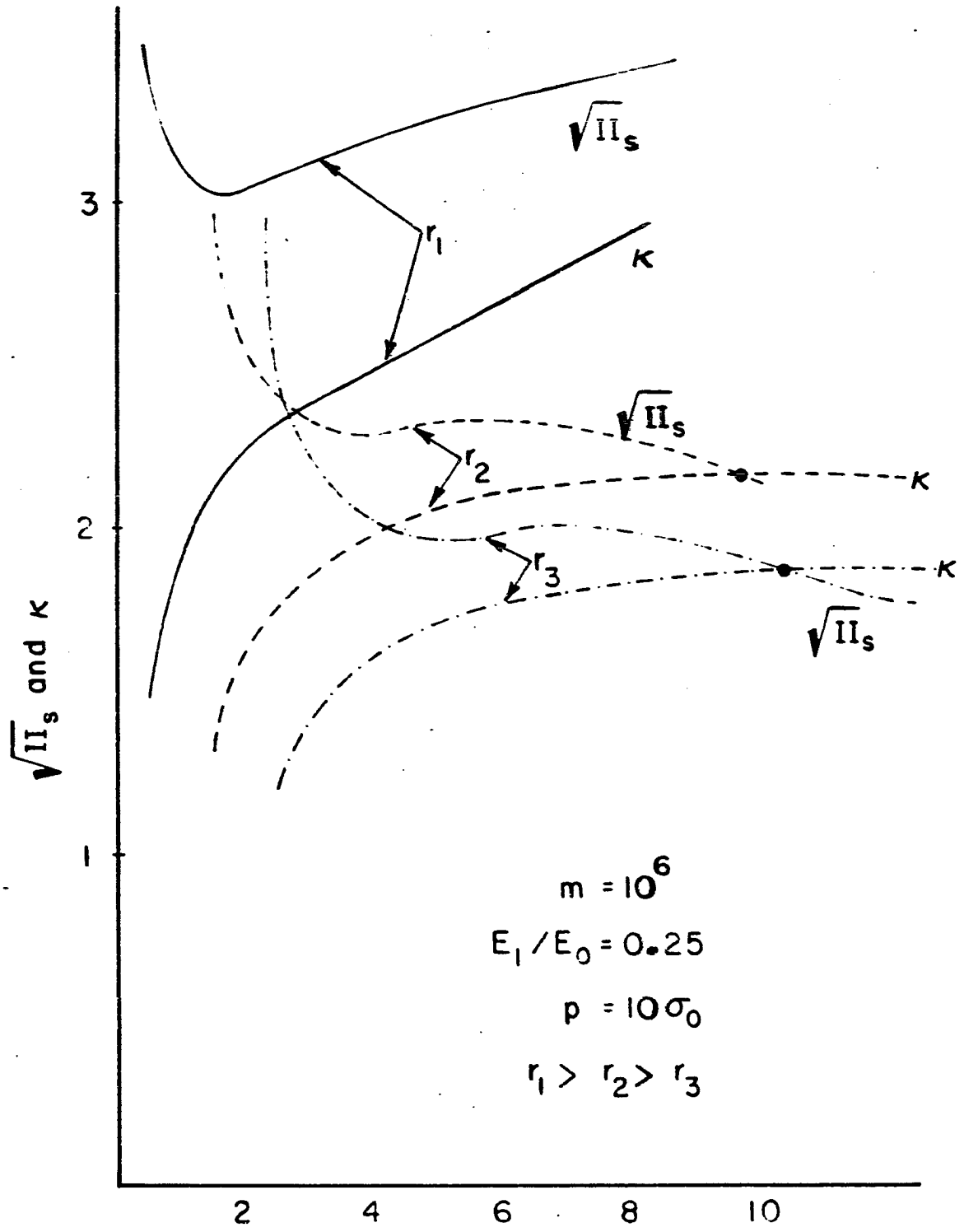

$\sqrt{II_s}$, and κ as a function of time at several points

FIG. 4.15

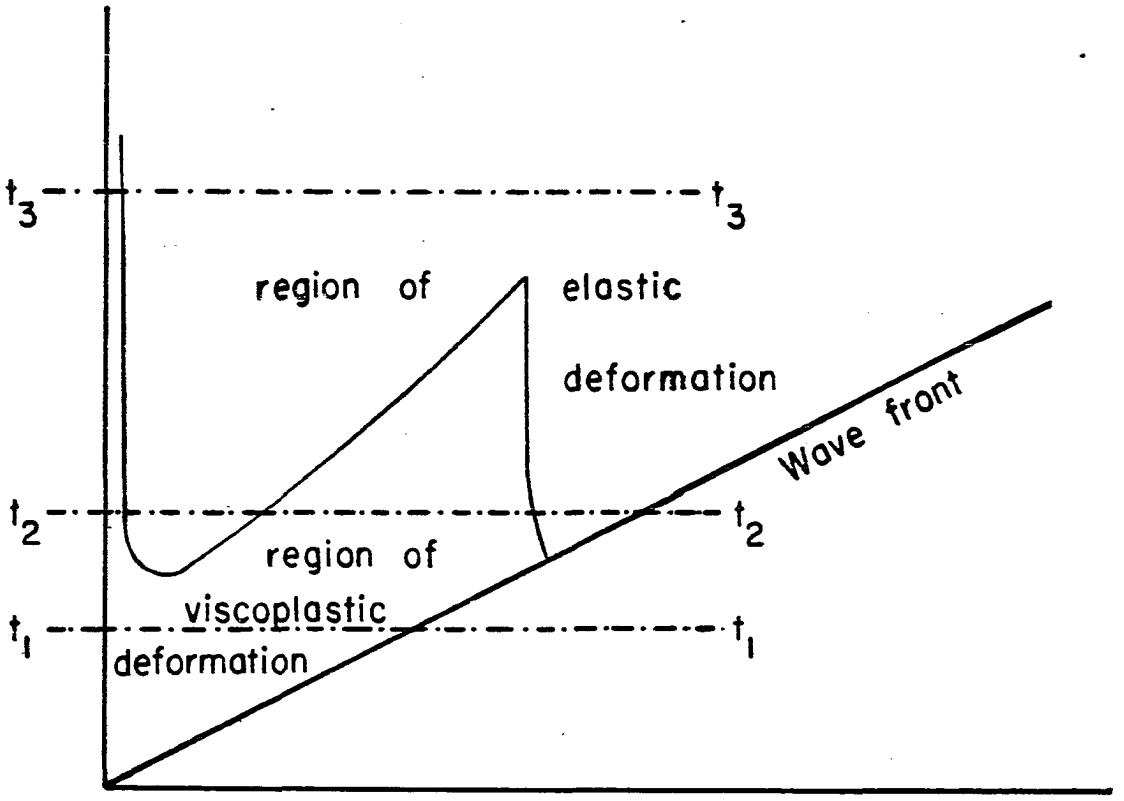

Radius r

Elastic viscoplastic boundary

($m=10^6$, $E_1/E_0=0.25$, $p=10\sigma_0$)

FIG. 4.16

figure 4.15, $\sqrt{II_S}$ always remains larger than K and therefore the deformation always remains viscoplastic.

The second mode of deformation is that corresponding to the points r_1 and r_2. In this case, the magnitude of $\sqrt{II_S}$ starts to increase again, but at a much lower rate than for r_1. After a certain period of time $\sqrt{II_S}$ starts to decrease again and eventually reaches the corresponding value of K_o. During the same period $\dot{K} > 0$ while $\ddot{K} < 0$.

After the intersection point between the two curves has been reached the deformation at the points r_1 and r_2 becomes elastic and consequently the radius of the yield surface remains constant.

These two modes of dynamic behavior give rise to a space-time diagram of the position of the elastic-viscoplastic boundary like that shown in figure 4.16. There we observe that points close to the cavity follow the first mode of viscoplastic behavior and consequently remain in the inelastic region throughout the entire transient phenomenon. On the other hand, points very far from the cavity behave only in an elastic manner since the geometric and viscous dispersions give rise to a magnitude of the second invariant of the deviatoric stress tensor that always lies inside the initial yield surface. For the points between these two regions the behavior is like that associated with the points r_2 and r_3 in figure 4.15.

Consider now the modes of dynamic behavior inside the elastic/viscoplastic medium at several times t_1, t_2, and t_3 ($t_3 > t_2 > t_1$).

At time t_1 all the points affected by the outwards travelling wave are deforming inelastically.

At a later time two elastically deforming regions arise. The first is associated with the geometrical dispersion and is close to the wave front. The second is due to a mode of dynamic behavior like that at the points r_2 and r_3 in figure 4.15. This region is formed inside what was initially the inelastically deforming region. The second region expands with time towards the cylindrical cavity on the one hand and towards the first elastic region on the other. As figure 4.16 indicates, the expansion towards the first elastic region is more rapid.

By the end of the transient phenomenon the two distinct elastic regions meet. At that time there is still a small region of inelastically deforming material close to the cylindrical cavity.

Figures 4.17 and 4.18 illustrate some of the features of the second region of elastic deformation, referred to above.

First we observe that for a given value of m a strengthening of the material due to work hardening effects (expressed in terms of decreasing values for E_1/E_o), delays the appearance of the second elastic region. This can easily be understood

since from figures 3.12 to 3.15 it is evident that the rate of increase for K is a decreasing function of E_1/E_o.

Secondly we observe that the time necessary for the second region to appear is almost independent of the magnitude of the applied pressure. By increasing p we shift the appearance of the elastic region to a slightly later time.

Thirdly we can see that this new elastic region occurs and expands always in the same region within the material independently of the work hardening parameter.

Finally figure 4.18 shows that for the same work hardening parameter E_1/E_o the viscosity coefficient affects the appearance of the second elastic region. Namely we observe that a large value of m accelerates the appearance of this region.

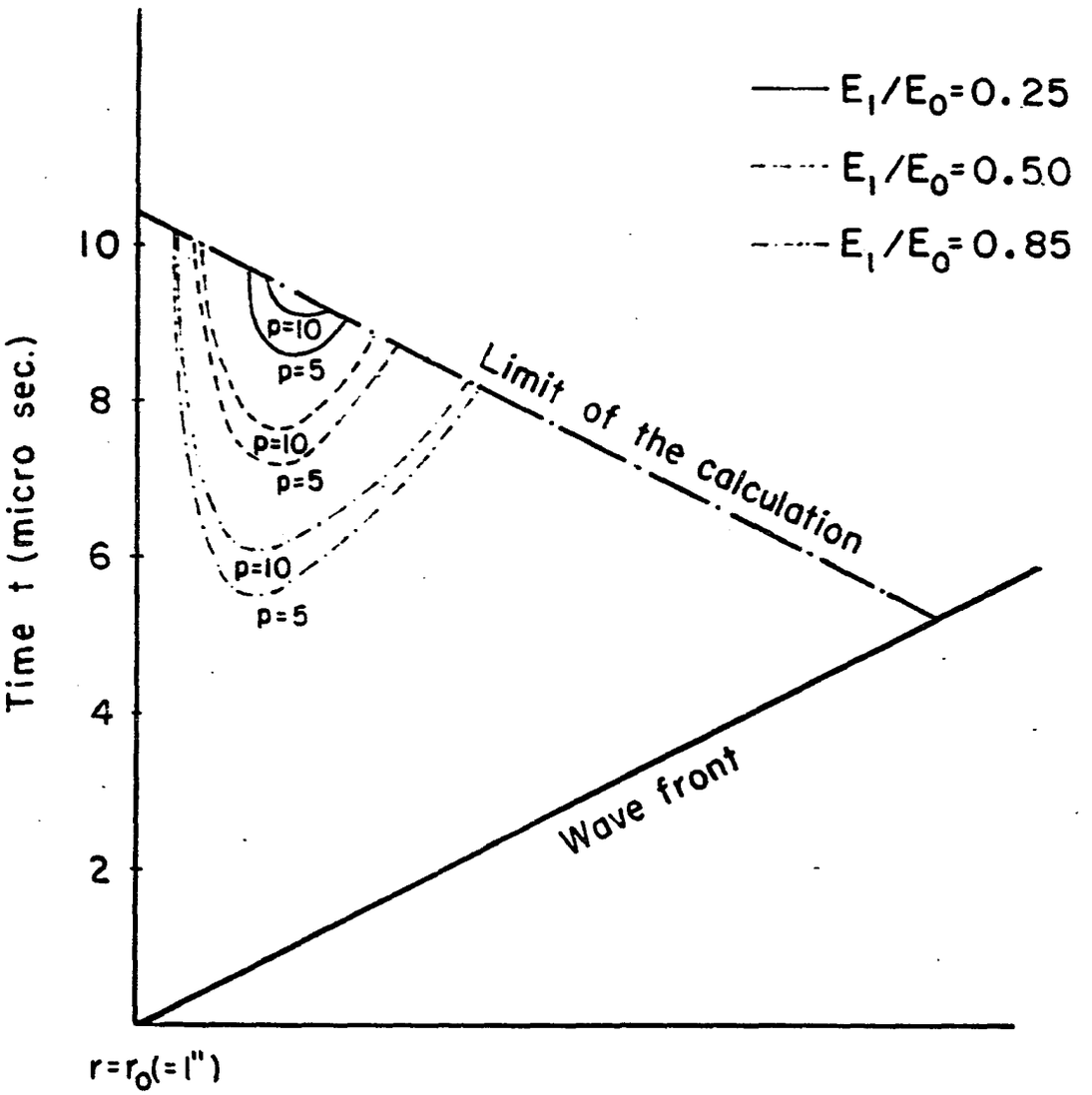

Elastic viscoplastic boundary

$(m=10^6)$

FIG. 4.17

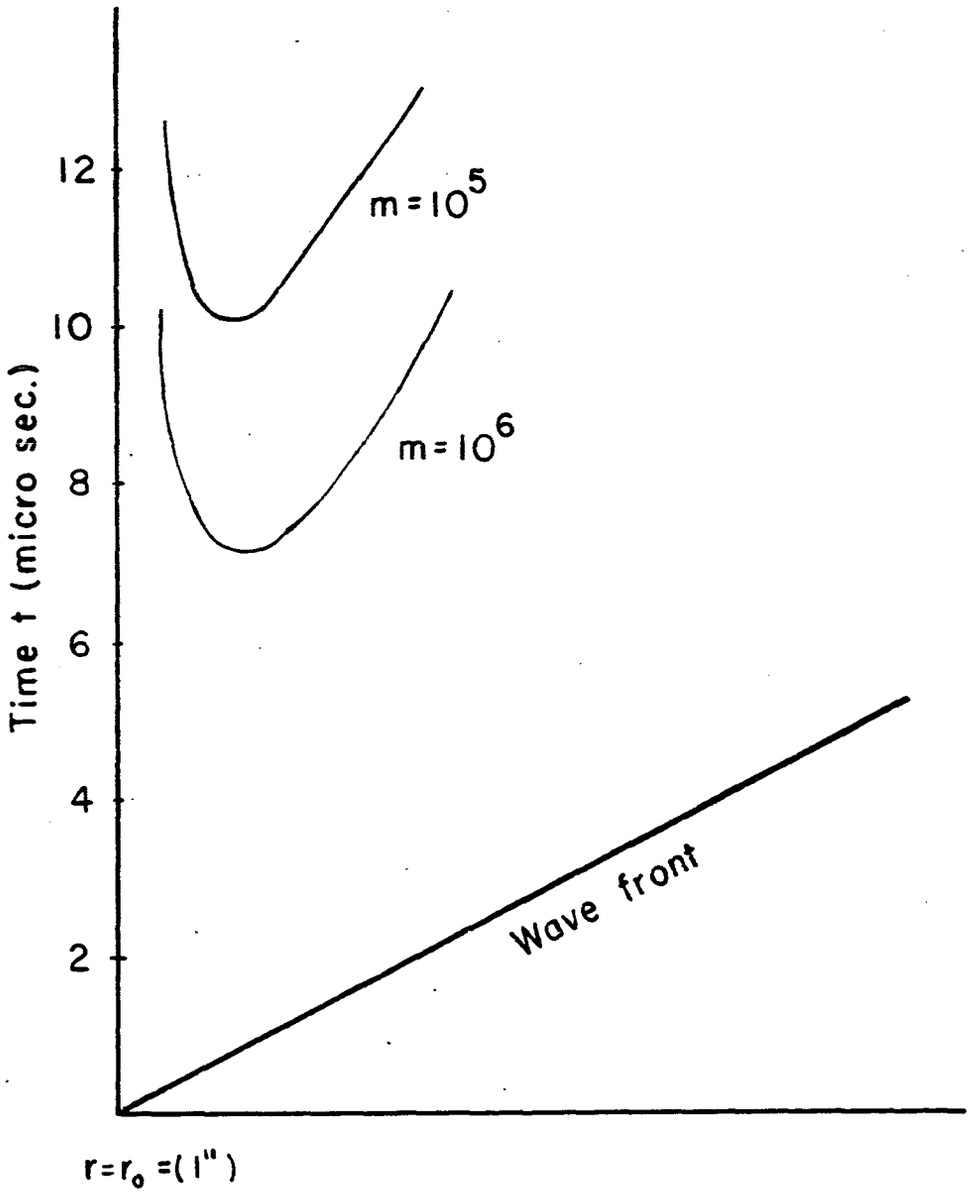

$E_1 / E_o = 0.50$

FIG. 4.18

C H A P T E R V

THE EXISTENCE OF A LOWER "QUASI-PLATEAU"

1. Introduction

In this chapter we again consider the classical problem of a semi-infinite bar subjected to an axially applied impact load. In chapter I, where the history of the inelastic waves was reviewed, the historical background for the present problem was also given.

The theory used in the following analysis is one that incorporates strain-rate effects into the dynamic stress-strain behavior. This theory, as was mentioned previously (Chapter I, section 2 and Chapter II, section 1) was introduced first by Malvern [44] and applied thereafter by Wood and Phillips [47] but only in the case of continuous loading of an elastic/viscoplastic bar.

The question to be discussed here is that of a semi-infinite bar of elastic/viscoplastic material subjected to a stress-history like that presented in figure 5.3. There it is shown that at time t = 0 a pressure p is applied to

the end of the bar. Thereafter it is assumed that the pressure remains constant for a certain period of time t_o, and is then gradually reduced to zero. As a result of this boundary condition, loading and subsequently unloading waves travel along the bar. The purpose of this chapter is to investigate these waves.

Initially, during the loading process, the transient phenomenon is very similar to that of continuous loading. According to Malvern, in the case of continuous loading, the inelastic strain-rate is positive, and therefore inelastic strains accumulate, whenever the dynamic stress point exceeds the stress that corresponds to the same strain on the quasi-static stress-strain curve.

It is therefore necessary to introduce a quasi-static stress-strain relationship. Figure 5.1 shows a typical experimental stress-strain curve. There we see that loading beyond the yield point $(\sigma_o, \varepsilon_o)$ introduces a new region of elastic behavior. This region starts at a point very close to the prestressing point A, extends along a straight line parallel to the original elastic stress-strain line and finally stops at a certain point σ_ℓ on that line. Thus every stress beyond the elastic limit σ_o introduces two new yield points called the upper, σ_u, and the lower, σ_ℓ, yield points. As experiments indicate, the locus of all upper yield points as well as that of the lower yield points can be approximated by two straight lines. Such an approxi-

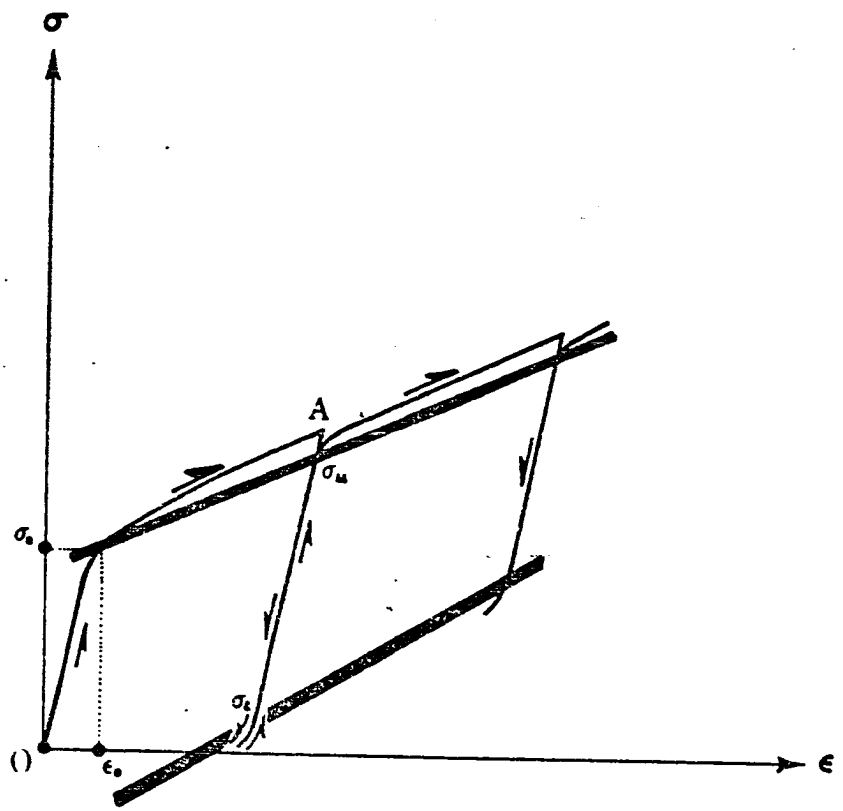

Typical experimental stress-strain curve

FIG. 5.1

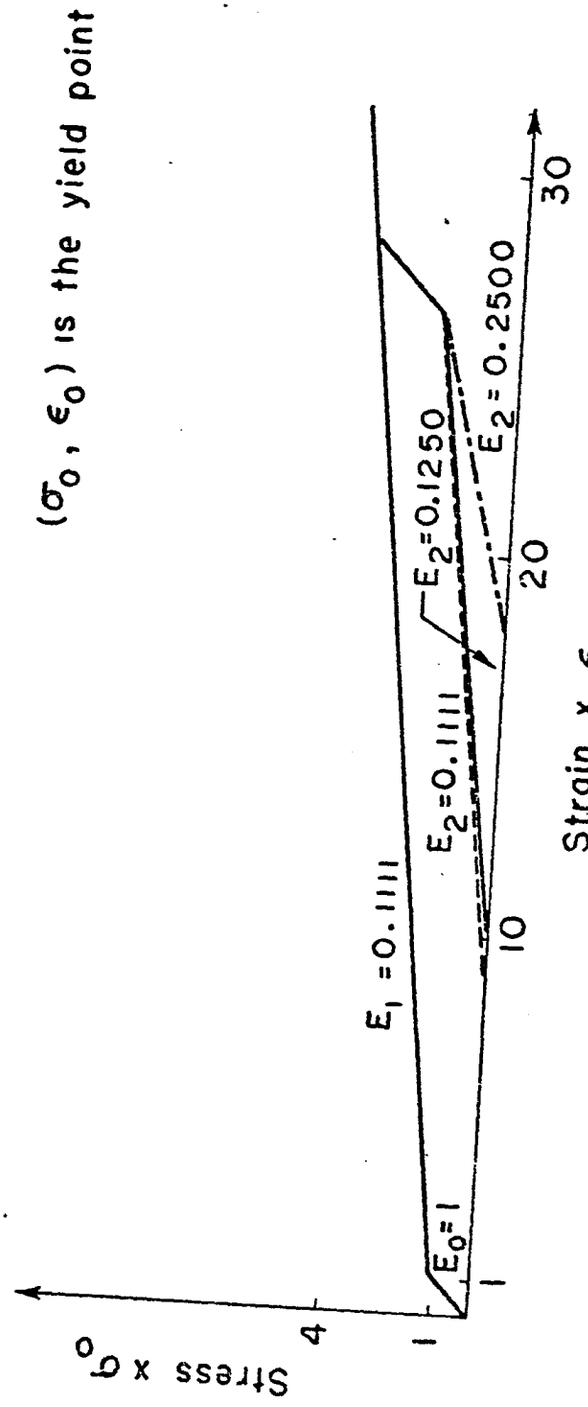

Dimensionless stess-strain curve

FIG. 5.2

mation is shown in figure 5.1. Figure 5.2 shows the quasi-static bilinear stress-strain curve used in connection with Malvern's theory throughout this chapter. Notice that KOLSKY [113] in 1963 recommended this as an approximation of the experimental stress-strain curve in figure 5.1. For reasons that will become clear at a later section (where a discussion of the results from the computations is given) the slope of the lower yield point line is assumed to differ slightly from that of the upper yield point line. This, in fact, gives a better approximation of the experimental curve.

During the unloading process, that accompanies the gradual removal of the applied pressure, the dynamic stresses decrease. It is therefore possible that they may reach at some points inside the bar values which are below the lower limit of elastic behavior. For those stress points we shall generalize Malvern's idea by assuming that inelastic loading takes place. This unloading is governed by a constitutive equation identical to that used to describe the mechanism of inelastic loading.

Work related to this particular problem was published by WOOD [114] in his doctoral dissertation. However the only question discussed there was the limited case of the sudden removal of the applied load at the end of the bar. The present problem could be viewed as a generalization of the work done by both, Malvern and Wood. By increasing the time t_o to infinity or by decreasing the slope γ to zero, we obtain the problem studied by Malvern. On the other hand, by

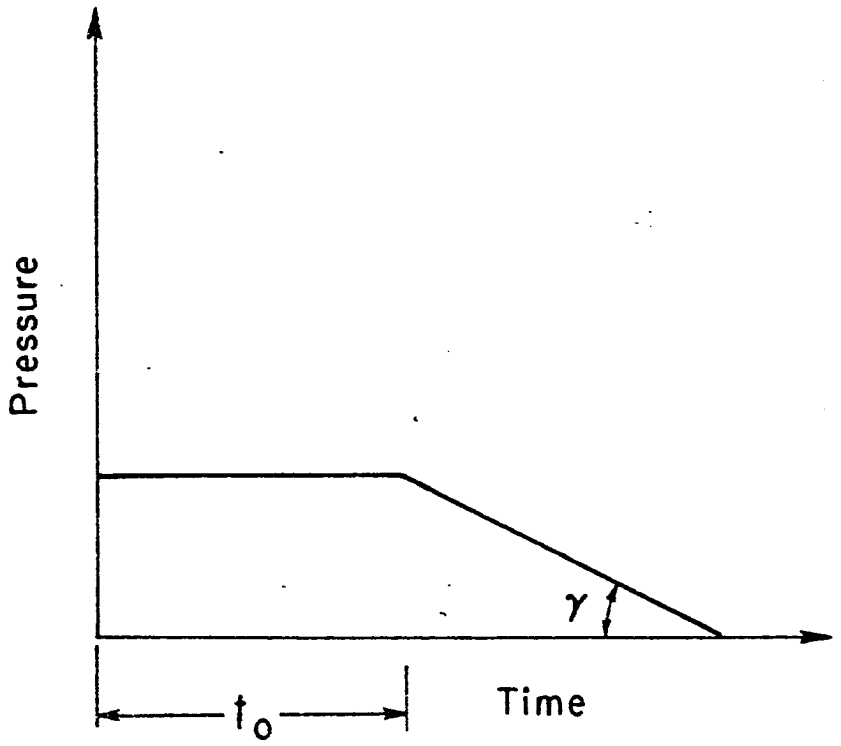

Stress-time boundary condition at the free end of the bar

FIG. 5.3

considering $\gamma = 90°$, we again obtain the particular case studied by Wood.

As it was done by the two previous authors for the case of continuous loading, special attention will be given to the residual strain distribution along the bar. The existence of a strain plateau and the effect of the several parameters shown in figures 5.2 and 5.3 on its shape, magnitude and length will be the basic questions discussed in the following sections.

Before proceeding to the next section, it is desirable to emphasize that the lower yield point described here is associated with unloading phenomena in aluminum. It is not in any way connected with the "lower yield point" observed in loading tests on certain metals (e.g., mild steel) immediately after the "upper yield point".

Summarizing we should bear in mind that our upper yield point σ_ℓ is associated with loading beyond the elastic region and that our lower yield point marks the beginning of inelastic phenomena during unloading.

2. Theoretical development

The present phase of the investigation considers wave propagation in an elastic/viscoplastic material having a bilinear quasi-static stress strain curve characterized by kinematic hardening. The quasi-static stress-strain curve can be expressed by the following 4 equations

a loading

$$\text{for } \sigma_o \geq \sigma > 0 \qquad \sigma = E_o\varepsilon$$

$$\text{for } p \geq \sigma > \sigma_o \qquad \sigma = \sigma_o + E_1(\varepsilon-\varepsilon_o)$$

b unloading (5.1)

$$\text{for } p \geq \sigma > p - 2\sigma_o \qquad \sigma = p - E_o(\varepsilon_p-\varepsilon)$$

$$\text{for } p - 2\sigma \geq \sigma \qquad \sigma = E_2\left\{(\varepsilon - \frac{p}{E_1}) + \varepsilon_o(1+\frac{E_o}{E_1})\right\}+p-2\sigma$$

where

1 $(\sigma_o, \varepsilon_o)$ is the yield point,

2 p is the maximum stress applied at the free end of the bar, and

3 ε_p is the strain that corresponds to p according to the quasi-static stress-strain curve.

Recall now the equations that describe the wave propagation in a rod according to the rate dependent theory proposed by Malvern [44], [45]

$$\frac{\partial \sigma}{\partial x} = \rho \frac{\partial u}{\partial t}$$

$$\frac{\partial \varepsilon}{\partial t} = \frac{\partial v}{\partial x} \tag{5.2}$$

$$E_o \frac{\partial \varepsilon}{\partial t} = \frac{\partial \sigma}{\partial t} + g(\sigma,\varepsilon)$$

For our current analysis the function $g(\sigma,\varepsilon)$ takes the following linear form

$$g(\sigma,\varepsilon) = k\ (\sigma - f(\epsilon)) \tag{5.3}$$

where $\sigma - f(\varepsilon)$ represents the excess of the instantaneous stress over the equivalent quasi-static stress for the same strain. In the equation (5.3), k is a multiplicative constant which may be selected empirically to match the strain rate characteristics of a specified material.

Using the bilinear form for $f(\varepsilon)$ the equation (5.3) can be written in the following way

a viscoplastic loading

$$g(\sigma,\varepsilon) = k \left\{ \sigma - \sigma_o\left(1 - \frac{E_1}{E_o}\right) - E_1\varepsilon \right\} \tag{5.4a}$$

b viscoplastic unloading

$$g(\sigma,\varepsilon) = k \left\{ \sigma - E_2 \left\{ \varepsilon - \frac{p}{E_1} + \varepsilon_o\left(1 + \frac{E_o}{E_1}\right) \right\} - p + 2\sigma_o \right\} \tag{5.4b}$$

Equations (5.2) are a hyperbolic system of quasi-linear partial differential equations which may be integrated by the method of characteristics (see eqs. (3.21) and (3.22) in chapter III, section 4) under appropriate boundary conditions. The characteristics in the x,t-plane are the three families of straight lines defined by the characteristic differential equations

$$\begin{aligned} dx &= 0 \\ dx - c_o dt &= 0 \\ dx + c_o dt &= 0 \end{aligned} \tag{5.5}$$

where

$$c_o = \sqrt{\frac{E_o}{\rho}} \tag{5.6}$$

is the (constant) speed of propagation of longitudinal elastic waves in the bar. The following three equations

$$\begin{aligned} E_o d\varepsilon - d\sigma &= g(\sigma,\varepsilon)dt \\ d\sigma - \rho c_o dv &= -g(\sigma,\varepsilon)dt \\ d\sigma + \rho c_o dv &= -g(\sigma,\varepsilon)dt \end{aligned} \tag{5.7}$$

hold along the three characteristics defined by eq. (5.5) respectively.

The boundary conditions are expressed in terms of the stress history at the point x = 0 of the bar. Figure 5.3

shows the plot of this stress-time curve. There we see that at time t = 0, a pressure p is suddenly applied at the free end of the bar. This pressure is kept constant for a certain period of time and then it is gradually removed. In order to introduce a concrete way of studying the effects of removing the applied load, the unloading part of the strain history has been assumed linear with slope γ. The parameter γ is a measure of the rate of unloading.

Initially the bar is assumed to be at rest and stress free. Immediately upon impact, a shock wave of elastic deformation begins to travel along the bar at speed c_o. This leading wave front is presented in figure 5.4 by the straight line $x = c_o t$. Let us denote by the subscript a the region of the bar an infinitesimal distance ahead of the wave front and by the subscript b the region just behind the front. Then we have

$$\sigma_a = \varepsilon_a = v_a = 0 \tag{5.8}$$

The shock wave conditions are

1. Momentum equation

$$\sigma_b - \sigma_\alpha = -\rho c_o (v_b - v_a) \tag{5.9a}$$

2. Continuity equation

$$v_b - v_a = - c_o (\varepsilon_b - \varepsilon_a) \tag{5.9b}$$

Using eq. (5.8) we have

$$\sigma_b = -\rho\, c_o v_b \tag{5.10a}$$

$$v_b = -\, c_o \varepsilon_b \tag{5.10b}$$

Equation (5.10a) together with the second of the equations (5.7) enables us to obtain a solution for the longitudinal stress along the wave front.

$$2d\sigma = -\, g\, dt \tag{5.11}$$

Equation (5.11) can be integrated immediately using the boundary condition that $\sigma = p$ at $x = 0$

$$\int_p^{\sigma} \frac{d\sigma}{g(\sigma)} = \int_p^{\sigma} \frac{d\sigma}{k\left\{(\sigma-\sigma_o)\left(1 - \frac{E_o}{E_1}\right)\right\}} = \int_o^t -\frac{1}{2}\, dt \tag{5.12}$$

(in eq. (5.4a) ε has been substituted with $\frac{\sigma}{E_o}$ using eqs. (5.10a) and (5.10b))

which results in

$$\frac{\sigma}{\sigma_o} = 1 + \left(\frac{p}{\sigma_o} - 1\right) e^{-\frac{1}{2}\left(1 - \frac{E_1}{E_o}\right)kt} \tag{5.13a}$$

and

$$\frac{\varepsilon}{\varepsilon_o} = 1 + \left(\frac{p}{\sigma_o} - 1\right) e^{-\frac{1}{2}\left(1 - \frac{E_1}{E_o}\right)kt} \tag{5.13b}$$

Along the axis $x = 0$, the stress history is prescribed by the boundary conditions. Since values along the two lines $x = 0$ and $x = c_o t$ are specified, it is now possible to carry out systematic stress-strain calculations in the x-t plane.

3. Numerical integration in the x-t plane

Numerical integration of equations (5.7) has been carried out in the x-t plane shown in figure 5.4. Here, a step by step finite difference solution has been obtained throughout a network formed by the characteristics. The process has been outlined in chapter III, section 5 of this dissertation. We assume again that the net can be selected fine enough so that the integrations on the right hand side of eqs. (5.7) may be approximated by the trapezoidal rule. From the previous discussion the values of σ, ε and v have been obtained along the two boundaries $x = 0$ and $x = c_o t$. With values along these two axes specified it is now possible to carry out systematically the calculations in the x-t plane. Calculations are initiated at the intersection of $x = 0$ and $x = c_o t$ axes. Here σ and ε are known and the computation may continue along the $x = c_o t$ axis for n points. When this is completed the same procedure is carried along the $x = 2k\Delta t + c_o t$ axis. Along this axis only n-1 points may be determined. Referring to the notation shown in figure 5.4 the finite difference form for the unknowns in eqs. (5.7) becomes

$$\sigma_N - \sigma_W - \rho c_o (v_N - v_W) = -\int_W^N g \, dt$$

$$\sigma_N - \sigma_E + \rho c_o (v_N - v_E) = -\int_E^N g \, dt \qquad (5.14)$$

$$E_o(\varepsilon_N - \varepsilon_S) - (\sigma_N - \sigma_S) = \int_S^N g \, dt$$

The trapezoidal rule simplifies eqs. (5.14) to the following system of equations for the unknowns σ_N, ε_N and v_N.

$$\sigma_N - \sigma_W - \rho c_o (v_N - v_W) = -\frac{1}{2}(g_N + g_W)\Delta t$$

$$\sigma_N - \sigma_E + \rho c_o (v_N - v_E) = -\frac{1}{2}(g_N + g_E)\Delta t \qquad (5.15)$$

$$E_o(\varepsilon_N - \varepsilon_S) - \sigma_N + \sigma_S = \frac{1}{2}(g_N + g_S)\Delta t$$

The calculation then shifts to the line $x = 4k\Delta t + c_o t$, along which n-2 points are determined, etc. In all $n\frac{n+1}{2}$ points have been determined by this method. Thus the final calculated stress-strain distribution presents the values of the unknowns within a triangular region of the x-t plane.

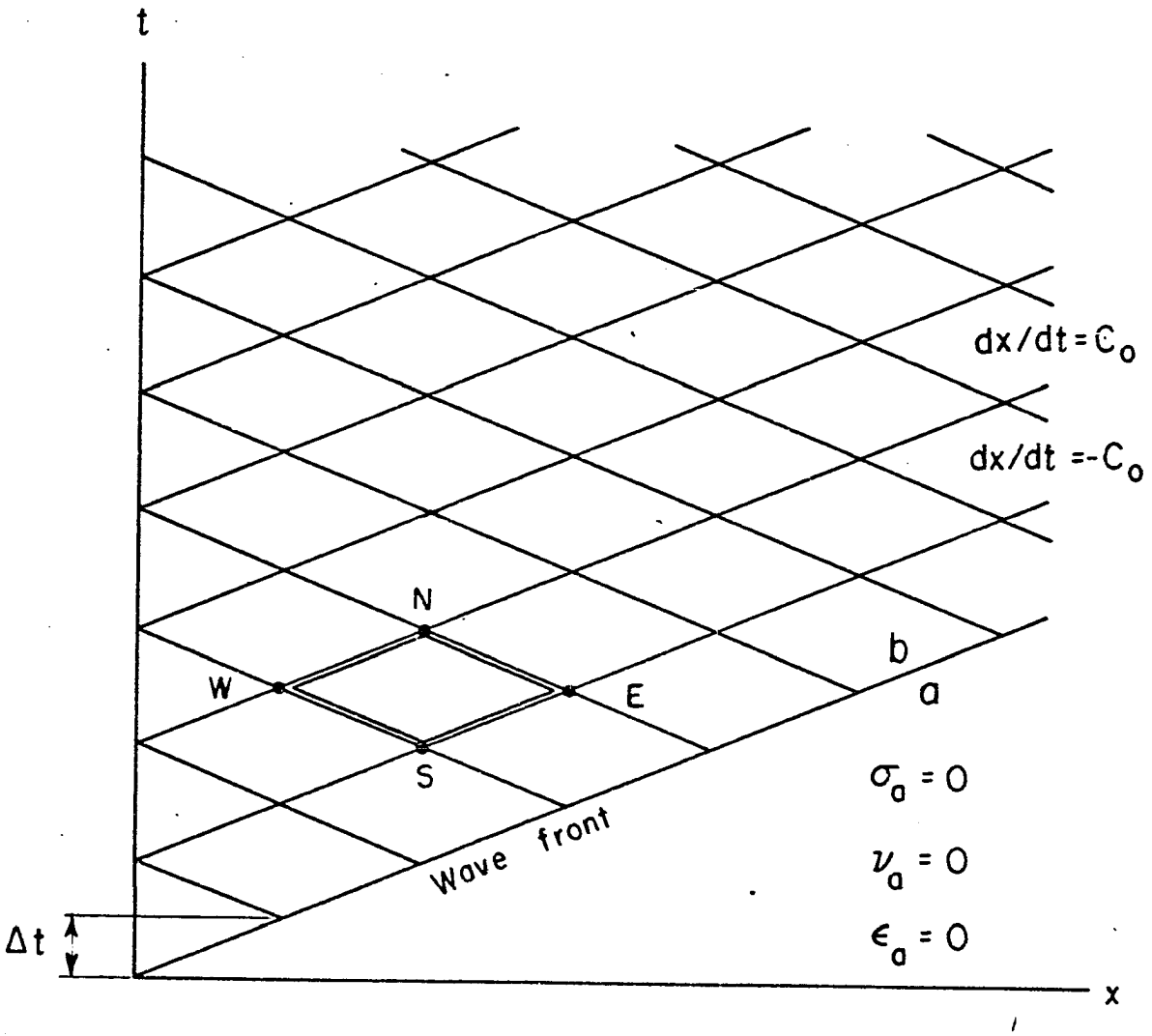

Characteristic net

FIG. 5.4

4. Discussion of results

In the previous sections the system of equations describing the wave propagation was obtained and a numerical method of integration was derived along the characteristic net. As equations (5.7) and (5.12) indicate, the transient phenomenon is governed by a number of parameters like the shape of the quasi-static stress-strain curve, the stress-time history etc. The purpose of this section is twofold. First the influence of the parameters will be studied, and, secondly, an attempt will be made towards a better understanding of the physical processes that give rise to the strain plateau.

The computer program, presented on Appendix II at the end of this dissertation, provided an excellent tool by which to probe physical concepts in rate-dependent plastic wave propagation. As programmed, a maximum number of 700 points along each characteristic and equivalent number of characteristics in the x-t plane could be taken into account. This made it possible to apply a stress pulse to one end of the bar, remove it gradually after a short period of time, and then allow the bar to come to complete equilibrium in order to establish the final residual strain distribution. Also the stress-strain curve of each point along the bar could be obtained and the time decay of stresses following unloading could be investigated for long-time effects.

The first phase of the computer analysis was to explore the influence of characteristic grid size on the accuracy of

computed stresses and strains. Results showed that a time increment of $\Delta t = 0.5/k$ provided a satisfactory accuracy compromise since the outputs approximated the results obtained with a time increment of $\Delta t = 0.05/k$ to within the sixth significant digit.

Following this, stress-strain histories were plotted. Figure 5.5 presents some of these curves. Results indicate that the nearer a location is to the impact end of the bar, the higher is its ratio of dynamic to static yield stress. This result was expected since locations nearer the impact end experience a more rapid loading history. The stress-strain histories also confirmed that those points well removed from the end of the bar, which experience a slow rate of loading, will tend to follow a stress-strain path closely approximating the quasi-static curve. Finally, points far away from the impact end will follow the elastic part of the quasi-static stress-strain curve.

Figure 5.5,and in a more detailed way,figure 5.6 show dynamic stress-strain curves for several points along the bar. There two different modes of dynamical behavior can be observed. First, up to a certain distance from the impact end, the points along the bar will experience a fast rate of loading history, enough to produce a part of the unloading stress-strain curve well below the corresponding lower yield point. Rate effects consequently will also take place during the unloading process. Behavior of this type produces residual strains contributing to the strain plateau

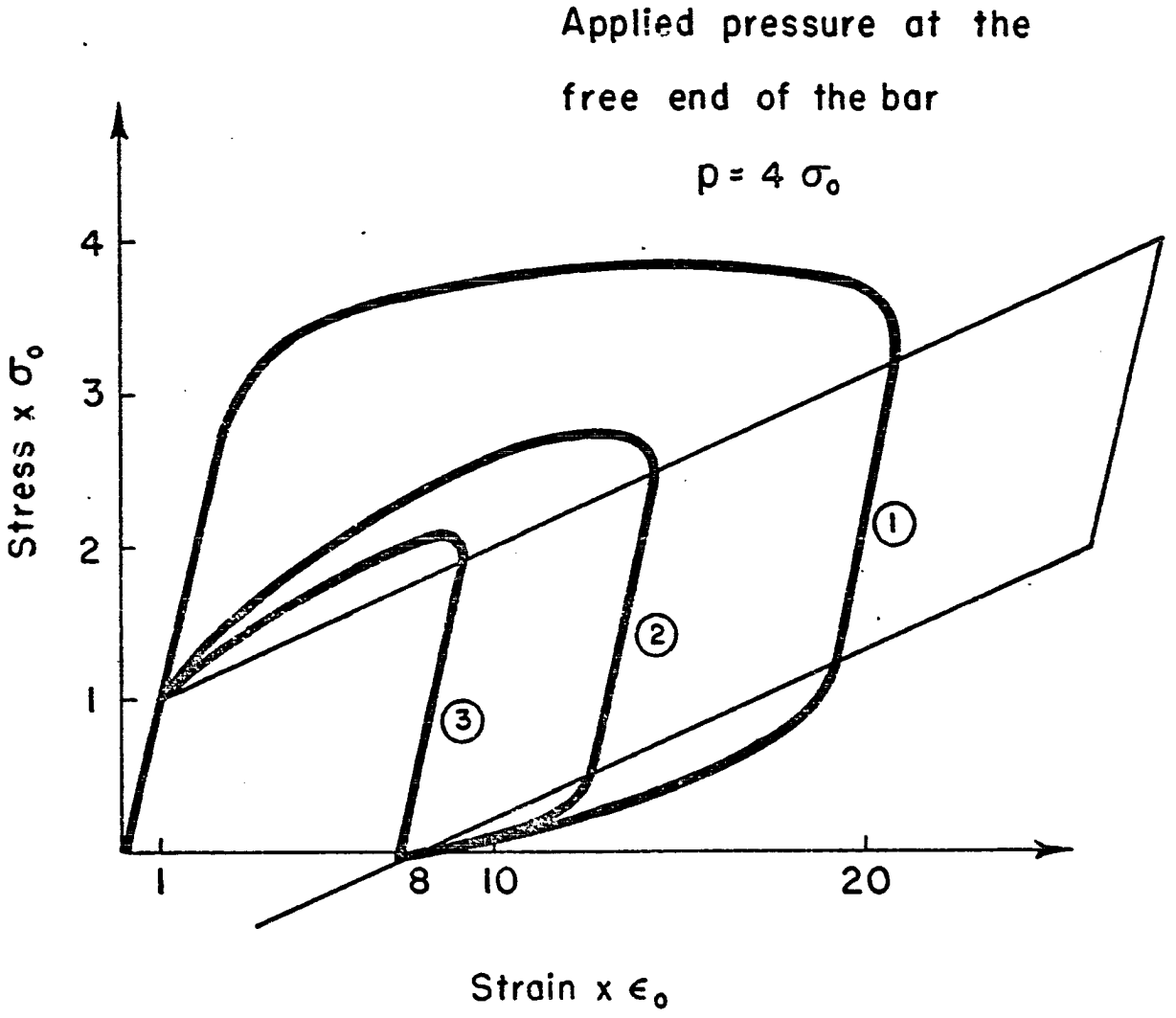

Dynamic stress-strain curves

($p = 4\sigma_0$, $\gamma = 0.063$, $E_2 = E_3 = 0.1111$)

FIG. 5.5

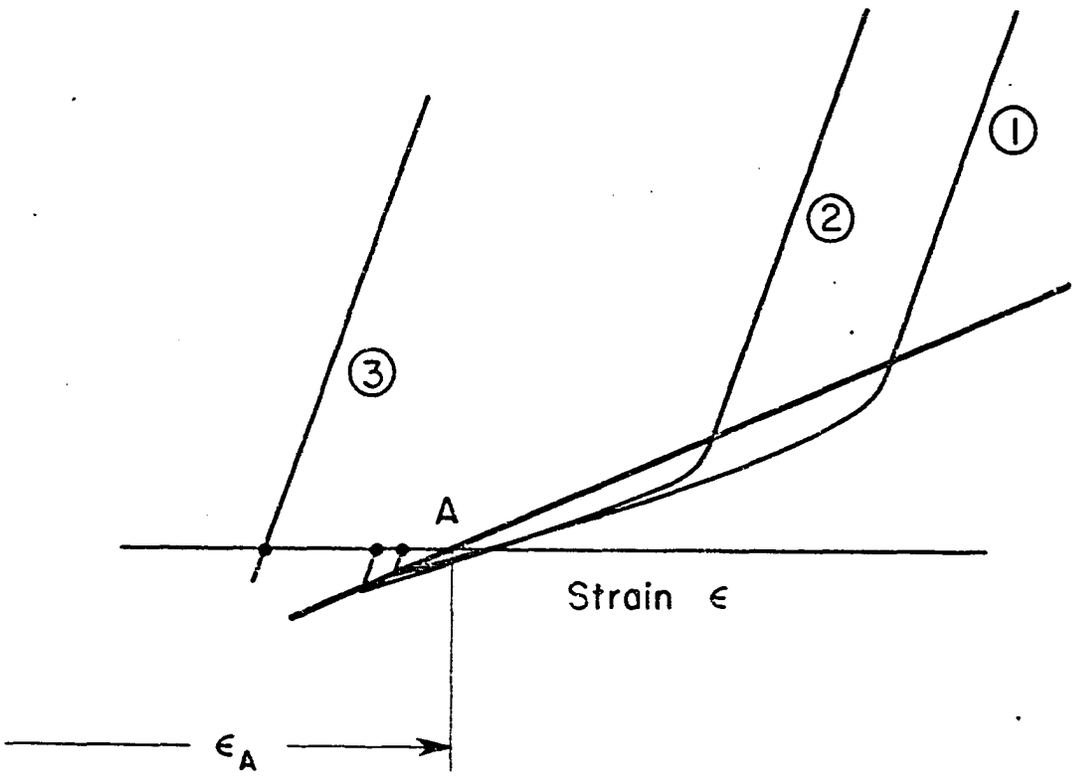

Intersections of the dynamic stress-strain curve with the strain axis

FIG. 5.6

shown in figure 5.8 or figure 5.9. On the other hand, points far away from the end follow a slow stress-strain curve. Therefore, during the unloading process, they will never reach the lower yield point and consequently the unloading part of the dynamic stress-strain curve remains purely elastic. In that case the residual strains decrease more rapidly as the distance from the free end increases. Points experiencing this type of dynamic behavior during unloading produce the second part of the "residual strain, position x along the bar" curve that marks the end of the strain plateau.

A decomposition of the dynamic stress-strain curves presented in figures 5.5 and 5.6 into several sections will allow us to understand the mechanism of dynamic response of each point along the bar to the applied boundary condition. These sections describing the different modes of elastic/viscoplastic behavior will be discussed next.

1. Instantaneous elastic response. As a result of the particular constitutive equation for the inelastic strain-rate, the initial strain is purely elastic, even for stresses exceeding the quasi-static yield limit.

2. Elastic/viscoplastic loading. The actual stress exceeds the stress $f(\varepsilon)$ (i.e. the stress that corresponds to the same total strain ε along the quasi-static stress-strain curve). The value of $g(\sigma,\varepsilon)$ is positive and consequently the inelastic strain rate is positive. With increasing strain ε the yield stress $f(\varepsilon)$ is also increasing and therefore $g(\sigma,\varepsilon) = \sigma - f(\varepsilon)$ is decreasing. By the end of this phase σ

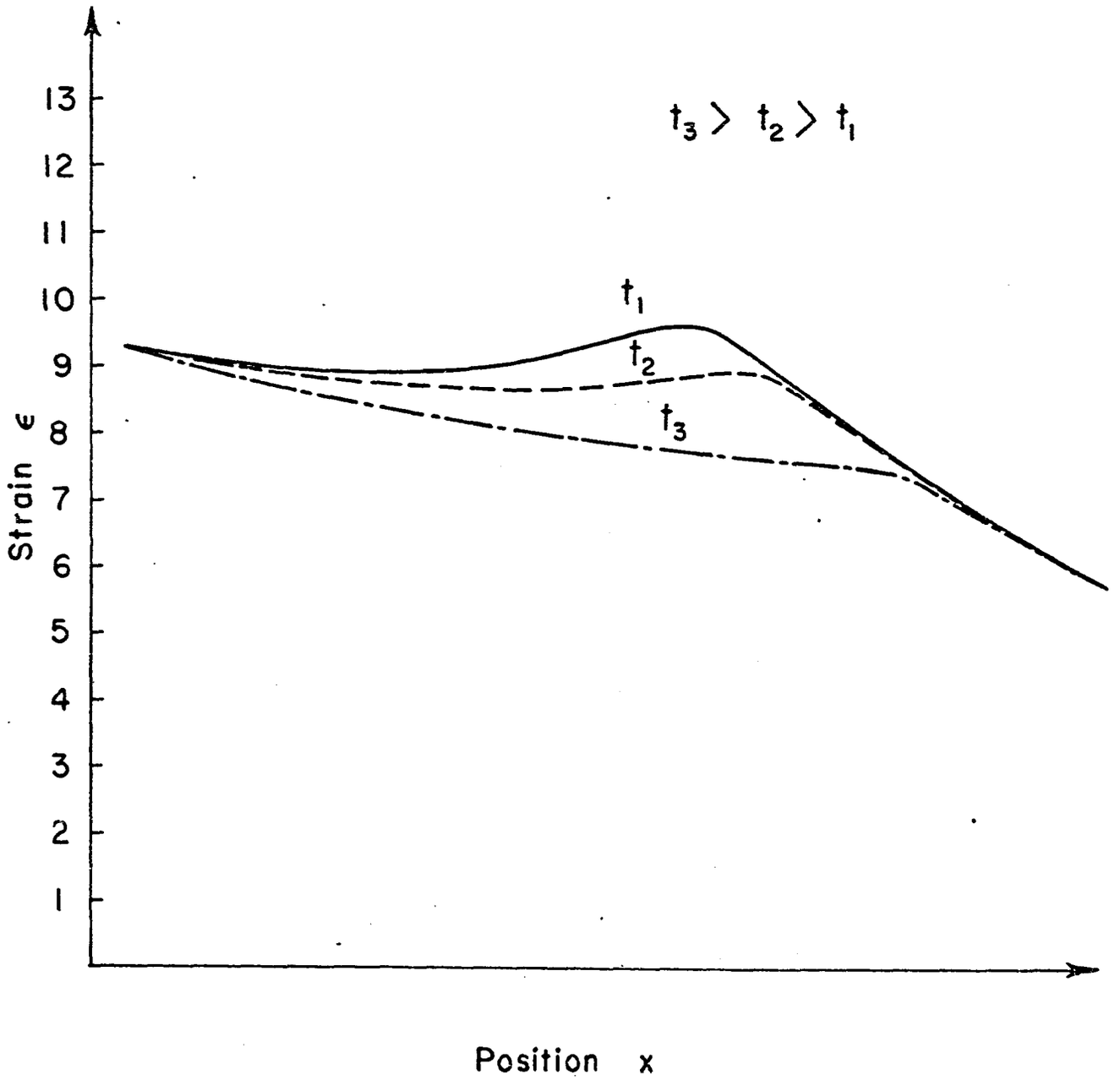

Residual Strain distribution along the bar at several times

FIG. 5.7

becomes equal to $f(\varepsilon)$, $g(\sigma,\varepsilon)$ will consequently be annihilated. This marks the beginning of the next process.

3. After the intersection of the dynamic and quasi-static stress-strain curve, elastic unloading takes place. This is a result of the particular boundary condition at the end of the bar. During the elastic unloading, the dynamic stress point moves along the straight line with slope E_o that passes through the intersection point. The inelastic strain therefore remains constant while $f(\varepsilon)$ is decreasing. The actual stress point decreases at most as far as the corresponding lower yield point.

4. Elastic/viscoplastic unloading. The dynamic stress point lies below the lower yield point line. The function $g(\sigma,\varepsilon)$ now has a negative value and the elastic and viscoplastic strain rates also have negative values. As the total strain decreases, $f(\varepsilon)$ also decreases and at a later time the distance $\sigma-f(\varepsilon)$ increases as the actual stress point approaches the quasi-static stress-strain curve again.

5. Second intersection of the dynamic and quasi-static stress-strain curve. The following phase is elastic loading. The dynamic stress point moves along a straight line with slope E_o that phases through the intersection point. The stress increases while the inelastic strain remains constant. This constant value of the inelastic strain is the residual strain and is shown at the corresponding point in figure 5.8, 5.9, and 5.10 who show the strain plateau. After a small

oscillation which takes place along the elastic loading/unloading line and about the intersection of this line with the strain axis, the stress goes to zero as the transient phenomenon dies out.

Notice that points experiencing dynamic behavior like the one described earlier complete the transient process at a point on the strain axis very close to the point A. Their residual strains, ε^r, ε^r is a slowly decreasing function of the position x along the bar.

This mode of dynamic response gives rise to the so-called "strain plateau", i.e. a region where the residual strain is a slowly decreasing function of x.

The second mode of dynamic behavior described hereunder differs from the above during the fourth phase. Namely, because of the slow rate of dynamic stress-strain response, the actual stress point cannot reach the lower yield point line, and consequently elastic/viscoplastic unloading cannot take place. Instead, the stress point moves as far as a certain point, below the strain axis, then reverses its direction of movement and goes upwards again along the same straight line, i.e. elastic loading takes place. After a few oscillations with decreasing amplitude, the transient process stops at the intersection point between the strain axis and the corresponding straight line of elastic dynamic behavior.

Observe now that the process described in phase II again produces residual strains. These strains can be ex-

pressed as a function of x which is very rapidly decreasing in contrast to the slow decrease of residual strains as a function of position (i.e., x) in phase I. The change in behavior is very abrupt as is evident by the sharp curve at the end of the strain plateau (see figures 5.8, 5.9, and 5.10). In summary, it was found that the plateau of the residual strains at the end of the transient process was the result of these two different modes of dynamic behavior in the vicinity of the point where the line presenting the lower yield points intersected the zero stress axis.

Several points should be brought out in regard to this finding. Observe that the plateau will only develop, according to this theory, if the bar is strained to a stress-strain point that lies on the right hand side of the straight line that is parallel to the elastic stress-strain line and passes through the point where the strain axis intersects with the lower yield point line. Otherwise the unloading phenomenon remains elastic and strain plateau will not develop. Also, note that if the bar is stressed sufficiently to produce a plateau, any additional stress will not increase the magnitude of the plateau, but instead its length. This is due to the fact that the amplitude of the plateau is determined by the fixed intercept of the lower yield point line with the strain axis. This conclusion is not in agreement with DUWEZ and CLARK [34] tests in 1947, which showed that the amplitude of the plateau increased with an increase

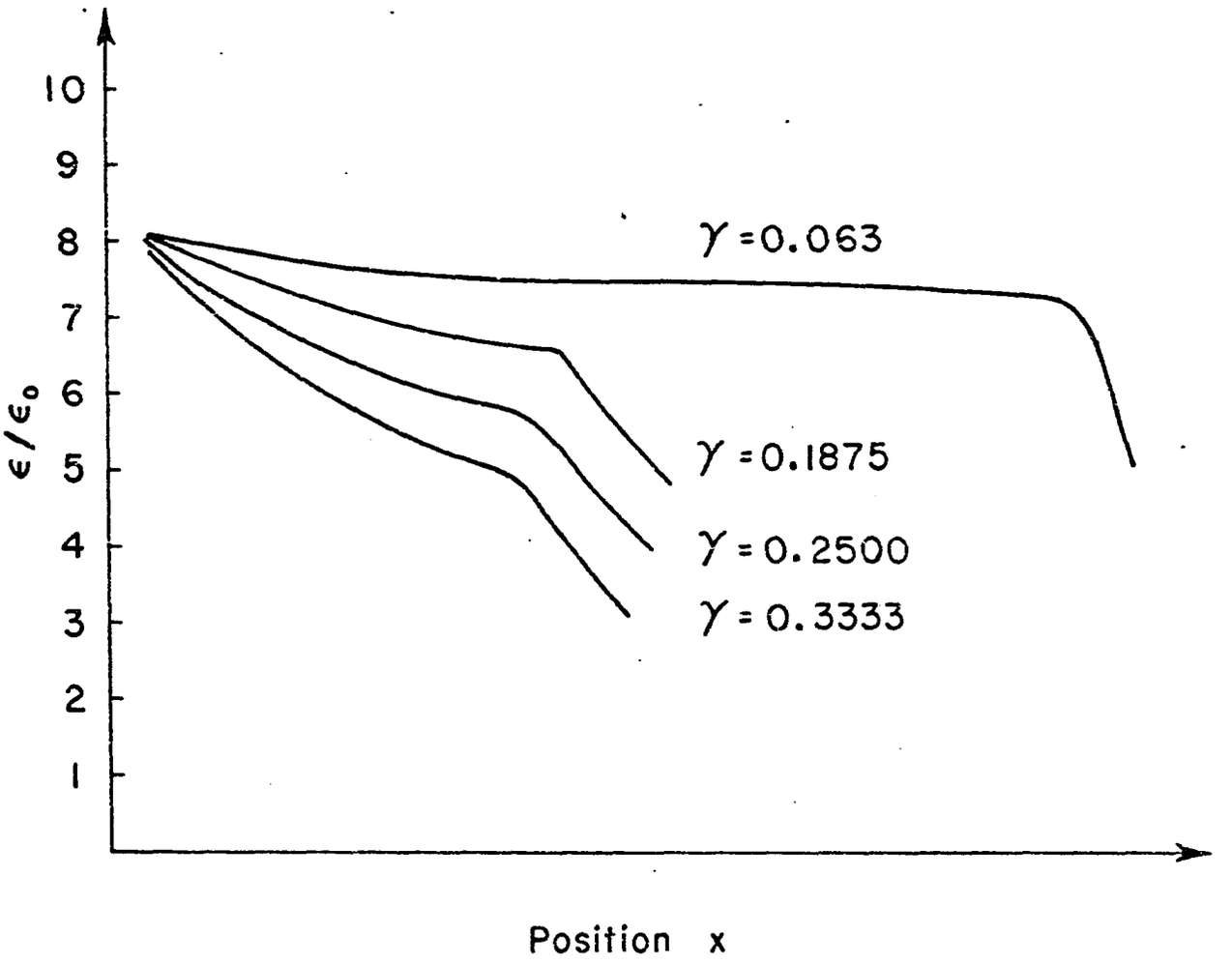

Residual Strain distribution along the bar for several slopes at the unloading part of the stress-time diagram

FIG. 5.8

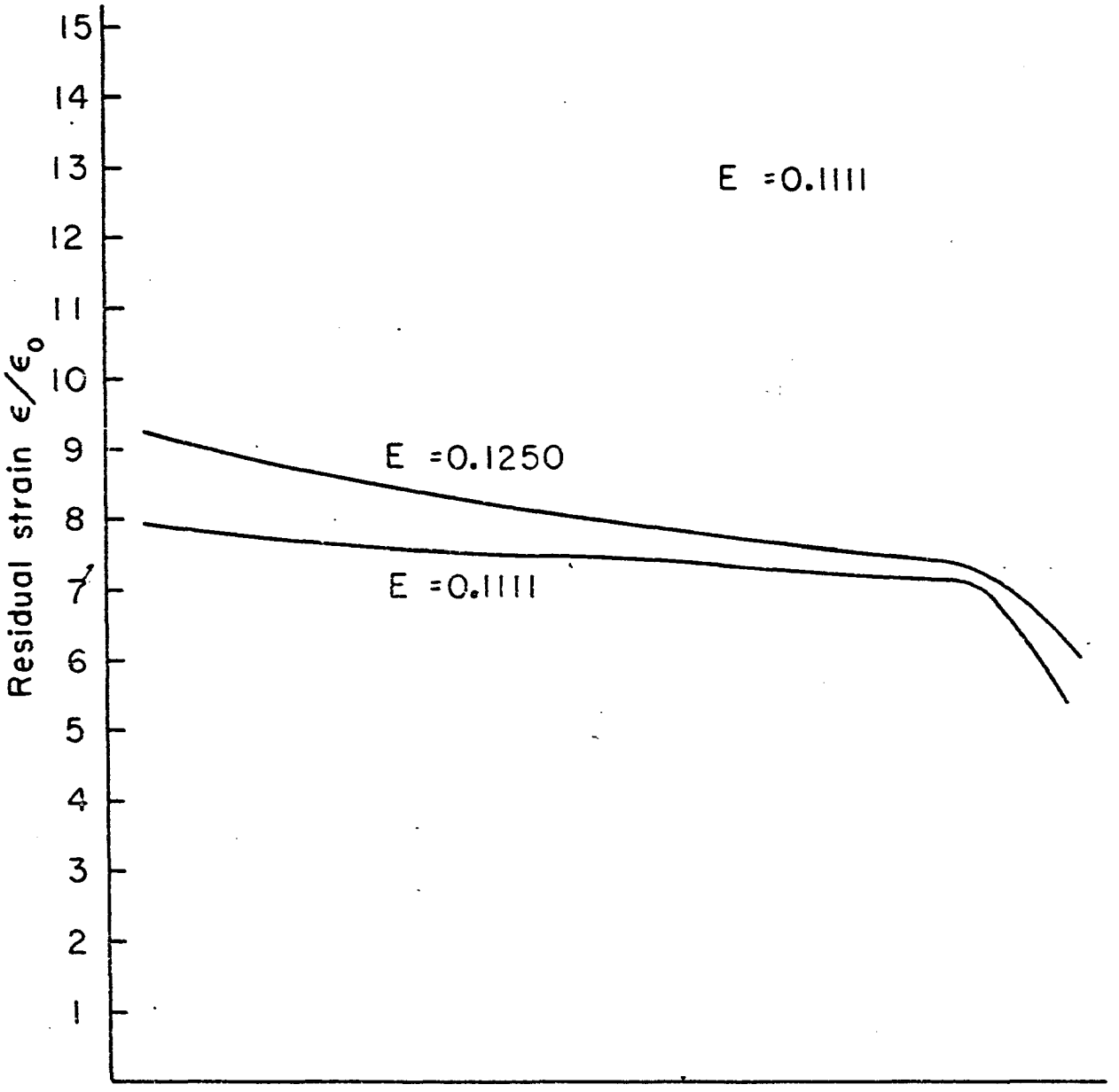

Residual strain distribution along the bar for the same stress-time diagram but for several slopes of the unloading part

FIG. 5.9

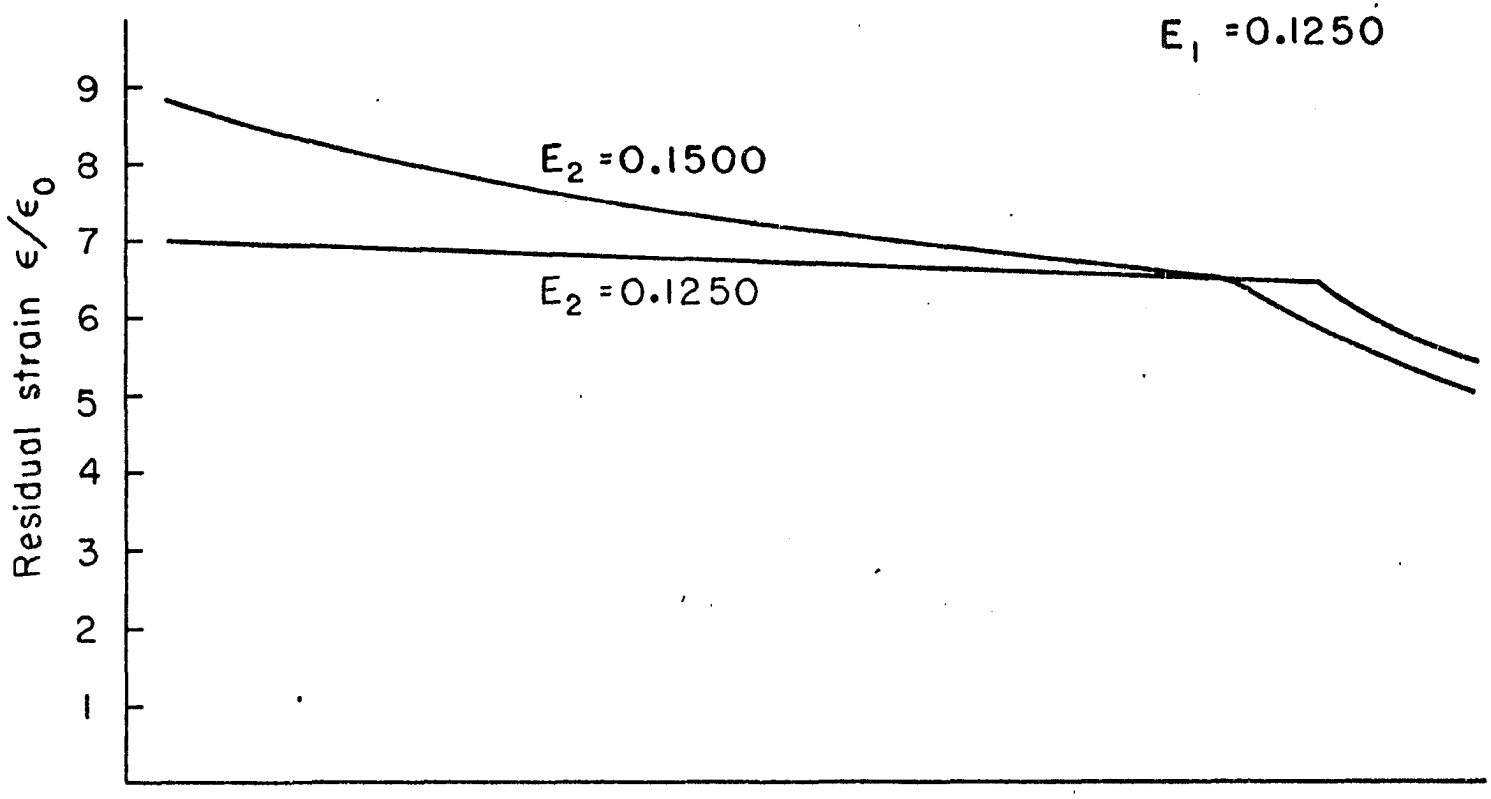

FIG. 5.10

Residual strain distribution along the bar
for the same stress-time diagram, the same strain hardening parameter
E_1 but two different slopes of the unloading part

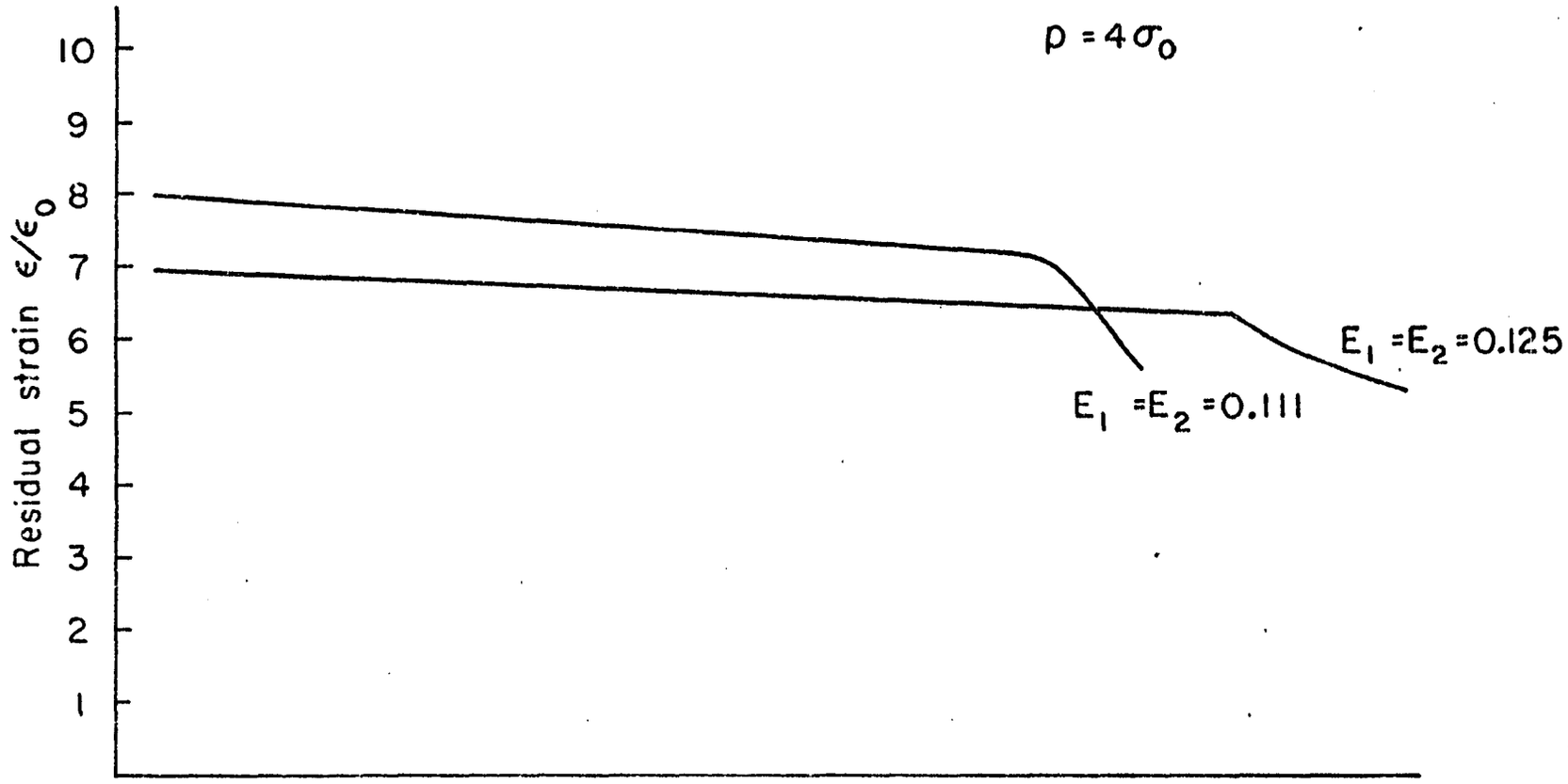

FIG. 5.11

Residual strain distribution along the bar for the same stress-time diagram but for two materials with different strain hardening and Bauschinger effects

in impact force. Whether this is true for strain-rate sensitive materials remains a question. If so, then this suggests that a shift in the intersection point depending on the magnitude of the applied load will be required to take this into account. This justifies a lower yield point line in the quasi-static stress-strain diagram with different slope than the slope of the upper yield point line. In that case, the intersection of the strain axis with the lower yield point line will depend on the applied pressure p at the end of the bar, as figure 5.3 shows. Consequently, the magnitude of the plateau will also depend on p. With regard to the length of the plateau, the calculations have shown that, for the same time duration of the applied load and the same quasi-static stress-strain curve, this is primarily a function of the magnitude of the applied load. Shown in figure 5.11 is the strain plateau for two different values of the applied load at the free end of the bar. Here, we observe the influence of the magnitude of the applied load on the length and the shape of the strain plateau.

Figures 5.9 and 5. 0 explain the influence of the lower yield point, expressed in terms of the slope E_2, on the strain plateau. By increasing the slope E_2, the length of the plateau decreases and also the residual strains change more rapidly with increasing distance from the impact end. A study of the mechanism by which the plateau is formed shows that this is not a surprising conclusion. Indeed, for a given slope E_1, a point inside the bar will experience the

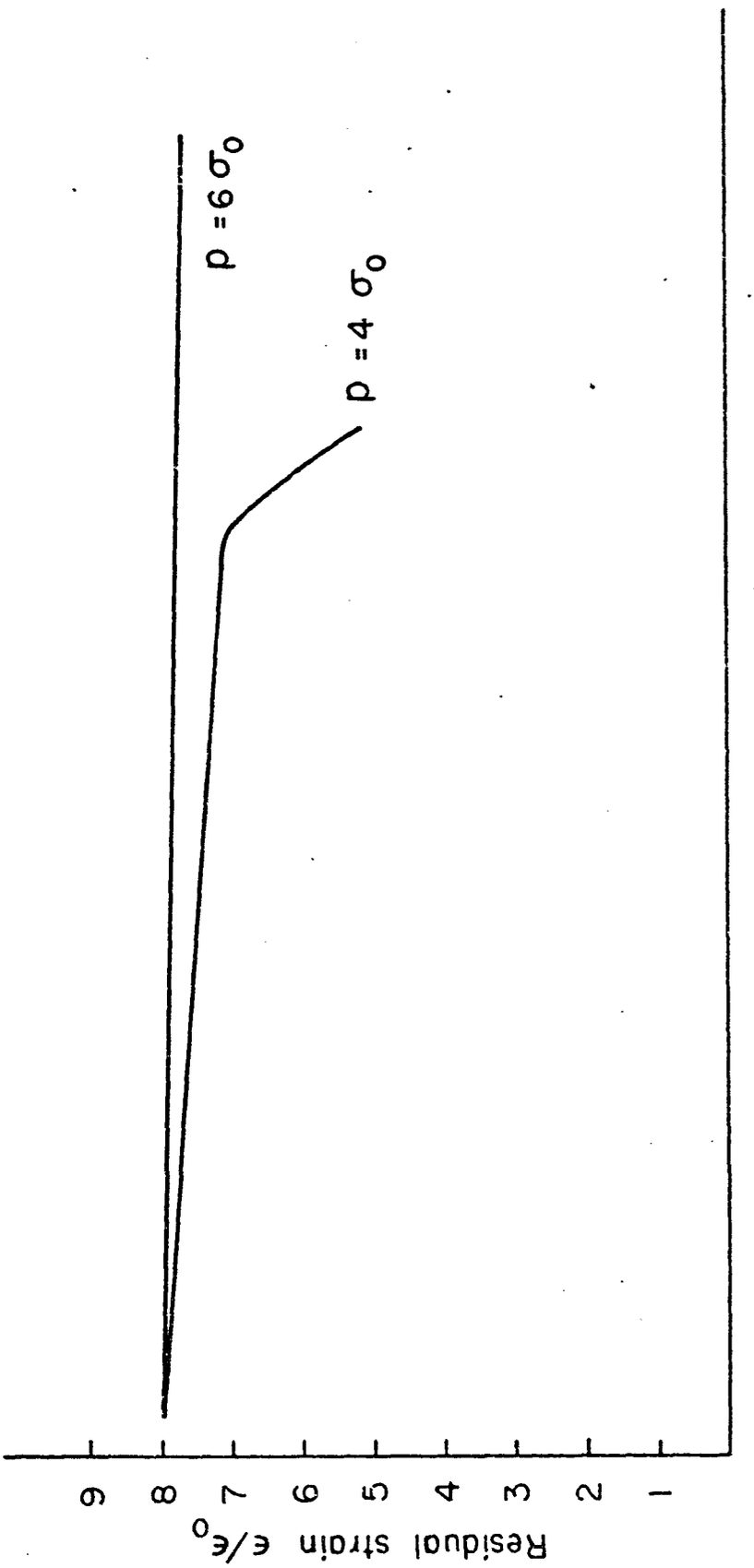

Residual strain distribution along the bar

for $E_1 = E_2 = 0.1111$, $\gamma = 0.063$

FIG. 5.12

first or second mode of dy namic behavior during unloading according to the intersection point of the dynamic stress-strain curve for the given point with the lower yield point line. By decreasing the slope E_2, more points will intersect into the region that produces residual strains which participate in the final strain plateau.

An interesting plot is that given by figure 5.7. Presented are the strain distributions along the bar at several times. They show the time history of buildup of the residual strain plateau. There we observe that the closer to the impact end a point lies, the sooner the strain will take its final value, while points farther inside the bar will still have strains larger than the final value of the corresponding residual strain. With increasing time, more points will reach the residual strain, that is a decreasing function of the distance from the free end, and will participate in the plateau.

REFERENCES

1 Taylor, Brook, "De Motu Nervi Tensi", Phil. Trans p. 26.

2 D'Alembert, J. D., "Recherces sur le Courbe que force une cord tendue mise en vibration", Royal Academy of Berlin, 1747, p. 241.

3 Euler, L., "Sur les Vibration des Cordes", Royal Academy of Berlin, 1748 .

4 Bernoulli, D., "Reflections et eclaircissemens sur les nouvelles vibrations des cordes exposes dans les Memoires de l'Academie de 1847 et 1848", Royal Academy of Berlin, 1850, p. 147.

5 Euler, L., "De Motu Vibratorio Laminarum Elasticarum, Ubi Plures Novae Vibratorum Species Hactenuo Non Pectractatae Evolvuntur", Novi Commentarii Academiae Petrop. Tom XVII (An Acad) 1772 pp. 449-457.

6 Biot, J. B., "Traité de Physique Expérimentale et Mathématique", Paris 1816, Chap. V.

7 Young, Thomas, A course of Lectures on Natural Philosophy and the Mechanical Arts, London 1807.

8 Cauchy, A., Exercises de Mathematique, Paris 1830.

9 Poisson, S. D., Paris Mém. de l'Academie, Vol. 8, 1829.

10 Poisson, S. D., Paris Mém. de l'Academie, Vol. 10, 1831.

11 Poisson, S. D., Traité de Mechanique, Paris 1883.

12 Saint Venant, B., Bull Soc. Philomath.,Paris 1853-1854 Compt. Rend, Vol. 45, p. 204, 1857.

13 Saint Venant, B. and Flamant, K., Compt. Rend. Vol. 97,

pp. 127, 214, 281 and 353.

14 Boussinesq, J., Applications des Potentiels, Paris, 1885.

15 Timoshenko, S. P., History of Strength of Materials, McGraw-Hill, New York, 1953.

16 Todhunter and Pearson, A History of the Theory of Elasticity and of the Strength of Materials, Dover Publications, New York, 1960.

17 Robert Bruce Lindsay, "Historical Introduction" to Lord Rayleigh's,Theory of Sound, Dover, New York, 1945.

18 Struik, D. J., A Concise History of Mathematics, Dover Publications, New York, 1948.

19 Love, A.E.H., The Mathematical Theory of Elasticity, Dover Publications, New York, 1944.

20 Hopkinson, J., "On the Rupture of Iron Wire by a Blow" Proc. Man. Lit. Phil. Soc., Vol. 11, pp. 40-45, Also "Further Experiments on the Rupture of Iron Wire", Proc. Man. Lit. Phil. Soc., Vol. 11, pp. 119-121.

21 Hopkinson, B., Phil. Trans. Royal Soc. of London, Series A, Vol. 213, 1914, p. 237.

22 Ludwik, P., "Uber den Einfluss der Deformationsgeschwindigkeit bei bleibenden Deformationen mit besonderey Berücksichtingung der Nachwirkungserscheinungen", Physicaliche Zeitschrift, Vol. 10, 1909, pp. 411-417.

23 Donnell, L. H., "Longitudinal Wave Transmission and Impact", Trans. Amer. Soc. Mech. Engrs., Vol. 52 (part 1), 1930,pp. 153-167.

24 Perzyna, P., "Fundamental Problems in Viscoplasticity", Advances in Applied Mechanics, Vol. 9, Academic Press, New York, 1966.

25 von Karman, Th., "On the Propagation of Plastic Deformation in Solids", NDRC Report A-103, 1942.

26 von Karman, Th., Bohnenblust, H. F., and Hyers, D. H., "The Propagation of Plastic Waves in Torsion Specimens of Finite Length", NDRC Report A-103, 1942.

27 Taylor, G. I., The Plastic Wave in a Wire Extended by an Impact Load. "The Scientific Papers of G. I. Taylor, Vol. 1, Mechanics of Solids", edited by G. K. Batchelor, Cambridge University Press, pp. 467-479.

28 von Karman, Th. and Duwez, P., "The Propagation of Plastic Deformation in Solids", presented at the Sixth International Congress for Applied Mechanics, Paris, France, 1946.

29 Zener, C. and Hollomon, J. H., "Addendum to von Karman's Theory of the Propagation of Plastic Deformation in Solids", NDRC Memo. A-37M (OSRD No. 659), 1942.

30 Bohnenblust, H. F., "A Note on von Karman's Theory of the Propagation of Plastic Deformation in Solids", NDRC Memo A-41M (OSRD No. 664), 1912.

31 Rakhmatun, K. A., "Propagation of a Wave of Unloading", Prikladnaia Matematika i Mekhanika, Vol. 9, 1945, pp. 91-100 (Russian).

32 Shapiro, G. S., "Longitudinal Oscillations of Bars", Prikladnaia Matematika i Mekhanika, Vol. 10, 1946, pp.

597-616 (Russian).

33 Rakhmatulin, K. A. and Shapiro, G. S., "On the Propagation of Plane Elastic-Plastic Waves", Prikladnaia Matematika i Mekhanika, Vol. 12, 1948, pp. 369-374 (Russian).

34 Duwez, P. E. and Clark, D. S., "An Experimental Study of the Propagation of Plastic Deformation under Conditions of Longitudinal Impact", Proc. Amer. Soc. Testing Mat'ls, Vol. 47, 1947, pp. 502-522.

35 Duwez, P. E. and Clark, D. S., "Discussion of the Forces Acting in Tension Impact Tests of Materials", Journal of Applied Mechanics, Trans. A.S.M.E., Vol. 70, 1948, pp. 243-247.

36 White, M. P. and Griffis, L., "The Permanent Strain in a Uniform Bar due to Longitudinal Impact", Journal of Applied Mechanics, Vol. 14, 1948, pp. A-337-343.

37 White, M. P. and Griffis, L., "The Propagation of Plasticity in Uniaxial Compression", Journal of Applied Mechanics, Vol. 15, 1948, pp. 256-260.

38 White, M. P., "On the Impact Behavior of a Material with a Yield Point", Journal of Applied Mechanics, Vol. 16, 1949, pp. 39-52.

39 De Juhosz, K. J., "Graphical Analysis of Impact of Bars Stressed above the Elastic Range", Journal of the Franklin Institute, Vol. 248, 1949, pp. 15-48, 113-142.

40 von Karman, Th. and Duwez, P., "The Propagation of Plastic Deformation in Solids", Journal of Applied

Physics, Vol. 21, 1950, pp. 987-994.

41 Bell, J. F., "Propagation of Plastic Waves in Pre-stressed Bars", Department of Mechanical Engineering, The Johns Hopkins University Technical Report No. 5, 1951.

42 Sternglass, E. J. and Stuart, D. A., "An Experimental Study of the Propagation of Transient Longitudinal Deformations in Elastoplastic Media", Journal of Applied Mechanics, Vol. 20, 1953,pp. 427-434.

43 Alter, B.E.K. and Curtis, C. W., "Effect of Strain Rate on the Propagation of a Plastic Strain Pulse along a Lead Bar", Journal of Applied Physics, Vol. 27, 1956, pp. 1079-1085.

44 Malvern, L. E., "The Propagation of Longitudinal Waves of Plastic Deformation in a Bar of Material Exhibiting a Strain-Rate Effect", Journal of Applied Mechanics, Vol. 17-18, 1950-51, pp. 203-208.

45 Malvern, L. E., "Plastic Wave Propagation in a Bar of Material Exhibiting a Strain-Rate Effect", Quarterly of Applied Mathematics, Vol. VIII, 1951, pp. 405-411.

46 Malvern, L. E., "Experimental Studies of Strain-Rate Effects and Plastic-Wave Propagation in Annealed Aluminum"in Behavior of Materials Under Dynamic Loading, edited by N. J. Huttington, ASME, New York, 1965., pp. 81-92.

47 Wood, E. R. and Phillips, A., "On the Theory of Plastic Wave Propagation in a Bar", Journal of the Mech. and Phys. of Solids, Vol. 15, 1967, pp. 241-254.

48 Ripperger, E. A. and Watson, H., "The Relationship between the Constitutive Equation and One-dimensional Wave Propagation" in Mechanical Behavior of Materials under Dynamic Loads, edited by U. S. Lindholm, Springer Verlag, New York, 1968, pp. 294-313.

49 Nicholson, D. W., The Dynamic Generalizations of Plasticity, Doctoral Dissertation, Yale University, 1971.

50 Wierzbicki, T., "A Thick-Walled Elasto-Visco-Plastic Spherical Container under Stress and Displacements Boundary Conditions", Arch. Mech. Stos., Vol. 15, 1963, p. 297.

51 Perzyna, P. and Bejda, J., "The Propagation of Stress Waves in a Rate Sensitive and Work Hardening Plastic Medium", Arch. Mech. Stos., Vol. 16, 1964, p. 1215.

52 Zabinski, M. P., Spherical Wave Propagation in Rate Dependent Media, Doctoral Dissertation, Yale University, 1969.

53 Jaerish, P.,"Uber die Elastischen Schwingungen einer Isotropen Kugel", Journal für die reine und Angewandte Mathematic, Vol. 88, 1880, pp. 131-145.

54 Jaerish, P., "Allgemeine Integration der Elasticitätsgleichungen für die Sahwingungen und das gleichgewicht Isotroper Rotationscörper", Journal für die reine und Angewandte Mathematik, Vol. 104, 1889, pp. 177-210.

55 Chree, C., "The Equations of an Isotropic Elastic Solid in Polar and Cylindrical Coordinates, their Solution and

Application", Transactions of the Cambridge Philosophical Society, Vol. 14, 1889, pp. 250-369.

56 Basset, A. B., "On the Radial Vibrations of a Cylindrical Elastic Shell", Proceedings of the London Mathematical Society, Vol. 21, 1889, pp. 53-58.

57 Sezawa, K., "Dilatational and Distortional Waves Generated from a Cylindrical or a Spherical Origin", Bulletin of the Earthquake Research Institute, Tokyo University, Vol. II, March 1927, p. 13.

58 Kromm, A., "Zur Ausbreitung von Stobwellen In Kreislochscheiben", Z. angew. Math. Mech., Bd. 28, 1948, pp.104-114 and pp. 297-303.

59 Selberg, H., "Transient Compression Waves from Spherical and Cylindrical Cavities", Arkiv for Fysik, Vol. 5, 1952, pp. 97-108

60 Goodier, J. N. and Jahsman, W. E., "Propagation of a Sudden Rotary Disturbance in an Elastic Plate in Plane Stress", Journal of Appl. Mech., Vol. 23, Trans. ASME, Vol. 78, 1956, pp. 284-286.

61 Jahsman, W. E., "Propagation of Abrupt Circular Wave Fronts in Elastic Sheets and Plates", Proceedings of the 3rd National Congress of Applied Mechanics, 1958, pp. 115-202.

62 Miklowitz, J., "Plane-Stress Unloading Waves Emanating from a Suddenly Punched Hole in a Stretched Elastic Plate", Journal of Applied Mechanics, Vol. 27, Trans.

ASME, Vol. 82, Series E, 1960, pp. 165-171.

63 Eringen, A. C., "Propagations of Elastic Waves Generated by Dynamic Loads on Circular Cavity", Journal of Appl. Mechanics, Vol. 83, Trans. ASME, 1961, pp. 218-222.

64 Plass, H. J. and Ellis, B. C., "Solution of Some Problems of Cylindrical Waves in Flat Elastic Plates" in Developments in Mechanics, edited by Ostrach and Scanlan, Vol. 2, Solid Mechanics, Pergamon Press, New York, 1965, pp. 402-418.

65 Pei Chi Chou and Koenig, H. A., "A Unified Approach to Cylindrical and Spherical Elastic Waves by Method of Characteristics", Journal of Applied Mechanics, Trans. ASME, Vol. 33, 1966, pp. 159-167.

66 Forrestal, M. J., "Transient Response at the Boundary of a Cylindrical Cavity in an Elastic Medium", Int. J. Solids Structures, 1968, Vol. 4, pp. 391-395.

67 Rader, D., "The Propagation of Extensional Cylindrical Pulses in Elastic Plates", J. Mech. Phys. Solids, 1969, Vol. 17, pp. 91-109.

68 Mehta, P. K. and Davids, N., "A Direct Numerical Analysis for Cylindrical and Spherical Elastic Waves", AIAA Journal, 1966, pp. 112-117.

69 Mehta, P. K., "Cylindrical and Spherical Elastoplastic Waves by a Unified Direct Analysis Method", AIAA Journal, Vol. 5, 1967, pp. 2242-2248.

70 Johnson, J. N., "Elastic Precursor Decay in Quartzite for

Cylindrical and Spherical Flow", Journal of Applied Physics, Vol. 39, 1968, pp. 290-296.

71 Ting, T.C.T., "Elastic-Plastic Boundaries in the Propagation of Plane and Cylindrical Waves of Combined Stress", Quarterly of Appl. Math., Vol. 27, 1970, pp. 441-449.

72 McNiven, H. D. and Mengi, Y., "Dispersion of Cylindrical Waves in a Viscoelastic Body", Report No. 69-24, University of California, Berkeley, 1969.

73 Eason, G., "Wave Propagation in Inhomogeneous Elastic Media; Normal Loading of Spherical and Cylindrical Surfaces", Appl. Sci. Res. 21, 1970, pp. 467-477.

74 Swift, R. P., "An Examination of an Elastic/Viscoplastic Theory using Radial Cylindrical Stress Wave Propagation", Doctoral Dissertation, University of Washington, 1969.

75 Murakami, S. and Bejda, J.,"Two-dimensional Cylindrical Problem of Elastic/Viscoplastic Wave Propagation", Archives of Mechanics, Vol. 23, 2, 1971, pp. 199-211.

76 Lindholm, U. S., "Dynamic Deformation of Metals", in Behavior of Materials Under Dynamic Loading, edited by N. J. Huffington, ASME, 1965, pp. 42-61.

77 Bell, J. F., "The Dynamic Plasticity of Metals at High Strain Rates: An Experimental Generalization", in Behavior of Materials Under Dynamic Loading, edited by N.J. Huffington, ASME 1965, pp.19-41.

78 Hauser, F. E., Simmons, D. A., and Dorn, D. E., "Strain Rate Effects in Plastic Wave Propagation", Response of

Metals to High Velocity Deformations, edited by Shewwon and Zackay, Interscience, New York, 1961.

79 Ensminger, R. R. and Fyfe, I. M., "Constitutive Model Evaluation Using Cylindrical Stress Wave Propagation", J. Mech. Phys. Solids, 1966, pp. 231-238.

80 Fyfe, I. M., "Plane-Strain Plastic Wave Propagation in Dynamically Loaded Hollow Cylinder" in Mechanical Behavior of Materials under Dynamic Loads", edited by U. S. Lindholm, Springer, New York, 1968, pp. 314-328.

81 Swift, R. P. and Fyfe, I. M., "Elastic/Viscoplastic Theory Examined using Radial Cylindrical Stress Waves", Journal of Applied Mechanics, Trans. of ASME, 1970, pp. 1134-1140.

82 Davies, R. M., "A Critical Study of the Hopkinson Pressure Bar", Phil. Trans. R. Soc. A240, 14375, 457

83 Cristescu, N., "European Contributions to Dynamic Loading and Plastic Waves"in Plasticity, Proceedings of the Second Symposium of Naval Structural Mechanics, edited by E. H. Lee and P. S. Symonds, Pergamon Press, New York 1960, p. 386-387.

84 Hencky, "Zur theorie plasticher Deformationen und der hierdurch im material hervorgerufenen Nachspannungen". Zeitschrift angen. Math. Mech. 4, 1924, p. 323-384.

85 Hohenemser, K. and Prager, W., "Über die Ansatze der Mechanik isotroper Kontinua", Zeitschrift für Angew. Math und Mech. 12, 1932, pp. 216-226.

86 Ilyushin, Ucheneye Zap. Mosk. Univ. Mekhanika, Vol. 39, 1940, p. 1.

87 Oldroyd, J. G., "A Rational Formulation of the Equations of Plastic Flow for a Bingham Solid", Proc. Cambridge Phil. Soc., Vol. 43, 1947, pp. 100-117.

88 Bingham, E. C., Fluidity and Plasticity, McGraw-Hill, New York, 1922, pp. 215-218.

89 Perzyna, P., "The Constitutive Equations for Rate Sensitive Plastic Materials", Quarterly of Appl. Math., Vol. 20, 1962, pp. 321-332.

90 Perzyna, P., "On the Constitutive Equations for Work-hardening and Rate Sensitive Plastic Materials", Bulletin de l'Académie de Sciences Polonaise, Vol. XII, 1964, pp. 249-256.

91 Wu, H. C., Viscoplasticity Under Complex States of Stress, Doctoral Dissertation, Yale University, 1970.

92 Cristescu, N. and Mihailescu, M., "On Dynamic Relaxation", Rheol. Acta, Vol. 6, 1967, pp. 144-146.

93 Cristescu, N., Dynamic Plasticity, North-Holland Publishing Co., Amsterdam, 1967.

94 Fridrichs, K. O., "Nonlinear Hyperbolic Differential Equations for Functions of Two Independent Variables", Am. J. Math., Vol. 70, 1948, pp. 555-588.

95 Courant, C. and Lax, W., "Remarks on Cauchy's Problem for Hyperbolic Partial Differential Equations with Constant Coefficients in Several Independent Variables", Communs. Pure and Appl. Math., Vol. 8, 1955, pp. 497-502.

96 Hartman, I. and Winter, H., "On Hyperbolic Differential Equations", Am. J. Math., Vol. 74, 1952, pp. 834-864.

97 Courant,C. and Hilbert, D., Methoden der Mathematischen Physik, Vol. 2, Springer, Berlin, 1937.

98 Clifton, R. J., "An Analysis of Combined Longitudinal and Torsional Plastic Waves in a Thin-Walled Tube", Proc. of 5th U.S. National Congress in Mechanics, 1966, pp. 465-480.

99 Hadamard, J., Lecons sur la Propagation des Ondes et les equations de l'hydrodynamique, New York, 1949, pp. 81-128.

100 Ziv, M., Elastic Wave Propagation in Plane Strain Problems", Dissertation, Iowa State University, 1968.

101 Ziv, M., "Two-spatial Dimensional Elastic Wave Propagation by the Theory of Characteristics", Int. J. Solids Structures, Vol. 5, 1969, pp. 1135-1151.

102 Ziv, M. "The Decay of Leading Elastic Waves by the Theory of Characteristics", Int. J. Eng. Sci., Vol. 8, pp. 483-497.

103 Thomas, T. Y., "Singular Surfaces and Flow Lines in the Theory of Plasticity", Journ. of Rational Mechanics and Analysis, Vol. 2, 1953, pp. 339-381.

104 Hopkins, H. G., "Dynamic Expansion of Spherical Cavities in Metals", Progress in Solid Mechanics I, 1960, pp. 83-164.

105 Tenenbaum, M. and Pollard, H., Ordinary Differential Equations, 1964, New York

106 Richarson, Lewis F. and Gount, A., "The Deterred Approach to the Limit", Transactions of the Royal Society of London, Vol. 226, Series A, 1926-27, p. 300.

107 Hartee, Douglas R., "Some Practical Methods of Using Characteristics in the Calculation of non-steady Compressible Flow", AECU-2713, September 1953.

108 Fox, P. and Ralston, A., "On the Numerical Solution of the Equations for Spherical Waves of Finite Amplitude, I", Journ. Math. and Phys., Vol. XXXVI, No. 4, Jan. 1958, pp. 313-328.

109 Roberts, L., "On the Numerical Solution of the Equations for Spherical Waves of Finite Amplitude, II, Journal of Math. and Phys., No. 4, Jan. 1958, pp. 329-337.

110 Lister, M., "The Numerical Solution of Hyperbolic Partial Differential Equations by the Method of Characteristics" in Mathematical Methods for Digital Computers, edited by Anthony Ralston and Herbert S. Wilf, J. Wiley, New York, 1960.

111 Carnahan, B., Luther, H. A. and Wilkes, J. O., Applied Numerical Methods, J. Wiley, New York, 1969.

112 Richtmyer, R. D., Difference Methods for Initial Value Problems, Interscience Publishers, New York, 1957.

113 Kolsky, H., Stress Waves in Solids, Dover, New York, 1963.

114 Wood, E. R., The Effect of Lower Yield on the Propagation of Plastic Waves, Doctoral Dissertation, Yale University 1967.

115 Mengi, Y. and McNiven, H. D., "Analysis of the Transient Excitation of an Elastic Rod by the Method of Characteristics", Int. J. Solids Structures, 1970, Vol. 6, pp. 871-892.

116 Courant, R., Isaacson, E. and Rees, M., "On the Solution of Nonlinear Hyperbolic Differential Equations by Finite Differences", Communication on Pure and Appl. Math., Vol. V, 1952, pp. 243-295.

117 Fox, P., "The Solution of Hyperbolic Partial Differential Equations by Difference Methods" in Mathematical Methods for Digital Computers, edited by A. Ralston and H. S. Wilf, John Wiley, New York, 1960.

A P P E N D I X I

Cylindrical waves

a. Flow chart of the computer program

b. Computer program

FLOWCHART OF THE COMPUTER PROGRAM

1. calculation of general parameters

2. calculation on the wave front

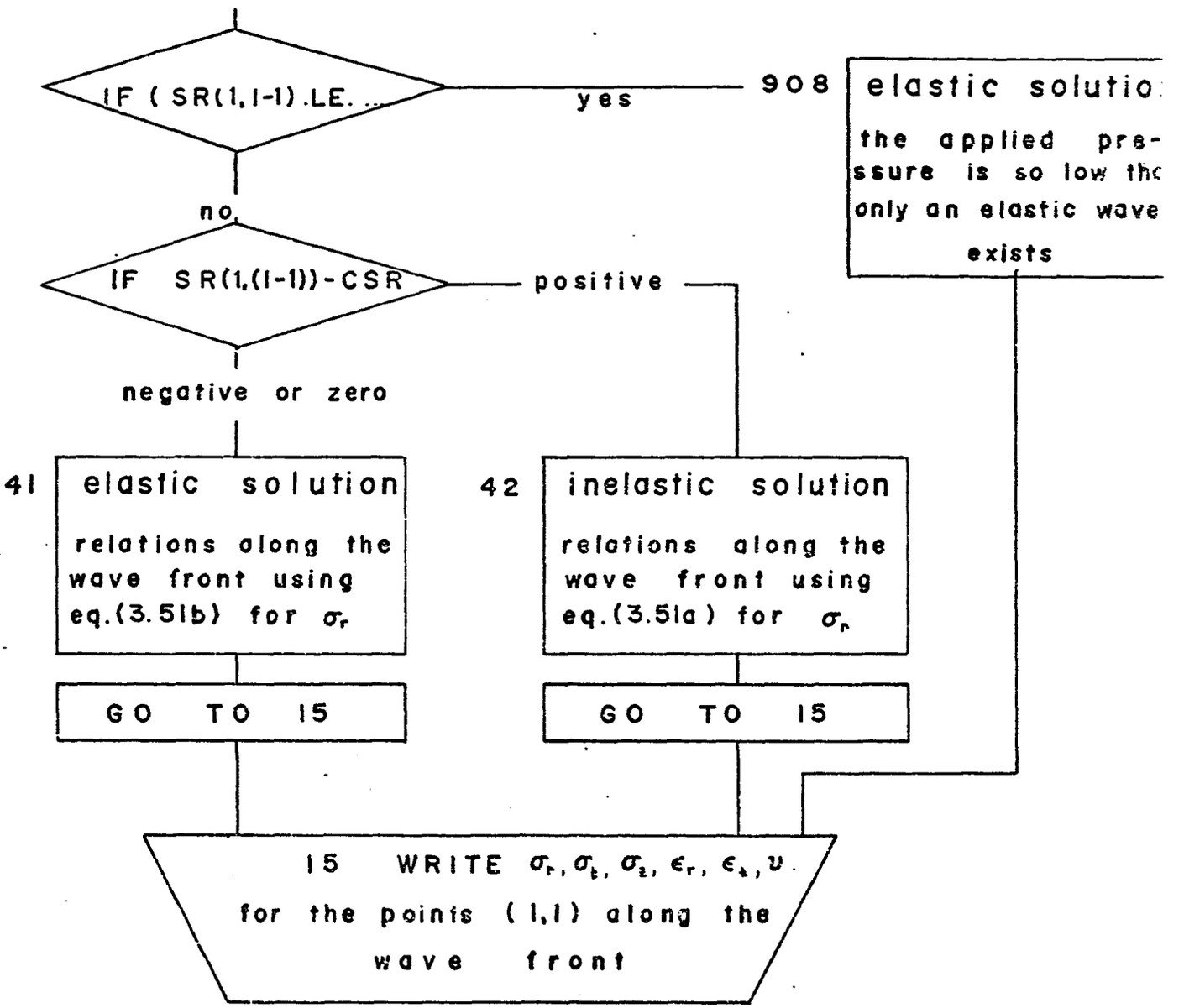

3. boundary conditions on the surface of the cylindrical cavity i.e.

4. calculations along the new characteristic II

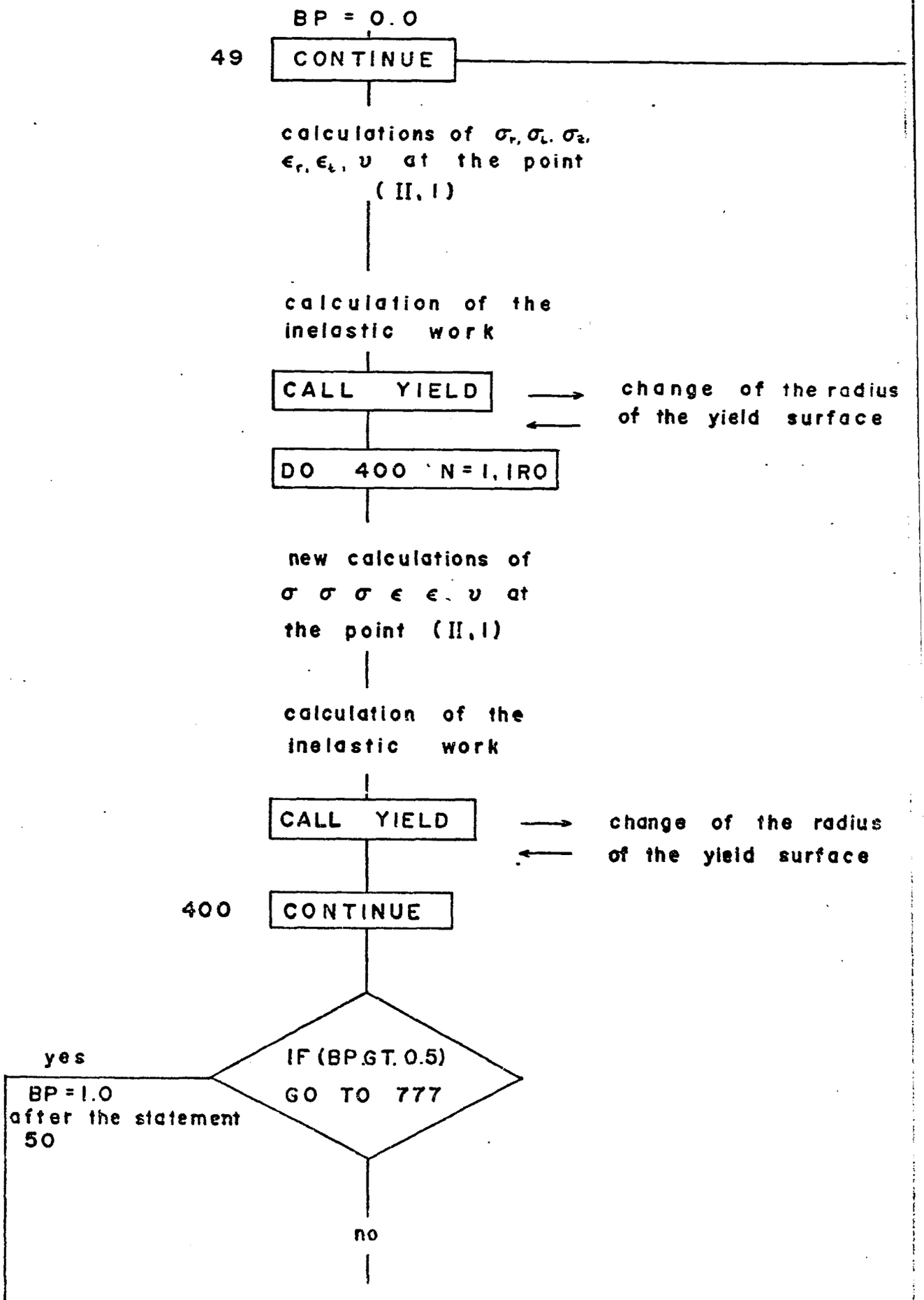

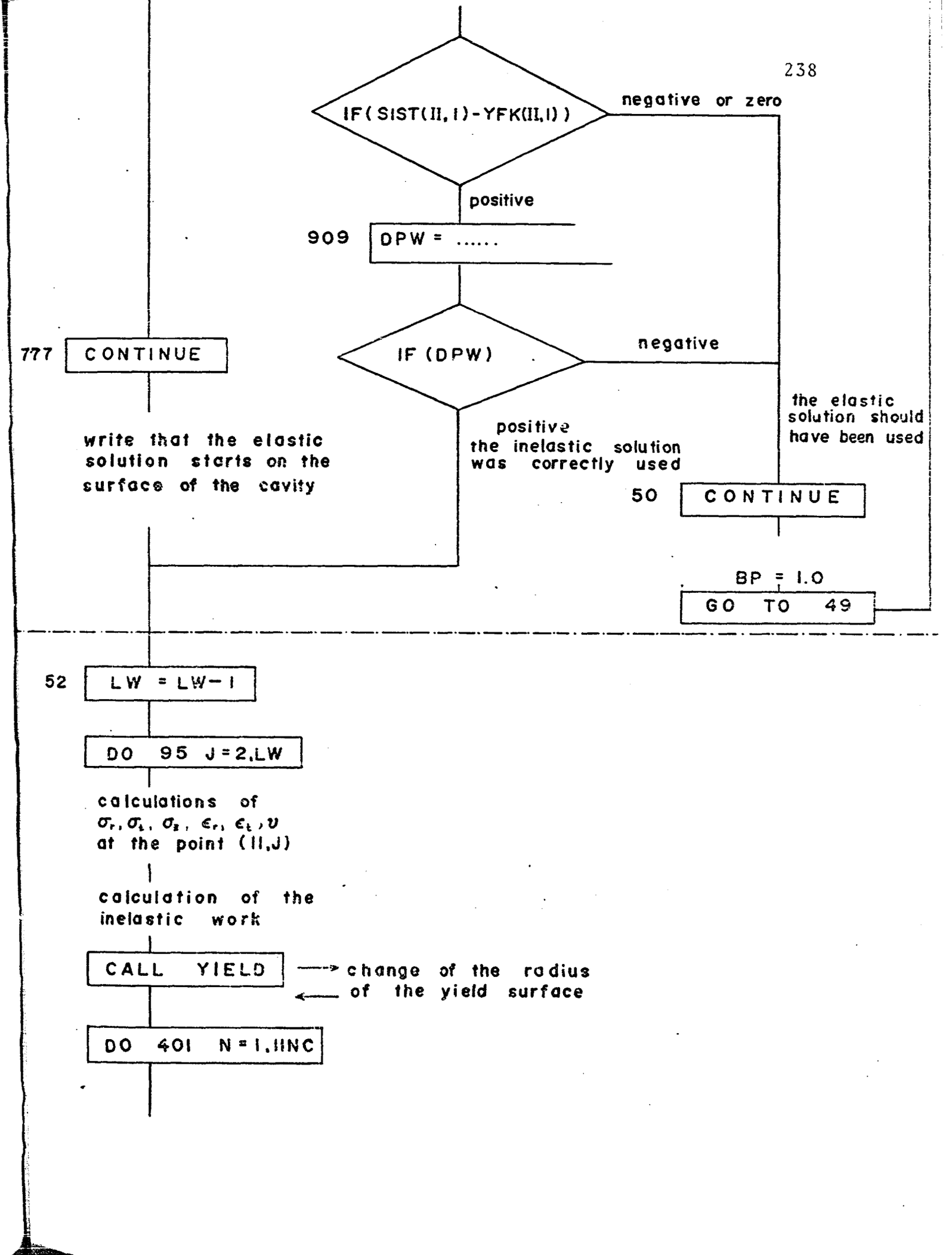

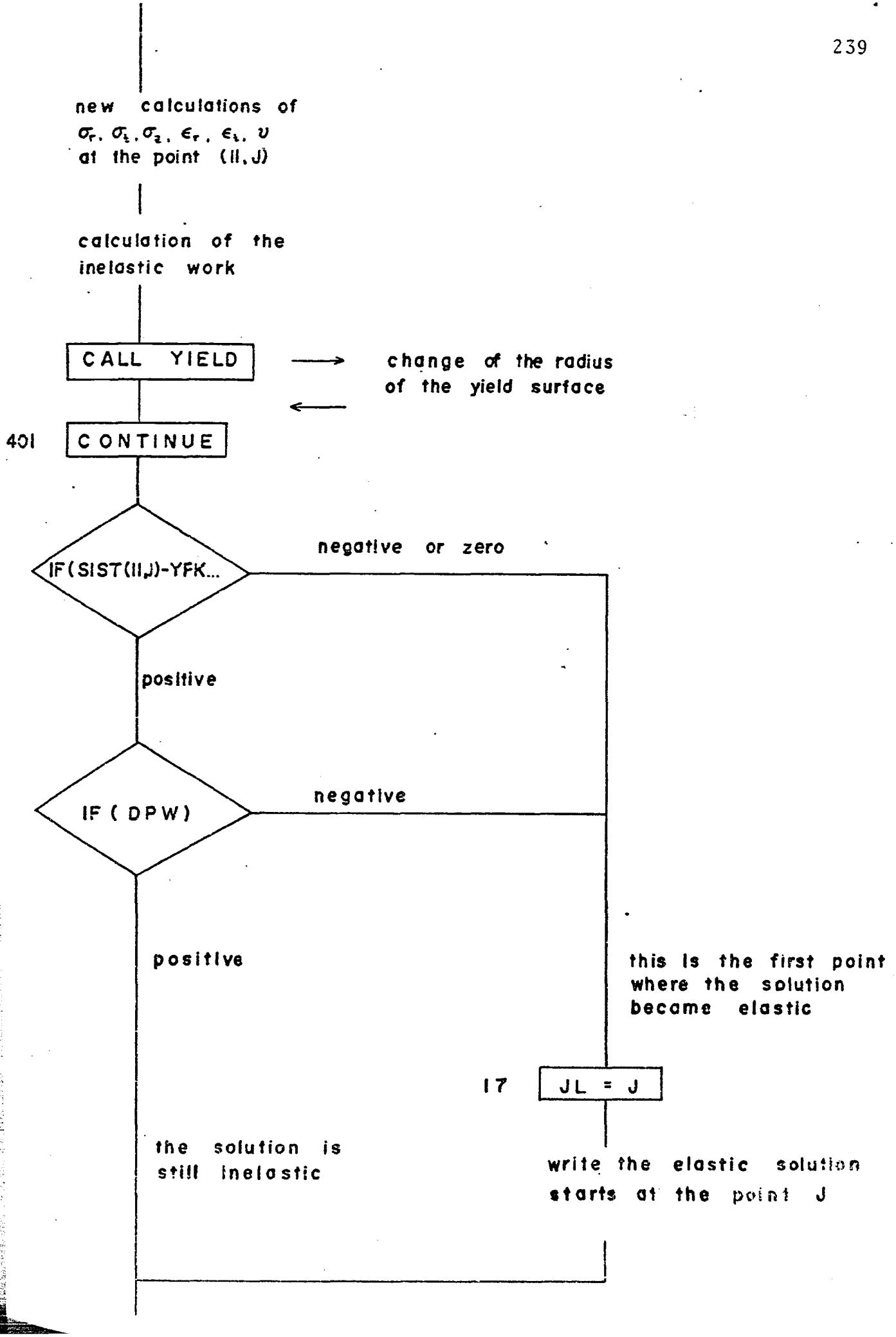

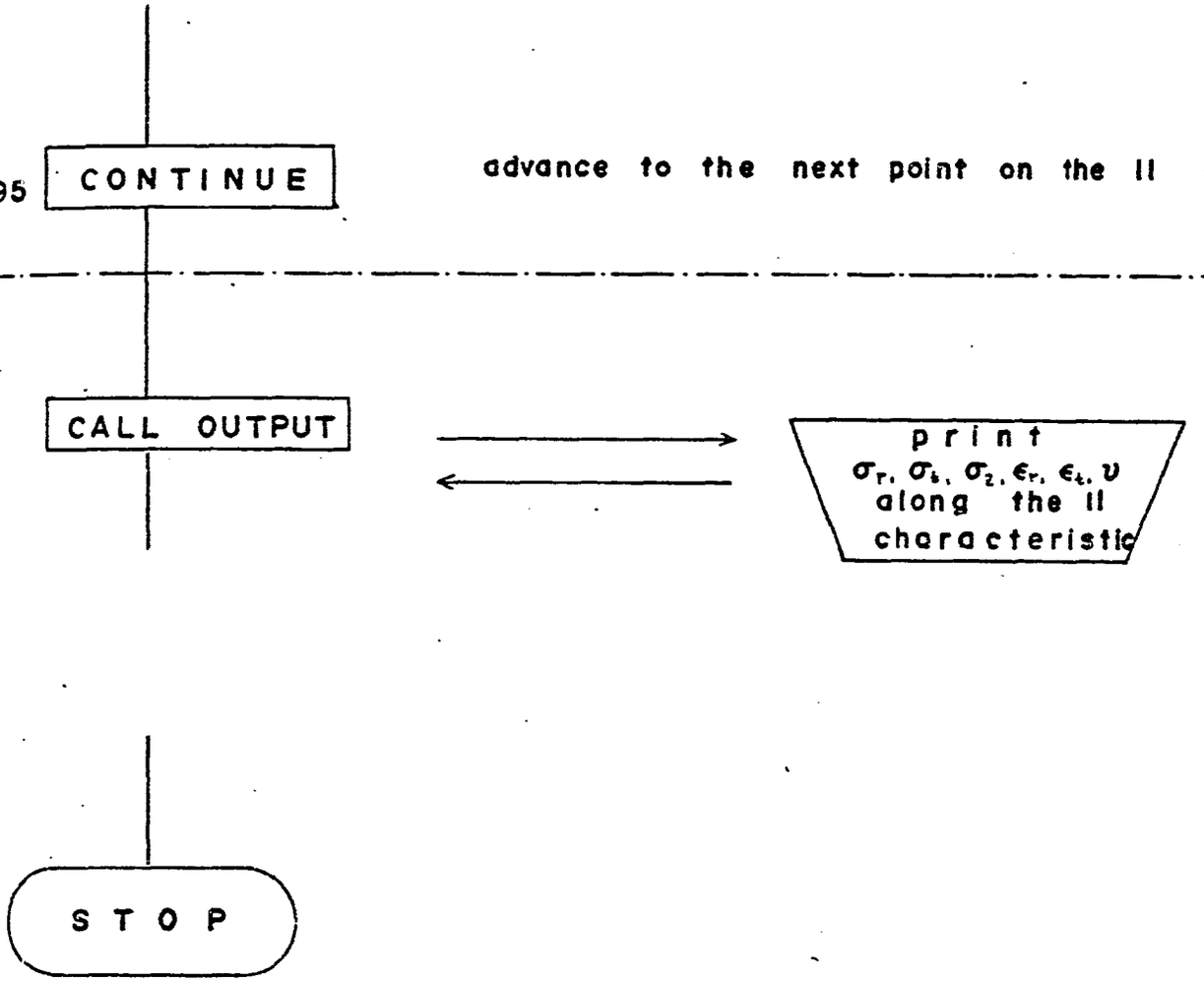

```
$PUFFT
PUFFT VERSION 3/1/68
      DIMENSION SR(2,151),ST(2,151),SZ(2,151),ER(2,151),ET(2,151),V(2,1
     251),SIST(2,151),CRC(2,151),COCO(2,151),EER(2,151),EET(2,151),PER(2
     3,151),PET(2,151),YFK(2,151),RR(151),R(151),PW(2,151),COCOA(2,151),
     4SP(151)
      COMMON LW,SR,ST,SZ,ER,ET,V,EER,EET,PER,PET,PW,YFK,IA,JINC,W,EX,FL,
     2 RO,I,STYL,EO,ERATIO,EMMA,BBB,I,SIST
    9 READ (5,30) EO,RHO,ALPHA,XN,PP,NP                                  11
   30 FORMAT(4F10.5,F10.5,I5)                                            12
   NW  MUST BE EQUAL OR LARGER TO (NWU+1)                                13
    2 FORMAT(4I5,E10.5,4F10.5)
    1 READ (5,2) NW,NBU,JINC,IINC,DT,P,ERATIO,RO
      IRO = IINC + 2                                                     16
      STYL = 1000.0
                                                                         1

      SK IN THIS PROGRAM REPRESENTS THE INITIAL VALUE OF THE RADIUS
      RJ OF THE YIELD SURFACE


      STYL IS THE YIELDING STRESS IN SIMPLE TENSION


      SK = 1.414214*STYL/1.73205


      P IS THE APPLIED PRESSURE

      P = P * STYL

      WRITE(6,20) EO,RHO,XN,DT,P,ERATIO,ALPHA
   20 FORMAT(1H1,'VISCOPLASTIC CYLINDRICAL WAVES'20X,'PAUL E. ZANNIS'///18
     1'YOUNG MODULUS'9X,'1/DENSITY'4X,'POISSON RATIO'2X,'TIME INCREMENT'19
     22X,'APPLIED PRESSURE'4X,'WORK HARDENING'/'EO='E15.7,4X,'RHO='F7.1,20
     32X,'XN='E10.4,2X,'DT='E10.4,'  ..P='E12.5,'..  ERATIO='F6.3//'VIS21
     4COSITY COEFFICIENT'/'ALPHA='E15.7//)                               22
                                                                         23
      WRITE(6,2020)NW,IINC,JINC,NP,PP,NBU
 2020 FORMAT('NUMBER OF POINTS'3X,'ITERATIONS'3X,'PRINTED RESULTS'/'NW='25
     1I3,13X,'IINC='I3,5X,'JINC='I3///'CASE TWO      UNLOADING'//'NUMBER26
     3 POINTS BEFORE GRADUAL UNLOADING'3X,'SLOPE FOR UNLOADING(1/SEC)'2X27
     4,'NUMBER OF POINTS BEFORE TOTAL-'/'NP='I3,35X,'PP='E15.7,10X,'NBU=28
     5'I3,14X,'UNLOADING'////////)                                       29
                                                                         31

      CALCULATION OF GENERAL PARAMETERS                                  33

                                                                         35
      CRS  MEANS THE VALUE OF SR ON THE WAVE FRONT THAT CORRESPONDS TO   36
      A SECOND INVARIANT OF THE DEVIATORIC STRESS TENSOR WITH MAGNITUDE  SK

                                                                         39
      FM = 1./(2.*(1.+XN))                                               40
      FK = 1./(3.*(1.-2.*XN))                                            41
      CSR = SK * (4.*FM + 3.*FK) / (4.898979*FM)                         42
      WRITE(6,7069)XN,CSR
 7069 FORMAT(17X,'POISSON,S  RATIO      '12X,'EQUIVALENT  SK            44
     2'//15X,E17.8,15X,E17.8//)
```

```
      RRR = 1.0 / RHO                                                    46
      FMFM = EC * FM                                                     47
      FKFK = EC * FK                                                     48
      FLL = (4.0*FMFM + 3.0*FKFK)/(3.0*RRR)                              49
      FL = SQRT(FLL)                                                     50
C                                                                        51
C     FL IS THE WAVE SPEED                                               52
C                                                                        53
      Z1 = 2.0*FMFM - 3.0*FKFK                                           54
      Z2 = - Z1/3.0
      Z3 = 4.0*FMFM+ 3.0*FKFK
      Z4 = Z3 / 3.0
      BETA = ALPHA * DT
      XLDT = DT * FL                                                     55
      WRITE(6,5136) XLDT
 5136 FORMAT(E17.8)
      XXL = XLDT / 100.0                                                 56
      SP3 = C.0                                                          57
      SP33 = 0.0
      NWW = NW - 1                                                       58
      R(1) = R0                                                          59
      EX = EC / (1.0+XN)                                                 60
      W = EX*RHO / FLL                                                    1
      FF = FL / RHO                                                      62
      LW = NW                                                            63
      F11 = 2.0 * DT                                                     64
C                                                                        65
C  CALCULATION OF THE COEFFICIENTS FOR THE DIFFERENTIAL EQUATION         67
C                                                                        68
C                                                                        69
      A = 0.5                                                            70
      B =-ALPHA * SK / (2.44949*FL)
      C = 0.66667 * (FMFM*ALPHA/(RRR * (FL**3)))
      SR1 = EXP(C)*P                                                     73A
      DO 4 I = 1,NWW                                                     74
    4 R(I+1) = R(I) + XLDT                                               75
      SR(2,1) = P                                                        76
      SR(1,1) = P                                                        77
      ST(1,1) = SR(1,1) * (1.0-W)                                        78
      SZ(1,1) = SR(1,1) * (1.0-W)                                        79
      ER(1,1) = SP(1,1) * W *(1.0/EX)                                    80
      ET(1,1) = 0.0
      V(1,1) = -ER(1,1) * FL                                             82
      P1 = - A*P
      P2 = -( B + C*P )
C                                                                        83
C                                                                        84
C  RELATIONS ALONG THE WAVE FRONT                                        8K
C                                                                        86
C
C
C                                                                        89
C  CHECK IF THE GIVEN PRESSURE  P  HAS SUCH A MAGNITUDE THAT THE         90
C    SECOND INVARIANT OF THE DEVIATORIC STRESS TENSOR IS LESS THAN       91
C    KO-SQ THAT THE ELASTIC SOLUTION (STATEMENT 908) CAN BE APPLIED      92
C      IMMEDIATELY THROUGHOUT THE WHOLE WAVE FRONT                       93
C                                                                        95
```

```
      DO 5 I = 2,NW                                                    96
      XI = I                                                           97
      IF(SR(1,I-1).LT.CSR.AND.XI.EQ.2.) GO TO 908                      98
          SRSR = SR(1,I-1)                                             99A
      IF(SR(1,I-1)-CSR) 41,41,42                                       99

      THE CASE .STATEMENT 42. MEANS APPLICATION OF THE INELASTIC SOLUTION
                                                                       103
   42 RR(1) = R(I-1)                                                   104
      DO 6666 J = 2,101                                                105
      RR(J) = RR(J-1) + XXL                                            106
      SRR2 = (RR(J) **A) * (EXP(C*RR(J)))*XXL
      SRR3 = (RR(J)**(A-1.)) * (EXP( C*RR(J))) * XXL
      SRR3 = SRR2 + SRR3
 6666 SR3 = SR3 + SR2                                                  108
      SR4 = P1 * SRR3 + P2 * SR3
      SR5 = (R(I) **A) *(EXP(C*R(I)))                                  110
      SR6 = SR4/SR5
      SR(1,I) = P + SR6
      CALL FRONT
    5 CONTINUE
      GO TO 15                                                         117

                                                                       119
    THE STATEMENT 41 MEANS THAT SOMEWHERE ALONG THE WAVE FRONT I CAME TO120
     A POINT WHERE THE SOLUTION IS ELASTIC AGAIN                       121

                                                                       123
   41 SR(1,I) = SRSR * ((R(I-1) / R(I))**0.5)                          124
      CALL FRONT
      JJJJ = I - 1                                                     129
      WRITE(6,43) JJJJ,CSR,SR(1,I-1)                                   29A
   43 FORMAT(//10X,'ELASTIC - PLASTIC BOUNDARY POINT IN R-T PLANE'//   130
     26X,'ACTUAL VALUE'12X,'VALUE USED AT THE BOUNDARY'/I3,20X,E17.8,18131
     3X,E17.8/)                                                        132
      ROS = R(I-1)                                                     133
      FPB = SR(1,I-1)                                                  134
      L = I+1                                                          135
      DO 7 I = L,NW                                                    136
      SR(1,I) = FPB * ((ROS/R(I)) **0.5)                               137
      CALL FRONT
    7 CONTINUE
      GO TO 15                                                         143


  908 CONTINUE                                                         150
      WRITE(6,7777) P                                                  151
 7777 FORMAT(1/10X,'CASE ONE -INITIAL PRESSURE PRODUCES ONLY ELASTIC DEFO152
     2RMATIONS ON THE WAVE FRONT'//30X,'P  =  ',E17.8///)              153


                                                                       156
      DO 906 I = 1,NW                                                  157
      SR(1,I) = P * ((R(1) / R(I)) **0.5)                              158
      CALL FRONT
  906 CONTINUE
   15 CONTINUE                                                         164
```

```
C  PRINT THE SR, ST, SZ, ER, ET, AND V ALONG THE WAVE FRONT
C
      WRITE(6,22) (SR(1,M),M=1,LW,JINC)
      WRITE(6,22)(ST(1,M),M=1,LW,JINC)
      WRITE(6,22) (SZ(1,M),M=1,LW,JINC)
      WRITE(6,22)(ER(1,M),M=1,LW,JINC)
      WRITE(6,22)(ET(1,M),M=1,LW,JINC)
      WRITE(6,22)(V(1,M),M=1,LW,JINC)

C
C     END OF THE CALCULATIONS ALONG THE WAVE FRONT

C
C  THIS PART OF THE PROGRAM INTRODUCES UNLOADING ON THE SURFACE OF THE
C  CYLINDRICAL CAVUTY
C
C
C  INS = 2  -CONTINUOUS LOADING AND THEN GRADUAL UNLOADING
C
C  INS = 0  -CONTINUOUS LOADING AND THEN SUDDEN UNLOADING
C
C  INS = 1  -CONTINUOUS LOADING ONLY
C

      INEW = NBU - 2
      READ(5,2) INS
      IF(INS.EQ.0) GO TO 556
      IF(INS.EQ.1) GO TO 5556

C
C     CASE ONE  *CONTINUOUS LOADING AND THEN GRADUAL UNLOADING
C
      DO 555 M = 1,INEW
      IF(NP.GT.M) GO TO 554
      X = M - NP
      SP(M) = P * (1.0 - X * 2. * DT * PP      )
      SSX = SP(M)
      IF(SSX.GT.0.0) GO TO 555
      SP(M) = 0.0
       GO TO 555
554   SP(M) = P
555   CONTINUE
      GO TO 557
C
C     CASE TWO  CONTINUOUS LOADING AND THEN SUDDEN UNLOADING
C
556   CONTINUE
      DO 558 M = 1,NBU
558   SP(M) = P
      NB = NBU + 1
      DO 559 M = NB,NW
559   SP(M) = 0.0
      GO TO 557
```

```
5556 DO 5656 M = 1,Nw                                                  216
5656 SP(M) = P                                                         217
557 CONTINUE                                                           218
                                                                       301
                                                                       302
   NOTICE THAT THE DEFORMATIONS ALONG THE WAVE FRONT ARE ELASTIC       303
                                                                       304
   DO 1234 I = 1,Nw                                                    305
   PER(1,I) = 0.0                                                      306
   PET(1,I) = 0.0                                                      307
    YFK(I,I) = SK                                                      308
1234 PW(I,I) = 0.0                                                     309
                                                                       310
                                                                       311
   I = 1                                                               312
   II = 2                                                              313

  CALCULATIONS ALONG A NEW CHARACTERISTIC                              315
                                                                       316
                                                                       317
                                                                       318
                                                                       318
                                                                       320
                              *  N = (II,J)                             21
                                                                       322
                                                                       323
                                                                       324
                                                                       325
                                                                       325
                                                                       326
                                                                       327
                                                                       328
                                                                       329
W = (II,JJJ)*                                  * E = (I,JJ)
                                                                        31
                                                                       332
                                                                       333
                                                                       334
                                                                       335
                                                                       336
                                                                       337
                                                                       338
                                                                       329
                              * S = (I,J)
                                                                       341
                                                                       342
                                                                       343
   DO 11 IA = 1,INEW                                                   344
   SP(2,1) = SP(IA)                                                    345

YFK(I,1) IS THE INITIAL VALUE OF KO OF THE YIELD SURFACE               348

                                                                       363
   CALCULATIONS AT THE POINT II,1
   BIC = (1./9.)*((2.*SR(I,2)-ST(I,2)-SZ(I,2))**2+(-SR(I,2)+2.*ST(I,2
  2)-SZ(I,2))**2+(-SR(I,2)-ST(I,2)+2.*SZ(I,2))**2)
   SIST(I,2) = SQRT(BIC)

   BIC = ((1./9.) * ((2.*SR(I,1)-ST(I,1)-SZ(I,1))**2+(-SR(I,1)+2.*
  2ST(I,1)-SZ(I,1))**2+(-SR(I,1)-ST(I,1)+2.*SZ(I,1))**2))
```

```
      SIST(I,1) = SQRT(BIO)

      COC(I,2) = 1. - YFK(I,2)/SIST(I,2)                                353
      COC(I,1) = 1. - YFK(I,1) / SIST(I,1)                              362
      WRITE(6,6543) BIO,BIC,SIST(I,1),SIST(I,2)
 6543 FORMAT(4E17.8)
      BP = 0.0
   49 CONTINUE
                                                                        372
      COCO(I,2) = (0.66667*EMM-FKFK)*V(I,2)/R(2) + 0.33333*ALPHA * COC(
     2I,2) * (2.*SR(I,2)-ST(I,2)-SZ(I,2))

      ET(II,1) = ET(I,1) + F11 * V(I,1) / R(1)

      V(II,1) = V(I,1) + (RHO/FL)*(SR(I,2)-SR(II,1) - (COCO(I,2) - FL *
     2(SR(I,2) - ST(I,2))/R(2) ) * D.)

      ER(II,1) = ER(I,1) + (Z1 * (ET(II,1)-ET(I,1)) + 3. * (SR(II,1)-SR(
     2I,1)) + ALPHA * COC(I,1) * (2.*SR(I,1)-ST(I,1)-SZ(I,1)) * F11) /Z3

      ST(II,1) = ST(I,1) - Z2 * (ER(I,1)-ER(II,1)) + Z4 * (ET(II,1)-ET(I
     2,1))- BETA * 0.66667 * (-SR(I,1) + 2.*ST(I,1)-SZ(I,1)) * COC(I,1)

      SZ(II,1) = 3.*FKFK*(ER(II,1)-ER(I,1)+ET(II,1)-ET(I,1)) - SR(II,1) 370A
     2+SR(I,1)-ST(II,1)+ST(I,1) + SZ(I,1)                               371A
      CALCULATION OF THE ELASTIC AND INELASTIC COMPONENTS OF THE STRAINS373
                                                                        374
      EER(II,1) = (SR(II,1) - XN * (ST(II,1)+SZ(II,1)))/ EO             375
      EET(II,1) = (ST(II,1) - XN * (SR(II,1)+SZ(II,1)))/EO              376
                                                                        377
      PER(II,1) = ER(II,1) - EER(II,1)                                  378
      PET(II,1) = ET(II,1) - EET(II,1)                                  379
                                                                        380
                                                                        381
      CALCULATION OF THE INELASTIC WORK FOR CHANGE OF THE RADIUS K (VALUE382
      OF YFK(I,J) ) IN THE FOLLOWING ITERATIONS                         382
                                                                        383
      PW(II,1) = PW(I,1) + 0.5 * ((SR(II,1)+SR(I,1))* (PER(II,1)-PER(I,1384
     2)) + (ST(II,1)+ST(I,1)) * (PET(II,1)-PET(I,1)) )                  385
      ROSI = PW(II,1)
      CALL YIELD

      YFK(II,1) = EMMA
      WRITE(6,6543)YFK(II,1)

      ITERATION STARTS                                                  390

      DO 400 N = 1,IRO                                                  392
                                                                        393
      BIB = ((2.*SR(II,1)-ST(II,1)-SZ(II,1))**2+(-SR(II,1)+2.*ST(II,1)-S
     2Z(II,1))**2+(-SR(II,1)-ST(II,1)+2.*SZ(II,1))**2)/9.
      SIST(II,1) = SQRT(BIB)
      WRITE(6,6543)SIST(II,1)
       IF(0.5-BP) 3322,3322,3323
 3322 COC(II,1) = 0.0
      WRITE(6,6543)COC(II,1)
      GO TO 3324
 3323 CONTINUE
      COC(II,1) = 1. - YFK(II,1) / SIST(II,1)                           399
                                                                        395
```

```
3324 CONTINUE                                                          372A
     COCO(II,1) = -Z2*V(II,1)/R(1) + 0.3333*ALPHA * (2.*SR(II,1)-ST(II,
    2I)-SZ(II,1) ) * COC(II,1)

     ET(II,1) = ET(I,1) + ( (V(II,1)+V(I,1))/R(1) ) * DT
     WRITE(6,6543)ET(I,1),V(I,1),V(II,1),ET(II,1)

     V(II,1) = V(I,1) + (RHO/FL) * ( SR(II,1)-SR(I,1) - (COCO(I,2) - FL
    2* (SR(I,2)-ST(I,2))/R(2)) *0.5*DT + ( COCO(II,1) - FL * (SR(II,1)-
    3ST(II,1))/R(1) )*0.5*DT )

     ER(II,1) = ER(I,1) + (ZI * (ET(II,1) - ET(I,1)) + 3.*(SR(II,1)-SR(
    2I,1)) + BETA * ( COC(I,1)*(2.*SR(I,1)-ST(I,1)-SZ(I,1)) + COC(II,1)
    3* (2.*SR(II,1)-ST(II,1)-SZ(II,1)) ) ) / Z3

     ST(II,1) = ST(I,1) + Z2 * (ER(II,1)-ER(I,1)) + Z4*(ET(II,1)-ET(I,1
    2)) - 0.3333*BETA* (COC(I,1)*(-SR(I,1)+2.*ST(I,1)-SZ(I,1)) +
    3COC(II,1) * (-SR(II,1)+2.*ST(II,1)-SZ(II,1)) )

     SZ(II,1) = 3.*FKFK*(ER(II,1)-ER(I,1)+ET(II,1)-ET(I,1)) - SR(II,1)  370
    2+SR(I,1)-ST(II,1)+ST(I,1) + SZ(I,1)                               371
     CALCULATION OF THE ELASTIC AND INELASTIC COMPONENTS OF THE STRAINS 373A
                                                                       374A
     EER(II,1) = (SR(II,1) - XN * (ST(II,1)+SZ(II,1)))/ EO             375A
     EET(II,1) = (ST(II,1) - XN * (SR(II,1)+SZ(II,1)))/EO              376A
                                                                       377A
     PER(II,1) = ER(II,1) - EER(II,1)                                  378A
     PET(II,1) = ET(II,1) - EET(II,1)                                  379A
                                                                       380A
                                                                       381A
   CALCULATION OF THE INELASTIC WORK FOR CHANGE OF THE RADIUS K (VALUE 382
   OF YFK(I,J) ) IN THE FOLLOWING ITERATIONS                           382A
                                                                       383A
     PW(II,1) = PW(I,1) + 0.5 * ((SR(II,1)+SR(I,1))* (PER(II,1)-PER(I,1384A
    2)) + (ST(II,1)+ST(I,1)) * (PET(II,1)-PET(I,1)) )                  385 A
     ROSI = PW(II,1)
     CALL YIELD
                                                                       450
     YFK(II,1) = EMMA
     WRITE(6,6543)YFK(II,1)
                                                                       452
400  CONTINUE                                                          53
                                                                       454
     CHECK IF THE MAGNITUDE OF THE SECOND INVARIANT OF THE DEVIATORIC  455
     STRESS TENSOR AT THE SURFACE OF THE CAVITY ,POINT (II,1) ,LIES     56
     INSIDE OF THE NEW -EXPANDED- YIELD SURFACE                        357
                                                                       358
     BIB = ((2.*SR(II,1)-ST(II,1)-SZ(II,1))**2+(-SR(II,1)+2.*ST(II,1)-S
    2Z(II,1))**2+(-SR(II,1)-ST(II,1)+2.*SZ(II,1))**2)/9.
     SIST(II,1) = SQRT(BIB)
     WRITE(6,6543)SIST(II,1)
     IF(BP.GT.0.5) GO TO 777

     IF(SIST(II,1)-YFK(II,1)) 50,50,909                                463
909  DPW = 0.5*((SR(II,1)+SR(I,1))*(PER(II,1)-PER(I,1))+ (ST(II,1)+ST(I464
    2,1))*(PET(II,1)-PET(I,1)))                                        465
     IF(DPW) 50,50,52                                                  466

     WRITE(6,6543)DPW
```

```
      STATEMENT NUMBER REQUIRED --- STATEMENT CAN NOT BE REACHED --- WARNING ONLY
                                                                        468
777   CONTINUE
                                                                        381A
      M = I + IA
      MM = J
      WRITE(6,801) M,MM,SIST(II,JJ) , YFK(II,JJ)
 52   LW = LW - 1                                                      469
      DO 95 J = 2,LW                                                   470
      SUMP = 0.0
      JJ = J + 1                                                       471
      JJJ = J - 1                                                      472
      ET(II,J) = ET(I,J) + FII*V(I,J)/R(J)                             473
      SIST(II,JJJ) =((1./3. )*((2.*SR(II,JJJ)-ST(II,JJJ)-SZ(II,JJJ))**2 474
     2+(-SR(II,JJJ)+2.*ST(II,JJJ)-SZ(II,JJJ))**2 + (-SR(II,JJJ)-ST(II,JJ475
     3J)+2.*SZ(II,JJJ))**2))**0.5                                      476
                                                                        477
       SIST(I,JJ) = ((1./3. )*((2.*SR(I,JJ)-ST(I,JJ)-SZ(I,JJ))**2+(-SR( 478
     2I,JJ)+2.*ST(I,JJ)-SZ(I,JJ))**2 + (-SR(I,JJ)-ST(I,JJ)+2.*SZ(I,JJ) 479
     3)**2))**0.5                                                      480
                                                                        481
      COC(II,JJJ) = 1. - YFK(II,JJJ)/SIST(II,JJJ)                        2
      IF(COC(II,JJJ)) 5055,5055,5056
5055  COC(II,JJJ) = 0.0
5056  CONTINUE
      COC(I,JJ) = 1. - YFK(I,JJ)/SIST(I,JJ)                           483
      IF(COC(I,JJ)) 5057,5057,5058
5057  COC(I,JJ) = 0.0
5058  CONTINUE
      COCO(II,JJJ) = -Z2*V(II,JJJ) / R(JJJ) + 0.3333* ALPHA *
     2(2.*SR(II,JJJ)-ST(II,JJJ)-SZ(II,JJJ)) *COC(II,JJJ)

      COCO(I,JJ) = -Z2 * V(I,JJ) / R(JJ) + 0.3333 * ALPHA *
     2(2.*SR(I,JJ)-ST(I,JJ)-SZ(I,JJ)) * COC(I,JJ)

      SR(II,J) = 0.5 * (SR(II,JJJ)+SR(I,JJ)) - 0.5*( COCO(II,JJJ)+COCO(I
     2,JJ)+ FL*(((SR(II,JJJ)-ST(II,JJJ))/R(JJJ)) - ((SR(I,JJ)-ST(I,JJ))/
     3R(JJ))) ) * DT

      V(II,J) = 0.5*(V(I,JJ)+V(II,JJJ))-(0.5*DT*RHO/FL) * (COCO(I,JJ)
     2-COCO(II,JJJ) - ( FL*(SR(I,JJ)-ST(I,JJ))/R(JJ) + FL*(SR(II,JJJ) -
     3ST(II,JJJ))/R(JJJ) ) )

      ER(II,J) = ER(I,J) + (Z1*(ET(II,J)-ET(I,J)) + 3.*(SR(II,J)-SR(I,J)
     2 ) * BETA * COC(I,J ) * (2.*SR(I,J)-ST(I,J)-SZ(I,J)) * 2.0 ) /Z3

      ST(II,J) = ST(I,J) + Z2*(ER(II,J)-ER(I,J)) + Z4*(ET(II,J)-ET(I,J))
     2 -BETA * 0.66667 * (-SR(I,J)+2.*ST(I,J)-SZ(I,J))

                                                                        503
      SZ(II,J) = 3.*FKFK*(ER(II,J)-ER(I,J)+ET(II,J)-ET(I,J))- SR(II,J)+ 504
     2SR(I,J)-ST(II,J)+ST(I,J)+SZ(I,J)                                 505
                                                                        506
  CALCULATION OF THE ELASTIC AND PLASTIC COMPONENTS OF THE STRAINS      507
                                                                        508
      EER(II,J) = (SR(II,J) -XN * (ST(II,J)+SZ(II,J)))/EO              509
      EET(II,J) = (ST(II,J) - XN * (SR(II,J)+SZ(II,J)))/EO             510
      PER(II,J) = ER(II,J) - EER(II,J)                                 511
      PET(II,J) = ET(II,J) - EET(II,J)                                 512
                                                                        513
```

```
C  CALCULATION OF THE INELASTIC WORK FOR THE NEW VALUE OF THE RADIUS K 514+
C   -VALUE YFK(II,J) -IN THIS PROGRAM                                  515
      PW(II,J) = PW(I,J) + 0.5 * ((SR(II,J)+SR(I,J))*(PER(II,J)-PER(I,J)516
     2) + (ST(II,J)+ST(I,J))*(PET(II,J)-PET(I,J)))                     517
      ROSI = PW(II,J)
      CALL YIELD
      YFK(II,J) = EMMA

C  ITERATION STARTS                                                   522
                                                                      523
      DO 401 N = 1,IINC                                               524
                                                                      526
      SIST(II,J) = ((1./9. )* ((2.*SR(II,J)-ST(II,J)-SZ(II,J))**2 + (-SR527
     2(II,J)+2.*ST(II,J)-SZ(II,J))**2 + (-SR(II,J)-ST(II,J)+2.*SZ(II,J)528
     3**2))**0.5                                                      529
                                                                      530
      COC(II,J) = 1. - YFK(II,J) / SIST(II,J)                         531
      IF(COC(II,J)) 5059,5059,5060
5059  COC(II,J) = 0.0
5060  CONTINUE
      COCO(II,J) = -Z2 * V(II,J)/R(II) + 0.33333 * ALPHA *
     2(2.0*SR(II,J)-ST(II,J)-SZ(II,J))* COC(II,J)
      ET(II,J) = ET(I,J) + (DT*(V(I,J) + V(II,J))/R(J) )

      SR(II,J) = 0.5*(SR(II,JJJ)+SR(I,JJ)) - 0.25 * (COCO(II,JJJ) + COCO
     2(I,JJ) + 2.0*COCO(II,J) + FL*( ((SR(II,JJJ)-ST(II,JJJ))/R(JJJ))
     3 - ((SR(I,JJ)-ST(I,JJ))/R(JJ)) ) )*DT

      V(II,J)= 0.25*(V(II,JJJ)+V(I,JJ)+2.*V(II,J)) - (0.25*RHO*DT/FL) *
     2( COCO(I,JJ)-COCO(II,JJJ) - ( ((SR(I,JJ)-ST(I,JJ))/R(JJ)) +
     3((SR(II,JJJ)-ST(II,JJJ))/R(JJJ)) + (2.*(SR(II,J)-ST(II,J))/R(J))
     4) * FL  )

      ER(II,J) = ER(I,J) + ( Z1*(ET(II,J)-ET(I,J)) + 3.*(SR(II,J)-SR(I,
     2J)) + (COC(I,J)*(2.*SR(I,J)-ST(I,J)-SZ(I,J)) + COC(II,J)*(2.*SR(I
     3I,J)-ST(II,J)-SZ(II,J)))*BETA ) /Z3

      ST(II,J) = ST(I,J) + Z2*(ER(II,J)-ER(I,J)) + Z4*(ET(II,J)-ET(I,J))
     2- 0.33333 * ((COC(I,J)*(-SR(I,J)+2.*ST(I,J)-SZ(I,J))) +(COC(II,J)*
     3(-SR(II,J)+2.*ST(II,J)-SZ(II,J)))) * BETA
                                                                      551
      SZ(II,J) = 3.*FKFK*(ER(II,J)-ER(I,J)+ET(II,J)-ET(I,J))- SR(II,J)+ 504AA
     2SR(I,J)-ST(II,J)+ST(I,J)+SZ(I,J)                                505AA
                                                                      506AA
C  CALCULATION OF THE ELASTIC AND PLASTIC COMPONENTS OF THE STRAINS    507AA
                                                                      508AA
      EER(II,J) = (SR(II,J) -XN * (ST(II,J)+SZ(II,J)))/EO             509AA
      EET(II,J) = (ST(II,J) - XN * (SR(II,J)+SZ(II,J)))/EO            510AA
      PER(II,J) = ER(II,J) - EER(II,J)                                511AA
      PET(II,J) = ET(II,J) - EET(II,J)                                512A
                                                                      513AA
C  CALCULATION OF THE INELASTIC WORK FOR THE NEW VALUE OF THE RADIUS K 514AA
C   -VALUE YFK(II,J) -IN THIS PROGRAM                                  515AA
      PW(II,J) = PW(I,J) + 0.5 * ((SR(II,J)+SR(I,J))*(PER(II,J)-PER(I,J)516 A
     2) + (ST(II,J)+ST(I,J))*(PET(II,J)-PET(I,J)))                    517AA
      ROSI = PW(II,J)
      CALL YIELD
      YFK(II,J) = EMMA
401   CONTINUE                                                        602
```

```
                                                                      603
C
C  CHECK IF THE MAGNITUDE OF THE DEVIATORIC STRESS TENSOR AT THE POINT 605
C  (II,J) IS LESS OR EQUAL TO YFK(II,J) SO THAT THE PROBLEM BECOMES   606
C  ELASTIC                                                            607
C                                                                     608
      IF(SIST(II,J)-YFK(II,J)) 17,17,16                               609
   16 DPW = 0.5*((SR(II,J)+SR(I,J)) * (PER(II,J)-PER(I,J)) + (ST(II,J) +610
     2ST(I,J)) * (PET(II,J) - PET(I,J)))                              611
      IF(DPW) 17,17,95                                                612
C  THE CASE -STATEMENT 17- MEANS THAT AFTER THE POINT J THE           613
C  DEFORMATION BECAME ELASTIC                                         614
C                                                                     615
   17 JL = J                                                          616
      IL = IA + 1                                                     617
      JX = JL + 1                                                     618
      WRITE(6,80) IL,JL,SIST(II,J),YFK(II,J)
   80 FORMAT(/2I4, 2E17.8)
      IF(BBP.GT.0.5) GO TO 95
      COC(II,J) = 0.0
      COCO(II,JJJ) = -Z2*V(II,JJJ) / R(JJJ)
      COCO(I,JJ) = -Z2*V(I,JJ) / R(JJ)
      BBP = 1.0
      GO TO 5060
   95 CONTINUE
                                                                      712
      CALL OUTPUT
      GO TO 11                                                        742
   50 CONTINUE
      COC(I,1) = 0.0
      COC(I,2) = 0.0
      BP = 1.0
      GO TO 49
                                                                      380A
   11 CONTINUE
   22 FORMAT(///(8E16.8))
      STOP
      END


      SUBROUTINE YIELD
      DIMENSION SR(2,151),ST(2,151),SZ(2,151),ER(2,151),ET(2,151),V(2,1
     251),SIST(2,151),COC(2,151),COCO(2,151),EER(2,151),EET(2,151),PER(2
     3,151),PET(2,151),YFK(2,151),RR(151),R(151),PW(2,151),COCOA(2,151),
     4SP(151)
      COMMON LW,SR,ST,SZ,ER,ET,V,EER,EET,PER,PET,PW,YFK,IA,JINC,W,EX,FL,
     2 ROSI,STYL,E0,ERATIO,EMMA,BBB,I,SIST
C  THIS PART OF THE PROGRAM INTRODUCES A CHANGE OF THE RADIUS
C  OF THE YIELD SURFACE AS A FUNCTION OF THE INELASTIC WORK

      ROSA = ROSI/((STYL**2)/E0)
      IF(ERATIO.GT.0.80) GO TO 4966
      IF(ERATIO.LT.0.60.AND.ERATIO.GT.0.40) GO TO 4967

      IF(ROSA.LE.15.0) GO TO 3303
      IF(ROSA.LE.50.0.AND.ROSA.GT.15.0) GO TO 3304
      IF(ROSA.LE.150.0.AND.ROSA.GT.50.0) GO TO 3305
      IF(ROSA.LE.400.0.AND.ROSA.GT.150.0) GO TO 3306
      IF(ROSA.LE.750.0.AND.ROSA.GT.400.0) GO TO 3307
```

```
      EMM = 15.92 + (ROSA-750.0) * 7.55/900.0
      GO TO 4968
3307  EMM = 11.72 + (ROSA-400.0)*4.20/350.0
      GO TO 4968
3306  EMM = 7.29 + (ROSA-150.0)*4.44/250.0
      GO TO 4968
3305  EMM = 4.28 + (ROSA-50.0)*3.00/100.0
      GO TO 4968
3304  EMM = 2.58 + (ROSA-15.0)*1.70/35.0
      GO TO 4968
3303  EMM = 1.0 + 1.58*ROSA/15.0
      GO TO 4968


4966  CONTINUE

      IF(ROSA.LE.6.0) GO TO 3301
      IF(ROSA.LE.17.5.AND.ROSA.GT.6.0) GO TO 3302
      IF(ROSA.LE.45.0.AND.ROSA.GT.17.5) GO TO 3315
      IF(ROSA.LE.101.0.AND.ROSA.GT.45.0) GO TO 3316
      EMM = 24.0 + 8.0 * (ROSA-101.0) / 79.0
      GO TO 4968
3316  EMM = 16.0 + 8.0 *(ROSA-45.0) / 56.0
      GO TO 4968
3315  EMM = 10.0 + 6.0 * (ROSA-17.5) / 27.5
      GO TO 4968
3302  EMM = 6.0+4.0 *(ROSA-6.0) / 11.5
      GO TO 4968
3301  EMM = 1.0 + 5.0*ROSA / 6.0
      GO TO 4968


4967  CONTINUE

      IF(ROSA.LE.5.0) GO TO 3308
      IF(ROSA.LE.20.0.AND.ROSA.GT.5.0) GO TO 3309
      IF(ROSA.LE.50.0.AND.ROSA.GT.20.0) GO TO 3310
      IF(ROSA.LE.100.0.AND.ROSA.GT.50.0) GO TO 3311
      IF(ROSA.LE.150.0.AND.ROSA.GT.100.0) GO TO 3312
      IF(ROSA.LE.200.0.AND.ROSA.GT.150.0) GO TO 3313
      IF(ROSA.LE.350.0.AND.ROSA.GT.200.0) GO TO 3314
      EMM = 18.82 + (ROSA-350.0)/250.0
      GO TO 4968
3314  EMM = 14.28 + 3.54*(ROSA-200.0)/150.0
      GO TO 4968
3313  EMM = 12.38 + 1.90*(ROSA-150.0)/50.0
      GO TO 4968
3312  EMM = 10.08 + 2.30 *(ROSA-100.0)/50.0
      GO TO 4968
3311  EMM = 7.28 + 2.80*(ROSA-50.0)/50.0
      GO TO 4968
3310  EMM = 4.82 + 2.66 * (ROSA-20.0)/30.0
      GO TO 4968
3309  EMM = 2.60 + 2.02 *(ROSA-5.0)/15.0
      GO TO 4968
3308  EMM = 1.0 + 0.32 * ROSA

4968  BBB = BBB + 1.0
      EMMA = EMM * STYL * 1.414214 / 1.73205
```

```
      RETURN
      END


      SUBROUTINE OUTPUT
      DIMENSION SR(2,151),ST(2,151),SZ(2,151),ER(2,151),ET(2,151),V(2,1
     251),SIST(2,151),CCC(2,151),COCO(2,151),EER(2,151),EET(2,151),PER(2
     3,151),PET(2,151),YFK(2,151),RR(151),R(151),PW(2,151),COCOA(2,151),
     4SP(151)
      COMMON LW,SR,ST,SZ,ER,ET,V,EER,EET,PER,PET,PW,YFK,IA,JINC,W,EX,FL,
     2 RUSI,STYL,EO,ERATIO,EMMA,BBB,I,SIST
      DO 97 LL = 1,LW                                                    713
      SR(1,LL) = SR(2,LL)                                                714
      ST(1,LL) = ST(2,LL)                                                715
      SZ(1,LL) = SZ(2,LL)                                                716
      ER(1,LL) = ER(2,LL)                                                717
      ET(1,LL) = ET(2,LL)                                                718
      V(1,LL) = V(2,LL)                                                  719
      EER(1,LL) = EER(2,LL)                                              720
      EET(1,LL) = EET(2,LL)                                              721
      PER(1,LL) = PER(2,LL)                                              722
      PET(1,LL) = PET(2,LL)                                              72
      PW(1,LL) = PW(2,LL)                                                724
      SIST(1,LL) = SIST(2,LL)
   97 YFK(1,LL) = YFK(2,LL)                                              725
      IN = IA + 1                                                        726
      WRITE(6,666)IN                                                     727
  666 FORMAT(1X,'I = ',I5)                                               728
      WRITE(6,22) (SR(1,M),M=1,LW,JINC)                                  729
      WRITE(6,23) (ST(1,M),M=1,LW,JINC)                                  730
      WRITE(6,23) (SZ(1,M),M=1,LW,JINC)                                  731
      WRITE(6,23) (ER(1,M),M=1,LW,JINC)                                  732
      WRITE(6,23) (ET(1,M),M=1,LW,JINC)                                  733
      WRITE(6,23) ( V(1,M),M=1,LW,JINC)                                  734
      WRITE(6,23) ( EER(1,M) ,M=1,LW,JINC)                               735
      WRITE(6,23) ( EET(1,M) ,M=1,LW,JINC)                               736
      WRITE(6,23) ( PER(1,M) ,M=1,LW,JINC)                               737
      WRITE(6,23) ( PET(1,M) ,M=1,LW,JINC)                               738
      WRITE(6,23) (  PW(1,M) ,M=1,LW,JINC)                               739
      WRITE(6,23)(SIST(1,M),M=1,LW,JINC)
      WRITE(6,23) ( YFK(1,M) ,M=1,LW,JINC)                               740
                                                                         741
   22 FORMAT(///(8E16.8))
   23 FORMAT(/(8E16.8))
      RETURN
      END


      SUBROUTINE FRONT
      DIMENSION SR(2,151),ST(2,151),SZ(2,151),ER(2,151),ET(2,151),V(2,1
     251),SIST(2,151),CCC(2,151),COCO(2,151),EER(2,151),EET(2,151),PER(2
     3,151),PET(2,151),YFK(2,151),RR(151),R(151),PW(2,151),COCOA(2,151),
     4SP(151)
      COMMON LW,SR,ST,SZ,ER,ET,V,EER,EET,PER,PET,PW,YFK,IA,JINC,W,EX,FL,
     2 RUSI,STYL,EO,ERATIO,EMMA,BBB,I,SIST
      ST(1,I) = SR(1,I) * (1.-W)                                         112
```

```
      SZ(1,I) = SP(1,I) * (1.0-W)                                    113
      SP(1,I) = SR(1,I) * W / EX                                     114
      ET(1,I) = 0.0                                                  115
    5 V(J,I) = -PR(1,I) * PL
      RETURN
      END
```

EXECUTION

A P P E N D I X II

Elastic/viscoplastic unloading waves in a rod

Computer program

```
      PROGRAM FOR COMPUTING THE TIME HISTORY OF STRESS AND STRAIN DUE TO
      A ONE-DIMENSIONAL PLASTIC WAVE INCLUDING STRAIN-RATE EFFECTS

C-----N=NO.OF POINTS ALONG INITIAL X=0 AXIS-----------------------------------
      NBU=NO. OF POINTS ALONG TIME AXIS BEFORE UNLOADING
      ERATIO=RATIO OF PLASTIC TO ELASTIC MODULUS
      DKT=DESIRED TIME INCREMENT
C-----P=MAGNITUDE OF NON-DIMENSIONAL LOAD-------------------------------------
      GAMMA=SLOPE OF UNLOADING FUNCTION,P/KT

      INTEGER SELU,SEPU,SEPUSR,GELU,GEPU,GEPUSR
C-----DIMENSION TKT(1001), SIG(2,1001),EPS(2,1001), H(2,1001),----------------
     1A(2,1001), B(2,1001),
     2 SIGL(1001), SIGU(1001), EPSL(1001), EPSU(1001), EX(1001), SLOP(10
     301), CXX(1001), S(1001,1), E(1001,1)
       N=1
      NM=1
000   CONTINUE
33    FORMAT (8E15.6)
      WRITE (6,7333)(SIGL(J), J=1,N,NM)
      WRITE (6,7333)  (EX(J), J=1,N,NM)
      WRITE (6,7333)(EPSL(J), J=1,N,NM)
      READ (5,1) N,NBU,ERATIO,DKT,P,GAMMA
      ER=ERATIO
       NM = 100
C-----FORMAT (2I10,F20.9,3F10.4)----------------------------------------------
      FORMAT (6I5)
      DO 5 I=1,2
      TKT(I)= 0.0
       CXX(I)=0.0
      DO 6 J=1,N
      CXX(J)=0.0
      SIG(I,J)= 0.0
                                  THE ARRAYS ARE ZEROED
      EPS(I,J)= 0.0
      H(I,J) = 0.0
      A(I,J) = 0.0
      B(I,J) = 0.0
      CONTINUE
      NED=0
      KATHY=N
      IF(KATHY.LT.1) GO TO 15
      NED=NED+KATHY
      KATHY=KATHY-1
      GO TO 10
C-----CONTINUE
                                  NO.OF POINTS IN THE TRIANGULAR NET
      TKT(1)=0.0
      DO 20 I=2,N
      TKT(I)= TKT(I-1) + DKT
      CONTINUE
                                  COMPUTES KT(I)
       DO 21 J=1,NBU
        S(J,1)= P
21     E(J,1)=(1./ERATIO)*(P+ERATIO-1.)-(P-1.)*((1./ERATIO)-1.)
```

```
WU -ZANNIS                EAS335-2737                          DATE 01/23/71
      PLWAVE     -  EFN    SOURCE STATEMENT  -  IFN(S)  -

   1*EXP(-ERATIO*2.0*TKT(J))
     DO 25 J=1,N
     SIG(1,J)=1.+(P-1.)*EXP(-.5*(1.-ERATIO)*TKT(J))
     EPS(1,J)=1.+(P-1.)*EXP(-.5*(1.-ERATIO)*TKT(J))
     H(1,J)=SIG(1,J)-(1.-ERATIO)-ERATIO*EPS(1,J)
     H(J,1)=  S(J,1)-(1.-ERATIO)-ERATIO*  E(J,1)
5    CONTINUE
     WRITE(6,100)
     WRITE (6,901)
01   FORMAT (1X,25X,78H GRADUAL REMOVAL OF LOAD, ELASTIC-PLASTIC UNLOAD
    1ING WITH STRAIN RATE EFFECTS    )
     WRITE (6,101) N,NBU,ER    ,DKT,P,GAMMA,NED ,ERATIO
     WRITE (6,102)
                    FINDS SIG, EPS, AND H ALONG X=CI AND X=0 AXES
     ASIG= 1.+ERATIO*DKT
     BSIG=ERATIO*DKT/2.
     DIVISR= 1.+DKT/2.+ERATIO*DKT/2.
     AEPS=1.+DKT
     BEPS=1.+DKT/2.
                    CALCULATES CONSTANTS FOR MAIN LOOP
                      I,J REFERS TO SOUTH POSITION
      MM=1
      I=1
      WRITE(6,3334) MM
     WRITE(6,1023) (SIG(I,J), J=1,N,NM)
     WRITE(6,1023) (EPS(I,J), J=1,N,NM)
     LAST=N-2
      L=NBU-1
     M=N-1
     DO 30 LL=1,L
     IF(M.LT.2) GO TO 30
     SIG(I+1,1)=S(LL+1,1)
     EPS(I+1,1)=E(LL+1,1)
     DO 40 J=2,M
     H(I,J)=SIG(I,J)-(1.-ERATIO)-ERATIO*EPS(I,J)
     A(I+1,J)=SIG(I+1,J-1)+SIG(I,J+1)-SIG(I,J)+H(I,J)*DKT/2.
    1 + (1.-ERATIO)*DKT/2.
     B(I+1,J)= EPS(I,J)-SIG(I,J)+H(I,J)*DKT-(1.-ERATIO)*DKT
     SIG(I+1,J)=(A(I+1,J)*ASIG+B(I+1,J)*BSIG)/(DIVISR)
                                              MAIN CALCULATION
     EPS(I+1,J)= (A(I+1,J)*AEPS+B(I+1,J)*BEPS)/(DIVISR)
0    CONTINUE
      DO 1201 J=1,M
     SLOP(J)= (SIG(I+1,J)-SIG(I,J))/(EPS(I+1,J)-EPS(I,J))
     SIG(I,J)=SIG(I+1,J)
201  EPS(I,J)=EPS(I+1,J)
      MM=LL+1
       WRITE(6,3334) MM
     WRITE(6,1023) (SIG(I,J), J=1,M,NM)
     WRITE(6,1023) (EPS(I,J), J=1,M,NM)
     WRITE(6,1023) (SLOP (J), J=1,M,NM)
     M=M-1
0    CONTINUE
                FINDS STRESSES AND STRAINS WITHIN THE NETWORK
00   FORMAT(1H1,42X,46H SOLUTION OF PLASTIC WAVE PROPAGATION PROBLEM  ,
    125X,'M. P. ZABINSKI')
```

WU -ZANNIS EAS335-2797 DATE 01/23/71

PLWAVE - EFN SOURCE STATEMENT - IFN(S) -

```
1   FORMAT (1HO,21X,2HN=,I3,3X,4HNBU=,I3,3X,'ERATIC LOADING = 'F12.9,
   13X,'DKT='
   2F6.3,3X,2HP=,F5.2,3X,6HGAMMA=,F6.3,3X,6HTOTAL=,I4/
   338X'ERATIO UNLOADING = 'F12.9)
2---FORMAT (1HO,31H-STRESS/STRAIN-DISTRIBUTION-IS--)----------
    K=N
    I=1 IS AT T=0, I=2 IS AT T=2*DKT, I=3 IS AT T=4*DKT, ETC.
    I=1
022-K=K-1----------
     R1=1./ER
---ERATIO = ER
    ASIG= 1.+ERATIO*DKT
    BSIG=ERATIO*DKT/2.
    DIVISR= 1.+DKT/2.+ERATIO*DKT/2.
---MLOC=7
    NUL=NBU+1
    NEW=N-NBU
    DO 991 J=1,NEW
    SIGL(J)=((EPS(1   ,J) +1.)- (SIG(1   ,J)+(1./ER)))/((1./ER)-1.)
    EPSL(J)= SIGL(J)-SIG(I+1 ,J)+ EPS(I+1,J)
91  EX(J)= SIGL(J)- ERATIO* EPSL(J)
    UKT=P/GAMMA
    NBAR=UKT/(2.*DKT)
    NU=NBU+NBAR
    DO 910 I=NUL,NU
    RI=I-NBU
     S(I,1)=P-GAMMA*RI*2.*DKT
0   CONTINUE
    NUM=NU+1
    DO 920 I=NUM,N
     S(I,1)=0.0
0   CONTINUE
    XX=DKT*ER
    E(NBU,1)= EPS(1   ,1)
    DO 933 I=NUL,NU
     E(I,1)=(  E(I-1,1)*(1.-XX)+  S(I,1)*AEPS+  S(I-1,1)*(DKT-1.)
   1-2.*DKT*(1.-ERATIO))/(1.+XX)
    RR=   E(I,1) -(  S(I,1) -(1.-ERATIO))/ ERATIO
    IF(RR.GT.0.0) GO TO 934
933 CONTINUE
    GO TO 935
934 IX=I
    DO 936  I=IX,NU
936   E(I,1)=  E(I-1,1)+  S(I,1)-  S(I-1,1)
935 LAST=N-2
    KM=NEW
---READ(5,3333) ERATIO
     R1=1./ER
     R2= 1./ERATIO
    SIGL(1)= ((  E(NU ,1)+1.)-(   S(NU ,1)+R1))/(R1-1.)
    EPSL(1)= SIGL(1)-  S(NU  ,1)+   E(NU ,1)
   EX(1)= SIGL(1)- ERATIO* EPSL(1)
    DO 8432 I=NUM,N
32    E(I,1)= -R2*EX(1)+(   E(NU ,1)  +R2*EX(1))
  1*EXP(-ERATIO*2.0*(TKT(I)-TKT(NUM)))
    ASI = 1.+ERATIO*DKT
```

```
      BSI =ERATIO*DKT/2.
      DIVIS = 1.+DKT/2.-ERATIO*DKT*(1.+DKT)*.5/ASI
      TT=1.
-----DO 940 M=NBU,LAST-----------------------------------------------
      IF(KM.LT.2) GO TO 1000
      IF(TT) 1902,1901,1902
1902  CONTINUE
-----IF(M-300) 1901,1900,1901----------------------------------------
1900  CONTINUE
       TT=0.0
       NM=1
-----CT =DKT
      READ(5,3333) DKT
-----WRITE(6,3732) DKT-----------------------------------------------
3732 FORMAT( /'AS OF NEXT I DKT = 'F6.3/)
-----I=1
      X=DKT/DT
      ID=X
      KS=KM/ID
-----LAST =M+KS-2
       DO1925 JJ=1,KS
      KL=ID*(JJ-1)+1
      SIG(1,JJ)= SIG(1,KL)
      EPS(1,JJ)= EPS(1,KL)
       CXX(JJ)= CXX(KL)
      SIGL(JJ)=SIGL(KL)
      SLOP(JJ)=SLOP(KL)
      EPSL(JJ)=EPSL(KL)
1925  EX (JJ)=EX  (KL)
     DO 1926 JJ=M,LAST
       KL=ID*(JJ-M)+M
      S(JJ,1)=S(KL,1)
      IF(S(JJ,1)) 1905,1905,1926
1926  CONTINUE
       GO TO 1927
1905  CONTINUE
      DO 1906 JX=JJ,LAST
1906  S(JX,1) =0.0
1927  CONTINUE
      M1=M+1
      DO 1907 LX= M1,LAST
1907  E(LX,1)= -R2*EX(1)
       WRITE(6,3334) M
     WRITE(6,1023) (SIG(I,J), J=1,KS,NM)
      WRITE(6,1023) (EPS(I,J), J=1,KS,NM)
-----WRITE(6,1023) (SLOP (J), J=1,KS,NM)
       KM=KS
     ASIG= 1.+ER     *DKT
      BSIG=ER     *DKT/2.
      DIVISR= 1.+DKT/2.+ER     *DKT/2.
      AEPS=1.+DKT
      BEPS=1.+DKT/2.
      ASI=1.+ERATIO*DKT
      BSI =ERATIO*DKT/2.
      DIVIS = 1.+DKT/2.-ERATIO*DKT*(1.+DKT)*.5/ASI
1901 CONTINUE
```

```
      I=1
      SIG(I+1,1)= S(M+1,1)
      EPS(I+1,1)= E(M+1,1)
      DO 941 J=2,KM
     H(I,J)=SIG(I,J)-(1.-ER    )-ER    *EPS(I,J)
      A(I+1,J)=SIG(I+1,J-1)+SIG(I,J+1)-SIG(I,J)+H(I,J)*DKT/2.
     1 + (1.-ER    )*DKT/2.
      B(I+1,J)= EPS(I,J)-SIG(I,J)+H(I,J)*DKT-(1.-ER    )*DKT
     SIG(I+1,J)=(A(I+1,J)*ASIG+B(I+1,J)*BSIG)/(DIVISR)
      EPS(I+1,J)= (A(I+1,J)*AEPS+B(I+1,J)*BEPS)/(DIVISR)
     RR=SIG(I+1,J)-ER    *EPS(I+1,J)-(1.-ER    )
      IF(RR.GT.0.0)GO TO 941
     IF(SIG(I+1,J).LT.SIGL(J)) GO TO 944
      SIG(I+1,J)=SIG(I+1,J-1)+SIG(I,J+1)-SIG(I,J)
     EPS(I+1,J)=EPS(I,J)+SIG(I+1,J)-SIG(I,J)
      IF(CXX(J)) 9111,9111,9112
111   SIGL(J)= ((EPS(I+1,J)+1.)-( SIG(I+1,J)+R1))/(R1-1.)
      EPSL(J)= SIGL(J)-SIG(I+1 ,J)+ EPS(I+1,J)
      EX(J)= SIGL(J)- ERATIO* EPSL(J)
      CXX(J)= 1.
112   CONTINUE
      IF(SIG(I+1,J).LT.SIGL(J)) GO TO 944
      GO TO  941
944   CONTINUE
      CXX(J)=1.
      H(I,J)=SIG(I,J)    -ERATIO        *EPS(I,J)-EX(J)
     SIG(I+1,J)=( SIG(I+1,J-1)+SIG(I,J+1)-SIG(I,J)+H(I,J)*DKT*.5+ (BSI
     1/ASI )*( EPS(I,J) -SIG(I,J)-DKT*EX(J)+H(I,J)*DKT)+DKT*.5*EX(J))/
     2DIVIS
      EPS(I+1,J)=(EPS(I,J)+ H(I,J)*DKT+SIG(I+1,J)*(1.+DKT)-SIG(I,J)-DKT
     1*EX(J))/ASI
      RR= ERATIO*EPS(I+1,J)+EX(J)
     IF(SIG(I+1,J).LT.RR) GO TO 941
      SIG(I+1,J)=SIG(I+1,J-1)+SIG(I,J+1)-SIG(I,J)
      EPS(I+1,J)=EPS(I,J)+SIG(I+1,J)-SIG(I,J)
941   CONTINUE
     DO 1102 J=1,KM
      SLOP(J)= (SIG(2,J)-SIG(1,J))/(EPS(2,J)-EPS(1,J))
      SIG(1,J)= SIG(2,J)
1102  EPS(1,J)= EPS(2,J)
      MM=M+1
      WRITE (6,3334) MM
     WRITE (6,1023) (SIG(1,J), J=1,KM,NM)
      WRITE (6,1023) (EPS(1,J), J=1,KM,NM)
      WRITE (6,1023)(SLOP(  J), J=1,KM,NM)
      KM=KM-1
940   CONTINUE
      GO TO 1000
33    FORMAT(3F10.9)
1023  FORMAT(/(8F16.8))
3334  FORMAT (//1X,'I=' I3)
      END
```